From Microevolutionary Processes to Macroevolutionary Patterns: Investigating Diversification at Multiple Scales in Southeast Asian Lizards

By

Anthony J. Barley

Submitted to the graduate degree program in Ecology and Evolutionary Biology and the Graduate Faculty of the University of Kansas in partial fulfillment of the requirements for the degree of Doctor of Philosophy.

Chairperson Dr. Rafe M. Brown

Dr. Mark Holder

Dr. John Kelly

Dr. Xingong Li

Dr. A. Townsend Peterson

Dr. Linda Trueb

Date Defended: April 14, 2014

The dissertation committee for Anthony J. Barley certifies that this is the approved version of the following dissertation:

From Microevolutionary Processes to Macroevolutionary Patterns: Investigating Diversification at Multiple Scales in Southeast Asian Lizards

____

Chairperson Dr. Rafe M. Brown

Date Approved: April 16, 2014

Abstract

A comprehensive understanding of the evolutionary processes responsible for generating biodiversity is best obtained using integrative approaches at multiple scales. In doing so, these investigations can provide complex insights into how fine-scale microevolutionary processes operating at the population level, translate into the large-scale macroevolutionary biodiversity patterns we see in evolutionary radiations. Due to the complex geography, historical climatic fluctuations, and remarkably high concentrations of land vertebrate biodiversity, Southeast Asia is an ideal place to investigate these processes. Lizards of the genus *Eutropis* represent one of the more recognizable radiations of lizards in Southeast Asia, due to their high abundances, broad geographic distribution, and generalized external morphology. However, their evolutionary history has remained enigmatic due to their highly conserved morphology and a lack of dense population sampling of individuals and species across their range.

In this dissertation, I first utilize a variety of approaches to delimit species in Philippine *Eutropis* and find that species diversity is vastly underestimated by current taxonomy, while more generally assessing how best to determine species limits in radiations where morphology is highly conserved. I then use a molecular phylogenetic framework to investigate biogeographic patterns and the timing of diversification within the genus across Southeast Asia. Lastly, I take a landscape genomic approach to determine the relative contributions of distance, and various geographic and environmental variables to population genetic differentiation and morphological diversity patterns in the common sun skink. This research contributes substantially to our understanding of species diversity in evolutionary radiations, as well as how historical and contemporary evolutionary processes shape the evolution of morphological and genetic diversity.

Acknowledgements

The research presented here, and my path to completing graduate school would not have been possible without the assistance and support of a large number people and institutions. Some chapters herein have been coauthored with Rafe Brown, Aniruddha Datta-Roy, Arvin Diesmos, Lee Grismer, Patrick Monnahan, K. Praveen Karanth, and Jordan White. I am grateful for the extensive financial support I have received during the course of my graduate career at KU from the Biodiversity Institute (Leonard Krishtalka), the Department of Ecology and Evolutionary Biology (Chris Haufler), the Office of Graduate Studies, and a number of professors (Andrew Short, Bill Duellman, and Linda Trueb) who provided me with research assistantship support that offered extra flexibility and valuable research time during my graduate career.

I thank my major advisor Rafe Brown for the extensive support he has provided throughout my time at KU, from both an academic and personal standpoint. Rafe's enthusiasm and mentorship has been instrumental in my success in research and my growth as a scientist. I also thank the other members of my dissertation committee Mark Holder, John Kelly, Xingong Li, Town Peterson, and Linda Trueb for being incredible academic resources and for challenging me intellectually. In particular I'd like to thank John for allowing me to work in his lab to collect genomic data for my dissertation research, and for answering a plethora of research questions over the years. Both of my undergraduate advisors Ronald Coleman and Brad Shaffer deserve thanks for providing me invaluable guidance, support, and opportunities, without which I likely would have never entered graduate school in the first place.

During my graduate career I have been fortunate to collaborate with numerous field biologists who have loaned specimens and tissue samples they collected, as well as obtain loans from museum collections; without which none of this research would have been possible. This includes A. Resetar (FMNH), J. Vindum, D. Blackburn, R. Crombie (CAS), A. Wynn, K. de Queiroz (USNM), J. McGuire (MVZ), T. LaDuc (TNHC), J. Hanken, J. Losos, J. Rosado (MCZ), J. Barnes, V. Papal-latoc (PNM), A. Schmitz, W. Böhme (ZMFK). Fieldwork during the course of my dissertation would not have been possible without support from the Philippine government and the hardworking Philippine field team I was privileged to work with, particularly Arvin Diesmos and Jason Fernandez.

I need to thank a large group of friends and colleagues that were important in making my graduate school experience at KU more enjoyable and successful, and providing intellectual input into my research, including: Mike Andersen, David Blackburn, Andrea Crowther, Matt Davis, Raul Diaz, Jake Esselstyn, Allison Fuiten, Rich Glor, Jesse Grismer, Boryana Koseva, Jacob Landis, Dean Leavitt, Andres Lira, Joe Manthey, Nick McCool, Julius Mojica, Rob Moyle, Jamie Oaks, Carl Oliveros, Karen Olson, Chan Kin Onn, Cameron Siler, Jeet Sukumaran, Scott Travers, Luke Welton, and Amber Wright. In particular, I thank Charles Linkem who was an important friend and mentor when I first moved to Lawrence, and provided me with much needed guidance during the early portion of my graduate school career. I would also like to thank members of the Tokyo Sandblasters including Michael Amick, Chris Coleman, Bob Jansen, Scott Cassaw, and Brian Finley; Monday night softball games were a much needed relaxation outlet from graduate school.

I thank Levi Gray, a close personal friend who has been tremendously supportive in both personal and professional contexts over the years. Being able to count on him for advice and herping trips has been incredibly important to me during graduate school, and I wouldn't be where I am today without his help. Phil Spinks is also a close friend who was a mentor to me as an undergraduate and was responsible for preparing me for graduate school in systematics; he spent countless hours working with me above and beyond what was expected. Bob Thomson is a close friend, mentor, and fellow California Gila Monster enthusiast; he has helped me on a variety of important fronts during graduate school for which I am extremely grateful.

Last, but not least, I would like to thank my entire family. My wife Laci has provided me with unlimited amounts of love, support, and encouragement, which has been integral to the completion of my dissertation. She has also provided countless insights during conversations that have helped me grow as both a person and a scientist while at KU. My parents Dave and Winnie Barley have always been role models for me, as well as provided encouragement and much needed financial support throughout my academic career. My brothers David, Dominic, and Michael have been there for me during my highest and lowest points, and the fishing trips and barbecues we've had during graduate school have been essential to my happiness. Additionally, Dave and Mike deserve credit for first teaching me how to noose lizards and find salamanders when I was a kid.

Table of contents

Chapter 1

The challenge of species delimitation at the extremes: diversification without morphological change in Philippine sun skinks

Barley AJ, White J, Diesmos AC, Brown RM. 2013. The challenge of species delimitation at the extremes: diversification without morphological change in Philippine sun skinks. *Evolution* 67:3556–3572.

Abstract

An accurate understanding of species diversity is essential to studies across a wide range of biological subdisciplines. However, delimiting species remains challenging in evolutionary radiations where morphological diversification is rapid and accompanied by little genetic differentiation or when genetic lineage divergence is not accompanied by morphological change. We investigate the utility of a variety of recently developed approaches to examine genetic and morphological diversity, and delimit species in a morphologically conserved group of Southeast Asian lizards. We find that species diversity is vastly underestimated in this unique evolutionary radiation, and find an extreme case where extensive genetic divergence among lineages has been accompanied by little to no differentiation in external morphology. Although we note that different conclusions can be drawn when species are delimited using molecular phylogenetics, coalescent-based methods, or morphological data, it is clear that the use of a pluralistic approach leads to a more comprehensive appraisal of biodiversity, and greater appreciation for processes of diversification in this biologically important geographic region. Similarly, our approach

demonstrates how recently developed methodologies can be utilized to obtain robust estimates of species limits in "non-adaptive" or "cryptic" evolutionary radiations.

Introduction

Due to its central importance in fields related to the evolutionary study of biodiversity, the practice of species delimitation has a long and contentious history (Wiley, 1978; Frost and Hillis, 1990; Mayden, 1997; de Queiroz, 1998; Sites and Marshall, 2003). Much of this debate stems from the difficulty of developing a universal species concept (de Queiroz, 1999; Esselstyn, 2007; Bauer et al., 2010) and involves determining which methodological approaches produce the most accurate results (Marshall et al., 2006; Fujita and Leaché, 2011). However, an accurate understanding of species diversity is an essential first step before studies in many other biological fields can be conducted, including studies of species diversification, character evolution, population genetics, ecology, comparative genomics, and conservation (Cracraft, 2002; Sites and Marshall, 2004; Fujita et al., 2012).

Problems associated with delimiting species are particularly pronounced in some systems and are characterized by challenges that can cause fundamental difficulties for evaluating species rich evolutionary assemblages (Fig. 1.1). These include many spectacular evolutionary radiations, which biologists are particularly motivated to understand. In several classic examples such as cichlid fishes (Moran and Kornfield, 1993; Seehausen, 2004; Wagner et al., 2012), passerine birds (Freeland and Boag, 1999; Petren et al., 2005; Moyle et al., 2009), Hawaiian silverswords (Baldwin, 1997), and ambystomatid salamanders (Shaffer, 1984; Shaffer and McKnight, 1996), species are well differentiated morphologically, but not genetically; making identification of unique evolutionary lineages challenging. This is often the case when species have diverged rapidly, recently, or when hybridization among lineages is common (Witter and Carr, 1988; Shaffer and Thomson, 2007; Wagner et al., 2012). Methodological advances in the fields of phylogenetics, population genetics, and molecular biology have led to the identification of an alternative paradigm in some systems which can make species delimitation just as problematic: when evolutionary lineages are well differentiated genetically, but not morphologically. These systems include “non-adaptive radiations” (Gittenberger, 1991; Jockusch and Wake, 2002; Rundell and Price, 2009) and “cryptic species diversity” in widespread species complexes (Stuart et al., 2006; Pfenninger and Schwenk 2007; Clare, 2011; Funk et al., 2012). Examples of these conceptually intriguing evolutionary phenomena include plethodontid salamanders (Wake et al., 1983; Highton, 1989; Jockusch and Wake, 2002; Kozak et al., 2006; Wake, 2006), tree snails (Holland et al., 2004), gekkonid lizards (Oliver et al., 2009), and cavefish (Niemiller et al., 2012).

Historically, morphological differences between populations were used as a proxy for reproductive isolation, and subsequent identification of species boundaries (Mayr, 1942; Simpson, 1951). However, the exclusive use of morphology in delimiting species can be problematic, particularly in cases in which species converge in external morphology (Derkarabetian et al., 2010; Serb et al., 2011; Heideman et al., 2011) or when speciation is not accompanied by morphological change. For example, morphological traits may experience similar selective pressures and evolve convergently (Schönrogge et al., 2002; Glor et al., 2003; Bickford et al., 2007; Revell et al., 2008; Wright, 2011). Conversely, some species may exhibit striking polymorphisms in morphology within or among populations, despite extensive gene flow (Wake, 1997; Petren et al., 2005; Harley et al., 2006; Wang and Summers, 2010).

Evolutionary biologists have widely embraced the notion that delimiting species ought to be guided by the principle that species are defined as distinct evolutionary lineages (Hennig, 1966; Wiley, 1978; Frost and Hillis, 1990; de Queiroz, 2005). Molecular datasets consisting of multiple, unlinked loci have allowed for more rigorous empirical studies delimiting evolutionary lineages that constitute species (Sinclair et al., 2004; Shaffer and Thomson, 2007; Carstens and Dewey, 2010; Linkem et al., 2010; Kubatko et al., 2011). Although phylogenetic and population genetic methods can be used to construct gene trees and examine population structure, identifying species-level lineages and determining if populations are isolated using genetic data can be challenging, particularly in the face of incomplete lineage sorting or hybridization (Shaffer and Thomson, 2007; Frankham et al., 2012; Fujita et al., 2012; Wagner et al., 2012; Welton et al., 2013).

Coalescent-based methods that permit the use of genetic sequence data to identify genetic isolation among—and cessation of gene flow between—lineages (or putative species) have just begun to be developed. Fundamentally, these methods evaluate the likelihood of competing species delimitation hypotheses based on an assumed evolutionary process (Pons et al., 2006; Yang and Rannala, 2010; Ence and Carstens, 2011; Reid and Carstens, 2012). Although these methods incorporate assumptions that may or may not be biologically realistic for a particular species group, they represent important progress towards the development of objective criteria for empirical evaluation of species limits (Leaché and Fujita, 2010; Fujita et al., 2012).

Lizards of the genus *Eutropis* (also referred to as "sun skinks") are some of the most common and conspicuous lizards in Southeast Asia, owing to their high abundance, diurnal activity patterns, and generalist habitat preferences. Despite this, the genus has had a long history of taxonomic confusion, due primarily to the fact that sun skinks represent a clade with a generalized external morphology, characterized as evolutionarily highly conserved (Miralles et al., 2005; Miralles and Caranza, 2010; Hedges and Conn, 2012). Within the Philippines, a region classified as both a Global Biodiversity Conservation Hotspot and a Megadiverse Nation (Conservation International, 2008; Brown and Diesmos, 2009), few distinct morphological characters clearly differentiate currently described species, and the geographic ranges of taxa are not well characterized (Brown and Alcala, 1980). Because extreme evolutionary radiations such as these are often characterized by discordance between genetic loci, data type, or other species recognition criteria, we take a pluralistic approach to examine lineage diversification and delimit species in Philippine sun skinks using extensive gene sampling and robust geographical coverage of populations from across this unique archipelago. Additionally, our study examines the effectiveness of utilizing recently developed methods and outlines an approach for investigating genetic and morphological diversity, and obtaining accurate estimates of species limits in "non-adaptive" or "cryptic" evolutionary radiations.

Methods

Taxonomic and genetic sampling and identification of evolutionary lineages

The core Philippine *Eutropis* radiation consists of five described species, one of which is divided into two subspecies (*E. indeprensa, E. cumingi, E. bontocensis, E. englei, E. multicarinata multicarinata*, and *E. multicarinata borealis*; Brown and Alcala, 1980). Two additional species in the genus occur in the Philippines (*E. multifasciata* and *E. rudis*), but these are members of a separate evolutionary radiation (Mausfeld and Schmitz, 2003; Datta-Roy et al., 2012) and are not included in the present study. Because of the poorly developed taxonomy and difficulty in assigning individuals to species in some cases, we sequenced a large sample of individuals (187) from across the archipelago for the nicotinamide adenine dinucleotide dehydrogenase subunit 2 (ND2) mitochondrial gene (Macey et al., 1997; Linkem et al., 2010) as an initial screen of genetic diversity (see Appendix 4 for specific locality information). Our sampling design included two individuals (when possible) of each putative species from each of 79 sampling localities. Previous studies of some species delimitation methods have shown that sampling two individuals dramatically improves both accuracy and precision (Camargo et al., 2012). We also included individuals from the type locality of all described *Eutropis* species in the Philippine radiation with exception of *E. englei*. Because this species is known to occur only in a portion of the country that is logistically challenging for biologists to access, we have been unable to include it in this study. Although the Philippine *Eutropis* radiation (exclusive of *E. multifasciata* and *E. rudis*) represents a monophyletic species group (Mausfeld and Schmitz, 2003; Datta-Roy et al., 2012), populations of several species in the group have been reported to occur in eastern Malaysia and the islands of Palau (Crombie and Pregill, 1999; Das, 2004); accordingly we included several individuals from these populations in our study.

Genomic DNA was extracted from soft tissue utilizing Fujita's guanidine thiocyanate protocol (Esselstyn et al., 2008). DNA was amplified using standard PCR protocols, and products were purified with a 20% dilution of ExoSAP-IT (Amersham Biosciences, Piscataway, NJ), incubated for 30 minutes at 37° C and then at 80° C for 15 minutes. Cleaned PCR products were dye-labeled using Big-Dye terminator 3.1 (Applied Biosystems, Foster City, CA), purified using Sephadex (Amersham Biosciences), and sequenced on an ABI 3730 automated capillary sequencer. All PCR products were sequenced in both directions. All DNA sequence data collected for this research was deposited in Genbank (see Appendix 3 for accession numbers). Sequences were edited and subsequently aligned using MAFFT in Geneious Pro v5.3 (Katoh et al., 2005). The alignments were visually examined and translated for coding regions using Mesquite v2.75 (Maddison and Maddison, 2011). Models of molecular evolution were selected using decision theory implemented in DT-ModSel (Minin et al., 2003). All alignments and phylogenetic trees generated for this research were deposited in Treebase (Accession S14377).

We then used a general mixed Yule-coalescent (GMYC) model in combination with the ND2 data to generate a preliminary species delimitation hypothesis. The GMYC model attempts to distinguish between interspecific (modeled by a Yule process) and intraspecific (modeled by the coalescent) branching events on a phylogenetic tree, based on the idea that the rate of coalescence within species should be much greater than between (Pons et al., 2006). There are currently three implementations of the model, all of which we tested on our dataset: a maximum likelihood (ML) method with a single threshold (Pons et al., 2006), a multiple threshold ML method that allows the depth of the coalescent-speciation transition to vary along branches of the tree (Monaghan et al., 2009), and a Bayesian method (bGMYC) that accounts for error in phylogeny estimation and uncertainty in model parameters (Reid and Carstens, 2012). To generate ultrametric trees for our analyses, we ran both strict clock and uncorrelated lognormal (UCLN) relaxed clock analyses of our 1017 base pair (bp) ND2 dataset using BEAST v1.7.3. Because the inclusion of identical sequences results in many zero length branches at the tip of the tree and can cause the model to over-partition the dataset (Reid and Carstens, 2012; also noted during preliminary analyses of our dataset), we pruned these sequences from our dataset for the final BEAST and GMYC analyses (resulting in 128 individuals in the alignment). We performed a likelihood ratio test to see if we could reject a molecular clock for the pruned ND2 dataset by comparing the likelihood of the tree after optimizing the branch lengths with and without enforcing a molecular clock using PAUP* v4.0b10 (Swofford, 2002). However, we were unable to reject a global molecular clock for the mtDNA dataset (p = 0.08)

We ran our BEAST analyses for 20 million generations, sampling every 2 x 10^3 generations and assessed convergence by assuring that all parameters had reached stationarity and sufficient (>200) effective sample sizes using Tracer v1.4 (Rambaut and Drummond, 2007), and that the posterior distributions differed from the priors. We checked for topological convergence by ensuring that posterior probabilities were stable and that split frequencies were similar across runs using Are We There Yet? (AWTY: Wilgenbusch et al., 2004; Nylander et al., 2007). For ML GMYC analyses, we utilized the maximum clade credibility tree generated from the posterior distribution of our BEAST analyses. For bGMYC analyses, we used 100 trees sampled from the posterior distribution of the BEAST analyses and ran the GMYC analyses on each tree for 50,000 generations, discarding the first 40,000 generations as burnin, and using a thinning interval of 100 (as recommended by the authors). Nei's genetic distance (D_{xy}; Nei, 1987) values (with a Jukes and Cantor distance correction) between the groups of populations identified as distinct evolutionary lineages by the GMYC analyses were calculated using DnaSP v5.10.1 (Librado and Rozas, 2009). Based on these analyses of the ND2 data, we then scaled our sampling of individuals down, targeting equal numbers of individuals across all divergent lineages for sequencing of nuclear genes, and further examination of species boundaries.

We chose exon-primed, intron-crossing (EPIC) markers for our study because the conserved exonic portions can anchor primers for use across a phylogenetically diverse species group; while the intronic regions typically have higher substitution rates than protein-coding DNA and consequently are more informative for studies of species level phylogenetics and phylogeography (Thomson et al., 2010). We developed markers by screening primers used in studies of closely related taxonomic groups (birds, turtles, and other squamates) and examining them for appropriate size, function across taxonomic diversity, and variation across species. In some cases, we designed new primers if the original primers failed to work across all taxonomic diversity in Philippine *Eutropis*, based on the collected sequence data and the *Anolis* genome (Alföldi et al., 2011). We sequenced each individual for six nuclear genes (see Appendix 2 for primer sequences and PCR protocols): the ATP synthetase-B subunit intron (ATPSB; Skinner, 2007), the selenoprotein-T intron (SELT; Jackson and Austin, 2009), the N-acetyltransferase 15 intron (NAT15; Kimball et al., 2009), the nitric oxide synthase 1 intron (NOS1), the forkheadbox P2 intron (FOXP2), and the L-lactate dehydrogenase M chain (LDHA) gene (Pasachnik et al., 2009). Because sequences from some individuals contained heterozygous insertions/deletions, the program Indelligent v1.2 (Dmitriev and Rakitov, 2008) was used to reconstruct the allelic sequences when necessary.

Full dataset phylogenetic analyses

To further investigate support for species boundaries in our dataset, we estimated phylogenetic trees for the full seven-gene dataset, the nuclear data only, and each gene individually. Bayesian inference (BI) phylogenetic analyses were performed with BEAST v1.7.3, using separate strict clock models for each gene, fixing the mean substitution rate to 1.0, and partitioning the dataset by gene (with separate substitution models for each partition). We ran our analyses for 100 million generations, sampling every 5 x 10^3 generations, and assessed convergence using Tracer and AWTY as discussed above. We examined the effect of analyzing the ND2 data as a single partition, partitioned by codon, or as two partitions (with the 1st and 2nd codon positions being one partition, and the 3rd codon position being the other) in all analyses of the full dataset. However, regardless of partitioning strategy, all analyses consistently produced the same topology, so we chose to analyze it as a single partition in our final analyses. Maximum likelihood gene tree estimates were obtained using RAxML v7.0.3 (Stamatakis, 2006) with nodal support assessed via 100 bootstrap replicates. The evolutionary models for each partition selected using DT-ModSel were used in all BI analyses, whereas all partitions were assigned a GTR + Γ model in the ML analyses, as this is the only option available in RAxML. Trees were rooted with *Eutropis macularia*, a closely related species that does not occur in the archipelago (Mausfeld and Schmitz, 2003; Datta-Roy et al., 2012).

Coalescent-based species delimitation using nuclear data

We then used the program Bayesian Phylogenetics and Phylogeography (BP&P) v2.1 in combination with our nuclear DNA (nuDNA) to evaluate potential species boundaries (Yang and Rannala, 2010) in several situations where species delimitation was still ambiguous despite an examination of gene trees, morphological data, and geographic range. This method utilizes a Bayesian framework and an explicit model of lineage sorting based on the coalescent process to estimate posterior probabilities for competing species delimitation models, while integrating over uncertainty in gene trees. It does this using a reversible-jump Markov Chain Monte Carlo (rjMCMC) algorithm in combination with a user-specified guide tree.

BP&P requires a prior on the population size parameter (θ) and the age of the root in the species tree (τ_0), which can affect the posterior probabilities for the models. Both priors are given a gamma distribution G(α,β) with mean α/β and variance α/β^2. Larger values for θ and smaller values for τ_0 favor conservative models with fewer species (Yang and Rannala, 2010). Estimates of θ exhibit a broad range (~0.0005–0.02) across extant plant and animal species (Zhang et al., 2011). We utilized a variety of combinations of priors that assumed large, medium, or small ancestral population sizes and shallow, moderate, or deep divergences. For our priors, we used $\theta \sim G(1, 10)$, $\theta \sim G(1, 100)$, $\theta \sim G(2, 2000)$. The same values were used for τ_0, using all the different possible combinations of values for these two parameters to evaluate their effect on the analysis. The program can implement two different rjMCMC algorithms, both of which we tested for consistency across each species delimitation hypothesis, while having the program auto-adjust the fine-tuning parameters. We also ran each analysis multiple times using different starting trees to ensure stability, as well as proper mixing and convergence across runs.

Because BP&P requires that the topology of the phylogeny be known with certainty in order to accurately delimit species (Yang and Rannala, 2010), we only used BP&P to evaluate species limits in clades with strongly supported topologies in all our phylogenetic analyses of the full dataset. Since the ND2 data were used to identify the clades for our species delimitation hypotheses (using the GMYC), we did not include them in the BP&P analyses, and included only the six nuclear genes. This approach allowed us to evaluate the species delimitation hypotheses with independent loci that were not used in the hypothesis formulation.

Morphological data

We also sought to examine the effectiveness of using variation in external meristic (scale counts) and mensural (body measurements) morphological characters to delimit species. In total, we collected morphological data for 145 individuals (see Appendix 4 for specimens examined).

For each individual, we collected 13 quantitative morphological traits: snout–vent length, axilla–groin distance, head length and head width (measured at the front of the auricular opening), forelimb length, hind limb length, total number of lamellae under toes I–V on the right foot, supra- and infralabial scale counts, ventral scale counts (counted as ventral scales between front and rear limbs), vertebral scale counts (the number of scale rows between the parietal scales and the base of the tail), midbody scale row counts, and number of keels per scale. Morphological data were deposited in the Dryad repository: doi:10.5061/dryad.307g0.

In addition to visually examining the morphological data for characters that could distinguish potential species, we performed three types of multivariate statistical analyses using the morphological data. Principal component analyses (PCA) were performed using a correlation matrix to examine the data for structure that could potentially correspond to species groups. We also performed linear discriminate function analysis (DFA) to determine if individuals could be assigned to the correct species groups identified by molecular data. Lastly we performed a two-step cluster analysis using Schwarz's Bayesian Criterion and a log-likelihood distance measure as an objective attempt to determine the number of morphological groups present in our dataset. All morphological measurements were log-transformed for multivariate analyses in order to reduce heteroscedasticity and improve normality. Analyses were performed using R v2.13.0 (The R Foundation for Statistical Computing; http://www.R-project.org), SPSS v20 (IBM Corp.), and JMP8 (SAS Institute Inc.).

Species tree analysis

After assessing species boundaries, species tree analysis was conducted using the program *BEAST (Heled and Drummond, 2010) in BEAST v1.7.3. *BEAST is a Bayesian method that uses a coalescent framework to simultaneously estimate a species-tree topology, divergence times, population sizes, and gene trees from multi-gene datasets. We ran both strict clock and UCLN relaxed clock analyses, fixing the mean substitution rate to 1.0. The species population-mean hyperprior and the species Yule process birth prior were both assigned exponential distributions, with means of 0.01 and 1.0 respectively. We utilized a piecewise linear and constant root population size model. In the strict clock analyses the relative clock rates for each gene were assigned an exponential prior distribution with a mean of 1.0. In the UCLN relaxed clock analyses, the clock means for each gene were also assigned exponential distributions with a mean of 1.0, and the standard deviations were assigned exponential distributions with a mean of 0.05. We ran each analysis for 200 million generations, sampling every 10^4 generations. Convergence was assessed using Tracer and AWTY as described above.

Lastly, as a cursory examination of diversification rates in Philippine *Eutropis*, we generated lineage through time plots for each of the post burin-in trees from the posterior distribution of our UCLN relaxed clock *BEAST analyses. We plotted the log number of lineages against relative time using the APE package (Paradis et al., 2004) in R. We tested for a significant departure from the null hypothesis of a constant rate of diversification through time using the constant-rate (CR) test (Pybus and Harvey, 2000). We calculated the γ-statistic for each of 10,000 trees drawn from the posterior distribution of two different *BEAST analyses: one employing a more conservative estimate of species diversity (13 species) and one with a more liberal estimate (15 species).

Results

General mixed Yule-coalescent analyses

Although topologies differed somewhat with respect to the poorly supported, deeper nodes in the tree, both strict and relaxed clock phylogenetic analyses of the ND2 data (when analyzed as a single partition and when partitioned by codon) identified the same strongly supported clades (Fig. 1.2). These slight changes in topology did not affect our GMYC analyses, which gave consistent results regardless of the tree used in the analysis. However, each of the different GMYC methods gave a slightly different result. The mean number of species estimated by the single threshold ML model was 19 [with the 95% highest posterior density (HPD) ranging from 4–27 species], whereas the mean number of species estimated by the multiple threshold ML model was 27 (with the 95% HPD ranging from 16–29). The mean number of species estimated by the bGMYC model was 19 (with the 95% HPD ranging from 9–33). After examining the geographic ranges (Fig. 1.2) and genetic divergences (Table 1.1) among the lineages identified in the analyses, we adopted the more conservative estimate of species diversity (19) as our working hypothesis. Additionally, several of the lineages identified in the GMYC analyses were represented by only 1 or 2 individuals (which could significantly impact the results in coalescent analyses). Because we had poor sampling in the regions where these lineages occur, and the populations together represented well-supported, monophyletic clades in this and subsequent phylogenetic analyses, we conservatively considered them to be a single species in later analyses (Fig. 1.2; clade numbers four and fifteen). This resulted in 16 divergent groups of populations we regarded as candidate species, which we targeted for further investigation.

Phylogenetic analyses

We collected nuclear sequence data for a subsample of 74 individuals for use in all subsequent analyses. This resulted in 3–6 individuals (mean n=4.6) per divergent clade. Our nuclear dataset consisted of a total of 4237 bp, and we were able to sequence all 74 individuals for NAT15 (572 bp), FOXP2 (634 bp), and LDHA (556 bp). ATPSB (1185 bp) was sequenced for 73 individuals, while SELT (694 bp) and NOS1 (596 bp) were sequenced for 72 individuals. The combined phylogenetic analyses of all the data identified the same 16 clades as the mtDNA data, and we unambiguously assigned existing species names (based on type localities and examination of type specimens) or clade letters to 13 of them (Fig. 1.3). Phylogenetic analyses of the combined nuclear gene data only, resulted in support for the monophyly of 15 of the 16 clades (with the exception being the split within Clade E in Figure 1.3 was not resolved).

Eleven of the 16 clades were found to be monophyletic (although support values were low in some instances) for each of the six nuclear genes (see Appendix 5 for individual gene tree estimates). This consisted of the clades that were assigned species names or clade letters in Figure 1.3, except that Clade D, *E. indeprensa*, and *E. cumingi* would be considered a single monophyletic clade in this case. We observed no instances of incongruence between analyses of mtDNA and nuDNA that might indicate hybridization or introgression, as all individuals were consistently assigned to the same 11 monophyletic clades among individual gene tree estimates. Relationships among these clades varied, however, this is not surprising given that most nodes in individual gene trees were not strongly supported, and gene tree heterogeneity is commonly observed in multi-locus phylogenetic datasets (Jennings and Edwards, 2005; Kubatko and Degnan, 2007; Edwards, 2008; Liu et al., 2008; Barley et al., 2010). Among Clade D, *E. indeprensa*, and *E. cumingi*, only three of six nuclear gene trees showed each clade to be monophyletic (ATPSB, SELT and NOS1). Analysis of mtDNA data revealed significant divergence between the Cordillera Mountain Range populations and all other populations of *E.*

cumingi; and actually showed both *E. indeprensa* and Clade D populations to be more closely related to other populations of *E. cumingi* than those in the Cordillera (Fig. 1.2; Table 1.1). However, none of the nuclear gene trees found the Cordillera Mountain populations to be reciprocally monophyletic with respect to other populations of *E. cumingi*. Within Clade E, only two of six nuclear gene trees (ATPSB and LDHA) showed the populations on Mindanao/Bohol and Siargao/Dinagat to form reciprocally monophyletic clades. Among *E. m. borealis* populations, three of six nuclear gene trees (LDHA, SELT, and NOS1) found populations from Luzon/Polillo/Catanduanes/Babuyan Islands and Negros/Panay/Siquijor to form reciprocally monophyletic clades.

Coalescent-based species delimitation using nuclear data

We focused our BP&P analyses on 3 different groups: the *E. indeprensa* species complex, Clade E, and the *E. m. borealis* clade. All analyses gave consistent results regardless of the rjMCMC algorithm and starting tree used (Fig. 1.3). For both Clade E and the *E. m. borealis* clade, our choice of prior distributions for (θ) and (τ_0) did not affect our results, and all analyses supported a split between the Siargao/Dinagat Islands populations and the Mindanao/Bohol populations in Clade E, as well as a split between the Luzon/Polillo/Catanduanes/Babuyan Island populations and the Negros/Panay/Siquijor populations of *E. m. borealis*, with a posterior probability for speciation of 1.0 (Fig. 1.3). For the *E. indeprensa* species complex, all BP&P analyses supported splits between all six clades with speciation posterior probabilities of 1.0 regardless of prior choice, with one exception (Fig. 1.3). In analyses utilizing our most conservative choice of priors [$\theta \sim G(1, 10)$ and $\tau_0 \sim G(2, 2000)$, which assume large ancestral population sizes and shallow divergence among species], a split between the Cordillera Mountain populations of *E. cumingi* and the rest of Luzon was not supported.

Morphology

Trait values for some morphological characters showed little variation across all Philippine *Eutropis* species; and the small variation present was as variable within taxa as between. This included the number of supralabial scales, infralabial scales, and midbody scale rows. Additionally, the number of keels per scale was often as variable within individuals as between individuals. Therefore, we excluded data for these morphological characters and performed all multivariate analyses using data from the remaining nine traits: snout–vent length, axilla-groin distance, head length, head width, forelimb length, hind limb length, total number of lamellae under the toes, vertebral scales rows, and ventral scale rows. We focused our morphological analyses on ten of the clades from Figure 1.3: Clade C, Clade E, Clade F, Clade G, *E. indeprensa, E. cumingi, E. bontocensis, E. m. multicarinata, E. m. borealis*, and the *Eutropis* species from Palau. For the other clades, the sample sizes from which we were able to collect morphological data were small, so extensive characterization of morphological variation within clades was not possible.

We found snout–vent length, axilla–groin distance, head length, head width, forelimb length, and hind limb length to be strongly correlated (r = 0.88–0.94; Appendix 1). Total lamellae number was moderately correlated with these variables (r = 0.69–0.77; Appendix 1). Vertebral and ventral scale rows did not show significant correlation with the other morphological variables, however, they were moderately correlated with each other (r = 0.73; Appendix 1). Principal component analysis found size to be the most important variable in explaining variance in our dataset (explaining 74.8%), as the loadings for PC1 all had similar values for all variables (with the exception of vertebral and ventral scale rows, which are not strongly associated with body size; Table 1.2). PC2 loaded strongly on the number of ventral and vertebral scale rows, and explained 14.6% of the total variance. PC3 loaded strongly on the total number of lamellae under the toes, and explained 3.7% of the total variance. However, most clades did not separate significantly along the axes of variation in morphological size and shape identified in the PCA (Fig. 1.4)

Discriminate function analyses of the morphological data was only able to assign all individuals correctly for three out of ten genetic clades (correctly assigning a total of 75.2% of individuals to their respective genetic clade), highlighting the extremely conserved external morphology of Philippine *Eutropis* (Table 1.3). Our cluster analysis found the optimal number of clusters in our dataset to be two, with Cluster 1 being composed of all individuals from the clades in the *E. multicarinata* species complex except for *E. bontocensis*, and Cluster 2 consisting of all individuals from the clades in the *E. indeprensa* species complex and *E. bontocensis* (Fig. 1.5). However, since our main concern was determining species boundaries, we were more interested in whether or not sister clades showed evidence of morphological differentiation.

Species tree analysis of the molecular data demonstrated strong support for a sister relationship between *E. bontocensis* and Clade F (Fig. 1.3). These clades were also found to be highly genetically distinct from each other (Table 1.1, Fig. 1.3), despite the fact they occur sympatrically; indicating the two taxa represent distinct species. Discriminate function analysis was able to correctly distinguish between the two clades, and individuals were not misassigned between them. *Eutropis bontocensis* was found to exhibit a generally smaller body size and a fewer total number of toe lamellae (Table 1.4). Similarly, *E. m. borealis* and Clade G appear to be highly genetically distinct sister clades (Table 1.1, Fig. 1.3). In this case, DFA was again able to distinguish between the two groups based on combinations of the morphological variables (Table 1.3, 1.4), as Clade G tended to have slightly larger body size and more vertebral scale rows; however there was significant overlap among all trait values. When comparing Clade E and the *Eutropis* species from Palau, trait values again overlapped, but in this case DFA was unable to correctly assign all individuals between each group. Discriminate function analysis correctly distinguished between individuals of *E. indeprensa* and *E. cumingi*, as *E. indeprensa* had a slightly longer hind limb/snout–vent length ratio and more total toe lamellae.

Discriminate function analysis performed best in distinguishing between the *E. multicarinata* and *E. indeprensa* species complexes, with body size generally being much larger in the *E. multicarinata* species complex. This result was also reflected in our cluster analysis, which identified two morphological clusters largely consisting of these two clades. Although *E. bontocensis* is an exception to this (having a generally smaller body size than other taxa in the species complex), DFA still assigned 97.8% of individuals correctly to the two groups. Among our comparisons, DFA performed most poorly in distinguishing among *E. m. borealis*, *E. m. multicarinata*, Clade E, Clade F, and the *Eutropis* species from Palau, only correctly assigning 68.1% of individuals to their actual genetic clade.

Species tree analysis

Our strict and relaxed clock species tree analyses using *BEAST resulted in identical topologies (Fig. 1.6). These results support the existence of two distinct species complexes in the

Philippines: the *E. indeprensa* species complex and the *E. multicarinata* species complex. Our diversification rate analyses using relative divergence times indicated there has been a significant decrease in speciation rate through time in the Philippine radiation, regardless of the number of species specified in the analysis (Fig. 1.6).

Discussion

Species delimitation

Despite a recent increase in interest in developing methods for delimiting species, conflicts between datasets, methodologies, and species recognition criteria often makes species delineation difficult in species-rich evolutionary radiations (de Queiroz, 1998, 1999; Frost and Hillis, 1990; Tobias et al., 2010). Traditionally, this has been examined in cases where species exhibit extensive morphological diversity, but little genetic divergence. This is often the result of rapid or recent divergences among species, or hybridization among lineages, and many well-studied examples exist (Witter and Carr, 1988; Seehausen, 2004; Petren, 2005). In this study, we find an extreme case of an alternative evolutionary phenomenon that poses a challenge to species delimitation: when many evolutionary lineages are highly genetically distinct, but morphologically indistinguishable.

Analysis of our dataset revealed that our current systematic knowledge of Philippine *Eutropis* vastly underestimates the actual lineage (species) diversity present within the archipelago. Concordant gene tree splits from multiple loci provide strong evidence for genetic isolation of populations representing distinct species (Knowles and Carstens, 2007; O'Meara, 2010), and therefore we find that conservatively, a minimum of eleven distinct species occur in our dataset, since each of these clades is supported by seven independent loci. Geographic range data for each of these groups of populations also indicate that these genetic clades are likely isolated from each other: either because they are separated by large geographic distances, or are highly divergent clades that occur sympatrically (Fig. 1.6, Table 1.5).

However, our coalescent-based analyses indicate strong support for species diversity being as high as fifteen candidate species, and provide limited support for as many as nineteen distinct evolutionary lineages. A lack of monophyly at all genetic loci does not necessarily preclude the possibility that speciation has occurred, as this could be the result of random variation in the coalescent process, or the failure of lineages to completely sort due to a recent speciation event. We find mixed support in our nuclear data for speciation having occurred among Clade D, *E. indeprensa*, and *E. cumingi* (Fig. 1.6). Additionally, these clades occur on adjacent islands and genetic divergences among clades could be the result of phylogeographic structure, with the potential for low rates of gene flow to occur among populations.

Our coalescent-based analyses supported a split between populations on the islands of Mindanao/Bohol and Siargao/Dinagat within Clade E. However, because we lacked sampling from NE Mindanao for this clade, we refrain from drawing any strong conclusions. Lastly, we found significant genetic divergence between populations of *E. m. borealis* on Luzon/Polillo/Catanduanes/Babuyan Islands and Negros/Panay/Siquijor. However, our dataset contains poor sampling in the central Philippine Visayan Islands, where there was evidence of extensive genetic structure among populations (including ~10% uncorrected "P" pairwise mtDNA sequence divergence among individuals from each island). We also lacked sampling on islands separating these two clades (e.g. Masbate), and thus the status of these populations warrants further field sampling and systematic investigation.

Coalescent modeling

Methods that attempt to model the coalescent process as it relates to species delimitation have only recently begun to be developed (Fujita et al., 2012). In this case, we applied two coalescent modeling methods to our dataset, one to generate an initial hypothesis for species delimitation based on mtDNA data (since the chaotic taxonomic history of the group made this problematic), and one to test these species limits using nuclear data. The coalescent models strongly supported the more liberal species delimitation hypotheses in most cases. The few simulation studies that have tested coalescent-based methods have been encouraging, often finding them to perform relatively well even when datasets are small (Yang and Rannala, 2010; Zhang et al., 2011; Reid and Carstens, 2012), and many recent empirical studies have tested their performance on datasets of various composition (Monaghan et al., 2009; Leaché and Fujita, 2010; Barrett and Freudenstein, 2011; Burbrink et al., 2011; Setiadi et al., 2011; Brown et al., 2012; Fujita et al., 2012; Spinks et al. 2012).

However, as with any statistical modeling method, it is important that they are utilized in appropriate systems. For example, the robustness of coalescent approaches to variations in geographic sampling and violations of model assumptions (which are often present in real world datasets such as this one) remain to be examined using simulated and empirical datasets. Of particular concern with respect to our dataset are the assumptions of no genetic structuring within lineages and constant population sizes, which are likely unrealistic in island archipelago systems. These assumptions may bias the method towards oversplitting, particularly since in this study we found the method to nearly always support the most liberal groupings.

Morphological data

Although sun skinks in general can be characterized as a group in which external morphology has been highly conserved through evolutionary time (Miralles et al., 2005; Miralles and Caranza, 2010; Hedges and Conn, 2012), our data demonstrate that Philippine *Eutropis* represent an extreme example of this. We found extensive genetic differentiation among species within the Philippine radiation, which has not been accompanied by even moderate levels of differentiation in external morphological traits. In some cases, we were unable to consistently diagnose species based on these morphological characters, and in cases where morphological differentiation appears to have occurred, most of these differences are rather minor, and often involved only slight differences in body size (i.e. species in the *E. indeprensa* species complex generally had a smaller body size than species in the *E. multicarinata* complex).

The fact that speciation in Philippine *Eutropis* is only sometimes associated with relatively small changes in external morphology renders these data problematic for species delimitation. Of course, even when small differences in morphological trait values appear to be diagnostic of certain populations, they could simply be the result of local adaptation. In many cases, we found that morphological trait values varied as much within populations as between them, and were not diagnostic of genetically defined groups that appear to represent distinct species. Interestingly, we also found two examples of sympatric species within the *E. multicarinata* species complex that we were unable to differentiate using morphological data, but which are clearly genetically isolated from each other. This included Clade F and *E. m. borealis*, which both occur syntopically in northern Luzon, as well as *E. m. multicarinata* and Clade E, which occur syntopically in northeastern Mindanao and on Dinagat Island.

In situations where species diverge rapidly or recently, and extensive morphological differentiation has not been accompanied by extensive genetic differentiation, strong directional selection acting on morphological traits, usually through sexual selection or adaptation, is often inferred. When species are well differentiated genetically, but not morphologically (as is the case in this study), it has previously been suggested to be the result of stabilizing selection on important adaptive traits (Schönrogge et al., 2002; Glor et al., 2003). We find it conceivable that a similar phenomenon may be occurring in Philippine *Eutropis*. All species appear to occupy similar microhabitat types and ecological niches (with the exception of *E. bontocensis* and *E. englei*, the two highly morphologically distinct species). Thus, strong selection may be acting to maintain external morphological traits, the values of which may be constrained since they are strongly associated with the similar ecologies of all species (Roughgarden, 1972; Stanley, 1989; Travis, 1989; Johnson and Barton, 2005).

Species diversification

Our species tree analysis and our partitioned analysis of the concatenated seven-gene dataset resulted in identical topologies, reflecting the strong signal in our dataset. The presence of two species complexes is consistent with previous morphological work (Brown and Alcala, 1980). Of those, the *E. indeprensa* Complex appears to be a more recent radiation, and some of the clades show evidence of incomplete lineage sorting in multiple gene trees if they should indeed be recognized as species. Within the *E. multicarinata* Complex, there does not appear to have been a historical split that divided the northern and southern populations (Fig. 1.6) as was previously hypothesized (Brown and Alcala, 1980).

Philippine sun skinks represent an extreme example of a species rich, morphologically conserved evolutionary radiation, although their overlapping geographic distributions make them a particularly intriguing system. Unfortunately, we lack calibration points for our phylogeny, and thus are unable to obtain a reliable estimate for the age of this species complex, although the high sequence divergences among lineages (Table 1.1) indicate species divergences are likely relatively old. Diversification rate analyses based on relative divergence times appear to indicate there has been a decrease in speciation rate through time. This could indicate that speciation rates were higher as this clade originally colonized the archipelago, and then slowed as they became more geographically widespread. The two species complexes exhibit overlapping distributions across the archipelago, with the *E. indeprensa* Complex being predominantly structured by geographic region (with the exception that two of the clades occur sympatrically on the island of Panay; Fig. 1.6). The *E. multicarinata* Complex exhibits more elaborate biogeographical relationships among candidate species, however, both complexes contain lineages that are restricted to small geographic regions, as well as lineages that appear to be capable of long distance dispersal across biogeographical regions. Additionally, unlike most morphologically conserved evolutionary radiations (e.g. “non-adaptive” radiations or “cryptic” species complexes), some morphologically indistinguishable lineages occur syntopically, raising the question of how these lineages can coexist.

Species delimitation in “non-adaptive” or “cryptic” species complexes

Our study outlines an approach that can be taken to obtain accurate estimates of species boundaries in species complexes where morphology is highly conserved. Our findings suggest that:

1. When lacking, preliminary hypotheses for species limits can be obtained using methods for discovering structure in data without *a priori* assumptions of species boundaries (in our case, mtDNA and the GMYC model).
2. EPIC markers can be used to obtain gene tree estimates to provide additional support for lineages that are defined as distinct by mitochondrial data. Introns (Benavides et al., 2007) and anonymous loci (Thomson et al., 2008; Camargo et al., 2012) are also likely to be useful in these situations.
3. Because results based on coalescent modeling can be dependent on model parameters, it is useful to utilize multiple methods and independent datasets when possible (e.g. using BP&P in combination with presumably unlinked nuclear loci).
4. Although in these systems external morphology can be limited in terms of its utility to delimit species, it can still provide valuable information regarding species boundaries in some cases, such as critically important data for diagnosing sister species.
5. Lastly, examining multiple lines of evidence (including geographic range data and ecological data) likely will produce the most biologically meaningful results when delimiting species.

Conclusions

We find that species diversity in this unique evolutionary radiation is at least 2 or 3 times higher than is currently described, and we identify an extreme case where lineage diversification has not been accompanied by divergence in external morphological traits. The surprising underestimate of species diversity in this group is particularly important since it occurs in a biodiversity conservation hotspot (Brown and Diesmos, 2009). Island archipelagos have historically and recently been regarded as models systems for studying evolutionary processes in a diverse range of fields (MacArthur and Wilson, 1967; Bock, 1970; Losos and Ricklefs, 2009; Oaks et al., 2013; Brown et al., 2013), however, an accurate understanding of species diversity is critical to these types of studies. Our study represents an empirical example of how recently developed methods can be used to arrive at an enhanced, evolutionary-informed understanding of cryptic biodiversity and reveal previously overlooked, but conceptually intriguing evolutionary radiations.

Table 1.1 Pairwise Nei's Genetic Distance (D_{xy}) values (with a Jukes and Cantor distance correction) between all combinations of each of the 16 clades identified in Figure 1.2.

	2	3	4	5	6	7	8	9	10	11	12
1	0.1301	0.1411	0.1268	0.1280	0.1310	0.1657	0.1581	0.1499	0.1638	0.1535	0.1548
2	–	0.1337	0.1285	0.1225	0.1364	0.1659	0.1726	0.1667	0.1629	0.1626	0.1667
3	–	–	0.1156	0.1119	0.1125	0.1712	0.1757	0.1652	0.1622	0.1337	0.1668
4	–	–	–	0.0974	0.1015	0.1643	0.1727	0.1573	0.1584	0.1683	0.1672
5	–	–	–	–	0.0912	0.1539	0.1659	0.1551	0.1680	0.1657	0.1681
6	–	–	–	–	–	0.1653	0.1711	0.1636	0.1625	0.1743	0.1654
7	–	–	–	–	–	–	0.1597	0.1542	0.1532	0.1604	0.1583
8	–	–	–	–	–	–	–	0.1459	0.1499	0.1382	0.1406
9	–	–	–	–	–	–	–	–	0.1393	0.1484	0.1446
10	–	–	–	–	–	–	–	–	–	0.1323	0.1353
11	–	–	–	–	–	–	–	–	–	–	0.1129

	13	14	15	16
1	0.1587	0.1569	0.1549	0.1497
2	0.1609	0.1685	0.1714	0.1571
3	0.1757	0.1676	0.1754	0.1634
4	0.1674	0.1611	0.1704	0.1615
5	0.1538	0.1568	0.1713	0.1587
6	0.1535	0.1667	0.1787	0.1630
7	0.1688	0.1665	0.1630	0.1446
8	0.1545	0.1518	0.1503	0.1449
9	0.1582	0.1526	0.1515	0.1429
10	0.1547	0.1472	0.1565	0.1434
11	0.1556	0.1470	0.1428	0.1510
12	0.1469	0.1471	0.1432	0.1395
13	–	0.1539	0.1601	0.1574
14	–	–	0.1554	0.1442
15	–	–	–	0.1384

Table 1.2 Results of principal component analysis. SVL = snout–vent length, AG = axilla–groin distance, HDLG = head length, HDWD = head width, ARM = forelimb length, LEG = hind limb length, LAM = total lamellae number, VERT = vertebral scale rows, and VEN = ventral scale rows.

	PC1	PC2	PC3	PC4
Eigenvalue	6.8024	1.3019	0.3136	0.2255
Percent of variation	75.5824	14.4658	3.4845	2.5057
SVL	0.3671	0.1436	-0.1861	0.0891
AG	0.3551	0.1540	-0.3832	0.0311
HDLG	0.3715	0.1073	-0.0250	0.0916
HDWD	0.3699	0.0616	-0.1574	0.1126
ARM	0.3639	0.1370	0.0284	0.0364
LEG	0.3697	0.0832	0.0466	0.0504
LAM	0.3309	0.0367	0.8578	-0.1968
VERT	-0.2476	0.5846	0.2155	0.7380
VEN	-0.1562	0.7560	-0.0888	-0.6187

Table 1.3 Results of the discriminate function analysis of ten clades based on nine morphological variables. Columns represent true identities of individuals based on their genetic clades, while rows indicate which group individuals were assigned to by analysis.

	E. m. borealis	*E. m. multicarinata*	*E. bontocensis*	*Eutropis sp.* Palau	Clade E	Clade F	Clade G	*E. indeprensa*
E. m. borealis	16	0	0	1	6	1	0	0
E. m. multicarinata	0	6	0	0	1	0	0	0
E. bontocensis	0	0	18	0	0	0	0	1
Eutropis sp. Palau	1	0	0	10	1	1	0	0
Clade E	5	0	0	0	6	1	0	0
Clade F	0	0	0	1	4	10	0	0
Clade G	0	0	0	1	0	0	5	0
E. indeprensa	0	0	2	0	0	0	0	4
E. cumingi	0	0	0	0	0	0	0	0
Clade C	0	0	0	0	0	0	0	1
Total *N*	22	6	20	13	18	13	5	6

	E. cumingi	Clade C
E. m. borealis	0	0
E. m. multicarinata	0	1
E. bontocensis	0	0
Eutropis sp. Palau	0	0
Clade E	0	0
Clade F	0	1
Clade G	0	0
E. indeprensa	0	2
E. cumingi	14	2
Clade C	0	14
Total *N*	14	20

Table 1.4 Ranges of morphological trait values for nine morphological variables for ten of the clades shown in Fig. 1.3. See Table 1.2 for character abbreviation interpretations.

	E. m. borealis (n=22)	*E. m. multicarinata* (n=6)	*E. bontocensis* (n=20)	*Eutropis sp.* Palau (n=13)	Clade E (n=18)	Clade F (n=13)	Clade G (n=5)
SVL	64.1–82.5	61.1–71.3	40.1–61.2	61.0–79.3	64.5–83.9	60.5–78.7	73.7–88.6
AG	27.4–41.4	29.6–36.1	22.4–29.5	29.2–40.3	28.6–40.7	27.0–40.3	35.0–41.2
HDLG	14.0–17.6	13.5–15.8	9.7–13.8	13.6–18.8	13.6–19.3	12.2–18.0	15.3–19.4
HDWD	10.4–13.3	10.0–12.9	6.8–9.8	9.5–12.8	10.0–14.6	10.2–13.0	11.5–17.4
ARM	11.0–18.7	14.6–16.9	9.4–13.6	14.8–19.2	13.4–19.8	12.0–19.3	17.9–22.2
LEG	15.1–24.8	18.0–23.1	11.4–16.6	18.1–24.3	17.4–24.7	15.6–22.2	21.8–27.3
LAM	79–88	71–82	67–74	77–88	73–88	74–87	82–89
VERT	37–42	35–38	44–50	39–46	35–43	37–46	41–47
VEN	24–28	22–28	29–33	27–30	26–30	26–30	29–30

	E. indeprensa (n=6)	*E. cumingi* (n=14)	Clade C (n=20)
SVL	54.0–63.8	43.5–60.0	45.6–69.7
AG	24.9–28.7	21.4–26.9	21.3–32.3
HDLG	10.3–13.5	8.6–11.6	9.6–14.0
HDWD	7.9–9.9	6.1–8.6	7.1–11.2
ARM	11.9–14.9	7.6–11.1	9.3–15.5
LEG	14.7–18.4	9.4–12.2	11.4–19.4
LAM	69–75	55–67	65–77
VERT	41–47	43–49	39–45
VEN	26–31	27–32	25–29

Table 1.5 Table indicating proximity of closest known populations among clades in Figure 1.6. Abbreviations indicate closest known populations occur on: AI = Adjacent Islands, NAI = Non-Adjacent Islands, SI = Same Island. Distances are approximate distance between closest populations sampled in study. Clades where both species were collected at same locality are denoted as sympatric.

	E. m. borealis	*E. bontocensis*	Clade A	Clade E	Clade F	Clade G
E. m. multicarinata	AI, 120 km.	NAI, 720 km.	SI, 200 km.	Sympatric	NAI, 770 km.	NAI, 350 km.
E. m. borealis	–	Sympatric	AI, 280 km.	AI, 70 km.	Sympatric	AI, 40 km.
E. bontocensis	–	–	NAI, 1100 km.	NAI, 800 km.	Sympatric	AI, 280 km.
Clade A	–	–	–	Sympatric	NAI, 1200 km.	NAI, 600 km.
Clade E	–	–	–	–	NAI, 900 km.	NAI, 380 km.
Clade F	–	–	–	–	–	AI, 460 km.

	E. cumingi	Clade B	Clade C	Clade D
E. indeprensa	AI, 15 km.	AI, 180 km.	AI, 120 km.	AI, 210 km.
E. cumingi	–	AI, 130 km.	SI, 150 km.	AI, 280 km.
Clade B	–	–	Sympatric	AI, 270 km.
Clade C	–	–	–	AI, 290 km.

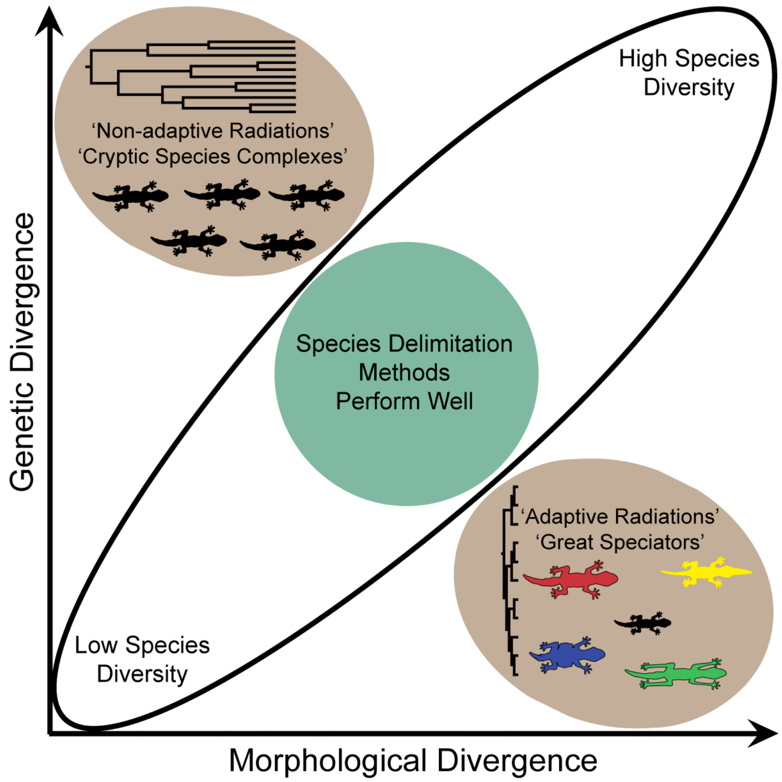

Figure 1.1 Hypothetical axes of morphological and genetic diversity within a species group. Area circumscribed by black ellipse represents systems where species delimitation is usually simple. The two areas circumscribed in brown represent conditions under which species delineation is often problematic, but conceptually interesting.

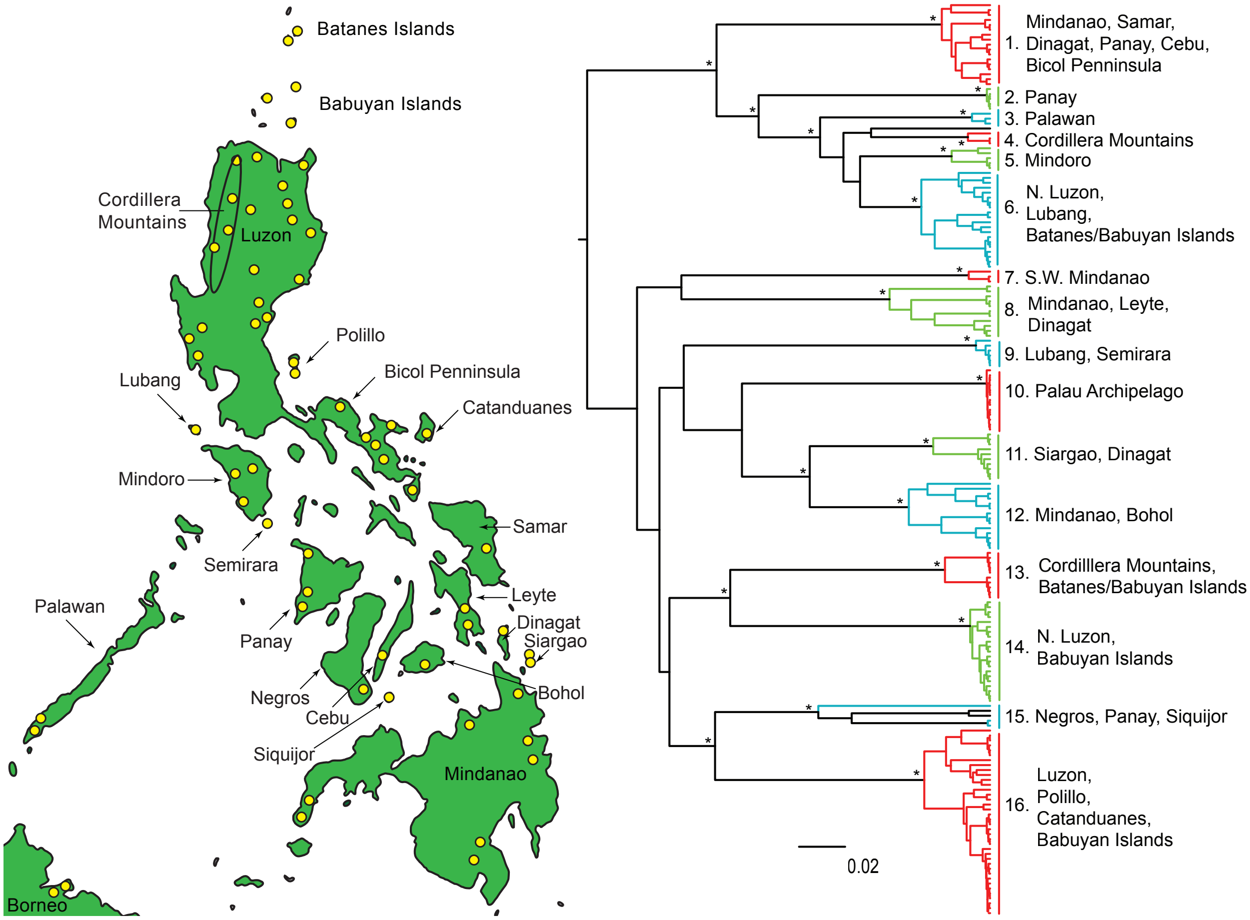

Figure 1.2 a) Map of Philippine Islands with dots indicating locations of sampled populations and b) Maximum clade credibility tree from strict clock analysis of ND2 data. Nodes with an asterisk represent nodes with posterior probabilities >.95. Different colored clades represent the distinct evolutionary lineages identified by the GMYC analyses.

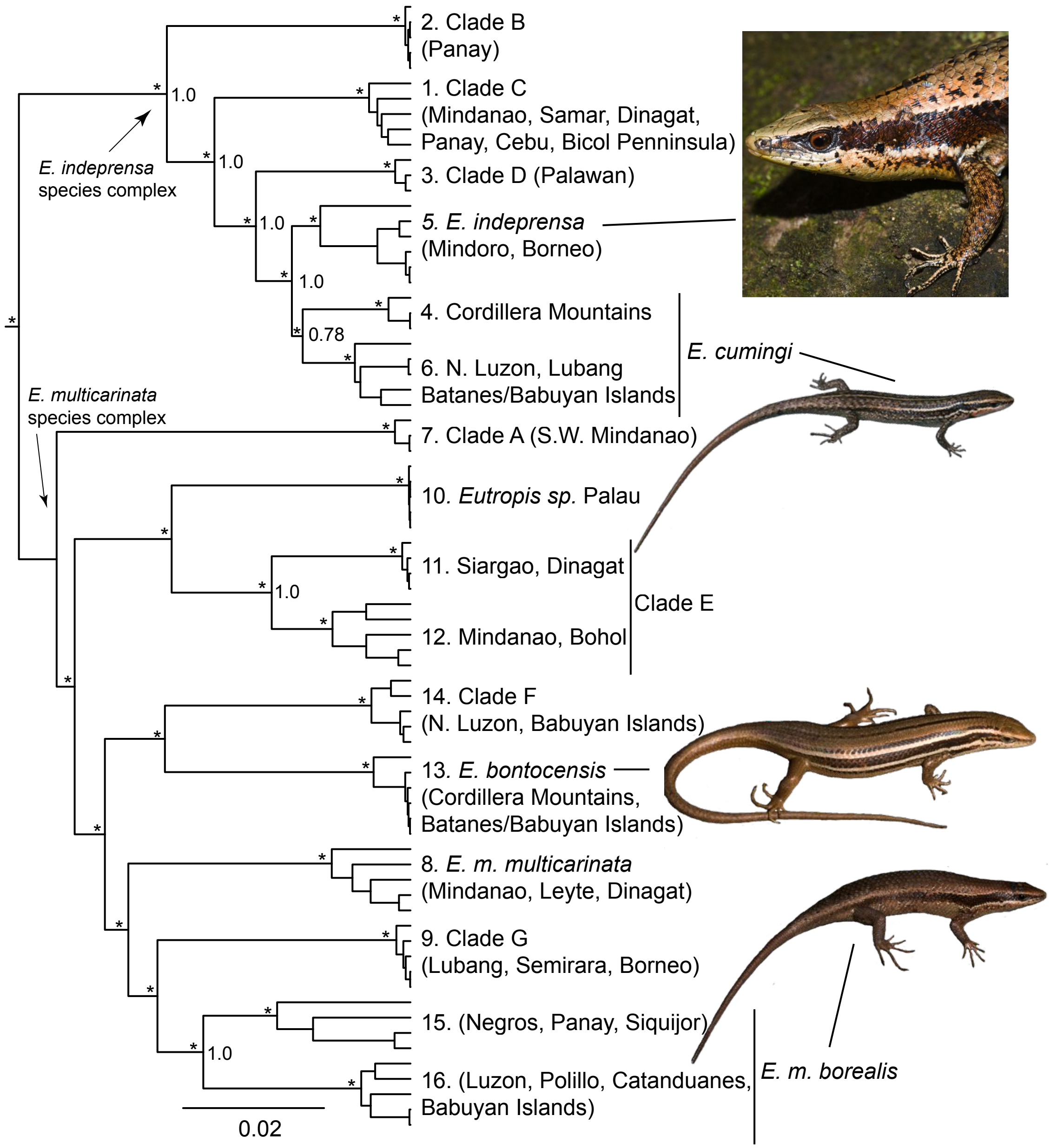

Figure 1.3 Maximum clade credibility tree from concatenated, partitioned Bayesian analysis of all genetic data. Nodes with an asterisks indicate posterior probabilities >.95. Numbers adjacent to nodes represent speciation posterior probabilities resulting from BP&P analyses using the most conservative prior distributions. Numbers at tips correspond to clades identified in Figure 1.2.

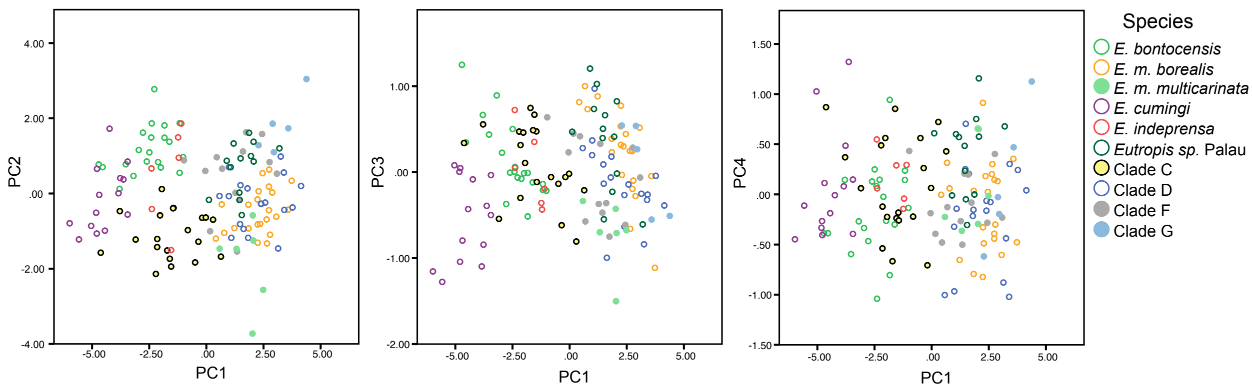

Figure 1.4 PCA biplots for nine morphological variables shown in Table 1.2.

Variables: 9	Clusters: 2
Cluster 1	Cluster 2
E. m. borealis (25)	*E. bontocensis* (20)
E. m. multicarinata (6)	*E. cumingi* (14)
Eutropis sp. Palau (13)	*E. indeprensa* (6)
Clade A (1)	Clade B (2)
Clade E (18)	Clade C (20)
Clade F (13)	Clade D (2)
Clade G (5)	n = 64, 44.1%
n = 81, 55.9%	

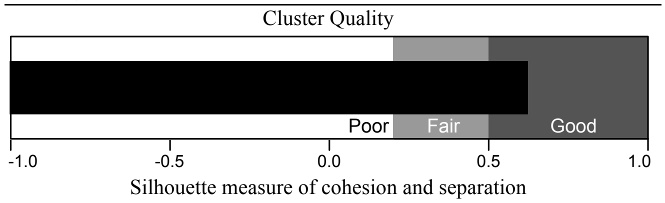

Figure 1.5 Results of two-step cluster analysis. Numbers in parentheses represent sample size for each clade. Clades correspond to those shown in Figure 1.3.

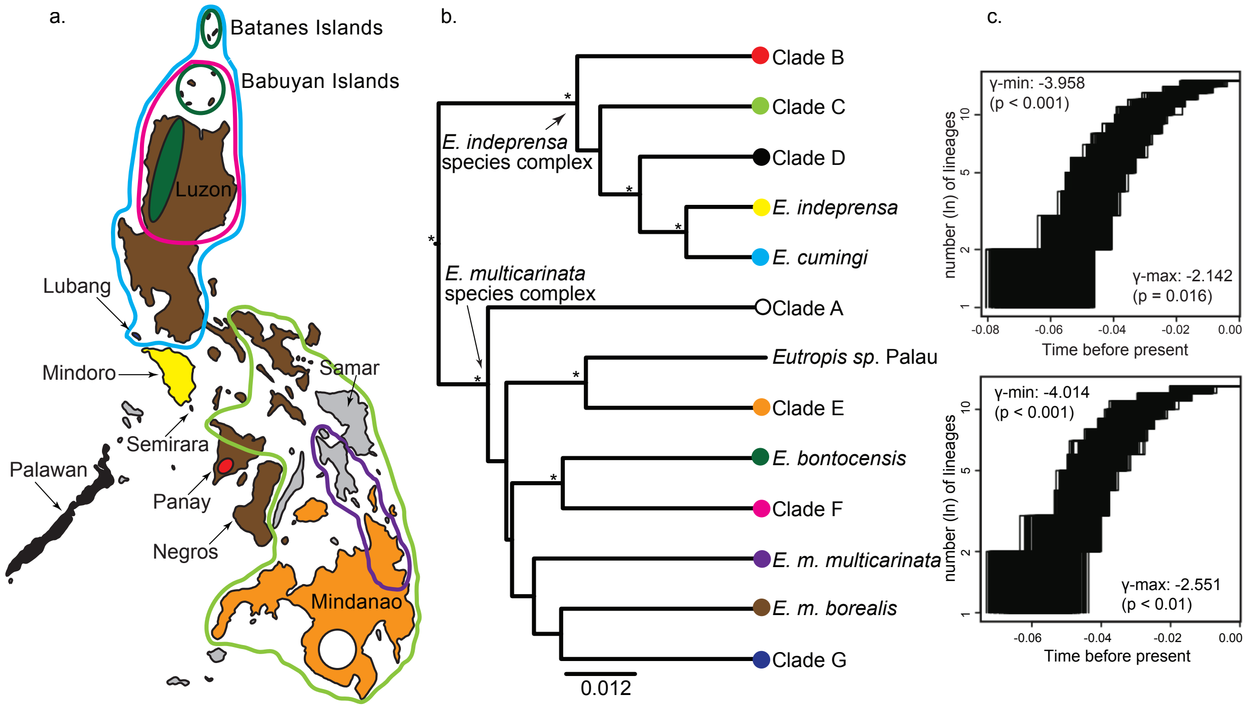

Figure 1.6 a) Map showing approximate distributions of clades identified in Figure 1.3; b) Maximum clade credibility tree from relaxed clock species tree analysis generated using all genetic data in *BEAST. Asterisks represent nodes with posterior probabilities >.95. All clades correspond to those identified in Figure 1.3; c) Lineage through time plots for 10,000 trees drawn from posterior distribution of species tree analysis with 13 lineages (bottom), and 15 lineages (top). Minimum and maximum γ-statistic values and associated p-values from posterior distribution of trees are indicated.

Chapter 2

Sun skink diversification across the Indian-Southeast Asian biogeographical interface

Abstract

Aim Widespread, trans-continental vertebrate groups represent ideal systems for biogeographic studies, because they can shed light on a wide range of questions relating to species diversification across the geographical template. We combined extensive geographic and genetic sampling from across multiple biogeographic realms to examine the timing and location of diversification in Asian sun skinks, a clade characterized by problematic species boundaries and a particularly enigmatic evolutionary history.

Location Southeast Asia, India, The Assam Region, Sundaland, and the Philippines.

Methods We sequenced one mitochondrial and nine nuclear genes for the majority of species in the genus *Eutropis* and we estimated phylogenetic relationships and divergence times using coalescent methods. To investigate the location of diversification events, we also estimated ancestral geographic ranges using several methods. Finally, we explored patterns of genetic diversity within several poorly understood but conspicuously widely distributed species.

Results Divergence time estimates indicate *Eutropis* began diversifying during the Eocene. Biogeographic reconstructions show that species diversification was clearly associated with dispersal into three biogeographical realms: India, Sundaland, and the Philippines. With respect to other classic studies of Southeast Asian vertebrate biogeography, Lydekker's line and the Assam region of northeastern India appear to have been prominent areas of faunal turnover in

Eutropis, whereas the Isthmus of Kra and Wallace's line do not appear to played a prominent role in shaping biogeographic history in this group.

Main conclusions Results of this study clarify several questions related to the evolutionary history of *Eutropis*, and provide a framework for understanding remaining questions regarding species diversity. Our study represents one of the first to compile a robust, heavily sampled, multilocus dataset across international boundaries in southern Asia that historically have prevented a unified understanding of biogeographic and evolutionary processes involving the Indian subcontinent, mainland Southern Asia, and the island archipelagos of Southeast Asia.

Introduction

Given the complex geography (Hall, 1998; Yumul et al., 2009), historical climatic fluctuations (Heaney, 1991; Woodruff, 2010), and remarkably high concentration of land vertebrate biodiversity (Myers et al., 2000) in Southeast Asia, the region represents an ideal setting to investigate species diversification and biogeographic patterns (Esselstyn et al., 2010; Stelbrink et al., 2012; Brown et al., 2013; Parnell, 2013). Consequently, a lengthy series of studies has lead to the identification of numerous biogeographic barriers and empirical tests of hypotheses to explain species distributions (Wallace, 1860; Van Steenis, 1950; Huxley, 1868; Inger, 1954; Diamond and Gilpin, 1983; Briggs, 1989). In many cases, researchers have found multiple, co-distributed taxa exhibiting shared biogeographic patterns, the examination of which has yielded insight into historical processes that may drive species diversification (Heaney, 1986; Corbet and Hill, 1992; Woodruff, 2003; Meijaard and Groves, 2006; Brown and Diesmos, 2009). However, empirical studies include nearly as many exceptions to predictions of common mechanisms (Brown and Guttman, 2002; Evans et al., 2003; Esselstyn et al., 2009; Jønsson et al., 2010; Esselstyn et al., 2010; Siler et al., 2010; Lim et al., 2011; Brown et al., 2013).

Studies of dispersal driven systems, such as the island archipelagos of Southeast Asia, often reveal how dispersal and colonization events facilitate species diversification (Mahler et al., 2010; Setiadi et al., 2011; Blackburn et al., 2013; Li et al., 2013; Linkem et al., 2013). Comparisons of species diversity patterns among geographic areas assist in the identification of regions where species diversification has been accelerated (Xang et al., 2004; Kozak and Wiens, 2010; Setiadi et al., 2011). Widespread taxonomic groups offer ideal systems for testing biogeographical hypotheses because they offer the opportunity to compare species diversity among geographic regions, and elucidate how geographic barriers interact with species dispersal abilities to determine biogeographic patterns of distribution (Irschick et al., 1997; Moyle et al., 2009; Alföldi et al., 2011). Although studies of such groups are important to understanding the general biogeographic history of a region, few clades contain both geographically widespread species and narrowly-distributed, microendemic taxa. Additionally, logistical obstacles to research across international boundaries historically have made studying widespread Southeast Asian vertebrate taxa problematic.

Lizards of the genus *Eutropis* are a species rich radiation of skinks that occur throughout tropical Asia (Taylor, 1922; Taylor, 1963; Mausfeld and Schmitz, 2003; Das, 2004; Grismer, 2011). The group represents an intriguing evolutionary radiation, both in terms of its large geographic distribution and the fact that it has not diversified substantially from an ecological perspective, as most species appear to occupy similar ecological niches. Although some previous studies have investigated coarse biogeographical patterns in *Eutropis* (Mausfeld and Schmitz, 2003; Whiting et al., 2006; Das et al., 2008; Skinner et al., 2011; Datta-Roy et al., 2012), poor taxonomic sampling, few data from nuclear markers, and cryptic species diversity (Barley et al., 2013) have prevented a comprehensive understanding of evolutionary history and patterns of diversification in this clade.

Many *Eutropis* lineages appear capable of long distance dispersal across oceanic barriers because presently they inhabit extensive geographic ranges spanning well-known biogeographic barriers between major geographic and faunal realms. (Kuhl, 1820; Hallowell, 1857; Mausfeld and Schmitz, 2003; Grismer, 2011; Holt et al., 2013). The pattern of large geographic ranges in selected *Eutropis* species may be indicative of this radiation being composed primarily of habitat non-specialist species that may be capable of surviving in a wide range of ecological and climatic environments. The consistently generalized and highly conserved external morphology exhibited by species in this group also suggest many *Eutropis* species may be ecological generalists (Miralles et al., 2005; Barley et al., 2013). In contrast, a number of *Eutropis* species are restricted to very small geographic ranges (Smith, 1935; Brown and Alcala, 1980; Bobrov, 1992; Barley et al., 2013).

In this paper we employ geographically comprehensive taxonomic sampling (including sampling from across the ranges of the widespread taxa), and data from multiple unlinked genetic markers, to investigate the timing of diversification and biogeographic patterns within *Eutropis*. In doing so, we relate biogeographic patterns to the complex geography of Southeast Asia in an attempt to understand the processes leading to speciation in this group. We also employ our phylogenetic estimate to infer the routes by which this group of diverse lizards colonized the different biogeographic regions of tropical Asia, and consider these results in the context of previously articulated Southeast Asian biogeographical hypotheses.

Methods

Taxonomic and genetic sampling

We obtained genetic samples for 20 of the 30 described species of *Eutropis*. Because several previous studies have indicated that cryptic and undescribed species diversity likely is present in multiple species complexes (Mausfeld and Schmitz, 2003; Das et al., 2008; Barley et al., 2013), we included multiple individuals from diverse sampling localities in an effort to include as many suspected species as possible (see Appendix 6 for details of sampling). We were unable to obtain genetic samples for several species (*E. andamanensis, E. tytleri. E. gansi, E. innotata, E. chapaensis, E. darevskii, E. floweri, E. tammanna*, and *E. englei*), however, because these rare taxa are endemic to small geographic areas, they are unlikely to have marked impacts on our broad scale phylogenetic and biogeographic analyses. As outgroups, we also included species from three genera that appear to be closely related to *Eutropis* (*Dasia grisea, Trachylepis perroteti*, and *Mabuya mabouya*), as well as a more distantly related species *Emoia atrocostata*.

Genomic DNA was extracted, amplified, and sequenced using the same methods as described in Barley et al. (2013). We sequenced one mitochondrial gene and nine nuclear genes for our study, seven of which have been previously shown to be informative in studies of *Eutropis* (ND2, ATPSB, SELT, NAT15, NOS1, FOXP2, LDHA; see Barley et al., 2013). We also sequenced the RNA fingerprint protein 35 (R35; Leaché, 2009), the melanocortin receptor 1 (MC1R) gene (Pinho et al., 2010), and the ribosomal protein 40 (RP40) gene (Friesen et al., 1999). The following redesigned primers were used for RP40: RP40.F 5’–

ATGTGGTGGATGYTGGCTCGTGAAGTC–3’ and RP40.R 5’–GCTTTCTCAGCWGCRGCCTGCTC–3’. Sequences were edited and subsequently aligned using MAFFT in Geneious Pro v5.3 (Katoh et al., 2005). All sequence data were deposited in Genbank (see Appendix 7 for details). The alignments were visually examined, translated for coding regions, and models of molecular evolution were selected using decision theory implemented in DT-ModSel (Minin et al., 2003).

Phylogenetic Analyses

We estimated phylogenetic relationships using several model-based methods. Maximum likelihood (ML) phylogenetic analysis was performed for each gene individually, and a partitioned, concatenated analysis was run for the full 10-gene dataset using RAxML v7.03 (Stamatakis, 2006). The data were partitioned by gene, and support was assessed via 1000 bootstrap replicates. A partitioned, concatenated Bayesian phylogenetic analysis of the full dataset was performed using MrBayes v3.2.1 (Ronquist et al., 2012) utilizing two replicates with four chains each for 20 million generations, sampling every 2×10^3 generations. To assess convergence, we checked that the average standard deviation of split frequencies approached zero, the potential scale reduction factor approached 1, and that the log likelihood scores had reached stationarity. We also used Tracer v1.4 (Rambaut and Drummond, 2007) to assess convergence, assuring that all the parameters and statistics had reached stationarity and sufficient effective sample sizes (>200). We checked for topological convergence by ensuring that posterior probabilities were stable and that split frequencies were similar across runs using Are We There Yet? (AWTY: Wilgenbush et al., 2004; Nylander et al., 2007).

Our goal was to obtain a temporal framework for examining biogeography and diversification in *Eutropis*, and utilize a coalescent species tree model to estimate phylogeny in a simultaneous analysis. Unfortunately no fossil calibration points exist for taxa within the genus, or closely related species, and ages of islands in Southeast Asia provide only a maximum bound for colonization times, with no minimum bounds. Therefore, as a crude approximation of the general temporal framework for diversification, we employed a mitochondrial DNA (mtDNA) substitution rate derived from closely related taxa to time-calibrate our tree. Although these limitations prevent precise divergence dating, using a molecular rate for calibration can provide a rough estimate for divergence times of the major radiations within the genus (Caccone et al. 1997; Calsbeek et al., 2003; Rabosky et al., 2007; Linkem et al., 2013).

We performed divergence time estimation with an uncorrelated relaxed lognormal clock in BEAST v1.7.5 (Drummond and Rambaut, 2007), using the species tree ancestral reconstruction (Heled and Drummond, 2010). Each gene was assigned a separate unlinked relaxed clock model in the analysis. For the ND2 data, we placed a 95% normal distribution prior (with a mean of 0.00895, and a standard deviation 0.0025) that was used as a substitution rate to calibrate our tree. This corresponded to a rate distribution of 0.483–1.31% Myr^{-1}, which has encompasses the mtDNA rate estimated for several different reptile groups, including skinks (Zamudio and Greene, 1997; Rabosky et al., 2007; Linkem et al., 2013). For the nuclear genes, the clock means were assigned a uniform distribution from 0–50, and the standard deviations were assigned exponential distributions with a mean of 0.05. The dataset was partitioned by gene for the nuclear data, and by codon for the mitochondrial data. We utilized a piecewise linear and constant root population size model in our analysis. The species population-mean hyperprior and the species Yule process birth prior were both assigned exponential distributions, with means of 0.01 and 1.0 respectively. We ran the analysis for 400 million generations, sampling every 32,000 generations. Convergence was assessed using Tracer and AWTY as discussed above. Sequence alignments and phylogenetic trees generated for this research were deposited in TreeBASE (Accession #).

Biogeographic Analyses

In order to examine biogeographic range evolution and test hypothesized colonization routes, we utilized several different methods to infer ancestral states across our species tree topology. We used a dispersal-extinction-cladogenesis (DEC) ML model implemented in the program Lagrange (Ree and Smith, 2008), and we employed the ML and rjMCMC models of character evolution available in BayesTraits (Pagel, 1999; Pagel and Meade, 2006). We reconstructed ancestral states to examine both broad scale biogeography across Southeast Asia, and more finescale patterns within the Philippine Islands. We coded species distributions into four biogeographic subregions: Peninsular India and Sri Lanka, Mainland Southeast Asia (starting from the Assam region of India and including Peninsular Malaysia), Sundaland (exclusive of the Malay Peninsula), and the Philippines. Although these regions share certain faunal elements and some level of connectivity exists among them, we chose to partition and code Southeast Asia up in this way because (1) significant geographic barriers separate each of these four regions, (2) previous biogeographic studies have shown each of these regions to harbor endemic radiations of species (Wallace, 1876; Mani, 1974; Corlett, 2009; Woodruff, 2010; Datta-Roy et al., 2013), (3) these regions separate the distributions of many of the species, and the major clades within *Eutropis*, and (4) many biogeographic range evolution models perform best when a small number of areas are considered in the analysis (Ree and Smith, 2008). For analyses of the endemic Philippine radiation, we divided the islands into four regions based on geography and the Pleistocene Aggregate Island Complex (PAIC) model (Inger, 1954; Heaney, 1985; Brown and Diesmos, 2009): 1) the Luzon PAIC + Mindoro, Lubang, and Semirara, 2) the Mindanao PAIC, 3) the Visayan PAIC, and 4) Palawan and Borneo.

For the Lagrange analyses we configured our analyses using the Lagrange configurator (beta) web tool (http://www.reelab.net/lagrange), estimating the baseline rates of dispersal and local extinction, and including no range or dispersal constraints. For the BayesTraits analyses of the entire genus, we estimated two free dispersal parameters: one for between India and the Philippines, since these were the only two geographic regions that were not directly adjacent to each other and thus direct dispersal between the two regions is not possible, and one for the remaining areas. For the BayesTraits analyses of the Philippine lineages, we estimated six free dispersal parameters, representing dispersal rates between each of the four geographic regions. The rjMCMC analyses were run for 1 x 10^8 generations, sampling every 25,000 generations, and discarding samples from the first 5.0 x 10^7 generations as burn-in. Stationarity of all model parameters was confirmed using Tracer.

Genetic structure in widely distributed species

We also sought to preliminarily characterize genetic diversity across the ranges of the biogeographically widespread *Eutropis* species. To do this, we sequenced a larger sampling of individuals for *E. longicaudata, E. macularia, E. multifasciata, E. rudis*, and *E. rugifera* from a diverse range of sampling localities for the ND2 gene. We then used this data to calculate several population genetics summary statistics using DnaSP v5.10.1 (Librado and Rozas, 2009) for each species.

Results

Our final dataset used for the phylogenetic analyses consisted of 1,016 base pairs (bp) of mitochondrial data (ND2) and 8,094 bp of nuclear data from nine different nuclear genes: ATPSB (1,293 bp), FOXP2 (671 bp), LDHA (589 bp), MC1R (661 bp), NAT15 (779 bp), NOS1 (1,685 bp), R35 (664 bp), RP40 (380 bp), and SELT (1372 bp) for 94 individuals. Our data matrix was mostly complete, containing only 5.4% missing data (see Appendix 7 for details). Topologies among individual gene trees were mostly congruent, though topologies varied for some poorly supported nodes deeper in the phylogeny (see Appendix 8).

Topologies of phylogenetic trees obtained from different analytical methods also were generally congruent. The concatenated phylogenetic analyses identified two cases in which populations of several species were strongly supported as non-monophyletic (*E. grandis* and *E. macropthalma*, as well as populations of *E. macularia* from India and mainland Southeast Asia; Fig. 2.1). Thus, in order to deal with the problematic taxonomy, we designated species identities for these individuals in the coalescent-based species tree analysis based on their appropriate genetic clade identified in the concatenated analyses. Our species-time tree analysis (Fig. 2.2) reveals that the earliest diverging clades consist of species with geographic ranges across mainland Southeast Asia. We also recover a clade consisting primarily of taxa endemic to India, another Sundaic clade consisting of *E. rugifera, E. multifasciata, E. grandis/macropthalma*, and *E. rudis*, and a third group of Philippines (+ Palau) species (Fig. 2.2). Our species tree analysis using *BEAST likely represents our best estimate of phylogenetic relationships within *Eutropis* because (1) we noted evidence of gene tree heterogeneity among loci, and (2) previous studies have shown that coalescent analyses are more appropriate and perform better than concatenation in many situations when analyzing multilocus datasets (Kubatko and Degnan, 2007; Liu and Pearl, 2007).

We utilized the maximum clade credibility tree from our *BEAST analysis to estimate ancestral states in the biogeographic analyses. Each of the biogeographic range evolution methods produced similar results for both the full phylogeny and the Philippine focused analyses (see Appendix 9). We focus primarily on the results from the Lagrange analyses since the DEC model can allow for widespread biogeographic ranges encompassing more than one area, and for lineage divergence within a species to occur either between a single area and the remainder of its range, or within an area (Ree and Smith, 2008). Because of this, we feel this model more accurately characterizes biogeographic range evolution in this group (Fig. 2.3).

Our characterization of genetic diversity within the widespread *Eutropis* species identified several different patterns, with some species exhibiting high genetic divergence among some sampling localities (potentially indicative of unrecognized species diversity), as well as some species showing low genetic differentiation across large geographic distances. Results of these analyses are summarized in Table 2.1.

Discussion

Biogeography and divergence times

Because skinks of the genus *Eutropis* are common and ubiquitous across their broad distribution, they represent a compelling system for obtaining insights into and testing classic hypotheses relating to Southeast Asian biogeography. However, their highly conserved morphology (Miralles et al., 2005; Barley et al., 2013) and distributions spanning many political boundaries has prevented a comprehensive range-wide understanding of species limits, diversification, and historical biogeography. This paucity of information includes shortcomings in our basic understanding of the group's phylogenetic relationships, species diversity, and species distributional data. By combing dense geographic, genetic, and taxonomic sampling, our study provides a robust examination of biogeographic patterns and sheds light on the origin and timing of diversification of *Eutropis* across some of tropical Asia's most celebrated biogeographic boundaries.

It appears that the initial lineages that gave rise to *Eutropis* began diversifying in mainland Southeast Asia 35–55 million years ago (mya; Fig. 2.2). Subsequently, the group's geographical distribution diffused outward, with three distinct lineages invading Sundaland, Peninsular India, and the Philippines (Fig. 2.3). This geographical spread of lineages, followed by a subsequent period of diversification gave rise to endemic species in each biogeographic region, and diversification appears to have been most extensive in India and the island archipelago of the Philippines (Fig. 2.4).

Interestingly, the complex biogeographic patterns exhibited by sun skinks reveal that there has likely been extensive back dispersal events out of, and multiple invasions into, each of the different biogeographic subregions by various species. Our results suggest a dispersal event from mainland Southeast Asia into India occurred relatively early as this group diversified (~28–42 mya), conceivably around the time India was colliding with mainland Asia (Atchison et al., 2007). Subsequently two independent back dispersals into mainland Southeast Asia from India occurred (Datta-Roy et al., 2012), the first of which involved the lineage that gave rise to *E.*

quadricarinata (Fig. 2.3). It also appears that the ancestor of the *E. macularia* species complex initially was distributed in India, and subsequently dispersed back into mainland Southeast Asia. The most likely route of these faunal exchanges would have been through the Assam region of northeastern India (Mani, 1974; Myers et al., 2000). Dispersal of *Eutropis* into Sundaland appears to have occurred slightly later, and this region appears to contain the lowest *Eutropis* species diversity within the range of the genus (Fig. 2.4). *Eutropis multifasciata* is the only species distributed across all four biogeographic subregions.

Our analyses show that the Philippines has been invaded multiple times (with at least two, but as many as four independent colonizations), but only one of these invasions has lead to significant *in situ* diversification (Fig. 2.3; Barley et al., 2013). Unfortunately, it remains difficult to determine the routes of colonization into the archipelago (Brown et al., 2013). Several species from the Sundaland group have relatively recently colonized the southwestern portion of the archipelago, with *E. rugifera* only being known from the Zamboanga Peninsula, and *E. rudis* from the Sulu Archipelago (Brown and Alcala, 1980). These species presumably were able to disperse into the southern Philippines either from Sulawesi, or from Borneo. Interestingly, it appears *E. rugifera* may have entered the archipelago around the same time the ancestor of the endemic Philippine radiation entered the archipelago, although unlike the latter (Barley et al., 2013) it did not colonize or diversify extensively. *Eutropis multifasciata* also has successfully colonized the entire archipelago, however this species has failed to diversify extensively (as in the rest of its biogeographic distribution) likely due to its impressive dispersal ability and resulting extensive gene flow among populations.

Interestingly, the Philippine radiation is not closely related to any species that currently occur in Sundaland, but rather is sister to a clade consisting of species distributed across India and mainland Southeast Asia (Fig. 2.2). The Philippine radiation is composed of two species complexes: the *E. multicarinata* species complex and the *E. indeprensa* species complex (Brown and Alcala, 1980; Barley et al., 2013), with the split between these two groups occurring during the Miocene, somewhere between 7–11 mya. Ancestral state reconstructions indicate the ancestor of the *E. indeprensa* species complex may have exhibited a broad distribution across the archipelago (Fig. 2.3). In contrast, our results show that the ancestor of the *E. multicarinata* species complex was likely distributed on islands that later formed the Mindanao PAIC, which at the time were located farther south than their present day position (with the exception of the Zamboanga Peninsula; Yumul et al., 2004, 2009). Subsequently lineages in this species complex dispersed northward and diversified, colonizing the Luzon PAIC somewhere between 6–9 mya. A long distance dispersal event into the Palau Archipelago also appears to have occurred from Mindanao. The species in the complex ultimately dispersed from Luzon into the West Visayan Islands (central Philippines), completing a counterclockwise colonization pattern of the archipelago. Our biogeographic range analyses also infer two recent back dispersal events out of the Philippines into Borneo, one by a species in the *E. multicarinata* complex, which likely dispersed from the Luzon PAIC, across Palawan, and into Borneo (Fig. 2.3). A divergent lineage that is most closely related to *E. indeprensa* (from Mindoro) also occurs on Borneo.

Phylogeographic patterns in "widespread species"

Although there are many examples of range restricted *Eutropis* species (Smith, 1935; Brown and Alcala, 1980; Bobrov, 1992; Barley et al., 2013), several species are curiously considered widespread across multiple biogeographic regions. The most widespread of these species is the large-bodied cosmopolitan *E. multifasciata*, with a distribution encompassing an area equivalent to that of the entire genus, from India throughout mainland Asia, and into the Indonesian, Malaysian, and Philippine archipelagos (Brown and Alcala, 1980; Das, 2004; Grismer, 2011). Remarkably, this species also exhibits the least geographically based genetic differentiation across its range when compared to other widespread species. Although we included samples from India, Myanmar, Indonesia, and the Philippines, we note little sequence divergence between individuals from adjacent geographic regions, and a maximum of ~8.0% uncorrected pairwise mtDNA sequence divergence across the entire range (Table 2.1). Among squamates, *E. multifasciata* is truly an exceptionally widespread species, now distributed on a scale realized by few other Southeast Asian vertebrate taxa; this suggests a capacity for long distance dispersal across ecologically diverse biogeographic regions.

Eutropis rugifera is distributed throughout the Sundaic Region of Southeast Asia, throughout Malaysia and Indonesia, and the Andanaman and Nicobar Islands. Here we identify an additional population from the Zamboanga Peninsula of southwestern Mindanao Island, from the extreme southern Philippines. Previously, the easternmost populations of this species were known from Borneo and Sulawesi (Das, 2004). Our phylogenetic analysis included specimens of *E. rugifera* from the Philippines, Sulawesi, Peninsular Malaysia, and Sarawak all of which are monophyletic. However, the newly discovered Philippine population is highly divergent from the other populations (~17–18% "p" distance for ND2). We also sampled populations of *E. longicaudata* (a species that is widespread across mainland Southeast Asia) from Myanmar, Laos, Thailand, and Peninsular Malaysia (Table 2.1). The populations from Laos and Thailand exhibited limited genetic divergence, while the remaining populations exhibited some geographic structure across the landscape (with "p" distance values for ND2 ranging between 13–18% among individuals).

One of the most taxonomically problematic *Eutropis* species groups has been the *E. macularia* species complex. Historically, a number of subspecies have been proposed, and a number of populations have been described as distinct species (Blythe, 1853; Schmidt, 1926; Inger *et al.*, 1984; *Das et al.*, 2008). We were able to amass the largest molecular dataset to date for this species complex, sampling within and across several geographical regions. We found that the species complex began to diversify sometime between 15–25 mya from an ancestor that was most likely distributed in India, and that there must have been a subsequent dispersal back to mainland Asia (Fig. 2.2, 2.3). Not surprisingly, our results also indicate there may be additional cryptic species diversity within the complex, and several described species render some populations of "*E. macularia*" paraphyletic (Fig. 2.2). Populations of *E. macularia* from mainland Southeast Asia appear to consist of at least to two distinct species, as we found two highly divergent clades (~23% "p" distance for ND2): one clade consisting of populations from Myanmar and Thailand and another consisting of populations from Thailand, Peninsular Malaysia, Cambodia, and Laos (Fig. 2.1, 2.2; Table 2.1). This result, suggesting multiple species may masquerade within *E. macularia* is consistent with a previous study that found variation in chromosome number in populations of *E. macularia* from Thailand (Ota et al., 2001).

Two of the most recently described *Eutropis* species are *E. macropthalma* (Mausfeld and Böhme, 2002) and *E. grandis* (Howard et al., 2007). Although both taxa were described as endemic to a single island (*E. macropthalma* from Java, and *E. grandis* from Sulawesi), our phylogenetic analyses of the genetic data for both species indicate they likely represent the same species, because they exhibit virtually no genetic divergence between these biogeographically distinct islands. There is no mention of populations on Sulawesi in Mausfeld and Böhme (2002) and no comparison of the two species in Howard et al. (2007). Thus, it appears this species may be more widely distributed across the Sundaic region than was originally thought; reconsideration of the taxonomic validity of the latter name (*E. grandis*) may be advisable in the near future.

Classic Southeast Asian biogeography and sun skink patterns

Tropical Asia has been the geographic setting for formulation of many seminal hypotheses in the field of biogeography (Wallace, 1860; Van Steenis, 1950; Huxley, 1868; Inger, 1954; Diamond and Gilpin, 1983; Briggs, 1989). Thus, consideration of how the biogeographic patterns observed in *Eutropis* fit within a more general context is warranted. Lydekker's line (Lydekker, 1903, 1915), which demarcates the easternmost zone of mixing between the Oriental and Australian faunal regions also represents the eastern edge of the distribution of the genus. Additionally, the Assam region of northeastern India (Fig. 2.4) appears to represent an important region of species turnover within *Eutropis*, as it separates the Indian radiation from the Southeast Asian species, although the region has potentially served as a corridor for dispersal in several cases as discussed above. It also marks the distributional edge for seven *Eutropis* species (*E. novemcarinata, E. longicaudata, E. macularia, E. bibronii, E. carinata, E. trivittata*, and *E. quadricarinata*), with *E. multifasciata* being the only species whose distribution actually spans both subcontinents.

In contrast, Wallace's line (Wallace, 1860) and Huxley's corresponding modification (Huxley, 1868) appear to have had little significance with regard to *Eutropis* diversification and no taxa exhibit ranges that abut or are bounded by this barrier. Wallace and Huxley's lines have each been crossed at least once by the Sundaland clade and the endemic Philippine radiation respectively (Fig. 2.3). The Sundaland clade consists of four taxa that have present day distributions spanning the original position of Wallace's line, and five *Eutropis* species have geographic ranges spanning Huxley's extension of Wallace's line into the Philippines (Fig. 2.3; *E. rudis, E. rugifera, E. multifasciata, E. indeprensa*, and Clade G in the Philippines). On mainland Southeast Asia, three *Eutropis* species exhibit distributions spanning the Isthmus of Kra (*E. longicaudata, E. macularia*, and *E. multifasciata*), while only one species shows a distributional break there (with *E. rugifera* only known to occur south of that point; Grismer, 2011). Lastly, within the Philippines, five taxa have distributions restricted to a single Pleistocene Aggregate Island Complex (Inger, 1954; Heaney, 1985; Brown and Diesmos, 2009), whereas seven species are distributed across multiple PAIC's (Fig 2.3). Back dispersals out of the Philippines to Borneo (Fig. 2.3) also appear to support Palawan as an important route facilitating faunal exchange (Diamond and Gilpin, 1983).

Conclusions

Our analyses provide a framework for understanding the evolutionary history in this widespread evolutionary radiation. Our divergence time analyses indicate that *Eutropis* likely began diversifying during the Eocene, and our estimates for the timing of diversification of various lineages agree well with the geological record. Results from our species tree analyses and ancestral state reconstructions indicate that diversification in *Eutropis* primarily occurred in three separate lineages that initially dispersed outward from mainland Southeast Asia into India, Sundaland, and the Philippines. Lastly, our broad geographic sampling of several widespread species provide insight into the historical processes that may have resulted in their pronounced genetic variation and indicate that future taxonomic and phylogeographic studies of these taxa may reveal additional undescribed species.

Table 1.1 Summary of sampling localities for several widespread species of *Eutropis* included in study, as well as numbers of polymorphic sites (P_N), nucleotide diversity (π), and ranges of pairwise sequence divergence (S) for ND2 data. *n* = number of individuals included, D = largest geographic distance (km) between populations sampled. *E. macularia* refers to Clades 1 & 2 (Fig. 2.1). See Appendix 6 for full details of sampling.

Species	*n*	Sampling Localities	P_N	π	S	D
E. longicaudata	6	Laos, Malaysia, Myanmar, Thailand, Vietnam	217	0.1136 ± 0.0169	0.4–16.0	2400
E. macularia	10	Cambodia, Laos, Malaysia, Myanmar, Thailand	282	0.1314 ± 0.0117	0.6–20.0	2080
E. multifasciata	23	India, Myanmar, Philippines, Sulawesi, Thailand	131	0.0438 ± 0.0049	0.0–7.7	3300
E. rudis	8	Sabah, Sarawak, Sulawesi	93	0.0379 ± 0.0055	0.3–5.9	1000
E. rugifera	7	Malaysia, Philippines, Sarawak, Sulawesi	203	0.1071 ± 0.0143	0.0–15.7	2105

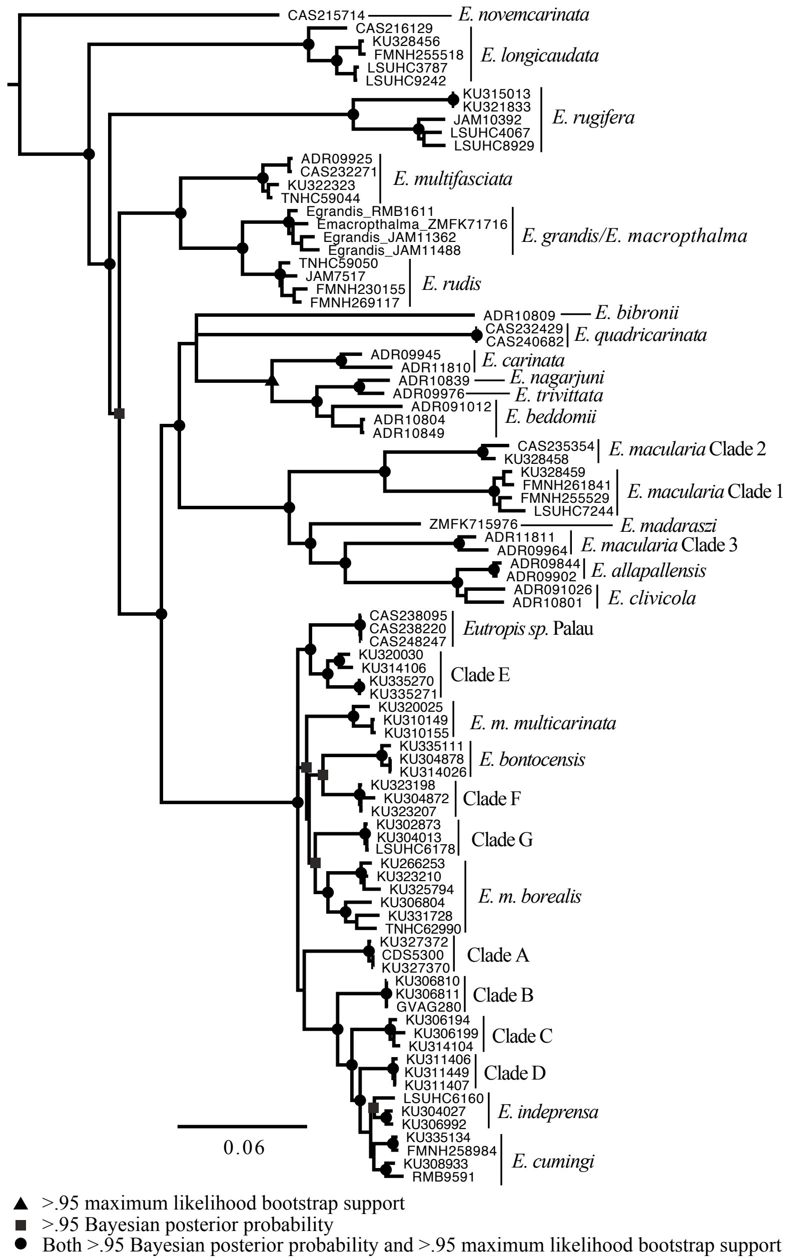

Figure 2.1. Majority-rule consensus tree from concatenated, Bayesian phylogenetic analysis of all genetic data. Specimen numbers are shown adjacent to species identities (see Appendix 6 for specimen information). *Eutropis macularia* Clades 1 and 2 consist of individuals from populations in mainland Southeast Asia, whereas Clade 3 represents populations from Peninsular India.

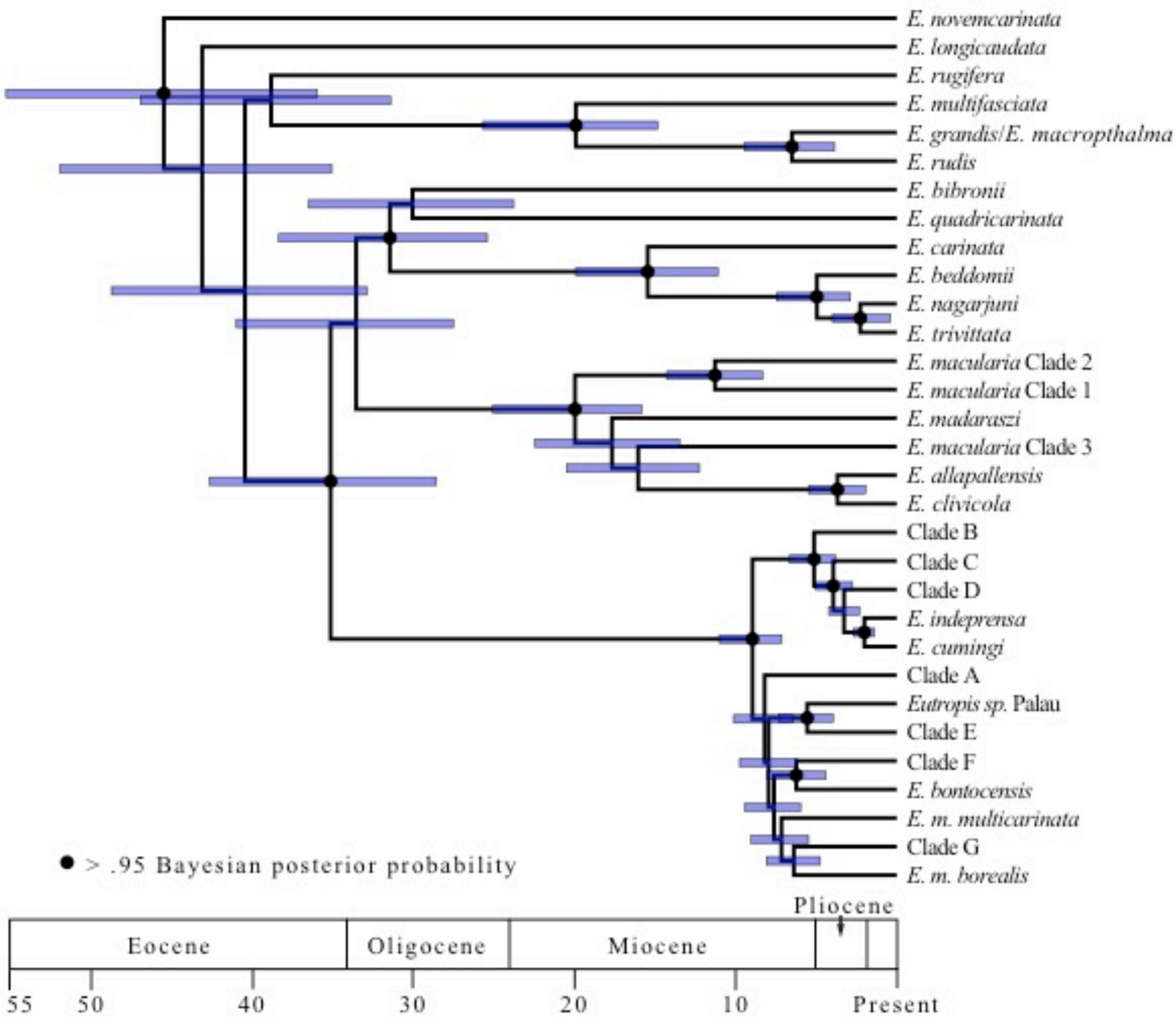

Figure 2.2. Maximum clade credibility tree from species tree/divergence time phylogenetic analysis of all genetic data. Confidence intervals show 95% highest posterior density for divergence times based on mtDNA substitution rate.

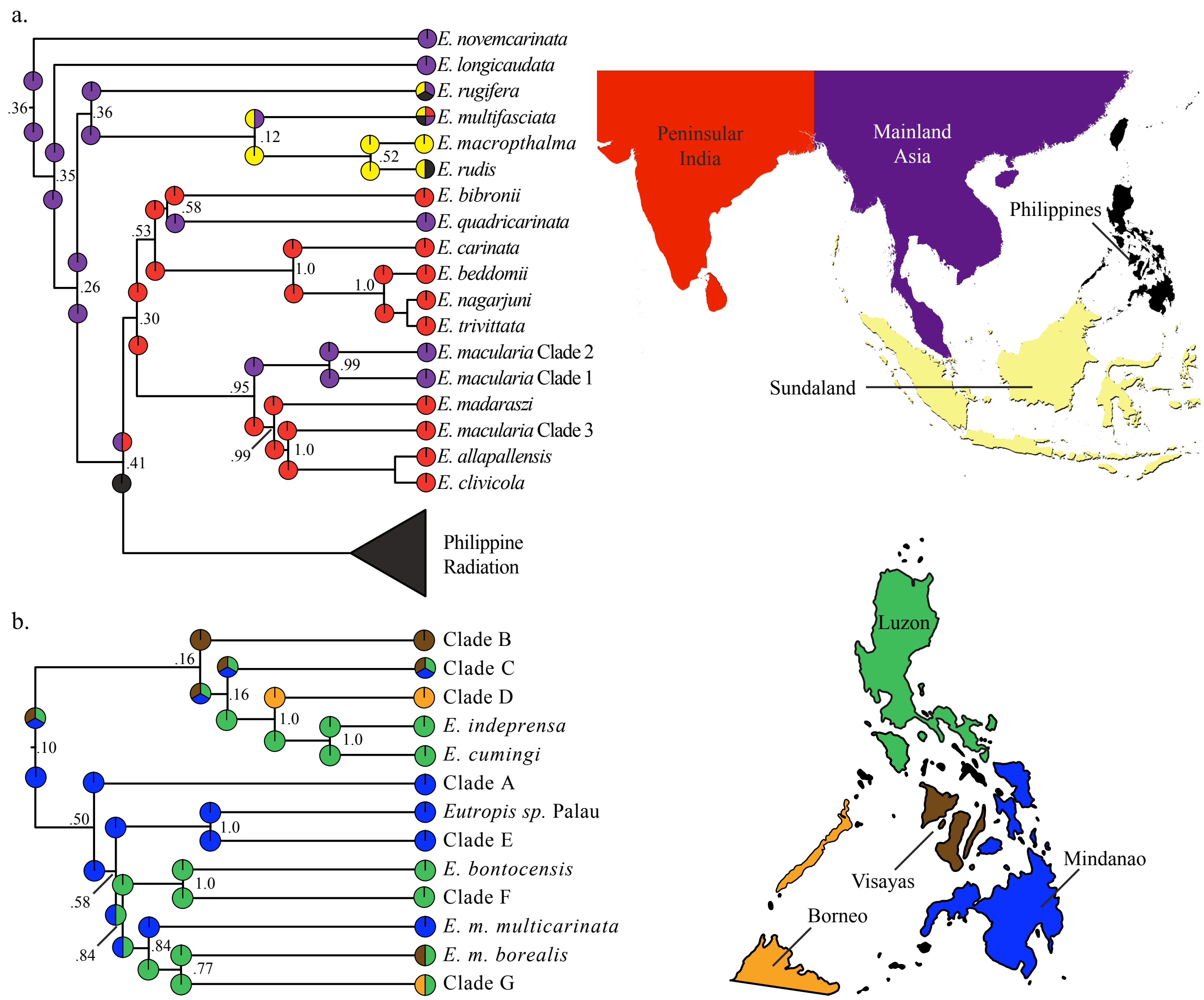

Figure 2.3. Results of biogeographic character-state reconstructions using the DEC model in Lagrange for a) the full phylogeny and b) the Philippine radiation. The biogeographic regions are coded on the associate maps. The maximum clade credibility trees from the species tree analyses were used in the Lagrange analyses (shown). The most probable range inheritance scenarios are shown for each node along with their probabilities.

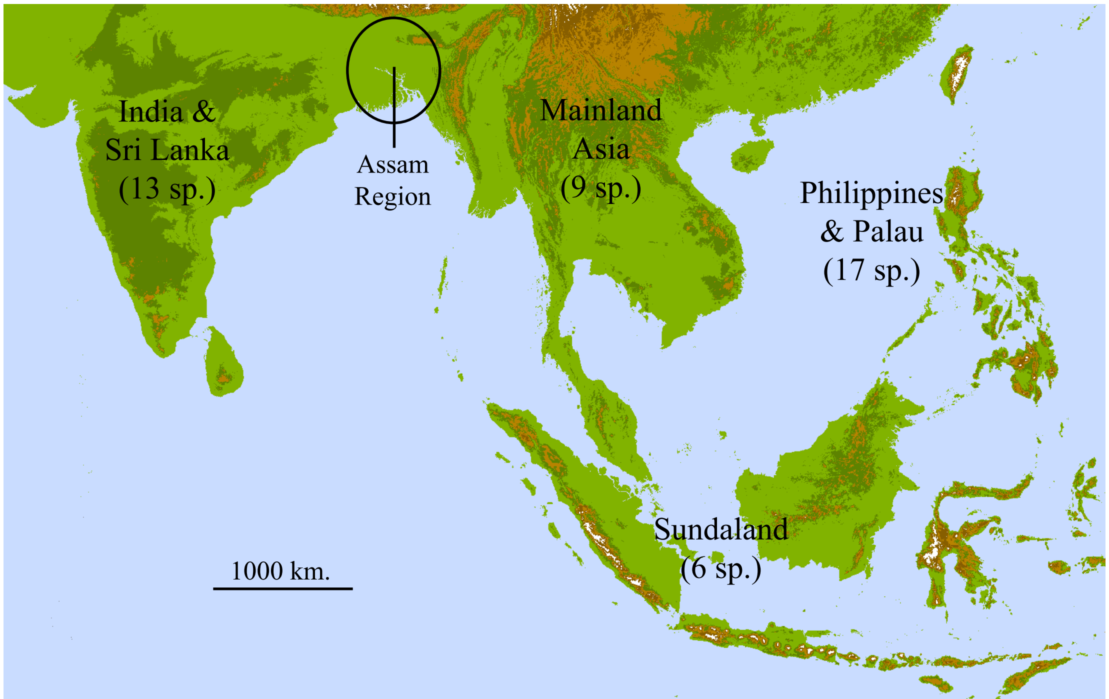

Figure 2.4. Map of tropical Asia showing the estimated number of species present in each of the four biogeographic regions discussed in the study. Species diversity estimates are based on current taxonomy, this study, and Barley et al., 2013.

Chapter 3

Landscape genomics across Southeast Asia: the evolution of genetic and morphological diversity in the common sun skink

Abstract

Incorporating genomic datasets into analyses employing landscape genetic approaches allows for powerful investigations of how population genetic and morphological diversity evolve across a landscape. Here we utilize an integrative approach to examine gene flow, and genetic and morphological population differentiation across Southeast Asia in the common sun skink, *Eutropis multifasciata*. We quantify the relative effects of geographic and ecological isolation in this system, finding evidence for more substantial genetic differentiation between populations distributed in the Philippine island archipelago than those on mainland Southeast Asia. We also identify how different methods of investigating morphological differentiation in natural populations could lead to different conclusions regarding the evolution of quantitative morphological traits. Ultimately, we discuss how studies of contemporary microevolutionary processes can potentially provide insights into the evolution of biodiversity patterns.

Introduction

Recent advances in genome sequencing technology as well as statistical methodologies has begun to unite the fields of population genomics and landscape genetics, which can provide revolutionary insights into the generation and maintenance of biodiversity (Storfer et al., 2010; Davey and Blaxter, 2011; Ekblom and Galindo, 2011; Glenn, 2011; Manel and Holderegger, 2013). Further, developments in genomic library preparation methods have enabled scientists to utilize these recent advances in studies of non-model organisms, providing a diversity of in-depth insights into population-level evolutionary processes (Davey et al., 2011; Petren, 2013; Shaffer and Purugganan, 2013). As the number of studies utilizing these methods grows, so too will our understanding of how genetic and morphological diversity evolve in evolutionary radiations.

Population genomic methods have broad utility across many fields including evolutionary genetics, speciation, conservation, and phenotypic evolution (Luikart et al., 2003; Michel, 2010; Ellegren, 2014). Recent studies have employed them to make powerful inferences regarding population demography, genome evolution, and neutral and adaptive molecular evolution in a variety of systems (Turner et al., 2005; Egan et al., 2008; Gompert et al., 2008; Hohenlohe, 2010; Yi et al., 2010). Applying population genomics to the field of landscape genetics (Manel et al., 2003; Storfer et al., 2010) will likely improve inferences regarding the impacts of distance, geographic features, and/or environmental variables on gene flow and population differentiation in natural populations. Variation in the relative importance of these factors in groups across the tree of life likely drive differences in population genetic structuring in individual species, and speciation patterns in evolutionary radiations (Petren et al., 2005; Sexton et al., 2014). By examining these differences in light of morphological differentiation, researchers can gain an understanding of the speciation process, and the evolution of biodiversity in different types of empirical systems.

Inferences about landscape and evolutionary genetics have historically been limited by dataset size and availability of analytical methods to model evolutionary processes (Luikart et al., 2003; Storfer et al., 2010; Guillot and Rousset, 2013). Now that genome scale datasets can be collected with relative ease and efficiency, limitation are more based on the power of computational and methodological approaches to analyze these large datasets. However, the recent development of a diverse array of analytical approaches now offer the exciting opportunity to apply these methods towards obtaining general insights into population genetics and landscape ecology (McRae and Beier, 2007; Barrett and Hoekstra; 2011; Bradburd et al., 2013; Wang, 2013; Wang et al., 2013).

Southeast Asia represents an ideal place for studies of landscape genetics given the complex geographic setting that exists there, and the dynamic environmental and geologic processes that have altered patterns of population connectivity through time (Heaney, 1991; Cannon et al., 2009; Yumul et al., 2009; Woodruff, 2010). These factors have likely contributed to the evolution of some of the highest concentrations of land vertebrate biodiversity in the world (Myers et al., 2000). Southeast Asia also offers the opportunity to examine how these processes contribute differentially to population dynamics of species in continental systems, and island archipelagos, which have formed the backdrop for many classic studies of population differentiation and speciation (Mayr, 1942; Williams, 1972; Carson and Kaneshiro, 1976). Though previous studies have investigated the historical processes that have shaped biodiversity in the region (Hall and Holloway, 1998; Lohman et al., 2011; Brown et al., 2013), few have focused on more contemporary time-scales and examined how fine-scale population differentiation contributes to patterns of morphological and genetic diversity. Studies at this scale are essential to revealing the initial evolutionary processes that contribute to the exceptional diversification of many vertebrate groups in Southeast Asia. In other words, we can begin to understand how microevolutionary processes acting at the population level ultimately result in broad-scale macroevolutionary biodiversity patterns.

Consisting of more than 1400 described taxa, skinks represent one of the most species-rich vertebrate groups worldwide (Pianka and Vitt, 2006). They are a particularly prominent component of squamate diversity in Southeast Asia, where limited gene flow between populations in island archipelagos likely promote high genetic differentiation and ultimately species diversity (Ciofi and Bruford, 1999; Reiff et al., 2007; Linkem et al., 2010; Siler et al., 2011). Although many groups of skinks exhibit diverse morphological and life history adaptations, other groups exhibit extensive conservation in external morphology across evolutionary timescales (Austin, 1995; Bruna et al., 1996; Barley et al., 2013; Rabosky et al., 2014). Within the skink genus *Eutropis*, many species also appear to occupy similar, generalist ecological niches, in addition to their highly conserved morphology (Brown and Alcala, 1980; Barley et al., 2013). Similarity in morphology and ecology are often correlated as a result of species filling similar ecological niches (Cody, 1969; Pianka, 1973; Losos, 1990), and this may explain why morphological and genetic differentiation are decoupled in these species groups.

In this study, we integrate recently developed population genomic and landscape genetic methodological approaches with genomic data to assess their functionality in elucidating fine-scale landscape genetic processes. We use the common sun skink, *Eutropis multifasciata*, to understand how gene flow connects natural populations across Southeast Asia. Our analyses focus on disentangling the relative effects of geographic distance, environmental heterogeneity, and geographic features on population genetic isolation in this system. Finally, we look for evidence of selection shaping morphological diversity patterns among populations and highlight sources of confusion and possible error with current methodologies. In doing this, we use this system as a model for understanding the evolution of genetic diversity in natural populations across Southeast Asia, and patterns of variation in external morphology in scincid lizards.

Materials and Methods

Genomic library preparation

Individuals were sampled from populations across Southeast Asia, with sampling being focused in two regions: mainland Southeast Asia and the Philippine Islands (Fig. 3.1). Genomic DNA was extracted from soft tissue using a Qiagen DNeasy Blood & Tissue Kit, quantified using a Qubit 2.0 Flourometer, and diluted to a concentration of 5 ng/µL. We utilized a Multiplexed Shotgun genotyping protocol, a modified form of RAD-seq (Andolfatto et al., 2011), to generate two genomic libraries, each with 96 individuals (192 in total; Fig. 3.1; Appendix 10). In both cases, DNA was digested with the NdeI restriction enzyme (New England BioLabs, Ipswich, MA), and unique barcoded adapters were ligated onto each of the 96 individuals in each library. Next, libraries were 'size-selected' to retain only digested/ligated fragments of a specific size. This served two purposes: it increases the likelihood of resequencing homologous sequences across samples, as well as aids with the sequencing process. For the first library, fragments were size selected manually using gel electrophoresis and excising a gel fragment ~450–550 base pairs (bp) according to adjacent run ladders. DNA was extracted from the gel fragment using a QIAquick Gel Extraction Kit. For the second library, fragments of size 475–525 bp were selected using a Pippin Prep (Sage Science, Beverly, MA). We amplified the libraries by PCR using Phusion High-Fidelity PCR Master Mix in order to obtain sequenceable quantities for each library. Libraries were then sequenced on separate lanes of an Illumina HiSeq 2500 sequencer using a single-end 100 bp read protocol. A step-by-step outline of the wetlab protocol is available in Appendix 11.

Morphological Data

We collected morphological data for six quantitative morphological traits: snout–vent length, axilla–groin distance, hind limb length, third finger length, head length, and head width. In total, we collected data for 93 individuals from 14 populations, most of which were the same individuals included in the genetic analyses, however, we excluded juveniles and included additional individuals for some populations when available in order to increase sample sizes (Appendix 10). These traits were chosen because they generally characterize body shape, and represent different axes of morphology on which many different groups of skinks have diversified (Wiens et al., 2006; Brandley et al., 2008; Siler and Brown, 2011; Rabosky et al., 2014).

Read parsing and assembly

Genomic data was initially visualized, and summaries of sequence quality were examined using FastQC (Andrews, 2012). All data was *de novo* assembled using the Stacks pipeline (Catchen et al., 2011), since a reference genome of a closely related species was not available. A substantial portion of the reads for one of the genomic libraries significantly decreased in quality towards the end. Data were initially demultiplexed and quality filtered using the process_radtags module, removing any reads with an uncalled base and discarding reads with low quality scores. This approach resulted in a high proportion of the reads from one library being discarded entirely, which substantially increased the amount of missing data. Because the Stacks pipeline requires all read lengths to be the same, we ultimately adopted an alternative quality filtering strategy where we first truncated all reads to 75 bp, and then quality filtered the data using process_radtags. Although this resulted in shorter read lengths, a smaller proportion of the total reads were thrown out due to low quality scores. Additionally, in subsequent analyses we only utilized data from one single nucleotide polymorphism (SNP) per locus anyway, to avoid using obviously linked SNPs. Reads were aligned, loci were assembled, and per-individual SNPs were detected in a maximum likelihood framework (Hohenlohe et al., 2010) using ustacks. A catalog of consensus loci for all individuals used in the study was created using cstacks, allowing for two mismatches between sample tags. The stacks of loci from ustacks were then searched against the catalog using sstacks to determine which individuals contain which alleles. SNP data was exported from the pipeline using the populations module.

Population Genomic Analyses and F_{ST} Outliers

General population genomic summary statistics (expected/observed heterozygosity, π, F_{IS}) and average pairwise F_{ST} were calculated using the populations module in Stacks (Hohenlohe et al., 2010). Because the number and density of individuals sampled across the geographic scope of the project varied, we utilized the program Structure (Pritchard et al., 2000) to identify the major population structure present in our dataset. Structure is a model-based clustering method that assigns individuals to an *a priori* determined number of populations in such a way to achieve Hardy-Weinberg equilibrium and linkage equilibrium within those groups. Final Structure analyses were run using the admixture model and a burn-in length of 100,000, followed by 100,000 MCMC reps. Estimates of migration rates among populations were obtained using BayesAss v1.3 (Wilson and Rannala, 2003). These analyses were run for 100 million generations, discarding the first 25 million generations as burn-in, and sampling every

5,000 generations. Convergence was assessed using Tracer, assuring that all parameters had reached stationarity and sufficient (>200) effective sample sizes; as well as by performing multiple analyses and assuring that the posterior mean parameter estimates were similar across runs.

We took an outlier approach to identify candidate loci under natural selection with the program BayeScan (Foll and Gaggiotti, 2008), which uses differences in allele frequencies among populations to assess if a model including selection fits the data significantly better than a neutral model. We ran several analyses, varying the prior odds for the neutral model from 10 to 1000 to assess how this impacted the number of loci identified as being under selection.

Landscape Genomics

We tested for the presence of isolation by distance in our dataset using matrices of genetic distance (calculated as average pairwise F_{ST}) and geographic distance (calculated as pairwise geographic great-circle distance) between populations. The Isolation By Distance Web Service v3.23 (IBDWS; Jensen et al., 2005) was employed to perform reduced major axis regression and Mantel tests using the matrices with 1000 randomizations. Geographic great-circle distances between populations were calculated using the 'fields' package in R version 3.0.1 (The R Foundation for Statistical Computing; http://www.R-project.org).

We examined the relative effects of specific geographic features and environmental variables in promoting genetic differentiation using BEDASSLE (Bradburd et al., 2013). Traditionally, these types of associations have been identified in landscape genetic studies using partial Mantel tests (Manel et al., 2003; Storfer et al., 2010). However, Mantel tests have been shown to perform poorly in many types of landscape genetic analyses (Legendre and Fortin, 2010; Guillot and Rousset, 2013). BEDASSLE is a geostatistical method that models allele frequencies as spatial Gaussian processes. It can be used to assess the relative contribution of any number of geographic or environmental variables to genetic differentiation compared to geographic distance. We examined the effect of two variables on genetic differentiation in our analyses: ocean channels and ecology.

Ecological niche models were generated based on occurrence data from 148 georeferenced museum specimens of *E. multifasciata* using Maxent (Phillips et al., 2006) and eight: bioclimatic variables (Hijmans et al., 2005) available from the WorldClim Database (www.worldclim.org): annual mean temperature, mean diurnal range, maximum temperature of the warmest month, minimum temperature of the coldest month, annual precipitation, precipitation of the wettest and driest months, and elevation. Ecological resistance distances between populations were calculated by using the ecological suitability profile generated by Maxent as the input conductance habitat raster in CircuitScape (McRae, 2006; McRae and Beier, 2007). CircuitScape uses circuit theory and models landscapes as a series of electrical resistors in order to calculate resistance distances between populations. This allows for an average resistance distance to be calculated between pairwise population comparisons by considering all possible pathways across a landscape simultaneously, rather than strictly a least cost path. We took this approach to examining ecological differentiation for two reasons. First, by scaling down the dimensionality of environmental space into a single variable (ecological habitat suitability), assessing a correlation between ecological and genetic differentiation becomes more manageable than trying to do it for multiple possibly correlated variables separately. Secondly, it allowed us to avoid making *a priori* assumptions about the relative costs of dispersal through different environments.

BEDASSLE analyses were run using a great circle geographic distance matrix, an ecological distance matrix, an ocean channel matrix, and raw allelic count data from 4,461 bi-allelic SNPs. The ecological and geographic distance matrices were continuous and standardized by their respective standard deviations, while the ocean channel matrix was binary (on the same landmass or separated by an ocean channel). Because climate fluctuations have altered the historical patterns of connectivity among islands across Southeast Asia, we employed two different ocean matrices in separate analyses. The first reflected contemporary patterns of connectivity among islands, while the second reflected the connectivity that existed during the mid to late Pleistocene when sea levels were ~120 m below current day levels (Voris, 2000; Brown and Diesmos, 2009).

There are two different models that can be employed to assess correlations between variables in BEDASSLE. In the standard model, all populations are assumed to have the same variance of allele frequencies about a global mean. However, this is often not the case when species inhabit a heterogeneous environmental landscape. Thus, a "beta-binomial" model that accounts for overdispersion by modeling the within-population correlations in allelic identity that are due to differences in among-population demographic histories can also be used. We analyzed each dataset using both models, running each analysis was run for 10 million generations, sampling every 1000 generations. Markov chain Monte Carlo marginal traces for each parameter were visually examined to assure convergence on a stationary distribution, and acceptance rates were checked to assure they were sufficient during the course of the run (~20–70%).

BEDASSLE also allows for the use of posterior predictive sampling to assess the model's fit to the empirical dataset, and to highlight features of the data that the model fails to capture. It does this by using draws of parameters from the posterior to simulate new datasets, which can then be used to assess how well the model can predict genetic differentiation based on geographic distance. Average pairwise F_{ST} is used as a summary statistic for the allelic count data in simulated and empirical datasets. We simulated 1000 posterior predictive datasets for the results of each BEDASSLE analysis.

F_{ST}-P_{ST} Comparisons

We also wanted to test whether morphological divergence among populations has been driven by selection. Although it was not possible to conduct common garden experiments to obtain Q_{ST} estimates, P_{ST} is an analogous measure that can be used to compare to F_{ST} in natural populations as it estimates the proportion of among-population variance in quantitative morphological trait values (Spitze, 1993). P_{ST} was calculated as:

$$P_{ST} = \frac{\sigma_{GB}^2}{(\sigma_{GB}^2 + 2\sigma_{GW}^2)}$$

where σ_{GB}^2 and σ_{GW}^2 are the among-population and within-population variance components for a phenotypic trait (Raeymaekers et al., 2007). We calculated P_{ST} for four different traits: third finger length/snout–vent length (TFL), axilla–groin distance/snout–vent length (AGD), hind limb length/snout–vent length (HLL), and head length/head width (HLHW). Individuals were drawn from 14 populations: Aurora Province, Bulacan Province, Cagayan Province, and Bicol Peninsula, Luzon Island, Philippines; Agusan del Sur Province and Zamboanga City Province, Mindanao Island, Philippines; Bohol Island, Mindoro Island, Palawan Island, Panay Island, and

Polillo Island, Philippines; and Ayeyawady State, Rakhine State, and Tanintharyi State, Myanmar.

Previously, several authors have compared pairwise P_{ST} and F_{ST} estimates among populations (e.g. Raeymaekers et al., 2007; Lehtonen, 2009; Wojcieszek and Simmons, 2011), citing non-overlapping confidence intervals (CI's) as significant differences presumably due to selection. In some cases, CI's have been generated by bootstrapping the pairwise F_{ST} and P_{ST} estimates, however, resampling pairwise estimates seemingly violates a major assumption of bootstrapping procedures: the independence of resampled units. This could have profound consequences for estimating CI's.

We propose an alternative method for generating CIs to compare among population F_{ST} and P_{ST} values. Rather than bootstrapping pairwise F_{ST} and P_{ST} estimates, we bootstrapped F_{ST} and P_{ST} estimates for all populations considered together. These global F_{ST}s for each locus were calculated as:

$$F_{ST} = \frac{\sigma_p^2}{\overline{p}(1-\overline{p})}$$

where σ_p^2 is the variance in allele frequencies among populations and $\overline{p}$ is the average allele frequency across populations. 95% confidence intervals for mean global F_{ST} were calculated by bootstrapping a dataset of 4460 SNPs using 10,000 replicates, where the resampled units were individual loci. Allele frequencies were only calculated for a locus in a population if at least 8 alleles were sampled, and only loci where at least 5 populations had allele frequency data were included in the global mean F_{ST} estimates. Confidence intervals for global P_{ST} were calculated by resampling the morphological data both within and among populations with replacement. For each bootstrap replicate, we sampled 14 populations, and individuals within each population were also resampled. This effectively samples from the empirical distributions for both among and within population variances, which are used to calculate P_{ST}.

The variance components were estimated using restricted maximum likelihood (REML) with population as a random variable ('lmer' function from the 'lme4' package in R). From the bootstrap distribution with 10,000 replicates, we estimated the average global P_{ST} as well as the 0.0275 and 0.975 quantiles as an estimate of the 95% CI. For comparison, we calculated bootstrapped means with 95% confidence limits for pairwise F_{ST} and P_{ST} values for each trait in R (Wojcieszek and Simmons, 2011), employing 10,000 replicates. Variance components for each trait and pairwise population comparison were estimated by fitting a linear mixed-effects model to the data as was done for the global P_{ST} estimates. We also tested for correlations between pairwise F_{ST} and P_{ST} for each morphological trait by conducting Mantel tests with 9999 permutations using the program PASSaGE (Rosenberg and Anderson, 2011).

Results

Genomic Datasets

Sequencing of the two genomic libraries resulted in a total of 218,864,422 total sequence reads. The amount of reads recovered per individual was highly variable in some cases. Consequently, two individuals were removed from the study due to insufficient read depth for the Stacks pipeline. When generating output datasets from Stacks using the populations module, we varied several data filtering parameters: -r (the minimum percentage of individuals required in a population), -p (the minimum number of populations a locus must be present in), and -m (the minimum stack depth at a locus). We noticed little effect on our analyses from varying these parameters and we present results from datasets generated requiring a locus be present in all populations, a minimum stack depth of eight (Nevado et al., 2014), and a minimum minor allele frequency of 0.05 before calculating F_{ST}.

Population Genomics and F_{ST} Outliers

Final structure analyses were performed on a dataset of 5,748 SNPs, utilizing a range of values for the number of assumed populations (K). Using K=3 appears to capture the majority of structure in the data, and beyond that likelihood scores begin to plateau (Fig. 3.2). This was also the optimal number of clusters inferred using the ad hoc metric Δ(K) (Evanno et al., 2005) in Structure Harvester (Dent and vonHoldt, 2012). The model was still able to infer population structure up to K=5, however, beyond that it was unable to split up distinct geographic localities in a way that was biologically meaningful. The three major population groups consisted of localities sampled from 1) mainland Asia, 2) the central Philippines, and 3) the northern and southern Philippines and Sulawesi, Indonesia. A K=4 split out the northern Philippines from the southern, and a K=5 splitting out eastern Myanmar from the rest of mainland Asia (Fig. 3.2). The Structure analyses also indicated a substantial amount of admixture among the major population groups. Asymmetrical migration rates among the three major population groups were estimated from datasets of 261, 337, and 338 SNPs using BayesAss (Table 3.1). The population admixture seen in the Structure results was reflected by substantial gene flow among each of the major population groups.

Our analyses showed a large range of variation in average pairwise F_{ST} values among sampling localities between the five population groups identified by Structure, many of which indicate significant genetic isolation (>0.25 average pairwise F_{ST}). Additionally, our analyses showed some average pairwise F_{ST} values between sampling localities within each of the five population groups that were indicative of moderate to high population differentiation (0.05–0.25). Thus, we scaled our sampling down to twenty localities for which we had sampled at least five individuals [as previous studies have shown the sampling of 3–4 individuals may be sufficient to detect specific genetic patterns in most situations (Prunier et al., 2013)], and used them in subsequent analyses, (Fig. 3.1). Average pairwise F_{ST} values among these populations are given in Table 3.2 and general population genetic summary statistics are given in Table 3.3, with each being derived from a dataset of 4,469 SNPs.

Genome-wide F_{ST} outlier analyses were run for the same 4,469 SNP dataset using individuals from the 20 populations discussed above. Using a false discover rate of 0.05 and prior odds on the neutral model of 10, 100, and 1000, we identified 38, 14, and 3 candidate loci under selection, respectively (Fig. 3.3). Interestingly, the majority of these SNPs showed a signature of diversifying selection rather than balance or purifying selection. However, the low proportion of loci under selection indicate the SNP data are potentially a good approximation of neutral divergence among populations.

Landscape Genomics

Mantel tests and reduced major axis regression of log-transformed pairwise geographic and genetic distance matrices showed a substantial signal of isolation by distance in our dataset (Fig. 3.4; $r = 0.44$, $p < 0.001$). In our BEDASSLE analyses using the standard model, the mean posterior $\alpha_E : \alpha_D$ ratio (describing the relative effects of the ecological variable compared to geographic distance) for the contemporary ocean channel matrix was 0.650 and the 95% credible set was 0.549–0.766. For the Pleistocene ocean channel matrix (POCM), the mean posterior $\alpha_E : \alpha_D$ ratio was 1.270, with a 95% credible set of 1.062–1.508. The mean posterior $\alpha_E : \alpha_D$ ratio for the ecological distance matrix using the standard model was 0.277 (0.385 in the POCM analysis), and the 95% credible set was 0.209–0.353 (0.322–0.456 in the POCM analysis).

However, results from posterior predictive sampling indicates that accounting for overdispersion using the beta-binomial model results in a better fit to the data (Fig 3.5); the mean Pearson's product moment correlation between the posterior predictive datasets and the observed dataset using the standard model was 0.64, whereas the mean correlation was 0.81 when the beta-binomial model was used. The mean posterior $\alpha_E : \alpha_D$ ratio for the contemporary ocean channel matrix analyses employing the beta-binomial model was 0.405, with a 95% credible set of 0.338–0.479. The mean posterior $\alpha_E : \alpha_D$ ratio for the POCM analyses was 1.336, with a 95% credible set of 1.080–1.609. The interpretation of these ratios is that being on opposite sides of an ocean channel has the impact of approximately 380–540 km of extra pairwise geographic distance on genetic differentiation (or ~1,200–1,800 km for deep water ocean channels). Thus, not surprisingly, much of the signal appears to be derived from islands separated by deep-water ocean channels, and that oceans that have been connected within the past 20,000 years show a much smaller signature of genetic isolation. The $\alpha_E : \alpha_D$ ratios from the beta-binomial model also indicate that ecological isolation has contributed little to genetic differentiation among populations, with a mean posterior of 0.117 for the ecological distance matrix in the contemporary analyses (0.109 for the POCM) and the 95% credible set being 0.093–0.143 (0.077–0.142 for the POCM). This is consistent with the results of a partial Mantel test showing no correlation between genetic and ecological distance when geographic distance is controlled for ($r = 0.04$; $p = 0.76$).

F_{ST}-P_{ST} Comparisons

Mantel tests showed no significant correlation between average pairwise F_{ST} and pairwise P_{ST} for any of the morphological variables (Fig. 3.6; all r values < 0.19; all p-values > 0.16), suggesting insufficient evidence that morphological differentiation follows the same neutral pattern of the genome. The only morphological variables that showed a significant correlation between pairwise P_{ST} values were HLL and TFL ($r = 0.46$; $p = 0.001$). Pairwise P_{ST} values were generally lower than average pairwise F_{ST} (Fig 3.6; Table 3.4), suggesting that stabilizing selection may be acting to maintain morphological trait values among genetically isolated populations. Accordingly, 95% confidence limits for mean pairwise F_{ST} did not overlap with the confidence limits for mean pairwise P_{ST} for any morphological variable, all of which had lower mean values (Table 3.4). Calculations of global P_{ST} and F_{ST} showed a similar pattern, with global P_{ST}s being slightly lower and average global F_{ST} being slightly higher than the pairwise means. However, the confidence intervals obtained from bootstrapping were significantly larger for global P_{ST} than those obtained from the pairwise estimates (Table 3.4). These confidence intervals are shown overlain on the genome wide distribution of global F_{ST} in Figure 3.6.

Discussion

Landscape Genetics

Landscape genomics provides a powerful framework for understanding how near-contemporary evolutionary processes operate in empirical systems. In this research, we present a landscape genomics approach where we investigate how distance, geography, and ecology shape genetic and morphological diversity in the common sun skink, a widely distributed Asian lizard. This is one of the first studies aimed at identifying recent population differentiation across Southeast Asia and the landscape factors that have promoted the evolution of exceptional biodiversity in the region. Although many broad-scaled studies of evolutionary radiations have focused on diversification across deep time scales, here, we use our approach to test several commonly invoked hypotheses in an attempt to better understand how genetic and morphological diversity are generated in this system.

Our results indicate that gene flow occurs among populations of *E. multifasciata* that are separated by large geographic distances and complex topography across Southeast Asia. However, we do see substantial genetic isolation among three main groups of populations: mainland Asia, the central Philippines, and the northern and southern Philippines. We identify geographic distance as an important predictor of genetic differentiation among populations, a commonly observed pattern in landscape genetic studies (Crispo and Hendry, 2005; Storfer et al., 2010; Sexton et al., 2014). In Southeast Asia, ocean channels have long been assumed to represent significant barriers to dispersal for many organisms (Lawlor, 1986; de Queiroz, 2005; Roberts, 2006), however, their relative isolating effect when compared to other factors such as geographic distance is largely unknown. Our study finds support for this on a number of levels, as the model based clustering method (Structure) more finely divided up populations in the Philippine Archipelago than on mainland Asia (Fig. 3.2). Additionally, our landscape genetic analyses provide empirical evidence for the relative ability of ocean channels to contribute to genetic differentiation from both a modern and historical perspective. In contrast, we find little evidence that ecological or environmental variables contribute substantially to population differentiation across this species range. These results suggest that *E. multifasciata* is able to disperse well across a diverse environmental landscape in Southeast Asia, and that geographic distance and ocean channels are the major mechanisms of population isolation in this system.

The specific isolating effects of the ecological and geographic variables discussed here should be interpreted with some caution, as the posterior predictive simulation results indicate that the model is unable to predict the specific patterns of observed genetic differentiation among pairwise populations in some cases (Fig 3.5). There are likely several explanations that could contribute to this. First, although we do see a significant correlation between genetic and geographic distance among populations, several pairwise population comparisons in our dataset do not conform precisely to that expectation (Fig. 3.4, 3.5). For example, some populations show substantial genetic connectivity with geographically distant populations (e.g. the sampled Sulawesi population is genetically similar to populations on northern Luzon Island in the Philippines). This could result from recent admixture between populations, and may reflect the more general pattern of random and opportunistic dispersal that occurs in species that inhabit island archipelagos (Diamond, 1969; Kelly et al., 2001; Crowie and Holland, 2006). There are also examples of populations in our dataset that exhibit higher genetic differentiation than expected based on geographic distance, and this may be a result of the substantial genetic isolation among the major population groups in our dataset that were revealed by the Structure analyses. Finally, the large geographic scope of this study (encompassing nearly 4,000 km) may also contribute to this issue, as the model often appears to have more difficulty predicting genetic differentiation in populations separated by large geographic distances. As geographic distance and complexity increase between populations, correlations between genetic and geographic distance have been shown to break down (Jaquiery et al., 2011). This may explain why specific pairwise population comparisons do not conform to their expectation.

Morphological differentiation

To determine the effects of selection across heterogeneous environments, researchers often compare population variation in neutral genetic markers to that in quantitative morphological traits (Lande, 1992; McKay and Latta, 2002; Whitlock, 2008; Leinonen et al., 2013). Many different studies have drawn conclusions about the effects of selection in natural populations by examining phenotypic differentiation (P_{ST}; Raeymaekers et al., 2007; Lehtonen, 2009; Brommer, 2011; Wojcieszek and Simmons, 2011). Some groups of scincid lizards have also been shown to exhibit extensive conservation in external morphology among species (Donnellan and Aplin, 1989; Austin, 1995; Bruna et al., 1996; Barley et al., 2013). When species are genetically isolated and separated by extensive evolutionary time, but exhibit little morphological differentiation, stabilizing selection on important adaptive traits is often suggested as an explanation for this pattern (Larson, 1989; Sturmbauer and Meyer, 1992; Schönrogge et al., 2002; Glor et al., 2003). However, few studies have actually attempted to demonstrate these types of selective processes in natural populations.

Our results indicate that average pairwise and global F_{ST} estimates were generally higher than pairwise and global P_{ST} estimates. However, substantial uncertainty accompanies individual F_{ST} and P_{ST} estimates, and F_{ST}–P_{ST} comparisons have been the subject of extensive debate due to the difficulty of interpreting these comparisons in relation to particular questions of interest (see Whitlock, 2008 and Leinonen et al., 2013 for reviews). Confidence intervals for bootstrapped pairwise F_{ST} estimates did not overlap with the bootstrapped pairwise P_{ST} CIs for any of the morphological traits examined, which has previously been cited as evidence for stabilizing selection acting to maintain trait values among genetically isolated populations (Wojcieszek and Simmons, 2011). In contrast, confidence intervals obtained from bootstrapping global F_{ST} and

P_{ST} broadly overlapped. The non-independence of the pairwise population bootstrap replicates may result in the narrow confidence intervals obtained using this method. Results from studies comparing P_{ST} to F_{ST} in natural populations should obviously be interpreted with caution when based on small sample sizes of individuals per population, as well as more general issues with inferences drawn from P_{ST} (reviewed in Brommer, 2011). However, we suggest future studies also consider the statistical validity of methods used to test for significant differences between P_{ST} and $F_{ST.}$ Therefore, the new method we present for comparing F_{ST} and P_{ST} in natural populations provides a more conservative interpretation of these comparisons.

Conclusions

In this study, we combine recently developed genomic and analytical approaches to illustrate the power of landscape genomics to reveal how microevolutionary processes contribute to population genetic and morphological diversity. This represents one of the first studies to do this in Southeast Asia, and we relate these processes to the evolution of exceptional biodiversity that has occurred in this region. Additionally, we discuss the importance of correctly deriving confidence intervals for studies of morphological differentiation in natural populations, as different conclusions can be drawn when they are unrealistically small. Future studies investigating other Asian vertebrate groups could provide contrasting examples of how microevolutionary processes function differentially and translate into biodiversity patterns in evolutionary radiations.

Table 3.1 Migration rate estimates among the three major population groups identified by structure. The direction of geneflow is from the population in the left column to the population along the top row. Numbers in parentheses represent 95% confidence intervals for the proportion of migrant individuals per population, per generation.

	Mainland	C. Philippines	N/S Philippines
Mainland	–	0.0354 (0.0082–0.0626)	0.0918 (0.0618–0.1308)
C. Philippines	0.0833 (0.0408–0.1258)	–	0.0854 (0.0421–0.1287)
N/S Philippines	0.0262 (0.0056–0.0468)	0.0134 (0.0–0.0283)	–

Table 3.2 Average pairwise F_{ST} values between 20 populations used in landscape genetic analyses. Ayeyarwady, Rakhine & Taninthary = Myanmar; Bicol, Bulacan, Pamplona, Cagayan & San Mariano = Luzon Island, Philippines; Langkawi & Pahang = Malaysia; Agusan del Sur & Zamboanga = Mindanao Island, Philippines.

	Ayeyarwady	Rakhine	Cambodia	Bicol	Bohol	Bulacan	Langkawi	Mindoro
Aurora	0.2829	0.1889	0.1254	0.0814	0.0389	0.0728	0.0865	0.3303
Ayeyarwady	–	0.0623	0.3143	0.3376	0.5742	0.2348	0.2298	0.3621
Rakhine		–	0.2605	0.2783	0.5714	0.1729	0.1531	0.3717
Cambodia			–	0.2222	0.3640	0.1606	0.0914	0.3674
Bicol				–	0.2150	0.0668	0.1570	0.3466
Bohol					–	0.1354	0.1117	0.1568
Bulacan						–	0.1316	0.3002
Langkawi							–	0.3187

	Agusan del Sur	Pahang	Palawan	Pamplona	Panay	Polillo	Tanintharyi	Zamboanga
Aurora	0.1415	0.1194	0.4475	0.1430	0.3027	0.1049	0.0734	0.2439
Ayeyarwady	0.5026	0.1897	0.4055	0.2545	0.3398	0.3355	0.2713	0.3466
Rakhine	0.4935	0.1110	0.4151	0.2195	0.3388	0.2854	0.1636	0.3301
Cambodia	0.3834	0.0770	0.4314	0.2213	0.3380	0.2495	0.1146	0.3170
Bicol	0.2427	0.1670	0.4398	0.1057	0.3148	0.1181	0.1882	0.2577
Bohol	0.3824	0.1292	0.1848	0.2094	0.0930	0.2077	0.2627	0.2796
Bulacan	0.1527	0.1421	0.4198	0.0887	0.2771	0.0903	0.1271	0.1982
Langkawi	0.1803	0.0272	0.4332	0.1935	0.2928	0.1704	0.0682	0.2458
Mindoro	0.3630	0.2817	0.1138	0.2958	0.0417	0.3261	0.3842	0.3196
Agusan del Sur	–	0.1845	0.4175	0.2064	0.3240	0.2526	0.3295	0.0810
Pahang		–	0.3942	0.1902	0.2658	0.1765	0.0730	0.2382
Palawan			–	0.3880	0.1005	0.4124	0.4542	0.3928
Pamplona				–	0.2713	0.1173	0.1934	0.2198
Panay					–	0.2888	0.3486	0.2938
Polillo						–	0.2057	0.2548
Tanintharyi							–	0.3103

	Cagayan	San Mariano	Sulawesi
Aurora	0.0527	0.0810	0.1006
Ayeyarwady	0.3082	0.4138	0.2424
Rakhine	0.2380	0.3540	0.2027
Cambodia	0.1928	0.2732	0.1879
Bicol	0.0835	0.1150	0.1257
Bohol	0.1242	0.2763	0.1740
Bulacan	0.0597	0.0674	0.1155
Langkawi	0.1352	0.1714	0.1727
Mindoro	0.3340	0.4064	0.2854
Agusan del Sur	0.1937	0.3045	0.1647
Pahang	0.1486	0.1763	0.1709
Palawan	0.4267	0.4643	0.3954
Pamplona	0.0474	0.0206	0.1457
Panay	0.2927	0.3477	0.2648
Polillo	0.1093	0.1385	0.14476
Tanintharyi	0.1465	0.2178	0.1715
Zamboanga	0.2388	0.2968	0.1934
Cagayan	–	0.0134	0.1159
San Mariano		–	0.1410

Table 3.3 Population genetic summary statistics for the 20 populations used in the landscape genetic analyses showing the number of individuals sampled per population (N), nucleotide diversity (Π), observed (H_O) and expected (H_E) heterozygosity, and the inbreeding coefficient (F_{IS}). PI = Philippines.

Population	N	Π	H_O	H_E	F_{IS}
Aurora (Luzon, PI)	7	0.0062	0.1103	0.0858	–0.0032
Ayeyarwady (Myanmar)	7	0.0014	0.0234	0.0210	0.0023
Rakhine (Myanmar)	5	0.0014	0.0224	0.0194	0.0041
Phnom Penh (Cambodia)	5	0.0030	0.0508	0.0384	0.0043
Bicol Peninsula (Luzon, PI)	7	0.0046	0.0683	0.0665	0.0231
Bohol (PI)	6	0.0025	0.0445	0.0247	0.0006
Bulacan (Luzon, PI)	7	0.0054	0.0927	0.0809	0.0051
Langkawi (Malaysia)	5	0.0050	0.0839	0.0708	0.0094
Mindoro (PI)	9	0.0020	0.0325	0.0309	0.0053
Agusan del Sur (Mindanao, PI)	5	0.0023	0.0414	0.0309	–0.0013
Pahang (Malaysia)	6	0.0047	0.0830	0.0690	–0.0010
Palawan (PI)	12	0.0018	0.0337	0.0287	0.0069
Pamplona (Luzon, PI)	9	0.0046	0.0738	0.0715	0.0153
Panay (PI)	8	0.0025	0.0429	0.0390	–0.0001
Polillo (PI)	7	0.0044	0.0647	0.0658	0.0249
Tanintharyi (Myanmar)	7	0.0041	0.0674	0.0515	0.0090
Zamboanga (Mindanao, PI)	6	0.0033	0.0545	0.0512	0.0070
Cagayan (Luzon, PI)	5	0.0049	0.0750	0.0709	0.0213
San Mariano (Luzon, PI)	5	0.0042	0.0706	0.0585	0.0067
Sulawesi (Indonesia)	7	0.0051	0.0770	0.0778	0.0273

Table 3.4 Mean pairwise and global F_{ST} and P_{ST} estimates, standard error, and 95% confidence limits following bootstrapping. See text for explanation of abbreviations.

	Mean	SE	Lower 95% limit	Upper 95% limit
Pairwise F_{ST}	0.2603	0.0132	0.2348	0.2863
Pairwise TFL P_{ST}	0.1214	0.0188	0.0857	0.1592
Pairwise AGD P_{ST}	0.0501	0.0096	0.0320	0.0696
Pairwise HLL P_{ST}	0.1317	0.0180	0.0986	0.1691
Pairwise HLHW P_{ST}	0.0789	0.0131	0.0548	0.1059
Global F_{ST}	0.3533	0.0045	0.3447	0.3624
Global TFL P_{ST}	0.1181	0.0881	0.0570	0.4016
Global AGD P_{ST}	0.0000	0.1283	0.0000	0.4975
Global HLL P_{ST}	0.0997	0.0897	0.0386	0.3871
Global HLHW P_{ST}	0.0569	0.0917	0.0033	0.3509

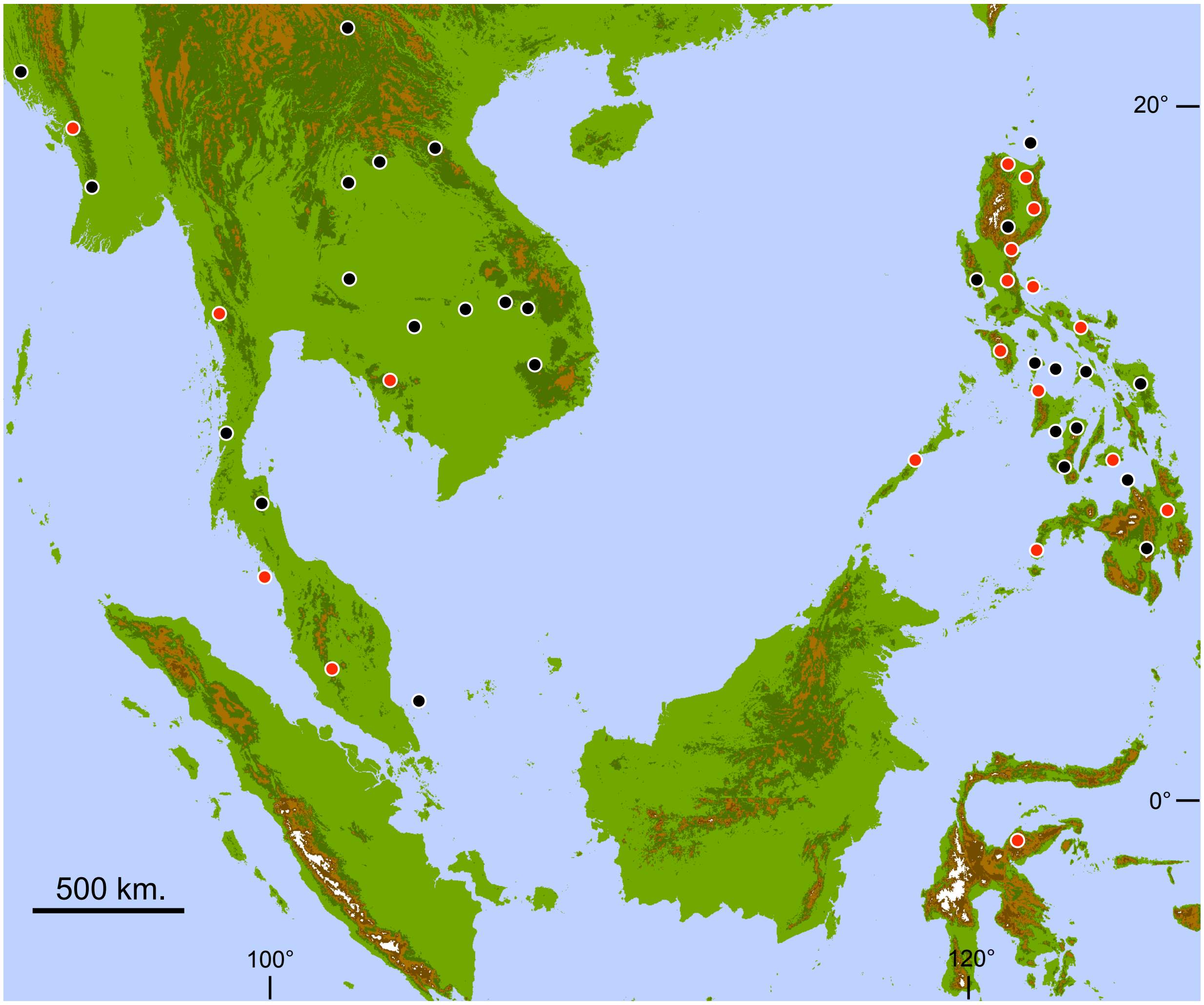

Figure 3.1 Sampling localities across map of Southeast Asia. Red dots indicate populations used in landscape genetic analyses where more than 5 individuals were sampled.

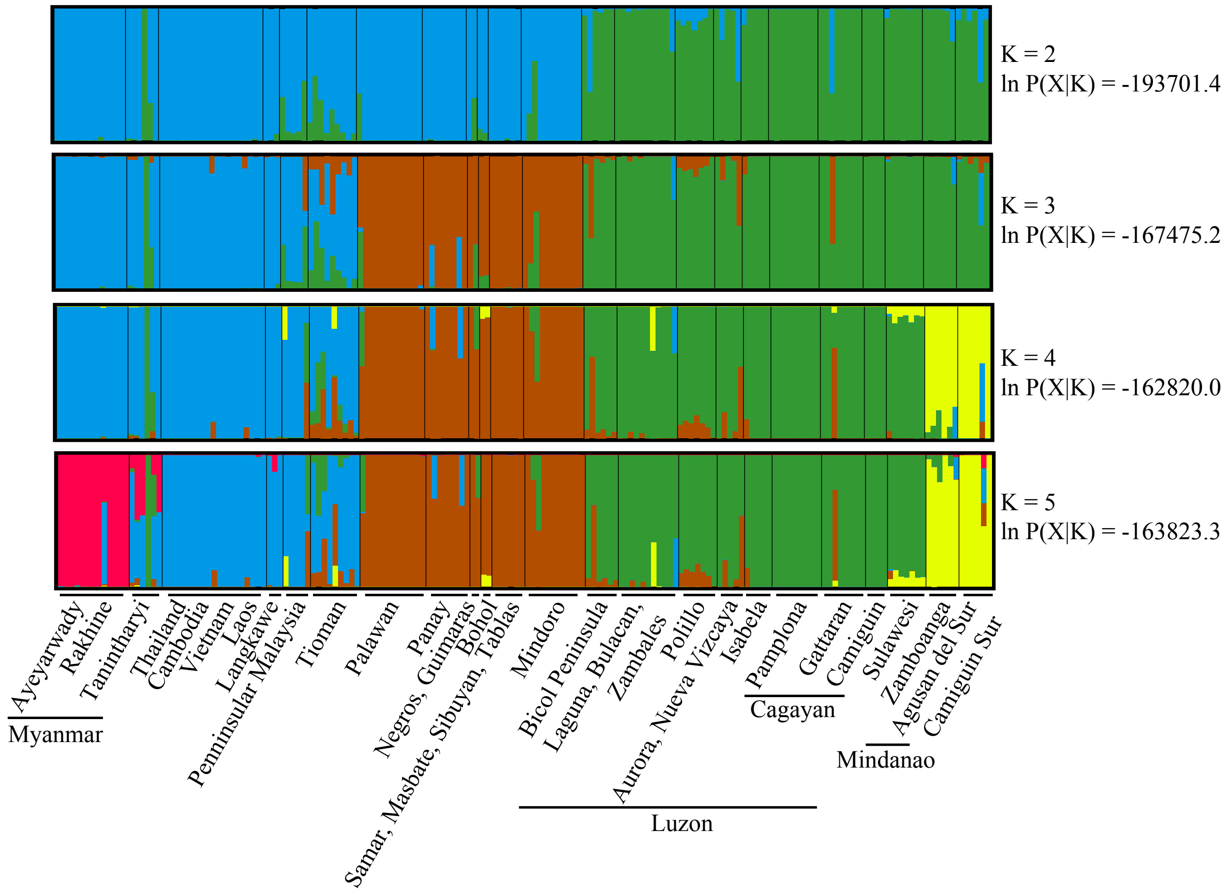

Figure 3.2 Plot of Structure results from analyses using the admixture model where K was varied from 2–5. The geographic sampling localities are listed across the bottom of the figure and each bar shows the posterior means estimates for the fraction of each individuals genome inherited from an ancestor in each population. The likelihood scores for the probability of the data given K are shown on the right.

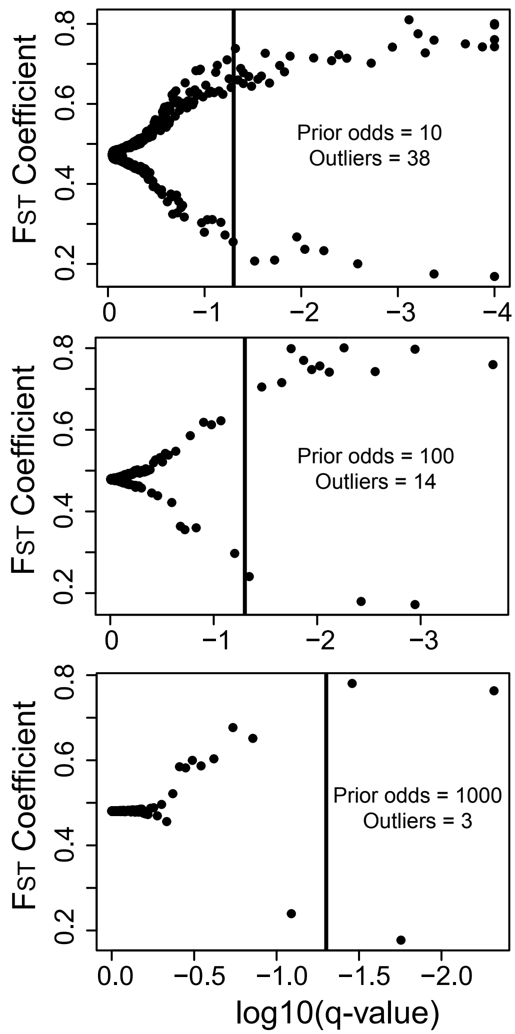

Figure 3.3 Volcano plot for each BayeScan analysis showing the F_{ST} coefficient averaged over populations against the logarithm of posterior odds to base 10 for the model including selection. The prior odds and number of outliers identified in each analysis are indicated.

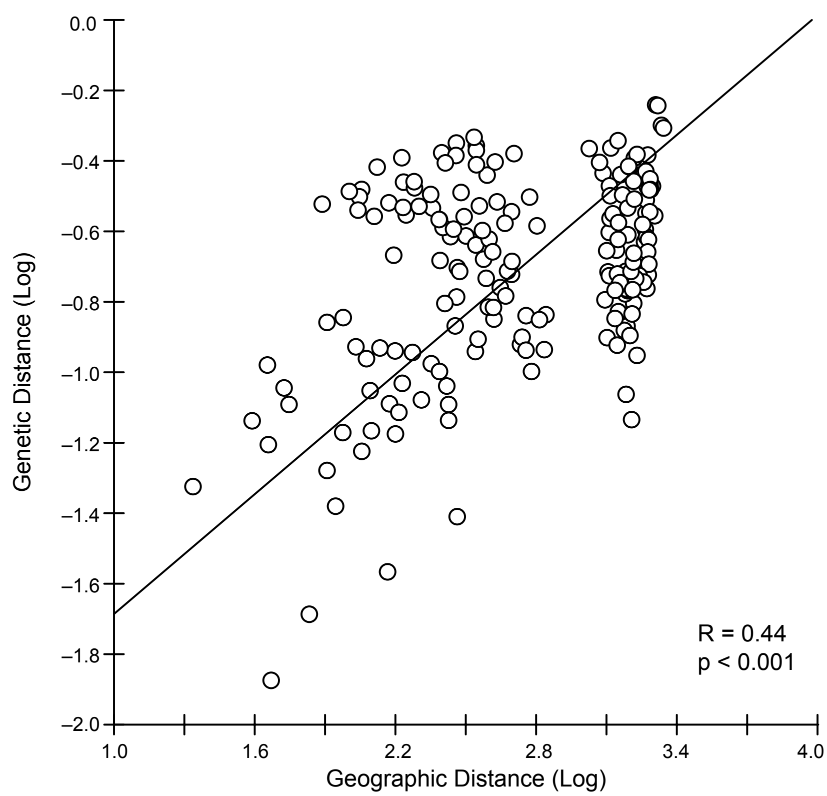

Figure 3.4 Results of IBDWS analyses including reduced major axis regression plot showing pairwise log genetic distance against log geographic distance between each population, as well as correlation coefficient and p-value from Mantel test.

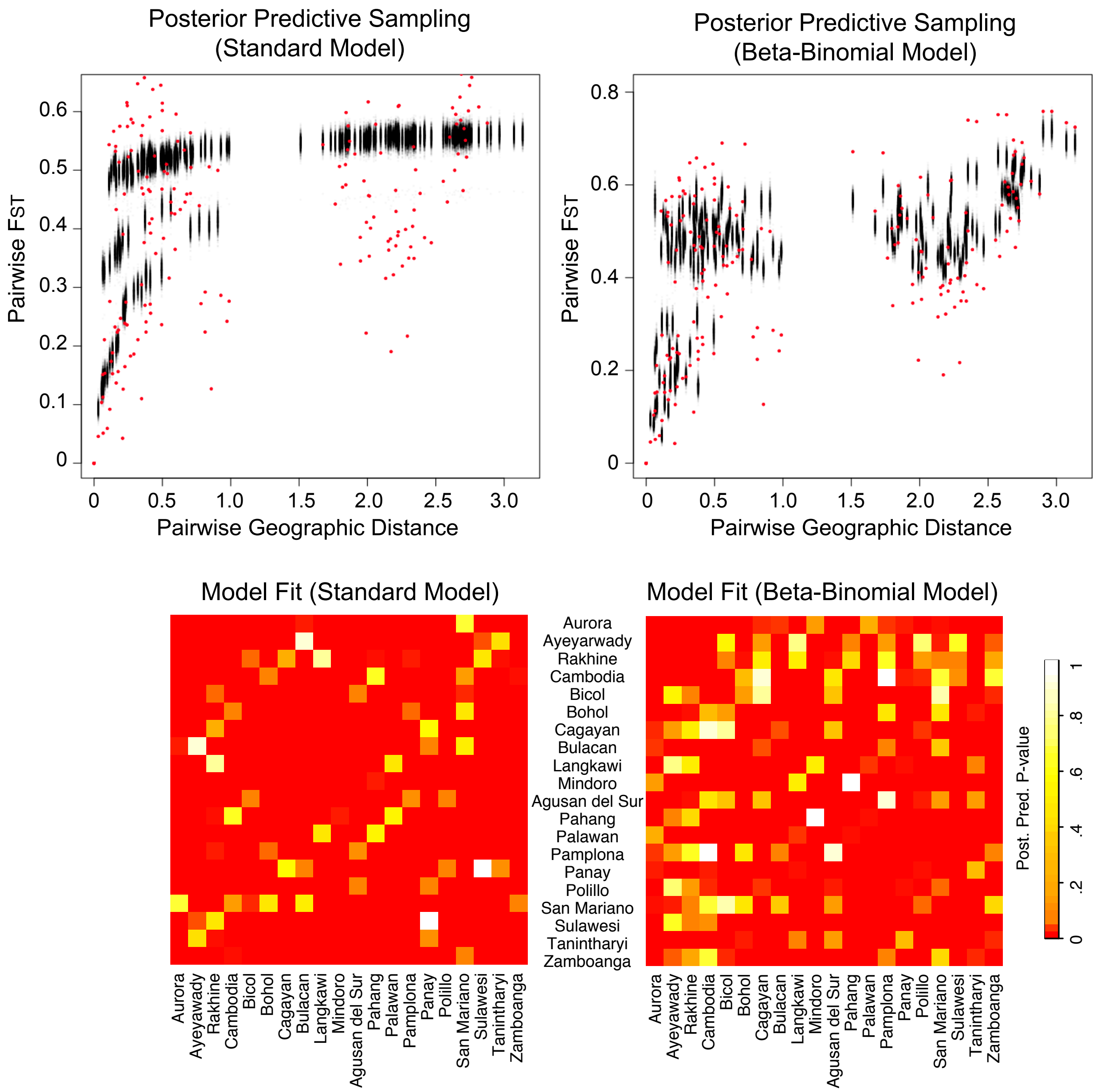

Figure 3.5 Posterior predictive sampling of 1000 simulated datasets for the standard and overdispersion models. Red dots indicate observed pairwise F_{ST} values and black dots indicate simulated pairwise F_{ST} values. Heatmapped matrices show the performance of the models for each pairwise population comparison, with higher posterior predictive p-values indicating better model fit (Bradburd et al., 2013).

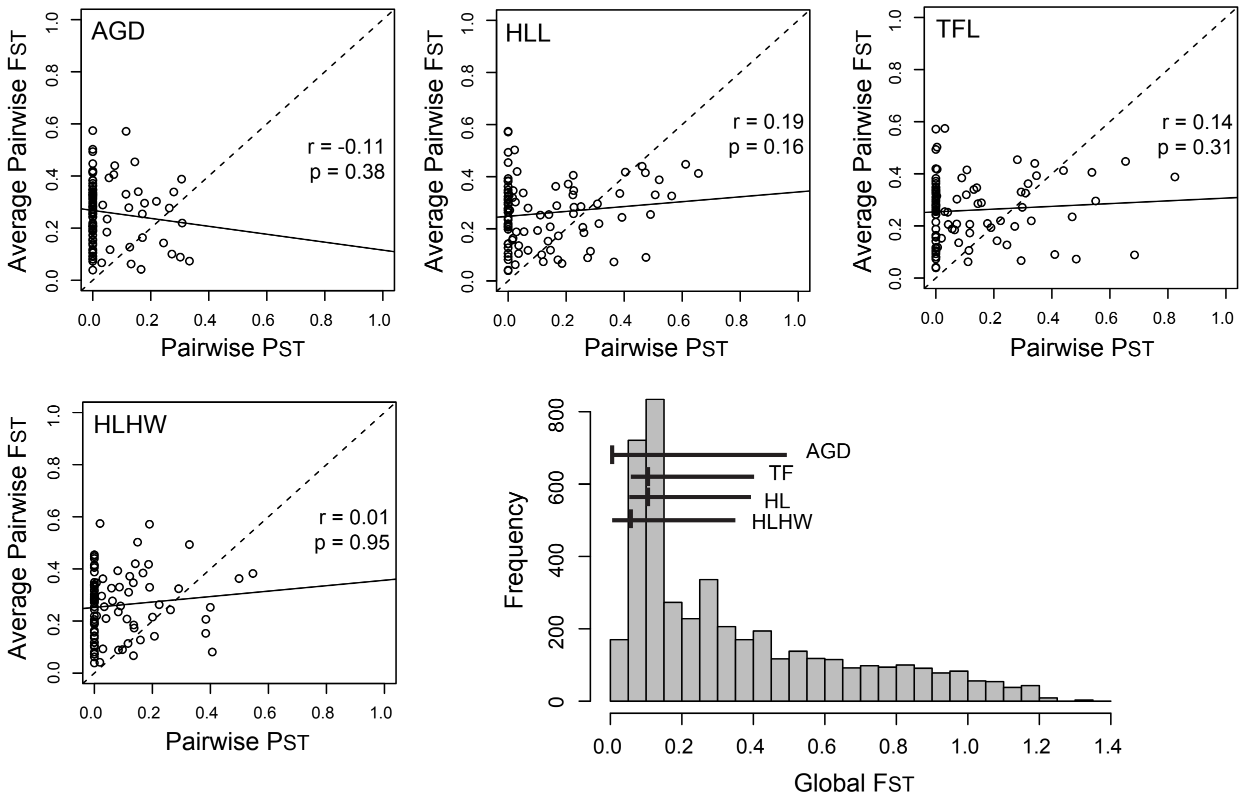

Figure 3.6 Scatterplot of average pairwise F_{ST} against pairwise P_{ST} for four phenotypic traits, with dashed line showing where $F_{ST} = P_{ST}$ and solid regression line. Correlation coefficients (r) and p-values from Mantel tests comparing pairwise values are indicated. Bottom-right plot shows distribution of genome-wide global F_{ST} estimates, with mean and 95% confidence intervals for global P_{ST} estimates overlain. See text for abbreviation meanings.

Chapter 4

Reconciling morphological conservatism, taxonomic chaos, and evolutionary history: a partial taxonomic revision of Philippine sun skinks of the genus *Eutropis* (Reptilia: Squamata: Scincidae)

Abstract

Species descriptions have traditionally relied exclusively reliant on the use of morphological data. Consequently, the underestimation of species diversity within radiations where morphology is highly conserved can be problematic. Using an integrative approach, a recent study examined the genetic and morphological diversity present in a nearly endemic Philippine radiation of skinks (*Eutropis*). Results of the study demonstrated that current taxonomy does not reflect evolutionary history in the radiation, and species diversity to be vastly underestimated. Here, we rectify the major taxonomic problems present in Philippine *Eutropis* by providing formal descriptions for five new species.

Introduction

Mabuyine skinks represent one of the of the most recognizable lizard groups worldwide, due to their circumtropical distribution, diurnal activity patterns, generalist habitat preferences, high abundances in certain regions, and their evolutionarily conserved and highly generalized external morphology (Miralles et al., 2005; Miralles and Carranza, 2010; Hedges and Conn, 2012; Sindaco et al., 2012). This conservative morphology has also resulted in a complex and chaotic taxonomic history for many species, with the Philippine members of this group being one of the most extreme examples of notoriously confusing taxonomy and problematic identifications (Taylor, 1922; Brown and Alcala, 1980; Barley et al., 2013). The genus *Mabuya* was described by Fitzinger (1826), and until recently was often considered a "wastebin taxon" and a convenient taxonomic receptacle into which over 100 species from Asia, Africa, the Middle East, Central and South America, and the Caribbean were deposited. Mausfeld and Schmitz (2003) proposed splitting *Mabuya* into three genera. This arrangement was based on a phylogenetic analysis of mitochondrial DNA for ~40 individuals. They found the genera *Apterygodon* and *Dasia* to be nested within *Mabuya*, and rather than subsume them, they placed Asian members of the genus in *Eutropis* (~31 species), New World taxa in *Mabuya* (~60 species), and the Middle East/African taxa in *Trachylepis* (~78 species). Although this taxonomic arrangement is in some ways problematic, many recent authors have adopted it (Howard et al., 2007; Das et al., 2008; Skinner et al., 2011; Datta-Roy et al., 2012; Sindaco et al., 2012).

Philippine species of the genus *Eutropis* belong to two groups: the first consisting of three separate invasions of the archipelago by widespread species that also possess distributions outside the archipelago (*E. multifasciata*, *E. rudis*, and *E. rugifera*), and another lineage that formed a nearly endemic radiation within the country (Mausfeld and Schmitz, 2003; Datta-Roy et al., 2012; Barley et al., 2013). *Mabuya multicarinata* (Gray, 1845) was the first described species from this nearly endemic Philippine radiation, a taxon that included populations from throughout the archipelago (Fig. 4.1). Subsequently, Taylor (1923, 1925) described two additional species, primarily on the basis of color pattern and body size differences: *M. bontocensis* being endemic to the Cordillera mountain range in northeastern Luzon, and *M. englei* from the coast of southeastern Mindanao.

The most recent taxonomic treatment of Philippine *Eutropis* was undertaken by Brown and Alcala (1980). They found that some specimens previously identified as juvenile *M. mulitcarinata* actually represented mature adults, and described them as *M. cumingi* (represented by populations from northern and southwestern Luzon Island) and *M. indeprensa* (consisting of populations from the rest of the Archipelago). They also divided the widespread taxon *M. mulitcarinata* into two subspecific pattern classes: *M. m. borealis* from the northern part of the archipelago, and *M. m. multicarinata* from the south. This last action was justified by the authors primarily on the basis of differences in color pattern (with individuals from southern populations usually having a dark vertebral stripe and small blackish blotches under the chin and northern populations lacking these color traits); as well as the tendency for the interparietal scale to be relatively long (and separating the parietal scales) in southern populations, and short (with the parietals being in contact posteriorly) in the north (Brown and Alcala, 1980).

In a recent paper, Barley et al. (2013) evaluated species limits in the Philippine *Eutropis* radiation, and employed a variety of approaches to survey molecular and morphological data. Consistent with previous morphological work, genetic data from the study supported the presence of two distinct species complexes: the *E. indeprensa* Complex (containing *E. indeprensa* and *E. cumingi*) and the *E. multicarinata* Complex (containing *E. m. multicarinata*, *E. m. borealis*, and *E. bontocensis*). Although they were unable to obtain genetic data for *E. englei* (a species that is only known from SW Mindanao, a region of the country that is logistically challenging for biologist to access), based on morphology, this species is likely a member the *multicarinata* species complex as well.

However, Barley et al.'s (2013) results indicated that external morphological trait values have been evolutionarily highly conserved and, as such, species limits confirmed with genetic data were poorly defined by characters of external morphology. Thus, it is clear that current species diversity within both the *E. indeprensa* and *E. multicarinata* species complexes is underestimated significantly by current taxonomy. Conservatively, Barley et al. (2013) found a minimum of 11 distinct evolutionary lineages deserving of species recognition in the Philippine radiation (which includes a species that is endemic to the islands of Palau; Crombie and Pregill, 1999). However, Barley et al. (2013) noted the presence of some substantial genetic divergence between additional clades, suggesting that as many as 19 species (and a minimum of 13 species if the closely related *E. indeprensa* and *E. cumingi* are to be considered distinct evolutionary lineages) may exist in the archipelago.

Although Brown and Alcala (1980) considered individuals from the southern portion of the archipelago (including Mindanao, Dinagat, Samar, Cebu, and the Bicol Peninsula of Luzon) to be *E. indeprensa*, they apparently did not measure specimens from these populations for the character they used to distinguish *E. indeprensa* from *E. cumingi* (the longer hind limb/snout–vent length ratio in *E. indeprensa*; Brown and Alcala, 1980). Barley et al. (2013) found that these populations do not form a clade with *E. indeprensa*, and represent a distinct species, which we formally describe here (Fig. 4.2). Accordingly, the taxon *E. indeprensa* should be restricted to populations from Mindoro (from which the type series was collected). The lone individual sampled from Borneo (Das, 2004) in their analysis also appeared to be part of this clade, though there was substantial divergence in mitochondrial and nuclear genes between this sample and the Mindoro population. Thus we refer them tentatively to *E. indeprensa* here, however, future work should attempt to clarify if they represent a distinct taxon. Within the *multicarinata* species complex, Barley et al. (2013) found that the northern and southern populations do not appear to represent distinct, monophyletic lineages, as was hypothesized by Brown and Alcala (1980). Barley et al. (2013) also found strong evidence for the presence of at least 8 species (including the undescribed Palau species, and excluding *E. englei*).

In this paper, we take a first step towards the rectification of the major taxonomic problems present in the Philippine *Eutropis* radiation as outlined by Barley et al. (2013). In doing so, we formally describe five new species endemic to the Philippine Archipelago, four in the *E. multicarinata* species complex, and one in the *E. indeprensa* species complex.

Materials and Methods

Specimens corresponding to genetic samples were collected primarily by hand between 1991 and 2012. Older historical specimens (including types of as many described species as possible) were examined simultaneously for the same characters (derived primarily from Brown and Alcala, 1980). All specimens were fixed in 10% buffered formalin and subsequently placed in 70% ethanol for long-term storage. Measurements were taken with digital calipers and sex was determined by gonadal inspection. Data for males, females, and immature specimens were examined separately and then combined when no significant differences were detected other than size. To eliminate inter-observer error, we analyzed only data collected by AJB.

For each specimen, we measured (see Brown and Alcala, 1980 for character definitions) snout-vent length, axilla-groin distance, head length, head width, frontlimb length, hind limb length. Snout–vent length was measured from the tip of the snout to the cloacal opening. Axilla–groin distance was measured from the posterior insertion of the forelimb to the anterior insertion of the hindlimb on the lateral side of the body. Head length was measured from the tip of the snout to the anterior edge of the ear opening, where head length was measured. Forelimb length was measured in two segments, from the body insertion, to the center of the elbow, and from the elbow to where the palmar scales begin on the posterior lateral edge. Hind limb length was also measure in two segments, from the body insertion to the center of the knee and from the knee to where the scales on the plantar surface begin on the anterior lateral edge. Our scale count measurements included: the number of lamellae under each of the toes on the right foot (including all lamellae beneath the digit, down to the base), upper and lower labial scale counts, ventral scale rows (counted as the number of scale rows on the ventral side between the central point on the front and rear limbs), vertebral scale rows (counted as the number of scale rows between the parietals and the base of the tail), midbody scale rows, and the number of keels per scale. See descriptions below and Appendix 12 for specimens examined.

Results

The theory and practice of defining and delimiting species has a long and contentious history (Wiley, 1978; Mayden, 1997, de Queiroz, 1998; Sites and Marshall, 2004). Any individual species concept has operational difficulties in specific situations (Frost and Hillis, 1990). We utilize the general lineage concept of species as a logical extension of the evolutionary species concept (Simpson, 1961; Wiley, 1978; Frost and Hillis, 1990; de Queiroz, 1998, 1999). Most importantly, this concept defines a species as the most inclusive ancestor-descendent series of populations (lineage) that can be identified as distinct from other such lineages, and within which there is reproductive cohesion.

Previous attempts to delimit species in Philippine *Eutropis* using morphological data were unable to identify distinct, monophyletic evolutionary lineages in many cases due to the extensive morphological conservatism/convergence in this group (Brown and Alcala, 1980; Barley et al., 2013); a common problem in scincid lizards (Austin, 1995; Bruna, 1996). Therefore, we utilize on the results of extensive coalescent and phylogenetic analyses of a robust molecular dataset to guide species delimitation in this group (Fig. 4.2; Barley et al., 2013). We focus our species delimitation on lineages that are: 1) geographically isolated and genetically or morphologically distinct; or 2) sympatric, but genetically or morphologically distinct. In this way, we are able to identify species based on multiple lines of evidence, but avoid being misled and underestimating diversity when external morphology is not indicative of species boundaries.

Species Descriptions

Eutropis caraga, new species

Tiliqua multicarinata (part) Gray, 1845.

Mabuia multicarinata (part) Boulenger, 1887.

Mabuya multicarinata multicarinata, Brown and Alcala, 1980

Mabuya multicarinata multicarinata, Ross and Lazell, 1990

Eutropis Clade E, Barley et al., 2013

Holotype.—KU 334226, collected by R. M. Brown 13 July 2012 on Mount Lumot, Misamis Oriental Province, Mindanao Island.

Paratopotypes.—KU 334228, 334229, collected by R. M. Brown, M. B. Sanguila, and V. Yngente 16 July 2012.

Other Paratypes.—KU 314106, collected by J. Fernandez, 13 May 2008, Barangay San Marcos, Municipality of Bunawan, Agusan del Sur Province, Mindanao Island; KU 315009, collected by R. M. Brown, 18 July 2008 at 760 m., Pasonanca Natural Park, Sitio Kalinga, Barangay Baluno, Municipality of Pasonanca, Zamboanga City Province, Mindanao Island; KU 320028, 320030, collected by A. C. Diesmos and M. B. Sanguila, 1 November 2008 at 430 m., Mt. Magdiwata, Barangay Bagusan, Municipality of San Francisco, Agusan del Sur Province, Mindanao Island; KU 332773, collected by J. Fernandez and V. Yngente, 21 May 2012 at 500 m., Rajah Sikatuna Protected Landscape, Sitio Napo, Barangay Omjon, Municipality of Valencia, Bohol Province, Bohol Island.

Referred specimens.—Dinagat Island, Dinagat Islands Province, Municipality of Loreto, Barangay Santiago, Sitio Cambinlia, Mount Cambinlia: KU 310152 310154; Barangay San Juan near Venus Dias Cave: KU 310156; Mindanao Island, Agusan del Sur Province, Municipality of Bunawan, Barangay San Marcos: KU 314098, 314105; Zamboanga City Province, Municipality of Pasonanca, Pasonanca Natural Park, Barangay Baluno: KU 315009; Siargao Island, Surigao del Norte Province, Municipality of Dapa: KU 335269, KU 335270; Municipality of Bilar: KU 335273–335275.

Diagnosis.—A species of *Eutropis* distinguished by the following combination of characters: (1) body size medium, SVL 64.5–83.9 in adults; (2) interparietal long, narrow, separating parietals; (3) paravertebrals 35–43; (4) total subdigital toe lamellae I–V 73–88; (5) ventral scale rows 26–30; (6) midbody scale rows 27–34; (7) geographically distributed on Mindanao, Bohol, Dinagat, and Siargao islands.

Comparisons.— Critical comparisons for *Eutropis caraga* include the sympatric taxa *E. lapulapu*, *E. englei, E. multifasciata*, and *E. rugifera*. Whether this species' distribution extends into the Sulu Archipelago is unknown. If so, the new species may also be sympatric with *E. rudis* at the southwesternmost extent of its range. *Eutropis rudis* and *E. multifasciata* can easily be distinguished from *E. caraga* by its larger, more robust body and the presence of only three (versus 8–11) strong keels on its dorsal scales. Keels on the dorsal scales of *E. rugifera* tend to be less numerous, but are more raised and sharply defined than in *E. caraga*. Adults of *E. rugifera* also have a slightly smaller SVL, have a smaller interparietal, with parietals in contact posteriorly, and lack the broad dorsolateral band (that is present in *E. caraga*). It can be readily distinguished from *E. englei* by color pattern, as it lacks this species' prominent series of dorsal and lateral stripes, and by more sharply raised keels on the dorsal scales than *E. englei*. It can be distinguished from *E. lapulapu* by its larger body size.

Description of holotype.— A large male (SVL 79.9 mm) with hemipenes everted. Body robust (axilla–goin distance/SVL = 0.5); limbs well developed (hind limb length/SVL = 0.3; front limb length/SVL = 0.2); tail long (SVL/tail length = 0.5); head robust (head length/SVL = 0.2), longer than wide (head width/head length = 0.9).

Snout tapered, rounded at tip. Rostral broader than high, in contact with frontonasal and nasals; frontonasal wider than long, in contact with nasals, frontal, prefrontals, rostral, and anterior loreal; prefrontals separated, contacting anterior and posterior loreals, 1st suprocular, frontal and rostral; frontal longer than wide, in contact with 1st and 2nd supraoculars; four supraoculars, 2nd largest; five supraciliaries; frontoparietals not fused; interparietal long and narrow; separating parietals.

Head scales embossed; one pair of enlarged nuchals; nasal pierced in center by naris, surrounded anteriorly by rostral, posteriorly by anterior loreal, dorsally by supranasal, and ventrally by 1st suprlabial; supranasals long and narrow, not in contact at midline; 6 supralabials, 5th elongate, beneath center of eye; 6 infralabials tympanum moderately sunk, without lobules.

Body elongate, with 38 paravertebrals, midbody scale rows 34, ventrals 29; dorsal and lateral scales with 8–11 keels, ventral scales smooth; tail elongate, 1.7 times body length. Forelimbs smaller than hind limbs, all limbs pentadactyl; forelimb scales smaller than body scales, keeled; relative digit length with subdigital lamellae in parentheses (Left/Right): IV(17/17) = III(18/18) > II(13/12) > V(12/12) > I (8/8). Hind limbs moderate (hind limb length/axilla–groin distance = 0.6); relative digit length with lamellae (L/R) in parentheses: IV(25/–) > III(21/–) > V(18/18) > II(13/13) > I(9/8).

Measurements of holotype (in mm).— SVL 79.9; tail length 155.6; axilla-groin distance 39.2; hind limb length 23.6; forelimb length 17.2; snout-forelimb length 27.7; head length 16.3; head width 14.6; interorbital distance 9.6; internarial distance 3.8; eye diameter 3.1; auricular opening diameter 1.6.

Coloration.— The following color description was written in 2013 following one year of storage in 70% ethanol. Dorsal ground color dark greenish-olive to brown, with dark brown spots randomly interspersed down the length of the body. Scales on the margins of the dorsum are slightly lighter on the anterior portion of the body. Thick, dark brown, longitudinal bands extend down lateral surfaces of body from posterior of eye to groin. Venter grayish tan to bluish, with lighter chin and precloacals, and dark flecks, randomly dispersed (primarily on the margins) and extending from the chin and throat, all the way down the length of the tail. Margins of ventral scales dark, grey, with central portions light tan.

On lateral surfaces of body, ventral coloration intergrades into dark brown; a faint, broken, light stripe from the upper labials extends down the lateral surface of the body until approximately just past the axilla. Dorsal surfaces of limbs and digits greenish-olive brown, mottled with dark brown spots. Ventral surfaces of limbs mostly light grayish to blue, intergrading with dark brown coloration on lateral surfaces. Ventral surfaces of digits dark brown, palmar surface of manus and plantar surface of pes tan to ivory. Head scales uniformly greenish-olive brown, as in the dorsal ground color. Upper portion of supralabials dark brown, lower portion light grey to bluish, lower labials also grey to bluish with several dark flecks. Color in life was unrecorded, but in our experience, *Eutropis* specimen coloration is very similar to that in preservative.

Variation.— Morphometric and meristic (scale count) data are summarized in Table 4.1. *Eutropis caraga* varies in the number of lamellae under each of the toes (8–10 under toe I, 9–13 under toe II, 19–23 under toe III, 22–27 under toe IV, and 14–19 under toe V). It also varies in the number of lamellae under finger III (16–19). Both the supralabials and infralabials vary in number (6 or 7), the supraciliaries (5 or 6) as well as the ventral scales (26–30), paravertebrals (35–43), and midbody scale rows (27–34). The number of keels on the dorsal scales is also highly variable, both within and among individuals (8–10). Whether or not the prefrontals are separated from the second supraocular also varies.

Dorsal color pattern varies slightly, in the degree of dark brown streaking present. The amount of dark flecking on the ventral surface varies from extensive to none. The thickness of the light stripe extending down the lateral side of the body also varies slightly between localities.

Distribution.— *Eutropis caraga* is known from localities throughout Mindanao Island, as well as Dinagat, Siargao, and Bohol islands.

Habitat and natural history.—*Eutropis caraga* inhabits primary and secondary growth mid-montane forest throughout its range, as well as the natural bonsai forest present on Dinagat Island. It also appears to be able to tolerate some disturbance, as it has been found in disturbed, agricultural areas, coconut groves, and residential areas near forest. It is a diurnally active species that has been collected in leaf litter on the forest floor, in open habitats near forest, on saplings, and under logs from sea level to 1500 m. This species can be found sympatrically with at least three other species of *Eutropis*: *E. Clade lapulapu*, *E. multicarinata*, and *E. multifasciata*. *Eutropis rugifera* is also known from nearby localities on the Zamboanga Peninsula, so it seems likely the two could be also found in sympatry at some sites there.

Etymology.—We derive the new species' specific epithet (used as a noun in apposition) from the name of the Caraga Region (the type locality) of northeastern Mindanao and the immediate offshore islands of Dinagat and Siargao. The name is feminine in gender.

Remarks.— Gray (1845) initially described *E. multicarinata*, but labeled the type locality only "Philippines" (BMNH 1946.8.15.13). Brown an Alcala (1980) determined the specimen was likely drawn from one of the southern populations in the archipelago based on the fact that the interparietal is relatively long and narrow, and the presence of dark markings under the chin and throat. They arbitrarily designated Leyte as the type locality for the subspecies *E. m.*

multicarinata based on the fact that Cuming (who collected the specimen) visited several islands in the southeastern portion of the archipelago, including Leyte. Barley et al. (2013) determined that these southern populations of *E. multicarinata* were actually composed of two distinct species, which we find to be morphologically indistinguishable, despite the fact they occur syntopically in northeastern Mindanao and on Dinagat Island. Because of the highly conserved external morphology in this species complex, determining which species the type specimen belongs to is not possible (because we cannot obtain genetic data from the type specimen). However, only one of these species has been found on Leyte Island, thus we consider those populations as representative of true *E. multicarinata*, and describe this new species here.

Eutropis borealis, new combination

Mabuia multicarinata (part) Boulenger, 1887.

Mabuya multicarinata (part) Taylor, 1917.

Mabuya multicarinata borealis, Brown and Alcala, 1980

Mabuya multicarinata borealis, Ota, 1991

Mabuya multicarinata borealis, Ross and Gonzales, 1992

Mabuya multicarinata borealis, Ferner et al., 2000

Eutropis multicarinata borealis (part) Siler et al., 2011

Eutropis multicarinata borealis (part) Brown et al., 2000, 2012, 2013

Eutropis multicarinata borealis (part) Devan-Song and Brown 2012

Eutropis multicarinata borealis, Barley et al., 2013

Holotype.—CAS 15447 (male, SVL 69.3) collected by J. C. Thompson 7 June, 1907 in the Subic Bay area, Luzon Island, Philippines.

Referred specimens.—Luzon Island, Zambales Province, Subic Bay: CAS 15448; Camarines del Sur Province, Municipality of Baao, Barangay La Medalla: KU 306196; Camarines Norte Province, Municipality of Labo, Barangay Tulay Na Lapa, 200 m: KU 313911; Aurora Province, Municipality of Maria Aurora, Barangay Villa Aurora, Sitio Dimani, Aurora Memorial National Park, 500 m: KU 323199–323202, 323204–323206; Municipality of Baler, Barangay Zabali, Aurora State College of Technology: KU 323210; Municipality of San Luis, Barangay Real Sitio Minoli, 600 m: KU 323223, 325050, 325051; Isabela Province, Municipality of San Mariano, Barangay Dibuluan, Sitio Apaya, Apaya Creek: KU 327366; Sitio Dunoy, Dunoy Lake, 200 m: KU 327549; Dibante Ridge, 250 m: KU 327562; Barangay Del Pilar, 200 m: KU 327557; Barangay San Jose, 200 m: KU 327567; Cagayan Province, Municipality of Gattaran, Gattaran DENR Reforestation Project Reserve: KU 335107, 335108; Babuyan Claro Island, Cagayan Province, Municipality of Calayan, Barangay Babuyan Claro: KU 304837; Catanduanes Island, Catanduanes Province Municipality of Gigmoto, Barangay San Pedro, 500 m: KU 308125; Polillo Island, Quezon Province: CAS 62280; Municipality of Burdeos, Barangay Aluyon, Sitio Malinao, 25 m: KU 327369.

Diagnosis.—A species of *Eutropis*, distinguished by the following combination of characters: (1) body size medium, SVL 64.1–82.6 in adults; (2) interparietal small, parietals in contact posteriorly; (3) paravertebrals 37–42, (4) total subdigital toe lamellae I–V 79–88; (5) ventral scales rows 24–28; (6) midbody scale rows 28–33; (7) geographically distributed in the northern Philippine (including Luzon, Polillo, and Catanduanes, as well as in the Babuyan Island Group) and central Philippine (including Negros, Panay and Siquijor) islands.

Comparisons.— Critical comparisons for *Eutropis borealis* include the sympatric taxa *E. cumingi, E. lapulapu, E. bontocensis, E. gubataas*, and *E. multifasciata*. *Eutropis borealis* can be distinguished from both *E. lapulapu* and *E. cumingi* by its larger, more robust body and fewer subdigital toe lamellae (79–88 vs. 65–77 or 55–67), and from *E. cumingi* by fewer vertebral scale rows (37–42 vs. 43–39). It can be distinguished from *E. multifasciata* by its smaller maximum body size, and more numerous and pronounced dorsal scale keels (3 vs. 6–9). It can be readily distinguished from *E. bontocensis* by color pattern, as it lacks this species' prominent series of dorsal and lateral stripes, by more strongly keeled dorsal scales than *E. bontocensis*, by fewer subdigital toe lamellae (79–88 vs. 67–74), and more numerous vertebral (37–42 vs. 44–50) and ventral (24–28 vs. 29–33) scale rows. However, this species appears to be morphologically indistinguishable from the broadly sympatric *E. gubataas.*

Description and variation (including holotype).—(based on 22 specimens, including holotype) A large species (adult SVL 64.11–82.52). Body robust (axilla–groin distance/SVL = 0.40–0.54), limbs well developed (hind limb length/SVL = 0.24–0.35; front limb length = 0.17–0.26); head robust (head length/SVL = 0.20–0.24), longer than wide (head width/head length = 0.70–0.85).

Snout tapered, rounded at tip. Rostral broader than high, in contact with frontonasal and nasals; frontonasal wider than long, in contact with nasals, frontal, prefrontals, rostral, and anterior loreal; prefrontals separated, contacting anterior and posterior loreals, 1st and 2nd suproculars, frontal and rostral; frontal longer than wide, in broad contact with 2nd (and rarely 1st) supraocular; four supraoculars, 2nd largest; supraciliaries usually five, rarely six; frontoparietals not fused; interparietal small, parietals in contact posteriorly.

Head scales embossed; one pair of nuchals, nasal pierced in center by naris, surrounded anteriorly by rostral, posteriorly by anterior loreal, dorally by supranasal, and ventrally by 1st suprlabial; supranasals long and narrow, not in contact at midline; 6 or 7 supralabials, 5th or 6th elongate, beneath center of eye; 6 or 7 infralabials; tympanum moderately sunk, without lobules.

Body elongate, with 37–42 paravertebrals (holotype 38); midbody scales 28–33 (holotype 28), ventrals 24–28 (holotype 28); dorsal and lateral scales with 6–9 keels, ventral scales smooth; tail elongate, approximately 1.6X body. Forelimbs smaller than hind limbs, all limbs pentadactyl; forelimb scales smaller than body scales, keeled; relative digit length IV = III > II > V > I. Hind limbs moderate (hind limb length/axilla–groin distance = 0.49–0.75), scales smaller than body scales, keeled; relative digit length IV > III > V > II > I; Toe IV lamellae 24–28 (holotype 27).

Coloration.—(based on 22 specimens, including holotype) Dorsal ground color dark greenish-olive to brown. The dorsal coloration is generally uniform, though some specimens exhibit dark streaks of brown at the margins (KU 306196, 323199, 327366). Thick, dark brown, longitudinal bands extend down lateral surfaces of body from posterior of eye to groin. Most specimens exhibit a light stripe extending down the body separating the dorsal surface and the dark brown bands on the lateral surface, though the extent and prominence of this stripe varies (being very distinct in KU 306196, extending down almost the entire length of the body in KU 323210, and nearly non-existent in KU 304837, 313911). Below the dark bands on the lateral surface, a faint, light stripe extends from the upper labials down the lateral surface of the body, though the length of this stripe varies (extending down the entire length of the body in some cases KU 306196, 327369, extending just past the axilla in KU 304837, 327366, 327562, and being discontinuous in KU 323223).

Venter grayish tan to bluish, with lighter chin and precloacals. Some individuals exhibit small. Dark flecks on the anterior portion of the lateral surface (KU 306196, 323223). The transition between the ventral and lateral surfaces exhibits a mottled pattern of grayish to bluish coloration interspersed with dark brown. Dorsal surfaces of limbs and digits greenish-olive brown, mottled with dark brown spots. The mottling is particularly prominent on the proximal portion of the forelimb. Ventral surfaces of limbs mostly light grayish to blue, intergrading with dark brown coloration on lateral surfaces. Ventral surfaces of digits dark brown, palmar surface of manus and plantar surface of pes tan to ivory. Dorsal ground color continues onto head scales, which are usually uniform, but exhibit dark brown flecks or spots in some cases (KU 306196, 323199). Upper labials dusky brown, lower labials lighter in color, both usually exhibiting dark bars at margins of scales, though this is more common in upper labials (KU 323210).

Distribution.— *Eutropis borealis* is known from localities throughout Luzon Island (Brown and Alcala, 1980; Brown et al., 2000, 2012, 2013; Siler et al., 2011; Devan-Song and Brown, 2012), as well as Babuyan island in the Babuyan Island group (Oliveros et al., 2011), Polillo Island, and Catanduanes Island (Ross and Gonzales, 1992). *Eutropis borealis* may occur on additional islands in the Babuyan and Batanes island groups, however, additional survey work is needed. Populations have also been reported from Lanyu Island, Taiwan (Ota, 1991). Closely related, highly divergent populations that may represent one or more distinct species are now also known from the biogeographically distinct central Philippine islands of Negros, Panay (Ferner et al., 2000), and Siquijor (Fig. 4.2). However, we refer them to this species pending further investigation. Presumably this species also occurs on other central Philippine islands within this range (e.g. Masbate, Ticao, and Burias islands).

Habitat and natural history.—*Eutropis borealis* can be considered a habitat generalist, as it has been collected in a wide variety of habitats across its distribution. It primarily occurs in primary and secondary growth, upper and lowland rainforest from sea level to 1500 m., where it is often one of the most common lizard species. It has also been found in limestone forest and dry, scrub forest on Luzon Island. This species can be found in many types of disturbed habitats including agricultural areas, coconut groves, bamboo forests, selectively logged forests, residential areas, and forest edge habitats. It is a diurnally active species that has been collected on leaf litter on the forest floor, tree trunks, and on branches of small shrubs, as well as on rocks on stream banks. It can also be found basking in disturbed, open areas, and on rotten coconut grove debris. Several specimens have been collected sleeping under rotten logs in the forest, and on leaf fronds over streams at night. This species can be found sympatrically with at least 4 other species of *Eutropis*: *E. gubataas, E. cumingi, E. lapulapu,* and *E. multifasciata*. Its range also encompasses that of *E. bontocensis*, however, the two species have not be collected at the same locality.

Eutropis gubataas, new species

Mabuia multicarinata (part) Boulenger, 1887.

Mabuya multicarinata (part) Taylor, 1917.

Mabuya multicarinata borealis, Brown and Alcala, 1980

Mabuya multicarinata borealis (part) Brown et al., 2000, 2012

Mabuya multicarinata borealis (part) Siler et al., 2011

Mabuya multicarinata borealis (part) Oliveros et al., 2011

Eutropis Clade F, Barley et al., 2013

Holotype.—KU 304620, collected R. M. Brown and J. Fernandez 7 March 2006 near Barangay Balatubat, in an area known locally as "Limandok," Municipality of Calayan, Cagayan Province, Camiguin Norte Island, Philippines.

Paratopotypes.—Six specimens, collected at the same locality, only differing from the holotype in the following: KU 304618, collected 6 March 2006; KU 304642, collected 7 March, 2006; KU 304688, KU 304689, collected 9 March 2006; KU 304727, KU 304750, collected 10 March, 2006. All collected by R. M. Brown and J. Fernandez.

Other Paratypes.—KU 304940, collected by R. M. Brown and J. Fernandez, 22 March 2006 at 300 m., Barangay Magsidel, Municipality of Calayan, Cagayan Province, Calayan; KU 323224, collected by A. C. Diesmos, 2 June 2009, Aurora Memorial National Park, Municipality of Maria Aurora, Aurora Province, Luzon; KU 329521, collected by R. M. Brown, 28 June 2011 at 475 m., Barangay Adams, Municipality of Adams, Ilocos Norte Province, Luzon.

Referred specimens.—Camiguin Norte Island, Cagayan Province, Municipality of Calayan, Barangay Balatubat: KU 304767; Calayan Island, Cagayan Province, Municipality of Calayan, Barangay Magsidel: KU 304871, 304872; Luzon Isand, Aurora Province, Municipality of Maria Aurora, Barangay Villa Aurora, Sitio Dimani, Aurora Memorial National Park: KU 323198; Ilocos Norte Province, Municipality of Adams, Barangay Adams, Mount Pao: KU 329522, 329523.

Diagnosis.—A species of *Eutropis*, distinguished by the following combination of characters: (1) body size medium, SVL 60.5–78.7 in adults; (2) interparietal small, parietals in contact posteriorly; (3) paravertebrals 37–46; (4) total subdigital toe lamellae I–V 74–87; (5) ventral scales rows 26–30; (6) midbody scale rows 30–36; (7) geographically distributed in the Babuyan Island Group, and northern Luzon Island.

Comparisons.—Critical comparisons for *Eutropis gubataas* include the sympatric taxa *E. cumingi, E. bontocensis*, *E. borealis*, and *E. multifasciata*. *Eutropis gubataas* can be easily distinguished from *E. cumingi* by its larger maximum body size, and more numerous subdigital toe lamellae (74–87 vs. 55–67). It can be readily distinguished from its closest relative *E. bontocensis* by lacking this species' characteristic series of prominent dorsal and lateral stripes, and by more strongly keeled dorsal scales than *E. bontocensis*. It can be distinguished from *E. multifasciata* by its smaller maximum body size, and more numerous (3 vs. 5–12) and more pronounced dorsal scale keels. Interestingly, this species appears to be morphologically indistinguishable from the broadly sympatric *E. borealis*; both are known to inhabit northern Luzon and the Babuyan Island Group (Oliveros et al., 2011).

Description of holotype.— A large male (SVL 77.9 mm) with hemipenes everted. Body robust (axilla–goin distance/SVL = 0.5); limbs well developed (hind limb length/SVL = 0.2; front limb length/SVL = 0.2); tail long (SVL/tail length = 0.6); head robust (head length/SVL = 0.2), longer than wide (head width/head length = 0.8).

Snout tapered, rounded at tip. Rostral broader than high, in contact with frontonasal and nasals; frontonasal wider than long, in contact with nasals, frontal, prefrontals, rostral, and anterior loreal; prefrontals separated, contacting anterior and posterior loreals, 1st and 2nd suproculars, frontal and rostral; frontal longer than wide, in broad contact with 2nd supraocular; four supraoculars, 2nd largest; five supraciliaries; frontoparietals not fused; interparietal small; parietals in contact posteriorly.

Head scales embossed; one pair of enlarged nuchals; nasal pierced in center by naris, surrounded anteriorly by rostral, posteriorly by anterior loreal, dorsally by supranasal, and ventrally by 1st suprlabial; supranasals long and narrow, not in contact at midline; 6 supralabials, 5th elongate, beneath center of eye; 6 infralabials; tympanum moderately sunk, without lobules.

Body elongate, with 41 paravertebrals, midbody scale rows 31, ventrals 30; dorsal and lateral scales with 8–11 keels, ventral scales smooth; tail elongate, 1.7 times body length. Forelimbs smaller than hind limbs, all limbs pentadactyl; forelimb scales smaller than body scales, keeled; relative digit length with subdigital lamellae in parentheses (L/R): IV(17/19) = III(18/16) > II(13/13) > V(11/11) > I (7/7). Hind limbs moderate (hind limb length/axilla–groin distance = 0.5), scales smaller than body scales, keeled; relative digit length with lamellae (L/R) in parentheses: IV(24/23) > III(20/20) > V(16/15) > II(14/14) > I(8/9).

Measurements of holotype.—SVL 77.9; tail length 130.4; axilla-groin distance 37.7; hind limb length 18.5; forelimb length 17.0; snout-forelimb length 26.6; head length 15.8; head width 13.1; interorbital distance 7.8; internarial distance 3.7; eye diameter 3.6; auricular opening diameter 1.5.

Coloration.—The following holotype color description was written in 2013 following seven years of storage in 70% ethanol. Dorsal ground color dark greenish-olive to brown, with some interspersed dark streaks of brown. Thick, dark brown, longitudinal bands extend down lateral surfaces of body from posterior of eye to groin. Venter grayish tan to bluish, with lighter chin and precloacals. Margins of ventral scales dark, grey, with central portions light tan. On lateral surfaces of body, ventral coloration intergrades into dorsal coloration in a mottled pattern; a faint, light stripe from the upper labials extends down the lateral surface of the body until approximately halfway between the axilla and groin.

Dorsal surfaces of limbs and digits greenish-olive brown, mottled with dark brown spots. Ventral surfaces of limbs mostly light grayish to blue, intergrading with dark brown coloration on lateral surfaces. Ventral surfaces of digits dark brown, palmar surface of manus and plantar surface of pes tan to ivory. Head a relatively uniform greenish-olive brown, with several dark brown blotches posteriorly, which are particularly prominent on the parietals. Upper labials dusky brown, lower labials lighter in color with dark splotches. Color in life was unrecorded but in our experience, *Eutropis* specimen coloration in life is very similar to that in preservative.

Variation.—Morphometric and scale count data are summarized in Table 4.1. *Eutropis gubataas* varies in the number of subdigital toe lamellae (8–10 under toe I, 9–12 under toe II, 18–22 under toe III, 23–27 under toe IV, and 14–19 under toe V). It also varies in subdigital finger III lamellae (16–19). Both the supralabials and infralabials vary in number (6 or 7), as well as ventral scale rows (26–30), paravertebrals (37–46), and midbody scale rows (30–34). The number of dorsal scale keels is also highly variable, both within and among individuals (5–12).

Dorsal color pattern varies slightly, in the degree of dark brown streaking present. Some individuals exhibit a light brown stripe between the dorsal ground color and the thick dark brown ventral band, starting just behind the head, and extending down past the forelimbs (KU 304689, 323224), however, the extent and distinctiveness of this stripe is variable among specimens. The extent to which ventral scales change from dark posteriorly to light on the chin is also variable, as is the variable presence of dark blotches on the posterior of the head.

Distribution.— *Eutropis gubataas* is known exclusively from several islands in the northern Philippines: from Calayan and Camiguin Norte islands in the Babuyan island group (Oliveros et al., 2011), as well as northeastern Luzon island from Cagayan and Aurora Provinces, and northwestern Luzon from Ilocos Norte Province (Brown et al., 2000, 2012, 2013; Siler et al., 20011). This species appears to be patchily distributed across northern Luzon (where the extent of its range is not well characterized). It may be restricted to mid– to high–elevation regions in the northern Cordillera and Sierra Madre mountain ranges, as a genetically divergent, but morphologically similar species (*E. borealis*) occurs at lower elevations in these same general areas. However, there is at least one locality where the two species have been collected syntopically in the Sierra Madre (mid-elevation in Aurora National Park; Brown et al., 2000; Siler et al., 2011). This species may potentially occur on additional islands in the Babuyan Island group (where *E. borealis* also occurs), as well as the Batanes Island group and Lanyu Island, Taiwan, however additional survey work will be needed to clarify this possibility.

Habitat and natural history.—*Eutropis gubataas* is known primarily from primary and secondary growth forest from sea level to 1000 m above sea level. However, this species appears to be able to tolerate a moderate amount of habitat disturbance, and specimens have been collected from agricultural and residential areas at the edge of forests, and in selectively logged areas. *Eutropis gubataas* can be found diurnally active in leaf litter on the forest floor, on the trunks of trees, on shrubs, and on rocky stream banks. This species can be found sympatrically with four other *Eutropis* species: *E. bontocensis, E. cumingi, E. borealis*, and *E. multifasciata*.

Etymology.—The specific epithet is an adjectival derivation from the Tagalog noun *gubat* (meaning forest) and adjective *mataas* (meaning "high" or "up high") in reference to the new species' preference for montane forested habitats. The name is feminine in gender.

Eutropis islamaliit, new species

Mabuia multicarinata (part) Boulenger, 1887.

Mabuya multicarinata (part) Taylor, 1917.

Mabuya multicarinata borealis, Brown and Alcala, 1980

Eutropis Clade G, Barley et al., 2013

Holotype.—KU 302873, collected by C. D. Siler 18 November 2000 near Barangay Tinogboc, Municipality of Caluya, Antique Province, Semirara

Paratypes.—KU 304013, collected by R. M. Brown, C.D. Siler, V. Yngente, and C.W. Linkem, 12 December 2005, Barangay Vigo, Municipality of Lubang, Occidental Mindoro Province, Lubang; KU 320491, collected by C. D. Siler, V. Yngente, and J. Fernandez, Sitio Dangay, Barangay Vigo, Municipality of Lubang, Occidental Mindoro Province, Lubang.

Referred specimens.—Lubang Island, Occidental Mindoro Province, Municipality of Lubang, Barangay Vigo, Sitio Dangay: KU 320490, 320492; Turtle Island, Sabah, Malaysia, LSUHC 6178.

Diagnosis.—A species of *Eutropis*, distinguished by the following combination of characters: (1) body size medium, SVL 73.7–88.6 in adults; (2) interparietal medium, parietals in touching posteriorly; (3) paravertebrals 41–47; (4) total subdigital toe lamellae I–V 82–89; (5) ventral scales rows 29–30; (6) midbody scale rows 30–32; (7) geographically distributed on Lubang and Semirara Islands in the Philippines, and Turtle Island, Malaysia.

Comparisons.—Critical comparisons for *Eutropis islamaliit* include *E. indeprensa*, *E. cumingi*, *E. borealis*, and *E. multifasciata*. *Eutropis semirara* can be readily distinguished from *E. indeprensa* and *E. cumingi* by its larger number of subdigital toe lamellae (82–89 vs. 69–75 or 55–67). It can be distinguished from *E. multifasciata* by its smaller maximum body size, and its more strongly and numerously (3 vs. 6–9) keeled dorsal scales. Due to our small sample size of specimens for this species, we are unable to confidently assess variation in this species. Thus, it is also difficult to reliably diagnosis of this species with respect to its sister species (*E. borealis*) based on morphology, although molecular data clearly indicate the distinctiveness of both taxa (Barley et al., 2013). *Eutropis islamaliit* does appear to exhibit a slightly larger body size and more vertebral scale rows (though there is substantial overlap in these characters). The new species also has a tendency towards a higher number of ventral scale rows and a larger interparietal than *E. borealis*.

Description of holotype.—A large male (SVL 88.6 mm). Body robust (axilla–goin distance/SVL = 0.5); limbs well developed (hind limb length/SVL = 0.3; front limb length/SVL = 0.3); tail long (SVL/tail length = 0.5); head robust (head length/SVL = 0.2), longer than wide (head width/head length = 0.9).

Snout tapered, rounded at tip. Rostral broader than high, in contact with frontonasal and nasals; frontonasal wider than long, in contact with nasals, frontal, prefrontals, rostral, and anterior loreal; prefrontals separated, contacting anterior and posterior loreals, 1st and 2nd suproculars, frontal and rostral; frontal longer than wide, in broad contact with 2nd supraocular, fused with frontoparietals; four supraoculars, 2nd largest; five supraciliaries; frontoparietals fused; interparietal medium; parietals touching posteriorly.

Head scales embossed; one pair of enlarged nuchals; nasal pierced in center by naris, surrounded anteriorly by rostral, posteriorly by anterior loreal, dorsally by supranasal, and ventrally by 1st suprlabial; supranasals long and narrow, not in contact at midline; 6 supralabials, 5th elongate, beneath center of eye; 6 infralabials; tympanum moderately sunk, without lobules.

Body elongate, with 47 paravertebrals, midbody scale rows 32, ventrals 30; dorsal and lateral scales with 7–9 keels, ventral scales smooth; tail elongate, 1.9 times body length. Forelimbs smaller than hind limbs, all limbs pentadactyl; forelimb scales smaller than body scales, keeled; relative digit length with subdigital lamellae in parentheses (L/R): IV(20/20) = III(18/19) > II(13/14) > V(12/12) > I (8/8). Hind limbs moderate (hind limb length/axilla–groin distance = 0.7), scales smaller than body scales, keeled; relative digit length with lamellae (L/R) in parentheses: IV(28/25) > III(22/21) > V(17/17) > II(13/13) > I(8/9).

Measurements of holotype.— SVL 88.6; tail length 171.7; axilla-groin distance 41.2; hind limb length 27.3; forelimb length 22.2; snout-forelimb length 31.2; head length 17.5; head width 12.2; interorbital distance 9.9; internarial distance 4.0; eye diameter 3.8; auricular opening diameter 1.4.

Coloration.— The following color description was written in 2013 following six years of storage in 70% ethanol. Dorsal ground color dark greenish-olive to brown, with some interspersed dark streaks of brown. Thick, dark brown, longitudinal bands extend down lateral surfaces of body from posterior of eye to groin. Above these bands, some light scales are interspersed that separate the brown bands from the dorsal ground color. Venter grayish tan to bluish, with lighter chin and precloacals, as well as some dark mottling under the chin and head. On lateral surfaces of body, ventral coloration becomes darker dorsal and mottled with dark brown; this coloration stretches from the upper labials to the groin up to the dark brown lateral bands.

Dorsal surfaces of limbs and digits greenish-olive brown, with some mottling of dark brown spots on the pes and manus. Ventral surfaces of limbs mostly light grayish to blue with tan and dark brown coloring in some regions, intergrading with dark brown coloration on lateral surfaces. Ventral surfaces of digits brown to grayish, palmar surface of manus and plantar surface of pes tan to ivory. Head scales a relatively uniform greenish-olive brown color. Upper portion of supralabials dusky brown, lower portion tan to ivory, with dark bars separating each scale. Anterior lower labial scales ivory to tan, posterior lower labials becoming grayish-brown with dark bars. Color in life was unrecorded but in our experience, *Eutropis* specimen coloration in life is very similar to that in preservative.

Variation.— Morphometric and scale count data are summarized in Table 4.1. *Eutropis islamaliit* varies in the number of subdigital toe lamellae (9–10 under toe I, 12–14 under toe II, 20–22 under toe III, 25–29 under toe IV, and 17–20 under toe V). This new species also exhibits a narrow range of variation in subdigital finger III lamellae (17–19). Both the supralabials and infralabials vary (6 or 7), and ventral scale rows (29–30), paravertebrals (37–46), and midbody scale rows (30–32) exhibit some variation. The number of keels on the dorsal scales ranges within and among individuals (6–9). Additionally, although the frontoparietals are fused in the holotype, this is the only specimen to exhibit this condition (all others have frontoparietals separate).

Dorsal color pattern varies slightly, in the degree of dark brown streaking present. The color of the dark brown lateral bands also varies, with some portions having a mottled dark and light brown color.

Distribution.—*Eutropis islamaliit* is known only from Lubang Island and Semirara Island in the Philippines. It has also been found on Turtle Island, Sabah, Malaysia. Presumably this species also occurs on the intervening large islands of Mindoro and Palawan, however, few historical specimens exist from these islands (Brown and Alcala, 1980), and recent, fairly extensive herpetofauna surveys (by RMB and ACD) have failed to secure additional specimens or genetic samples that could confirm if this species is indeed present there. The presence of this species only on small islands on the periphery of larger landmasses suggests an interesting biogeographical phenomenon or competitive interactions between species. This species curious distribution leaves questions for future research.

Habitat and natural history.—This species is known from very few specimens, however, it can be found in both primary and secondary growth forest. Specimens have been collected when found active on stream banks, tree trunks, and the forest floor. *Eutropis islamaliit* is known to occur sympatrically with *E. cumingi* and *E. multifasciata*.

Etymology.—The specific epithet is an adjectival derivation from the Tagalog noun *isla* (meaning island) and adjective *maliit* (meaning small) in reference to fact that the only specimens that have been collected for which there are genetic samples to confirm their identity are from three small, offshore islands. We name this species to draw attention to the importance of these small peripheral islands, which are often disregarded for conservation management planning. The name is feminine in gender.

Eutropis lapulapu new species

Mabuia multicarinata (part) Boettger, 1893.

Mabuya multicarinata (part) Taylor, 1917.

Mabuya indeprensa, Brown and Alcala, 1980

Mabuya indeprensa, Ferner et al., 2000

Eutropis Clade C, Barley et al., 2013

Holotype.—KU 310781, Collected by C. D. Siler and C. W. Linkem 13 October 2007, Barangay San Rafael, Municipality of Taft, Eastern Samar Province, Samar Island.

Paratypes.—KU 302876, collected by C. D. Siler and C.W. Linkem 24 November 2001 at 180 m., Barangay Duyong, Municipality of Pandan, Antique Province, Panay Island; KU 306194, collected by C. W. Linkem and C. D. Siler 24 June 2006, near Barangay Esperanza, Municipality of Loreto, Dinagat Islands Province, Dinagat Island; KU 306195, collected by C. W. Linkem 26 June 2006 at 40 m., Barangay San Juan, Municipality of Loreto, Dinagat Islands Province; KU 306200, 306201 (collected by C. D. Siler 16 June 2006), KU 310340 (collected by R. M. Brown 3 October 2007), 310781 (collected by C. D. Siler 13 October 2007), Barangay San Rafael, Municipality of Taft, Eastern Samar Province, Samar Island; KU 331836, collected by J. Fernandez 11 December 2011 at 400 m., Mt. Lantoy, Municipality of Argao, Cebu Province, Cebu Island; KU 306197, 306199, collected by C. W. Linkem and C. D. Siler 7 July 2006 at 30 m., Barangay Maangas, Municipality of Presentacion, Camarines del Sur Province, Luzon Island; CAS 27478 collected by L. C. Alcala 9 March 1967, Buhisan Barrio, Cebu City Province, Cebu Island; CAS 24673 collected by D. S. Rabor 31 May 1964, Municipality of Mahaplag, Leyte del Sur Province, Leyte Island.

Referred specimens.—Panay Island, Antique Province, Municipality of Pandan, Barangay Duyong: KU 302874, 302875, 305175–305177; Samar Island, Eastern Samar Island, Municipality of Taft, Barangay San Rafael, Taft Forest: KU 306202, 306204, 306205, 310783; Mindanao Island, Agusan del Sur Province, Municipality of San Francisco, Barangay Kaimpugan, Agusan Marsh: KU 314104; Zamboanga City Province, Municipality of Pasonanca, Pasonanca Natural Park, Barangay Baluno: KU 315006; Cebu Island, Cebu Province, Municipality of Argao, Mount Lantoy: KU 331837.

Diagnosis.—A species of *Eutropis*, distinguished by the following combination of characters: (1) adult body size small to medium, SVL 45.6–69.7; (2) interparietal relatively large, separating parietals; (3) paravertebrals 39–45; (4) total subdigital toe lamellae 65–77; (5) ventral scales rows 25–29; (6) midbody scale rows 27–33; (7) geographically distributed in the southern and central Philippine islands (including Mindanao, Samar, Dinagat, Panay, Cebu, and the Bicol Peninsula of Luzon).

Comparisons.— Critical comparisons for *Eutropis lapulapu* include sympatric taxa *E. caraga*, *E. multicarinata, E. borealis, E. rugifera*, and *E. multifasciata.* If this species distribution extends into the Sulu Archipelago, the new species may also exist sympatrically with *E. rudis*. *Eutropis lapulapu* can easily distinguished from the much larger, more robust species *E. rudis* and *E. multifasciata* by its small body size. It also has 5–9 dorsal scale keels (vs. only three in *E. multifasciata* and *E. rudis*). *Eutropis lapulapu* can easily be distinguished from *E. rugifera*, which has a much larger body size, a smaller interparietal, and parietals in contact posteriorly (vs. not in contact in *E. lapulapu*). *Eutropis rugifera* also has dorsal body scale keels that are more raised and sharply defined, and lacks the broad, dark dorsolateral body (present in *E.*

lapulapu). As a member of the *E. indeprensa* species complex, *E. lapulapu* can be distinguished from *E. multicarinata, E. borealis,* and *E. caraga* by its smaller maximum body size (Table 4.1). It can also be distinguished from *E. borealis* by having a large interparietal that separates the parietals (vs. small with parietals in contact).

Description of holotype.—A large, gravid female (SVL 58.0 mm). Body robust (axilla–goin distance/SVL = 0.5); limbs well developed (hind limb length/SVL = 0.2; front limb length/SVL = 0.2); regenerated tail; head robust (head length/SVL = 0.2), longer than wide (head width/head length = 0.7).

Snout tapered, rounded at tip. Rostral broader than high, in contact with frontonasal and nasals; frontonasal wider than long, in contact with nasals, prefrontals, rostral, and anterior loreal; prefrontals in contact, also in contact with anterior and posterior loreals, 1st and 2nd suproculars, frontal and rostral; frontal longer than wide, in broad contact with 2nd supraocular; four supraoculars, 2nd largest; five supraciliaries; frontoparietals not fused; interparietal large, separating parietals.

Head scales embossed; one pair of enlarged nuchals; nasal pierced in center by naris, surrounded anteriorly by rostral, posteriorly by anterior loreal, dorsally by supranasal, and ventrally by 1st suprlabial; supranasals long and narrow, not in contact at midline; 6 supralabials, 5th elongate, beneath center of eye; 7 infralabials; tympanum moderately sunk, without lobules.

Body elongate, with 42 paravertebrals, midbody scale rows 31, ventrals 28; dorsal and lateral scales with 8–9 keels, ventral scales smooth; tail elongate, but regenerating, 0.8 times body length. Forelimbs smaller than hind limbs, all limbs pentadactyl; forelimb scales smaller than body scales, keeled; relative digit length with subdigital lamellae in parentheses (L/R):

IV(19/16) = III(16/16) > II(12/13) > V(11/11) > I (8/7). Hind limbs moderate (hind limb length/axilla–groin distance = 0.5), scales smaller than body scales, keeled; relative digit length with lamellae (L/R) in parentheses: IV(24/23) > III(19/19) > V(15/15) > II(11/12) > I(8/7).

Measurements of holotype (in mm).—SVL 58.0; tail length 44.7; axilla-groin distance 26.1; hind limb length 14.1; forelimb length 12.1; snout-forelimb length 12.0; head length 12.4; head width 9.0; interorbital distance 6.2; internarial distance 2.7; eye diameter 3.1; auricular opening diameter 0.9.

Coloration.— The following color description was written in 2013 following six years of storage in 70% ethanol. Dorsal ground color nearly solid dark greenish-olive to brown, though some dark streaks of brown mark the margins of some scales. Thick, dark brown, longitudinal bands extend down lateral surfaces of body from posterior of eye to groin. A light stripe extending from behind the head, down the body halfway between the axilla and groin separates the dorsal surface and the dark brown bands on the lateral surface. Venter grayish tan to bluish, with lighter chin and precloacals. Margins of ventral scales dark, grey, with central portions light tan. On lateral surfaces of body, ventral coloration becomes mottled with streaks of dark brown; a prominent, light stripe from the upper labials extends down the lateral surface of the body, below the ear, to the groin.

Dorsal surfaces of limbs and digits greenish-olive brown, mottled with dark brown spots. Ventral surfaces of limbs mostly light grayish to blue, intergrading with dark brown coloration on lateral surfaces. Ventral surfaces of digits dark brown, palmar surface of manus and plantar surface of pes tan to ivory. Head scales uniformly greenish-olive brown, as in the dorsal ground color. Upper labials mostly tan to ivory, though the upper edge of some scales exhibits a dark brown color. Lower labials also tan to ivory, with dark bars on the more posterior scales. Color in life was unrecorded but in our experience, *Eutropis* specimen coloration is very similar to that in preservative.

Variation.— Morphometric and scale count data are summarized in Table 4.1. *Eutropis caraga* varies in numbers of subdigital toe lamellae (8–10 under toe I, 8–11 under toe II, 17–19 under toe III, 18–24 under toe IV, and 12–17 under toe V). Both the supralabials and infralabials vary slightly (6 or 7), as do supraciliaries (4 or 5), ventral scale rows (25–29), paravertebrals (39–45), and midbody scale rows (27–33). Numbers of dorsal body scale keels ranges both within and among individuals (5–9). Prefrontals usually separated (KU 302875, 302876, 306204, 331836), but sometimes in contact (KU 306201).

Dorsal color pattern varies in terms of the amount of dark streaking and blotches present. The ventral surface of most individuals is relatively uniform, though some individuals have several small dark flecks dispersed randomly. The thick dark stripe on the lateral surface of the body varies in color from solid brown to extensively mottled throughout. The light stripe above the dorsolateral band varies from faint and short (KU 310340, 310783) to bright and long (KU 306200, 306202). The stripe below the dorsolateral band also varies from short (KU 302876) to and long (KU 306201). Some individuals exhibit dark spots on the head scales (KU 306200, 306205).

Distribution.— *Eutropis lapulapu* appears to be distributed throughout the islands of the central and southern Philippines, and is known from the Bicol Peninsula on Luzon island, localities throughout Mindanao island, as well as Samar, Dinagat, Panay, and Cebu islands.

Habitat and natural history.—*Eutropis lapulapu* can be found in primary and secondary growth forest throughout its range, and in peat swamp forest on Mindanao Island. It also appears to tolerate disturbance well, as it has been found in agricultural and residential areas, as well as coconut field. It is a diurnally active species that can be found under logs, on stream banks, and on the forest floor, as well as in open areas near forest from sea level to 800 m. This species can be found sympatrically with five other species of *Eutropis*, but only one (*E. multifasciata*) is sympatric throughout its range. *Eutropis lapulapu* occurs sympatrically with *E. multicarinata* in northeastern Mindanao and on Dinagat, Siargao, and Leyte, with *E. caraga* throughout Mindanao, Dinagat, Siargao, and Bohol, with *E. borealis* in the Visayan Islands and the Bicol Peninsula (Luzon), and with *E. rugifera* in the Zamboanga Peninsula (Mindanao). A morphologically indistinguishable, but genetically divergent population (known only from several specimens) that appears to represent a distinct species (see "Clade B" in Fig. 4.2) also occurs on the island of Panay (Barley et al., 2013). However, the ranges of these two distinct genetic clades are not well understood on Panay Island, as only a single population of each has been sequenced to confirm its genetic identity. *Eutropis lapulapu* is known from a population in the Municipality of Pandan in the extreme northwest portion of the island, and the other distinct population is known only from the southern Panay population in the Municipality of San Remigio.

Etymology.—We are pleased to name this species in honor of the Philippine National Hero, Lapu-Lapu who is considered to be the first Filipino native to have resisted Spanish colonization. Lapu-Lapu was a ruler on the island of Mactan in the Visayas, where this species is known to occur.

Discussion

Philippine *Eutropis* historically have been a taxonomically confusing group, representing the more complex and difficult end of the species delimitation spectrum (Barley et al., 2013). In systems like Philippine *Eutropis*, distinct evolutionary lineages (species) may be well differentiated genetically, but not morphologically, presumably because morphological differentiation may not have accompanied speciation. Pluralistic approaches to species delimitation, utilizing multiple datasets (e.g. morphology, geographic range, and multiple genetic loci) and analyses, can help identify species level lineages in these poorly understood vertebrate clades (Barley et al., 2013; Linkem and Brown, 2013; Siler et al., 2013; Welton et al., 2013). However, species delineation can remain problematic even when rigorous approaches are employed, as is the case in Philippine *Eutropis*. In this island radiation, morphological divergence is only associated with speciation in some instances. This variation in the association of morphological and molecular divergence renders reliance on morphological data to delimit species problematic. It also makes determining if lineages are truly genetically isolated tantamount to the species delimitation process. Although newly developed analytical approaches represent important progress on this front (e.g. Yang and Rannala, 2010; Carstens et al., 2013; Grummer et al., 2014), and genomic approaches now allow for more robust datasets to be collected, challenges still remain, particularly when species divergences are relatively recently, or if they occurred rapidly (Petren et al., 2005; Shaffer and Thomson, 2007).

In this paper and Barley et al. (2013) we have taken an arguably conservative approach to delimiting Philippine sun skink diversity. Consequently, several taxonomic ambiguities remain. Future research should focus on addressing the following in order to clarify the taxonomic status of several distinct populations. As mentioned previously, genetic data have yet to be obtained for the enigmatic *E. englei*, although several characteristics of this taxon indicate it likely represents a distinct species. It possesses a highly distinctive morphology that is remarkably similar to *E. bontocensis*, and unlike any other species in the southern Philippines. Both taxa posses a bright contrasting series of stripes down the length of the body, are smaller bodied, and possess less distinctly keeled dorsal body scales than other species in the *E. multicarinata* species complex. However, both also have small geographic ranges and documented populations are separated by considerable geographic distances. *Eutropis englei* also exhibits a unique habitat preference, appearing to be restricted to coastal beach habitats or open areas along river mouths (Taylor, 1925). Thus, determining which species *E. englei* is most closely related to remains an intriguing question. Future taxonomic inquires in this group should focus on additional population and/or genetic sampling to determine if several of the morphologically indistinguishable divergent gene lineages identified by Barley et al. (2013) are genetically isolated and characterized by a lack of gene flow with congeners.

Barley et al. (2013) identified two additional, highly distinct populations based on genetic data of individuals that lack corresponding voucher specimens (Clade A and Clade B). We refrain from describing them here because each is represented by a single adult specimen. The two populations appear to represent isolated lineages, one being endemic to South Cotobato Province in extreme southwestern Mindanao (Clade A; KU 327372) and the other to San Remigio in Southwestern Panay (Clade B; KU 306810). Future surveys targeting these regions would be valuable for obtaining additional specimens for morphological characterization and determining if these species occur syntopically with other *Eutropis* species.

Eutropis borealis populations in the Visayan Islands also warrant future investigation, as individuals from Negros, Panay, and Siquijor are somewhat genetically divergent from each other, and from populations in the northern Philippines. Surveys targeting populations on these islands, and those between them (e.g. Mindoro, Sibuyan, Masbate) would allow for the range of this species to be better characterized, and dense sampling would allow for the determination of whether genetic divergence is based purely on geographic distance between populations, or due to one or more speciation events.

Lastly, the collection of population genomic data (e.g. RADseq SNP data) that could be used to obtain robust gene flow and/or divergence time estimates would be valuable for determining the extent of genetic isolation among some of the less divergent population groups. This includes populations of *E. caraga* (from Mindanao, Bohol, Siargao, and Dinagat), as well as populations of *E. cumingi* (in the Cordillera Mountain range vs. the rest of Luzon), *E. indeprensa*, and Clade D (on Palawan; Fig. 4.2).

Conclusions

Although taxonomy and species identification within Philippine *Eutropis* (and the genus in general) will continue to be a complex problem for future studies, a biologically accurate understanding of species diversity in this evolutionary radiation is an obtainable goal, which will allow for more appropriate conservation and management decisions to be made. Although in some cases, species identification in the field will be problematic due to highly conserved external morphology, the use of a species' geographic range information, in combination with the morphological traits we have surveyed, will allow for straightforward species identification in most cases. Additionally, future ecological studies that may provide additional data for distinguishing sympatric species are grounds for future inquiry.

Key to Philippine *Eutropis*

1a.	Dorsal scale keels 3, body size large (61–97 mm)	2
1b.	Dorsal scale keels >3, body size small to medium (40–89 mm)	3
2a.	Head scales smooth, dorsal scale keels weak, prefrontals in contact	*E. multifasciata*
2b.	Head scales embossed posteriorly, dorsal scale keels strong, prefrontals separate, Southwestern Philippines	*E. rudis*
3a.	Broad, dark lateral bands absent, sharply defined dorsal scale keels, Southwestern Philippines	*E. rugifera*
3b.	Broad, dark lateral bands present, dorsal keels less sharply defined	4
4a.	Bright dorsolateral stripes extending the length of the body present, dorsal scale keels less sharply raised	5
4b.	Distinct dorsolateral stripes not present, dorsal scale keels more sharply raised	6
5a.	Mindanao Island	*E. englei*
5b.	Luzon, Babuyan, or Batanes Islands	*E. bontocensis*
6a.	Body size medium (60–89 mm), robust	7
6b.	Body size small (43–69 mm), slender	11
7a.	Interparietal large, parietals separate, Southern Philippines	8
7b.	Interparietal small, parietals in contact, Northern/Central	

	Philippines/Borneo	9
8a.	NE Mindanao, Leyte, Dinagat	*E. multicarinata*
8b.	Siargao, Dinagat, Mindanao, Bohol	*E. caraga*
9a.	Lubang, Semirara, Borneo	*E. islamaliit*
9b.	Northern/Central Philippines	10
10a.	N. Luzon, Babuyan Islands	*E. gubataas*
10b.	Luzon, Babuyan Islands, Polillo, Catanduanes, Negros, Panay, Siquijor	*E. borealis*
11a.	Northern Philippines	12
11b.	Southern Philippines (Mindanao, Samar, Dinagat, Panay, Cebu, Bicol Peninsula)	*E. lapulapu*
12a.	Mindoro/Borneo; hind limb length/SVL ratio generally larger (0.45–0.58)	*E. indeprensa*
12b.	N. Luzon, Batanes/Babuyan Islands, Lubang; hind limb length/SVL ratio generally smaller (0.37–0.45)	*E. cumingi*

Table 4.1 Summary of morphometric, meristic, and sample size data for Philippine *Eutropis*. For interparietal, parietals: S = interparietal small, L = interparietal large, C = parietals in contact, N = parietals not in contact. Measurements in millimeters.

	E. bontocensis (n=20)	*E. borealis* (n=22)	*E. caraga* (n=18)	*E. cumingi* (n=14)	*E. gubataas* (n=13)
Snout–vent length	40.1–61.2	64.1–82.5	64.5–83.9	43.5–60.0	60.5–78.7
Axilla–groin	22.4–29.5	27.4–41.4	28.6–40.7	21.4–26.9	27.0–40.3
Head Length	9.7–13.8	14.0–17.6	13.6–19.3	8.6–11.6	12.2–18.0
Head Width	6.8–9.8	10.4–13.3	10.0–14.6	6.1–8.6	10.2–13.0
Forelimb length	9.4–13.6	11.0–18.7	13.4–19.8	7.6–11.1	12.0–19.3
Hind limb length	11.4–16.6	15.1–24.8	17.4–24.7	9.4–12.2	15.6–22.2
Total toe lamellae	67–74	79–88	73–88	55–67	74–87
Vertebral scale rows	44–50	37–42	35–43	43–49	37–46
Ventral scale rows	29–33	24–28	26–30	27–32	26–30
Midbody scale rows	29–34	28–33	27–34	28–33	30–36
Interparietal, parietals	S, C	S, C	L, N	L, N	S, C

	E. indeprensa (n=6)	*E. lapulapu* (n=20)	*E. multicarinata* (n=6)	*E. islamaliit* (n=5)
Snout–vent length	54.0–63.8	45.6–69.7	61.1–71.3	73.7–88.6
Axilla–groin	24.9–28.7	21.3–32.3	29.6–36.1	35.0–41.2
Head Length	10.3–13.5	9.6–14.0	13.5–15.8	15.3–19.4
Head Width	7.9–9.9	7.1–11.2	10.0–12.9	11.5–17.4
Forelimb length	11.9–14.9	9.3–15.5	14.6–16.9	17.9–22.2
Hind limb length	14.7–18.4	11.4–19.4	18.0–23.1	21.8–27.3
Total toe lamellae	69–75	65–77	71–82	82–92
Vertebral scale rows	41–47	39–45	35–38	41–47
Ventral scale rows	26–31	25–29	22–28	29–30
Midbody scale rows	29–33	27–33	30–33	30–32
Interparietal, parietals	L, N	L, N	L, N	S, C

Figure 4.1 Map of Philippine Archipelago indicating islands of particular significance for Philippine *Eutropis*.

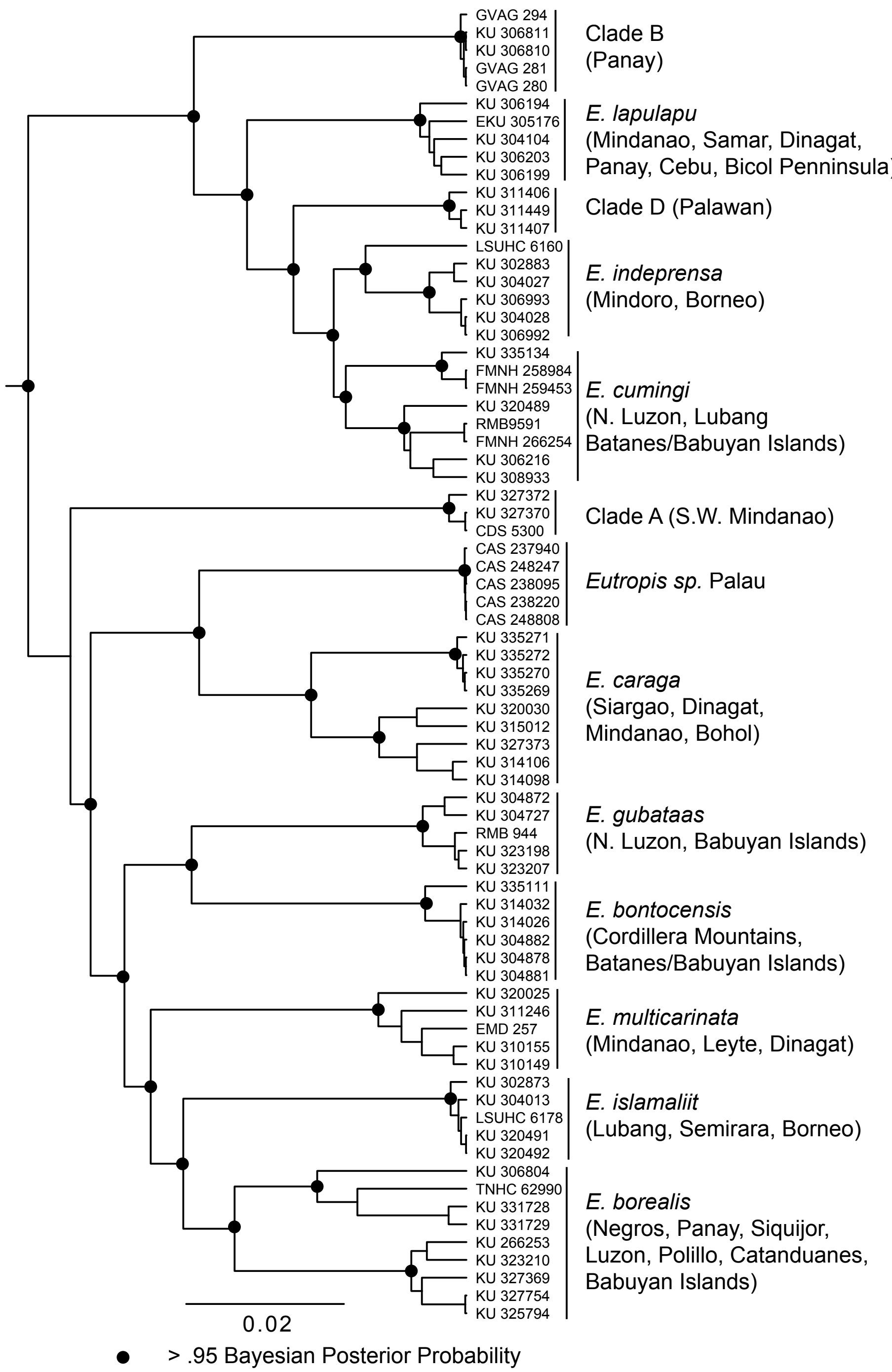

Figure 4.2 Maximum clade credibility tree from concatenated BEAST phylogenetic analysis for 74 individuals, 7 genes (1 mitochondrial, 6 nuclear) for Philippine *Eutropis* (figure adapted from Barley et al., 2013).

Literature Cited

Alföldi J, et al. 2011. The genome of the green anole lizard and a comparative analysis with birds and mammals. *Nature* 477:587–591.

Andolfatto P, Davison D, Erezyilmaz D, Hu TT, Mast J, Sunayama-Morita T, Stern DL. 2011. Multiplexed shotgun genotyping for rapid and efficient genetic mapping. *Genome Research* 21:610–617.

Andrews S. 2012. Fast QC Version 0.10.1. Available: http://www.bioinformatics.babraham.ac.uk/projects/fastqc/

Atchison JC, Ali JR, Davis AM. 2007. When and where did India and Asia collide? *Journal of Geophysical Research: Solid Earth* 112:1–19.

Austin CC. 1995. Molecular and morphological evolution in south Pacific scincid lizards: morphological conservatism and phylogenetic relationships of Papuan *Lipinia*. *Herpetologica* 51:291–300.

Baldwin BG. 1997. Adaptive radiation of the Hawaiian silversword alliance: Congruence and conflict of phylogenetic evidence from molecular and non-molecular investigations. In: Givnish TJ, Systma K (Eds.). *Molecular Evolution and Adaptive Radiation*. Cambridge University Press, Cambridge, pp. 103–128.

Barley AJ, Spinks PQ, Thomson RC, Shaffer HB. 2010. Fourteen nuclear genes provide phylogenetic resolution for difficult nodes in the turtle tree of life. *Molecular Phylogenetics and Evolution* 55:1190–1194.

Barley AJ, White J, Diesmos AC, Brown RM. 2013. The challenge of species delimitation at the extremes: diversification without morphological change in Philippine sun skinks. *Evolution* 67:3556–3572.

Barrett CF, Freudenstein JV. 2011. An integrative approach to delimiting species in a rare but widespread mycoheterotrophic orchid. *Molecular Ecology* 20:2771–2786.

Barrett RDH, Hoekstra HE. 2011. Molecular spandrels: tests of adaptation at the genetic level. *Nature Reviews Genetics* 12:767–780.

Bauer AM, Parham JF, Brown RM, Stuart BL, Grismer LL, Papenfuss TJ, Böhme W, Savage JM, Carranza S, Grismer JL, Wagner P, Schmitz A, Anajeva NB, Inger RF. 2010. Availability of new Bayesian-delimited gecko names and the importance of character-based species descriptions. *Proceedings of the Royal Society London B Biological Sciences* 278:490–492.

Benavides E, Baum R, McClellan D, Sites Jr. JW. 2007. Molecular phylogenetics of the lizard genus Microlophus (Squamata: Tropiduridae): aligning and retrieving indel signal from nuclear introns. *Systematic Biology* 56:776–797.

Bickford D, Lohman DJ, Sodhi NS, Ng PKL, Meier R, Winker K, Ingram KK, Das I. 2007. Cryptic species as a window on diversity and conservation. *Trends in Ecology and Evolution* 22:148–155.

Blackburn DC, Siler CD, Diesmos AC, McGuire JA, Cannatella DC, Brown RM. 2013. An adaptive radiation of frogs in a Southeast Asian island archipelago. *Evolution* 67:2631–2646.

Blythe E. 1853. Notices and descriptions of various reptiles, new or little-known. *Journal of the Asiatic Society of Bengal* 22:639–655.

Bobrov VV. 1992 A new scincid lizard (Reptilia Sauria Scincidae) from Vietnam. *Zoologichseskii Zhurnal* 71:156–158.

Bock W. 1970. Microevolutionary sequences as a fundamental concept in macroevolutionary models. *Evolution* 24:704–722.

Boetteger O. 1893. Katalog der Reptilien – Sammlung im Museum der Senckenbergischer Naturforschender Gesellschaft in Frankfurt am Main, Frankfurt.

Boulenger GA. 1887. Catalogue of Lizards in the British Museum (Natural History), London.

Bradburd GS, Ralph PL, Coop GM. 2013. Disentangling the effects of geographic and ecological isolation on genetic differentiation. *Evolution* 67:3258–3273.

Brandley MC, Huelsenbeck JP, Wiens JJ. 2008. Rates and patterns in the evolution of snake-like body form in squamate reptiles: evidence for repeated re-evolution of lost digits and long-term persistence of intermediate body forms. *Evolution* 62:2042–2064.

Briggs JC. 1989. The historic biogeography of India: isolation or contact? *Systematic Zoology* 38:322–332.

Brommer JE. 2011. Whither P_{ST}? The approximation of Q_{ST} by P_{ST} in evolutionary and conservation biology. *Journal of Evolutionary Biology* 24:1160–1168.

Brown RM, McGuire JA, Ferner JW, Icarangal Jr. N, Kennedy RS. 2000. Amphibians and reptiles of Luzon Island, II: preliminary report on the herpetofauna of Aurora Memorial National Park, Philippines. *Hamadryad* 25:175–195.

Brown RM, Guttman SI. 2002. Phylogenetic systematics if the *Rana signata* complex of Philippine and Bornean stream frogs: reconsideration of Huxley's modification of Wallace's Line at the Oriental-Australian faunal zone interface. *Biological Journal of the Linnean Society* 76:393–461.

Brown RM, Diesmos AC. 2009. Philippines, Biology. In: Gillespie R, Clague D (Eds.). *Encyclopedia of Islands*. University of California Press, Berkeley, CA, pp. 723–732.

Brown RM, Oliveros CH, Siler CD, Fernandez JB, Welton LJ, Buenavente PAC, Diesmos MLD, Diesmos AC. 2012. Amphibians and Reptiles of Luzon Island (Philippines), VII: Herpetofauna of Ilocos Norte Province, Northern Cordillera Mountain Range. *Check List* 8:469–490.

Brown RM, Siler CD, Grismer LL, Das I, McGuire JA. 2012. Phylogeny and cryptic diversification in Southeast Asian flying geckos. *Molecular Phylogenetics and Evolution* 65:351–361.

Brown RM, Siler CD, Oliveros CH, Esselstyn JA, Diesmos AC, Hosner PA, Linkem CW, Barley AJ, Oaks JR, Sanguila MB, Welton LJ, Blackburn DS, Moyle RG, Peterson AT, Alcala AC. 2013. Evolutionary processes of diversification in a model island archipelago. *Annual Review of Ecology, Evolution, and Systematics* 44:1–24.

Brown RM, Siler CD, Oliveros CH, Welton LJ, Rock A, Swab J, Van Weerd M, van Beijnen J, Jose E, Rodriguez D, Jose E, Diesmos AC. 2013. The amphibians and reptiles of Luzon Island, Philippines, VIII: the herpetofauna of Cagayan and Isabela Provinces, northern Sierra Madre Mountain Range. *ZooKeys* 266:1–120.

Brown WC, Alcala AC. 1980. *Philippine lizards of the family Scincidae*. Silliman University Press, Dumaguete City, Philippines.

Bruna EM, Fisher RN, Case TJ. 1996. Morphological and genetic evolution appear decoupled in Pacific skinks (Squamata: Scincidae: *Emoia*). *Proceedings of the Royal Society London B: Biological Sciences* 263:681–688.

Burbrink FT, Yao H, Ingrasci M, Bryson Jr. RW, Guiher TJ, Ruane S. 2011. Speciation at the Mongolian Rim in the Arizona Mountain Kingsnake (*Lampropeltis pyromelana*). *Molecular Phylogenetics and Evolution* 60:445–454.

Caccone A, Milinkovitch MC, Sbodoni V, Powell JR. 1997. Mitochondrial DNA rates and biogeography in European newts (Genus *Euproctus*). *Systematic Biology* 46:126–144.

Calsbeek R, Thompson JN, Richardson JE. 2003 Patterns of molecular evolution and diversification in a biodiversity hotspot: the California Floristic Province. *Molecular Ecology* 12:1021–1029.

Camargo A, Avila LJ, Morando M, Sites Jr. JW. 2012. Accuracy and precision of species trees: effects of locus, individual, and base pair sampling on inference of species trees in lizards of the *Liolaemus darwinii* Group (Squamata, Liolaemidae). *Systematic Biology* 61:272–288.

Cannon CH, Morley RJ, Bush ABG. 2009. The current refugial rainforests of Sundaland are unrepresentative of their biogeographic past and highly vulnerable to disturbance. *Proceedings of the National Academy of Sciences* 106:11188–11193.

Carson JL. 1976. *Drosophila* of Hawaii: Systematics and ecological genetics. *Annual Review of Ecology and Systematics* 7:311–345.

Carstens BC, Dewey TA. 2010. Species delimitation using a combined coalescent and information-theoretic approach: an example from North American *Myotis* bats. *Systematic Biology* 59:400–414.

Carstens BC, Pelletier TA, Reid NM, Satler JD. 2013. How to fail at species delimitation. *Molecular Ecology* 22:4369–4383.

Catchen J, Amores A, Hohenlohe P, Cresko W, Postlethwait JH. 2011. *Stacks*: Building and genotyping loci *de novo* from short-read sequences. *G3: Genes, Genomes, Genetics* 1:171–182.

Ciofi C, Bruford MW. 1999. Genetic structure and gene flow among Komodo dragon populations inferred by microsatellite loci analysis. *Molecular Ecology* 8:S7–S30.

Clare EL. 2011. Cryptic species? Patterns of maternal and paternal gene flow in eight neotropical bats. *PLoS ONE* 6:1–13.

Cody ML. 1969. On the methods of resource division in grassland bird communities. *American Naturalist* 102:107–147.

Conservation International. 2008. Biological diversity in the Philippines. In: Cleveland CJ, McGinley M, (Eds.). *Encyclopedia of Earth*. National Council for Science and the Environment, Washington, DC.

Corlett RT. 2009. *The ecology of tropical East Asia*. Oxford University Press, Oxford.

Cracraft J. 2002. The seven great questions of systematic biology: an essential foundation for the conservation and sustainable use of biodiversity. *Annals of the Missouri Botanical Garden* 89:127–144.

Crispo E, Hendry AP. 2005. Does time since colonization influence isolation by distance? A meta-analysis. *Conservation Genetics* 6:665–682.

Crombie RI, Pregill GK. 1999. A checklist of the herpetofauna of the Palau Islands (Republic of Belau), Oceania. *Herpetological Monographs* 13:29–80.

Crowie RH, Holland BS. 2006. Dispersal is fundamental to biogeography and the evolution of biodiversity on ocean islands. *Journal of Biogeography* 33:193–198.

Das I. 2004. Lizards of Borneo. Natural History Publications, Kota Kinabalu, Borneo.

Das I, De Silva A, Austin CC. 2008. A new species of *Eutropis* (Squamata: Scincidae) from Sri Lanka. *Zootaxa* 1700:35–52.

Datta-Roy A, Singh M, Srinivasulu C, Karanth KP. 2012. Phylogeny of the Asian *Eutropis* (Squamata: Scincidae) reveals an 'into India' endemic Indian radiation. *Molecular Phylogenetics and Evolution* 63:817–824.

Davey JW, Blaxter ML. 2011. RADSeq: next-generation population genetics. *Briefings in Functional Genomics* 9:416–423.

Davey JW, Hohenlohe PA, Etter PD, Boone JQ, Catchen JM, Blaxter ML. 2011. Genome-wide genetic marker discovery and genotyping using next-generation sequencing. *Nature Reviews Genetics* 12:499–510.

de Queiroz A. 2005. The resurrection of oceanic dispersal in historical biogeography. *Trends in Ecology and Evolution*, 20:68–73.

de Queiroz K. 1998. The general Lineage concept of species, species criteria, and the process of speciation. In: Howard DJ, Berlocher SH (Eds.). *Endless forms: species and speciation*. Oxford University Press, New York, NY, pp. 57–75 de Queiroz K. 1999. The general Lineage concept of species and the defining properties of the species category. In: Wilson RA (Ed.). *Species: new interdisciplinary essays*. Massachusetts Institute of Technology Press, Cambridge, MA, pp. 49–89

de Queiroz K. 2005. A unified conceot of species and its consequences for the future of taxonomy. *Proceedings of the National Academy of Sciences USA* 56:196–215.

Dent EA, vonHoldt BM. 2012. STRUCTURE HARVESTER: a website and program for visualizing STRUCTURE output and implementing the Evanno method. *Conservation Genetics Resources* 4:350–361.

Derkarabetian S, Steinmann DB, Hedin M. 2010. Repeated and time-correlated morphological convergence in cave-dwelling harvestmen (Opiliones, Laniatores) from montane western North America. *PLoS ONE* 5:1–13.

Devan-Song A, Brown RM. 2012. Amphibians and Reptiles of Luzon Island, Philippines, VI: the Herpetofauna of the Subic Bay Area. *Asian Herpetological Research* 2012:1–20.

Diamond JM. 1969. Avifaunal equilibria and species turnover rates on the Channel Islands of California. *Proceedings of the National Academy of Sciences* 64:57–63.

Diamond JM, Gilpin ME. 1983. Biogeographic umbilic and the origin of the Philippine avifauna. *Oikos* 41:307–321.

Dmitriev DA, Rakitov RA. 2008. Decoding of superimposed traces produced by direct sequencing of heterozygous indels. *PLoS Computational Biology* 4:1–10.

Donnellan SC, Aplin KP. 1989. Resolution of cryptic species in the New Guinean lizard *Sphenomorphus jobiensis* (Scincidae) by electrophoresis. *Copeia* 1989:81–88.

Drummond AJ, Rambaut A. 2007. BEAST: Bayesian evolutionary analysis by sampling trees. *BMC Evolutionary Biology* 7:214.

Edwards S. 2008. Is a new and general theory of molecular systematics emerging? *Evolution* 63:1–19.

Egan SP, Nosil P, Funk DJ. 2008. Selection and genomic differentiation during ecological speciation: isolating the contributions of host associations via a comparative genome scan of *Neochlamisus bebbianae* leaf beetles. *Evolution* 62:1162–1181.

Ekblom R, Galindo J. 2011. Applications of next generation sequencing in molecular ecology of non-model organisms. *Heredity* 107:1–15.

Ellegren H. 2014. Genome sequencing and population genomics in non-model organisms. *Trends in Ecology & Evolution* 29:51–63.

Ence DD, Carstens BC. 2011. SpedeSTEM: a rapid and accurate method for species delimitation. *Molecular Ecology Resources* 11:473–480.

Esselstyn JA. 2007. Should universal guidelines be applied to taxonomic research? *Biological Journal of the Linnean Society* 90:761–764.

Esselstyn JA, Garcia HJD, Saulog MG, Heaney LR. 2008. A new species of *Desmalopex* (*Pteropodidae*) from the Philippines, with a phylogenetic analysis of the Pteropodini. *Journal of Mammalogy* 89:815–825.

Esselstyn JA, Timm RM, Brown RM. 2009. Do geological or climatic processes drive speciation in dynamic archipelagos? The tempo and mode of diversification in Southeast Asian shrews. *Evolution* 63:2595–2610.

Esselstyn JA, Oliveros CH, Moyle RG, Peterson AT, McGuire JA, Brown RM. 2010. Integrating phylogenetic and taxonomic evidence illuminates complex biogeographic patterns along Huxley's modification of Wallace's Line. *Journal of Biogeography* 37:2054–2066.

Evans BJ, Brown RM, McGuire JA, Supriatna J, Andayani N, Diesmos AC, Iskandar D, Melnick DJ, Cannatella DC. (2003) Phylogenetics of fanged frogs: testing biogeographical hypotheses at the interface of the Asian and Australian faunal zones. *Systematic Biology* 52:794–819.

Evanno G, Regnaut Sm Goudet J. 2005. Detecting the number of clusters of individuals using the software STRUCTURE: a simulation study. *Molecular Ecology* 14:2611–2620.

Ferner JW, Brown RM, Sison RV, Kennedy RS. 2001. The amphibians and reptiles of Panay Island, Philippines. *Asiatic Herpetological Research* 9:34–70.

Fitzinger LJ. 1826. Neue classification der Reptilien nach ihren naturlichen verwandtschaften, Vienna.

Foll M, Gaggiotti OE. 2008. A genome scan method to identify selected loci appropriate for both dominant and codominant markers: A Bayesian perspective. *Genetics* 180:977–993.

Frankham R, Ballou JD, Dudash MR, Eldridge MDB, Fenster CB, Lacy RC, Mendelson JR, Porton IJ, Ralls K, Ryder OA. 2012. Implications of different species concepts for conserving biodiversity. *Biological Conservation* 153:25–31.

Freeland JR, Boag PT. 1999. The mitochondrial and nuclear genetic homogeneity of the phenotypically diverse Darwin's ground finches. *Evolution* 53:1553–1563.

Friessen VL, Congdon BC, Kidd MG, Birt TP. 1999. Polymerase chain reaction (PCR) primers for the amplification of five nuclear introns in vertebrates. *Molecular Ecology* 8:2147–2149.

Frost DR, Hillis DM. 1990. Species in concept and practice: herpetological applications. *Herpetologica* 46:87–104.

Fujita MK, Leaché AD. 2011. A coalescent perspective on delimiting and naming species: a reply to Bauer et al. *Proceedings of the Royal Society London B Biological Sciences* 278:493–495.

Fujita MK, Leaché AD, Burbrink FT, McGuire JA, Moritz C. 2012. Coalescent-based species delimitation in an integrative taxonomy. *Trends in Ecology and Evolution* 27:480–488.

Funk CM, Caminer M, Ron SR. 2012. High levels of cryptic species diversity uncovered in Amazonian frogs. *Proceedings of the Royal Society London B Biological Sciences* 279:1806–1814.

Gittenberger E. 1991. What about non-adaptive radiation? *Biological Journal of the Linnean Society* 43:263–272.

Glenn T. 2011. Field guide to next-generation DNA sequencers. *Molecular Ecology Resources* 11:759–769.

Glor RE, Kolbe JJ, Powell R, Larson A, Losos JB. 2003. Phylogenetic analysis of ecological and morphological diversification in Hispaniolan trunk-ground anoles (*Anolis cybotes* group). *Evolution* 57:2283–2397.

Gompert Z, Forister ML, Fordyce JA, Nice CC, Williamson RJ, Buerkle A. 2010. Bayesian analysis of molecular variance in pyrosequences quantified population genetic structure across the genome of *Lycaedeis* butterflies. *Molecular Ecology* 19:2455–2473.

Gray JE. 1845. Catalogue of the specimens of lizards in the collection of the British Museum. London.

Grismer LL. 2011. *Lizards of Peninsular Malaysia, Singapore, and their adjacent archipelagos*. Edition Chimaira, Frankfurt.

Grummer JA, Bryson Jr. RW, Reeder TW. 2014. Species delimitation using Bayes factors: simulations and application to the *Sceloporus scalaris* species group (Squamata: Phrynosomatidae). *Systematic Biology* 63:119–133.

Guillot G, Rousset F. 2013. Dismantling the Mantel tests. *Methods in Ecology and Evolution* 4:336–344.

Hall R. 1998. The plate tectonics of Cenozoic SE Asia and the distribution of land and sea. In: Hall R, Holloway JD (Eds.). *Biogeography and geological evolution of SE Asia*. Backhuys Publishers, Leiden, pp. 99–131.

Hallowell E. 1857. Notice of some new and rare species of Scincidae in the collection of the Academy of Natural Sciences of Philadelphia. *Transactions of the American Philosophical Society, Philadelphia* 11:71–82.

Harley CDG, Pankey MS, Wares JP, Grosberg RK, Wonham MJ. 2006. Color polymorphism and genetic structure in the sea star *Pisaster ochraceus*. *Biological Bulletin* 211:248–262.

Heaney LR. 1985. Zoogeographic evidence for middle and late Pleistocene land bridges to the Philippine Islands. *Modern Quaternary Research in Southeast Asia* 9:127–144.

Heaney LR. 1986. Biogeography of mammals in SE AsiaL estimates of rates of colonization, extinction, and speciation. *Biological Journal of the Linnean Society* 28:127–165.

Heaney LR. 1991. A synopsis of climatic and vegetational change in Southeast Asia. *Climatic Change* 19:53-61.

Hedges SB, Conn CE. 2012. A new skink fauna from Caribbean islands (Squamata, Mabuyidae, Mabuyinae). *Zootaxa* 3288:1–244.

Heideman JL, Mulcahy DG, Sites Jr. JW, Hendricks MGJ, Daniels SR. 2011. Cryptic diversity and morphological convergence in the genus *Scelotes* (Squamata: Scincidae) from the Western Cape Coast of South Africa: Implications for species boundaries, digit reduction and conservation. *Molecular Phylogenetics and Evolution* 61:823–833.

Heled J, Drummond AJ. 2010. Bayesian inference of species trees from multilocus data. *Molecular Biology and Evolution* 27:570–580.

Hennig W. 1966. *Phylogenetic systematics*. University of Illinois Press, Urbana.

Highton R. 1989. Biochemical evolution in the slimy salamanders of the *Plethodon glutinosus* complex in the eastern United States. Chapter 1. Geographic protein variation. *Illinois Biological Monographs* 57:1–78.

Hijmans RJ, Cameron SE, Parra JL, Jones PG, Jarvis A. 2005. Very high resolution interpolated climate surfaces for global land areas. *International Journal of Climatology* 25:1965–1978.

Hohenlohe PA, Bassham S, Etter PD, Stiffler N, Johnson EA, Cresko WA. 2010. Population genomics of parallel adaptation in threespine stickleback using sequenced RAD tags. *PLoS Genetics* 6:e1000862.

Holland BS, Hadfield MG. 2004. Origin and diversification of the endemic Hawaiian tree snails (Achatinellidae: Achatinellinae) based on molecular evidence. *Molecular Phylogenetics and Evolution* 32:588–600.

Holt BG, Lessard JP, Borregaard MK, Fritz SA, Araújo MB, Dimitrov D, Fabre PH, Graham CH, Graves GR, Jønsson KA, Nogués-Bravo D, Wang Z, Whittaker RJ, Fjeldså J, Rahbek C. 2013. An update of Wallace's zoogeographic regions of the world. *Science* 339:74–78.

Howard SD, Gillespie GR, Riyanto A, Iskandar D. 2007. A new species of large *Eutropis* (Scincidae) from Sulawesi, Indonesia. *Journal of Herpetology* 41:604–610.

Huxley TH. 1868. On the classification and distribution of the Alectoromorphae and Heteromorphae. *Proceedings of the Zoological Society London* 1868:294–319.

Inger RF. 1954. Systematics and zoogeography of Philippine Amphibia. *Fieldiana* 33:181–531.

Inger RF, Shaffer HB, Koshy M, Bakde R. 1984. A report on a collection of amphibians and reptiles from Ponmudi, Kerala, South India. *Journal of the Bombay Natural History Society* 81:551–570.

Irschick DJ, Vitt LJ, Zani PA, Losos JB. 1997. A comparison of evolutionary radiation in mainland and West Indian *Anolis* lizards. *Ecology* 78:2191–2203.

Jackson ND, Austin CC. 2009. The combined effects of rivers and refugia generate extreme cryptic fragmentation within the common ground skink (*Scincella lateralis*). *Evolution* 64:409–428.

Jaquiery J, Broquet T, Hirzel AH, Yearsley J, Perrin N. 2011. Inferring landscape effects on dispersal from genetic distances: how far can we go? *Molecular Ecology* 20:692–705.

Jennings WB, Edwards SV. 2005. Speciational history of Australian grass finches (Poephila) inferred from 30 gene trees. *Evolution* 59:2033–2047.

Jensen JL, Bohonak AJ, Kelley ST. 2005. Isolation by distance, web service. *BMC Genetics* 6:13.

Jockusch EL, Wake DB. 2002. Falling apart and merging: diversification of slender salamanders (Plethodontidae: *Batrachoseps*) in the American West. *Biological Journal of the Linnean Society* 76:361–391.

Johnson T, Barton N. 2005. Theoretical models of selection and mutation on quantitative traits. *Philosophical Transactions of the Royal Society London B Biological Sciences* 360:1411–1425.

Jønsson KA, Bowie RCK, Moyle RG, Christidis L, Norman JA, Benz BW, Fjeldsa J. 2010. Historical biogeography of an Indo-Pacific passerine bird family (Pachycephalidae): different colonization patterns in the Indonesian and Melanesian archipelagos. *Journal of Biogeography* 37:245–257.

Katoh K, Kuma K, Toh H, Miyata T. 2005. MAFFT version 5: improvement in accuracy of multiple sequence alignment. *Nucleic Acids Resources* 33:511–518.

Kelly LC, Bilton DT, Rundle SD. 2001. Population structure and dispersal in the Canary Island caddisfly *Mesophylax asperses* (Trichoptera, Limnephilidae). *Heredity* 86:370–377.

Kimball RT, Braun EL, Barker FK, Bowie RCK, Braun MJ, Chojnowski JL, Hacket SJ, Han K, Han J, Harshman J, Heimer-Torres V et al. 2009. A well-tested set of resources to amplify nuclear regions across the avian genome. *Molecular Phylogenetics and Evolution* 50:654–660.

Knowles LL, Carstens BC. 2007. Delimiting species without monophyletic gene trees. *Systematic Biology* 56:887–895.

Kozak KH, Weisrock DW, Larson A. 2006. Rapid lineage accumulation in a non-adaptive radiation: phylogenetic analysis of diversification rates in eastern North American woodland salamanders (Plethodontidae: *Plethodon*). *Proceedings of the Royal Society London B Biological Sciences* 273:539–546.

Kozak KH, Wiens JJ. 2010. Accelerated rates of climate-niche evolution underlie rapid species diversification. *Ecology Letters* 11:1378–1389.

Kubatko LS, Degnan JH. 2007. Inconsistency of phylogenetic estimates from concatenated data under coalescence. *Systematic Biology* 56:17–24.

Kubatko LS, Gibbs HL, Bloomquist EW. 2011. Inferring species-level phylogenies and taxonomic distinctiveness using multilocus datasets in *Sistrurus* rattlesnakes. *Systematic Biology* 60:393–409.

Kuhl H. 1820. Beiträge zur Zoologie und vergleichenden Anatomie. Hermannsche Buchhandlung, Frankfurt.

Lande R. 1992. Neutral theory of quantitative genetic variance in an island model with local extinction and colonization. *Evolution* 46:381–389

Larson A. 1989. The relationship between speciation and morphological evolution. In: Otte D, Ender JA (Eds.). *Speciation and its consequences*. Sinauer, Sunderland, MA, pp. 579–598.

Lawlor TE. 1986. Comparative biogeography of mammals on islands. *Biological Journal of the Linnean Society* 28:99–125.

Leaché AD. 2009. Species tree discordance traces to phylogeographic clade boundaries in North American fence lizards (*Sceloporus*). *Systematic Biology* 58:547–559.

Leaché AD, Fujita MK. 2010. Bayesian species delimitation in West African forest geckos (*Hemidactylus fasciatus*). *Proceedings of the Royal Society London B Biological Sciences* 277:3071–3077.

Legendre P, Fortin MJ. 2010. Comparison of the Mantel test and alternative approaches for detecting complex multivariate relationships in the spatial analysis of genetic data. *Molecular Ecology Resources* 10:831–844.

Lehtonen PK, Laaksonen T, Artemyev AV, Belskii E, Both C, Bures S, Bushuev AV, Krams I, Moreno J, Mägi M, Nord A, Potti J, Ravussin PA, Sirkiä PM, Sætre GP, Primmer CR. 2009. Geographic patterns of genetic differentiation and plumage colour variation are different in the pied flycatcher (*Ficedula hypoleuca*). *Molecular Ecology* 18:4463–4476.

Leinonen T, McCarirns RJS, O'Hara RB, Merilä J. 2013. Q_{ST}–F_{ST} comparisons: evolutionary and ecological insights from genomic heterogeneity. *Nature Reviews Genetics* 14:179–190.

Li JT, Li Y, Klaus S, Rao DQ, Hillis DM, Zhang YP. 2013. Diversification of rhacophorid frogs provides evidence for accelerated faunal exchange between India and Eurasia during the Oligocene. *Proceedings of the National Academy of Sciences* 110:3441–3446.

Librado P, Rozas J. 2009. DnaSP v5: A software for comprehensive analysis of DNA polymorphism data. *Bioinformatics* 25:1451-1452.

Lim HC, Rahman MA, Lim SLH, Moyle RG, Sheldon FH. 2011. Revisiting Wallace's haunt: coalescent simulations and comparative niche modeling reveal historical mechanisms that promoted avian population divergence in the Malay Archipelago. *Evolution* 65:321–334.

Linkem CW, Hesed K, Diesmos AC, Brown RM. 2010. Species boundaries and cryptic lineage diversity in a Philippine forest skink complex (Reptiltia; Squamata; Scincidae; Lygosominae). *Molecular Phylogenetics and Evolution* 56:572–585.

Linkem CW, Brown RM, Siler CD, Evans BJ, Austin CC, Iskandar DT, Diesmos AC, Supriatna J, Andayani N, McGuire JA. 2013. Stochastic faunal exchanges drive diversification in widespread Wallacean and Pacific island lizards (Squamata: Scincidae: *Lamprolepis smaragdina*). *Journal of Biogeography* 40:507–520.

Liu L, Pearl DK. 2007. Species trees from gene trees: Reconstructing Bayesian posterior distributions of a species phylogeny using estimated gene tree distributions. *Systematic Biology* 56:504-514.

Liu L, Pearl DK, Brumfield RT, Edwards SV. 2008. Estimating species trees using multiple-allele DNA sequence data. *Evolution* 62:2080–2091.

Lohman DL, de Bruyn M, Page T, von Rintelen K, Hall R, Ng PKL, Shih HT, Carvalho GR, von Rintelen T. 2011. Biogeography of the Indo-Australian Archipelago. *Annual Review of Ecology, Evolution, and Systematics* 42:205–226.

Losos JB. 1990. Ecomorphology, performance capability, and scaling of West Indian *Anolis* lizards: an evolutionary analysis. *Ecological Monographs* 60:369–388.

Losos JB, Ricklefs RE. 2009. Adaptation and diversification on islands. *Nature* 457:830–836.

Luikart G, England PR, Tallmon D, Jordan S, Taberlet P. 2003. The power and promise of population genomics: from genotyping to genome typing. *Nature Reviews Genetics* 4:981–994.

Lydekker FRS. 1903. *Mostly Mammals*. Dodd Mead and Co., New York.

Lydekker FRS. 1915. *Wild Life of the World*. Fredrick Warne and Co. Ltd., New York.

MacArthur RH, Wilson EO. 1967. *The Theory of Island Biogeography*. Princeton University Press, Princeton, NJ.

Macey JR, Larson A, Anajeva NB, Fang Z, Papenfuss TJ. 1997. Two novel gene orders and the role of light-strand replication in rearrangement of the vertebrate mitochondrial genome. *Molecular Biology and Evolution* 14:91–104.

Maddison WP, Maddison DR. 2007. Mesquite: a modular system for evolutionary analysis. Version 2.0, http://mesquiteproject.org

Mahler DL, Revell LJ, Glor RE, Losos JB. 2010. Ecological opportunity and the rate of morphological evolution in the diversification of Greater Antillean anoles. *Evolution* 64:2731–2745.

Manel S, Schwartz MK, Luikart G, Taberlet P. 2003. Landscape genetics: combining landscape ecology and population genetics. *TRENDS in Ecology and Evolution* 18:189–197.

Manel S, Holderegger R. 2013. Ten years of landscape genetics. *Trends in Ecology & Evolution* 28:614–621.

Mani MS. 1974. Biogeographical evolution in India. In: Mani MS (Ed.). *Ecology and Biogeography of India*. Dr. W. Jukn b.v. Publishers, The Hague, pp. 698–724.

Marshall JC, Arévalo E, Benavides E, Sites JL, Sites Jr. JW. 2006. Delimiting species: Comparing methods for Mendelian characters using lizards of the *Sceloporus grammicus* (Squamata: Phrynosomatidae) complex. *Evolution* 60:1050–1065.

Mausfeld P, Böhme W. 2002. A new Mabuya from Java, Indonesia, *Salamandra* 38:135–144.

Mausfeld P, Schmitz A. 2003. Molecular phylogeography, intraspecific variation and speciation of the Asian scincid lizard genus *Eutropis* Fitzinger, 1843 (Squamata: Reptilia: Scincidae): taxonomic and biogeographic implications. *Organisms Diversity & Evolution* 3:161–171.

Mayden RL. 1997. A hierarchy of species concepts: The denouement in the saga of the species problem. In: Clardge MF, Dawah HA, Wilson MR (Eds.). *Species*. Chapman and Hall, London, pp. 381–424

Mayr E. 1942. *Systematics and the origin of species, from the viewpoint of a zoologist*. Columbia University Press, New York.

McKay JK, Latta RG. 2002. Adaptive population divergence: markers, QTL and traits. *Trends in Ecology and Evolution* 17:285–291.

McRae BH. 2006. Isolation by resistance. *Evolution* 60:1551–1561.

McRae BH, Beier P. 2007. Circuit theory predicts gene flow in plant and animal populations. *Proceedings of the National Academy of Sciences* 104:19885–19890.

Méhely L. 1897. Zur Herpetologie von Ceylon. Termes Fuzetek, Budapest, xx, 55–70.

Meijaard E, Groves CP. 2006. The geography of mammals and rivers in mainland South-East Asia. In: Lehman SM, Fleagle JG (Eds.). *Primate Biogeography*. Springer, New York, pp. 305–329.

Michel AP, Sim S, Powell THQ, Taylor MS, Nosil P, Feder JL. 2010. Widespread genomic divergence during sympatric speciation. *Proceedings of the National Academy of Sciences* 107:9724–9729.

Minin V, Abdo Z, Joyce P, Sullivan J. 2003. Performance-based selection of likelihood models for phylogeny estimation. *Systematic Biology* 52:674–683.

Miralles A, Fuenmayor GR, Barrio-Amoros CL. 2005. Taxonomy of the genus *Mabuya* (Reptilia, Squamata, Scincidae) in Venezuela. *Zoosystema* 27:825–837.

Miralles A, Carranza S. 2010. Systematics and biogeography of the Neotropical genus *Mabuya*, with special emphasis on the Amazonian skink *Mabuya nigropunctata* (Reptilia, Scincidae). *Molecular Phylogenetics and Evolution* 54:857–869.

Monaghan MT, Wild R, Elliot M, Fujisawa T, Balke M, Inward DJG, Lees DC, Ranaivosolo R, Eggleton P, Barraclough TG, Vogler AP. 2009. Accelerated species inventory on Madagascar using coalescent-based models of species delineation. *Systematic Biology* 58:298–311.

Moran P, Kornfield I. 1993. Retention of an ancestral polymorphism in the Mbuna species flock (Teleostei, Cichlidae) of Lake Malawi. *Molecular Biology and Evolution* 10:1015–1029.

Moyle RM, Filardi CE, Smith CE, Diamond J. 2009. Explosive Pleistocene diversification and hemispheric expansion of a "great speciator". *Proceedings of the National Academy of Sciences USA* 106:1863–1868.

Myers N, Mittermeier RA, Mittermeier CG, da Fonseca GAB, Kent J. 2000. Biodiversity hotspots for conservation priorities. *Nature* 403:853–858.

Nei M. 1987. *Molecular Evolutionary Genetics*. Columbia University Press, New York.

Nevado B, Ramos-Onsins S, Perez-Enciso. 2014. Re-sequencing studies of non-model organisms using closely-related reference genomes: optimal experimental designs and bioinformatics approaches for population genomics. *Molecular Ecology* DOI:10.1111/mec.12693.

Niemiller ML, Near TJ, Fitzpatick BM. 2012. Delimiting species using multilocus data: diagnosing cryptic diversity in the southern cavefish, *Typhlichthys subterraneus* (Teleostei: Amblyopsidae). *Evolution* 66:846–866.

Nylander JA, Wilgenbusch JC, Warren DL, Swofford DL. 2007 AWTY (Are We There Yet?) a system for graphical exploration of MCMC convergence in Bayesian phylogenetics. *Bioinformatics* 24:581–583.

Oaks JR, Sukumaran J, Esselstyn JA, Linkem CW, Siler CD, Holder MT, Brown RM. 2013. Evidence for climate driven diversification? A caution for interpreting ABC inferences of simultaneous historical events. *Evolution,* 67:992–1010.

Oliver PM, Adams M, Lee MS, Hutchinson MN, Doughty P. 2009. Cryptic diversity in vertebrates: molecular data double estimates of species diversity in a radiation of Australian lizards (Diplodactylus, Gekkota). *Proceedings of the Royal Society London B Biological Sciences* 24:1–7.

Oliveros CH, Ota H, Crombie RI, Brown RM. 2011. The herpetofauna of the Babuyan group of islands, northern Philippines. *Scientific Publications of the Natural History Museum of the University of Kansas* 43:1–20.

O'Meara BC. 2010. New heuristic methods for joint species delimitation and species tree inference. *Systematic Biology* 59:59–73.

Ota H. 1991. Taxonomic Status of *Mabuya multicarinata* (Gray, 1845) (Scincidae: Squamata: Reptilia) from Taiwan, with comments on the herpetofauna of Lanyu Island. *Bulletin of the College of Science University of the Ryukyus* 51:11–18.

Ota H, Hikida T, Nabhitabhata J, Panka S. 2001. Cryptic taxonomic diversity in two broadly distributed lizards of Thailand (*Mabuya macularia* and *Dixonius siamensis*) as revealed by chromosomal investigations (Reptilia: Lacertilia). *The Natural History Journal of Chulalongkorn University* 1:1–7.

Pagle M. 1999. The maximum likelihood approach to reconstructing ancestral character states of discrete characters on phylogenies. *Systematic Biology* 48:612–622.

Pagle M, Meade A. 2006. Bayesian analysis of correlated evolution of discrete characters by reversible-jump Markov chain Monte Carlo. *American Naturalist* 167:808–825.

Paradis E, Claude J, Strimmer K. 2004. APE: analyses of phylogenetics and evolution in R language. *Bioinformatics* 20:289–290.

Parnell J. 2013. The biogeography of the Isthmus of Kra region: a review. *Nordic Journal of Botany* 31:1–15.

Pasachnik SA, Fitzpatrick BM, Near TJ, Echternacht AC. 2009. Gene flow between an endangered endemic iguana, and its wide spread relative, on the island of Utila, Honduras: when is hybridization a threat? *Conservation Genetics* 10:1247–1254.

Petren K, Grant PR, Grant BR, Keller LF. 2005. Comparative landscape genetics and the adaptive radiation of Darwin's finches: The role of peripheral isolation. *Molecular Ecology* 14:2943–2957.

Petren K. 2013. The evolution of landscape genetics. *Evolution* 67:3383–3385.

Pfenninger M, Schwenk K. 2007. Cryptic animal species are homogeneously distributed among taxa and biogeographical regions. *BMC Evolutionary Biology* 7:1–6.

Phillips SJ, Anderson RP, Schapire RE. 2006. Maximum entropy modeling of species geographic distributions. *Ecological Modelling* 190:231–259.

Pianka ER. 1973. The structure of lizard communities. *Annual Review of Ecology and Systematics* 4:53–74.

Pianka ER, Vitt LJ. 2006. *Lizards: windows to the evolution of diversity*. University of California Press, Berkely, CA.

Pinho C, Rocha S, Carvalho BM, et al. 2010. New Primers for the amplification and sequencing of nuclear loci in a taxonomically wide set of reptiles and amphibians. *Conservation Genetics Resources* 2:181–185.

Pons J, Barraclough TG, Gomez-Zurita J, Cardoso A, Duran DP, Hazell S, Kamoun S, Sumlin WD, Vogler AP. 2006. Sequence-based species delimitation for the DNA taxonomy of undescribed insects. *Systematic Biology* 55:595–609.

Pritchard JK, Stephens M, Donnelly P. 2000. Inference of population structure using multilocus genotype data genotype data. *Genetics* 155:945–959.

Prunier JG, Kaufmann B, Fenet S, Picard D, Pompanon F, Joly P, Lena JP. 2013. Optimizing the trade-off between spatial and genetic sampling efforts in patchy populations: towards a better assessment of functional connectivity using an individual-based sampling scheme. *Molecular Ecology* 22:5516–5530.

Pybus OG, Harvey PH. 2000. Testing macroevolutionary models using incomplete molecular phylogenies. *Proceedings of the Royal Society London B Biological Sciences* 267:2267–2272.

Rabosky DL, Donnellan SC, Talaba AL, Lovette LJ. 2007. Exceptional among-lineage variation in diversification rates during the radiation of Australia's most diverse vertebrate clade. *Proceedings of the Royal Society B: Biological Sciences* 274:2915–2923.

Rabosky DL, Donnellan SC, Grundler M, Lovette IJ. 2014. Analysis and visualization of complex macroevolutionary dynamics: an example from Australian scincid lizards. *Systematic Biology* doi: 10.1093/sysbio/syu025.

Rambaut, A., and A. J. Drummond. 2007. Tracer, Version 1.4, Available: http://beast.bio.ed.ac.uk/Tracer

Raeymaekers JAM, Van Houdt JKJ, Larmuseau MHD, Geldof S, Volckaert FAM. 2007. Divergent selection as revealed by P_{ST} and QTL-based F_{ST} in three-spined stickleback (*Gasterosteus aculeatus*) populations along a coastal-inland gradient). *Molecular Ecology* 16:891–905.

Ree RH, Smith SA. 2008. Maximum likelohood inference of geographic range evolution by dispersal, local extinction, and cladogenesis. *Systematic Biology* 57:4–14.

Reid NM, Carstens BC. 2012. Phylogenetic estimation error can decrease the accuracy of species delimitation: a Bayesian implementation of the general mixed Yule-coalescent model. *BMC Evolutionary Biology* 12:1–11.

Reiff DM, Kaneko A, Taleo G, Amos M, Lum JK. 2007. Population structure and gene flow of *Anopheles farauti s.s.* (Diptera:Culicidae) among ten sites on five islands of Vanuatu: implications for malaria control. *Journal of Medical Entomology* 44:601–607.

Revell LJ, Harmon LJ, Collar DC. 2008. Phylogenetic signal, evolutionary process, and rate. *Systematic Biology* 57:591–601.

Roberts TE. 2006. Multiple levels of allopatric divergence in the endemic Philippine fruit bat *Haplonycteris fischeri* (Pteropodidae). *Biological Journal of the Linnean Society* 88:329–349.

Rosenberg MS, Anderson CD. 2011. PASSaGE: pattern analysis, spatial statistics and geographic exegesis. Version 2. *Methods in Ecology and Evolution* 2:229–232.

Ross CA, Lazell JD. 1990. Amphibians and reptiles of Dinagat and Siargao Islands, Philippines. *The Philippine Journal of Science* 119:257–286.

Ross CA, Gonzales PC. 1992. Amphibians and reptiles of Catanduanes Island, Philippines. *National Museum Papers (Manila)* 2:50–76.

Roughgarden J. 1972. Evolution of niche width. *American Naturalist* 106:683–718.

Rundell RJ, Price TD. 2009. Adaptive radiation, nonadaptive radiation, ecological speciation and nonecological speciation. *Trends in Ecology and Evolution* 24:394–399.

Schmidt KP. 1926. Amphibians and reptiles of the James Simpson-Roosevelt Asiatic Expedition. *Field Museum of Natural History Zoological Series* 12:167–173.

Schönrogge K, Barr B, Wardlaw JC, Napper E, Gardner MG, Breen J, Elmes GW, Thomas JA. 2002. When rare species become endangered: cryptic speciation in myrmecophilous hoverflies. *Biological Journal of the Linnean Society* 75:291–300.

Seehausen O. 2004. Hybridization and adaptive radiation. *Trends in Ecology and Evolution* 19:198–207.

Serb JM, Alejandrino A, Otárola-Castillo E, Adams DC. 2011. Morphological convergence of shell shape in distantly related scallop species (Mollusca: Pectinidae). *Zoological Journal of the Linnean Society* 163:571–584.

Setiadi MI, McGuire JA, Brown RM, Zubairi M, Iskandar DT, Andayani N, Supriatna J, Evans BJ. 2011. Adaptive radiation and ecological opportunity in Sulawesi and Philippine fanged frog (*Limnonectes*) communities. *American Naturalist* 178:221–240

Sexton JP, Hangartner SB, Hoffman AA. 2014. Genetic isolation by environment or distance: which pattern of gene flow is most common? *Evolution* 68:1–15.

Shaffer HB. 1984. Evolution in a paedomorphic lineage. II. Allometry and form in the Mexican Ambystomatid Salamanders. *Evolution* 28:1207–1218.

Shaffer HB, McKnight ML. 1996. The polytypic species revisted: genetic differentiation and molecular phylogenetics of the tiger salamander *Ambystoma tigrinum* (Amphibia: Caudata) complex. *Evolution* 50:417–433.

Shaffer HB, Thomson RC. 2007. Delimiting species in recent radiations. *Systematic Biology* 56:896–906.

Shaffer HB, Purugganan MD. 2013. Introduction to theme: "Genomics in Ecology, Evolution, and Systematics". *Annual Review of Ecology, Evolution and Systematics* 44:1–4.

Siler CD, Oaks JR, Esselstyn JA, Diesmos AC, Brown RM. 2010. Phylogeny and biogeography of Philippine bent-toed geckos (Gekkonidae: *Cyrtodactylus*) contradict a prevailing model of Pleistocene diversification. *Molecular Phylogenetics and Evolution* 55:699–710.

Siler CD, Brown RM. 2011. Evidence for repeated acquisition and loss of complex body-form characters in an insular clade of Southeast Asian semi-fossorial skinks. *Evolution* 65:2641–2663.

Siler CD, Diesmos AC, Alcala AC, Brown RM. 2011. Phylogeny of Philippine slender skinks (Scincidae: *Brachymeles*) reveals underestimated species diversity, complex biogeographical relationships, and cryptic patterns of lineage diversification. *Molecular Phylogenetics and Evolution* 59:53–65.

Siler CD, Welton LJ, Siler JM, Brown J, Bucol A, Diesmos AC, Brown RM. 2011. Amphibians and reptiles, Luzon Island, Aurora Province and Aurora Memorial National Park, Northern Philippines: new island distribution records. *Check List* 7:182–195.

Siler CD, Dececchi AA, Merkord CL, Davis DR, Christiani TJ, Brown RM. 2013. Cryptic diversity and population genetic structure in the rare, endemic, forest-obligate, geckos of the Philippines. *Molecular Phylogenetics and Evolution* 70:204–209.

Simpson GG. 1951. The species concept. *Evolution* 5:285–298.

Simpson GG. 1961. *Principles of Animal Taxonomy*. Columbia University Press, New York.

Sinclair EA, Bezy RL, Bolles K, Camarillo JL, Crandall KA, Sites JW. 2004. Testing species boundaries in an ancient species complex with deep phylogeographic history: genus *Xantusia* (Squamata: Xantusidae). *American Naturalist* 164:396–414.

Sindaco R, Metallinou M, Pupin F, Fasola M, Carranza S. 2012. Forgotten in the ocean: systematics, biogeography, and evolution of the *Trachylepis* skinks of the Socotra Archipelago. *Zoologica Scripta* 41:346–362.

Sites JW, Marshall JC. 2003. Delimiting species: a Renaissance issue in systematic biology. *Trends in Ecology and Evolution* 18:462–470.

Sites JW, Marshall JC. 2004. Operational criteria for delimiting species. *Annual Review of Ecology Evolution and Systematics* 35:199–227.

Skinner A. 2007. Phylogenetic relationships and rate of early diversification of Australian *Sphenomorphus* group scincids (Scincoidea, Squamata). *Biological Journal of the Linnean Society* 92:346–366.

Skinner A, Hugall AF, Hutchinson MN. 2011. Lygosomine phylogeny and the origins of Australian scincid lizards. *Journal of Biogeography* 38:1044–1058.

Smith MA. 1935. The fauna of British India, including Ceylon and Burma. Reptiles and Amphibia, Vol. II. Sauria. Taylor and Francis, London.

Spinks PQ, Thomson RC, Hughes B, Moxley B, Brown RM, Diesmos AC, Shaffer HB. 2012. Cryptic variation and the tragedy of unrecognized taxa: the case of international trade in the spiny turtle *Heosemys spinosa* (Testudines: Geoemydidae). *Zoological Journal of the Linnean Society* 164:811–824.

Spitz K. 1993. Population structure in *Daphnia obtuse*: quantitative genetic and allozyme variation. *Genetics* 135:367–374.

Stamaktakis A. 2006. RAxML-VI-HPC: Maximum Likelihood-based phylogenetic analysis with thousands of taxa and mixed models. *Bioinformatics* 22:2688–2690.

Stanley SM. 1989. Fossils, macroevolution, and theoretical ecology. In: Roughgarden J, May RM, Levin SA (Eds.). *Perspectives in Ecological Theory*. Princeton University Press, Princeton, NJ, pp. 125–134

Stelbrink B, Albrecht C, Hall R, von Rintelen T. 2012. The biogeography of Sulawesi revisited: is there evidence for a vicariant origin of taxa on Wallace's "Anomalous Island". *Evolution* 66:2252–2271.

Storfer AS, Murphy MA, Spear SF, Holderegger R, Waits LP. 2010. Landscape genetics: where are we now? *Molecular Ecology* 19:3496–3514.

Stuart BL, Inger RF, Voris HK. 2006. High level of cryptic species diversity revealed by sympatric lineages of Southeast Asian forest frogs. *Biology Letters* 2:470–474.

Sturmbauer C, Meyer A. 1992. Genetic divergence and morphological stasis in a lineage of African cichlid fishes. *Nature* 358:578–581.

Swofford DL. 2002. PAUP*. Phylogenetic Analysis using Parsimony (*and Other Methods). Version 4. Sinauer Associates, Sunderland.

Taylor EH. 1917. Snakes and lizards known from Negros, with descriptions of new species and subspecies. *Philippine Journal of Science* 12:358–381.

Taylor EH. 1922. The lizards of the Philippine Islands. *Manila: Philippine Bureau of Science, Monograph* 17:1–178.

Taylor EH. 1923. Additions to the herpetological fauna of the Philippine Islands, III. *Philippine Journal of Science* 22:515–557.

Taylor EH. 1925. Additions to the herpetological fauna of the Philippine Islands, IV. *Philippine Journal of Science* 26:97–111.

Taylor EH, Elbel RE. 1958. Contribution to the Herpetology of Thailand. *University of Kansas Science Bulletin* 38:1033–1189.

Taylor EH. 1963 The lizards of Thailand. *University of Kansas Science Bulletin* 44:687–1077.

Thomson RC, Shedlock AM, Edwards SV, Shaffer HB. 2008. Developing markers for multilocus phylogenetics in non-model organisms: a test case with turtles. *Molecular Phylogenetics and Evolution* 49:514–525.

Thomson RC, Wang IJ, Johnson JR. 2010. Genome-enabled development of DNA markers for ecology, evolution, and conservation. *Molecular Ecology* 19:2184–2195.

Tobias JA, Seddon N, Spottiswoode CN, Pilgrim JD, Fishpool LDC, Collar NJ. 2010. Quantitative criteria for species delimitation. *IBIS* 152:724–746.

Travis J. 1989. The role of optimizing selection in natural populations. *Annual Review of Ecology and Systematics* 20:279–296.

Turner TL, Hahn MW, Nuzhdin SV. 2005. Genomic islands of speciation in *Anopheles gambiae*. *PLoS Biology* 3:e285.

Van Steenis CGGJ. 1950. The delimitation of Malaysia and its main plant geographical divisions. In Van Steenis CGGJ (Ed.). *Flora Malesiana Vol. 1 Spermatohyta*. Noordhoff-Kolff NV, Djarkarta, pp. LXX–LXXV.

Voris HK. 2000. Maps of Pleistocene sea levels in Southeast Asia: shore lines, river systems and time durations. *Journal of Biogeography* 27:1153–1167.

Wagner CE, Keller I, Wittwer S, Selz OM, Mwaiko S, Greuter L, Sivasundar A, Seehausen O. 2012. Genome-wide RAD sequence data provide unprecedented resolution of species boundaries and relationships in the Lake Victoria cichlid adaptive radiation. *Molecular Ecology* 22:787–798.

Wake DB, Roth G, Wake MH. 1983. On the problem of stasis in organismal evolution. *Journal of Theoretical Biology* 101:211–224.

Wake DB. 1997. Incipient species formation in salamanders of the *Ensatina* complex. *Proceedings of the National Academy of Sciences USA* 94:7761–7767.

Wake DB. 2006. Problems with species: patterns and processes of species formation in salamanders. *Annals of the Missouri Botanical Garden* 93:8–23.

Wallace AR. 1876. *The geographical distribution of animals*. Macmillan, London.

Wallace AR. 1860 On the zoological geography of the Malay Archipelago. *Journal of the Proceedings of the Linnean Society London* IV:172–184.

Wang IJ, Summers K. 2010. Genetic structure is correlated with phenotypic divergence rather than geographic isolation in the highly polymorphic strawberry poison-dart frog. *Molecular Ecology* 19:447–458.

Wang IJ. 2013. Examining the full effects of landscape heterogeneity on spatial genetic variation a multiple matrix regression approach for quantifying geographic and ecological isolation. *Evolution* 67:3403–3411.

Wang IJ, Glor RE, Losos JB. 2013. Quantifying the roles of ecology and geography in spatial genetic divergence. *Ecology Letters* 16:175–182.

Welton LJ, Siler CD, Oaks JR, Diesmos AC, Brown RM. 2013. Multilocus phylogeny and Bayesian estimates of species boundaries reveal hidden evolutionary relationships and cryptic diversity in Southeast Asian monitor lizards. *Molecular Ecology* 22:3495–3510.

Whiting AS, Sites Jr. JW, Pellegrino KCM, Rodrigues MT. 2006. Comparing alignment methods for inferring the history of the new world lizard genus *Mabuya* (Squamata: Scincidae). *Molecular Phylogenetics and Evolution* 38:719–730.

Whitlock MC. 2008. Evolutionary inference from Q_{ST}. *Molecular Ecology* 17:1885–1896.

Wiens JJ, Brandley MC, Reeder TW. 2006. Why does a trait evolve multiple times within a clade? Repeated evolution of snake-like body form in squamate reptiles. *Evolution* 60:123–141.

Wiley EO. 1978. The evolutionary species concept reconsidered. *Systematic Zoology* 27:17–26.

Wilgenbusch JC, Warren DL, Swofford DL. 2004. AWTY: a system for graphical exploration of MCMC convergence in Bayesian phylogenetic inference. Available: http://ceb.csit.fsu.edu/awty. Accessed December 1, 2012.

Williams EE. 1972. The origin of faunas. Evolution of lizard congeners in a complex island fauna: a trivial analysis. *Evolutionary Biology* 6:47–89.

Wilson GA, Rannala B. 2003. Bayesian inference of recent migration rates using multilocus genotypes. *Genetics* 163:1177–1191.

Wojcieszek JM, Simmons LW. 2011. Evidence for stabilizing selection and slow divergent evolution of male genitalia in a millipede (*Antichiropus variabilis*). *Evolution* 66:1138–1153.

Witter MS, Carr GD. 1988. Adaptive radiation and genetic differentiation in the Hawaiian silversword alliance (Compositae: Madiinae). *Evolution* 42:1278–1287.

Woodruff DS. 2003. Neogene marine transgressions, paleogeography, and biogoegraphic transition on the Thai-Malay Penninsula. *Journal of Biogeography* 30:551–567.

Woodruff DS. 2010. Biogeography and conservation in Southeast Asia: how 2.7 million years of repeated environmental fluctuations affect today's patterns and the future of the remaining refugial-phase biodiversity. *Biodiversity and Conservation* 19:919–941.

Wright JJ. 2011. Conservative coevolution of Müllerian mimicry in a group of rift lake catfish. *Evolution* 65:395–407.

Xang QY, Zhang WH, Ricklefs RE, Qian H, Chen ZD, Wen J, Hua JL. 2004. Regional differences in rates of plant speciation and molecular evolution: a comparison between eastern Asia and eastern North America. *Evolution* 58:2175–2184.

Yang Z, Rannala B. 2010. Bayesian species delimitation using multilocus sequence data. *Proceedings of the National Academy of Sciences USA* 107:9264–9269.

Yi X, et al. 2010. Sequencing of 50 human exomes reveals adaptation to high altitude. *Science* 329:75–78.

Yumul GP, Dimalanta CB, Marquez EJ, Queaño KL. 2009. Philippines, geology. In: Gillespie R, Clague D (Eds.). *Encyclopedia of Islands*. University of California Press, Berkeley, pp. 732–738.

Yumul GP, Dimalanta CB, Tamayo RA, Maury RC, Bellon H, Polve M, Maglambayan VB, Querubin CL, Cotton J. 2004. Geology of the Zamboanga Peninsula, Mindanao, Philippines: an enigmatic South China continental fragment? *Geological Society, London, Special Publications* 266:289–312.

Zamudio KR, Greene HW. 1997. Phylogeography of the bushmaster (*Lachesis muta*: Viperidae): implications for neotropical biogeography, systematics, and conservation. *Biological Journal of the Linnean Society* 62:421–442.

Zhang C, Zhang D, Zhu T, Yang Z. 2011. Evaluation of a Bayesian coalescent method of species delimitation. *Systematic Biology* 60:747–761.

Appendices

Appendix 1 Correlation coefficients between each of the nine morphological variables (Chapter 1).

	Head length	Head width	Arm length	Leg length	Total lamellae	Vertebral scale rows	Ventral scale rows
SVL	0.9395	0.9403	0.9111	0.9155	0.6940	-0.4203	-0.2552
Head length		0.9289	0.9333	0.9386	0.7699	-0.4708	-0.2932
Head width			0.9077	0.9278	0.7251	-0.4894	-0.3323
Arm length				0.9441	0.7563	-0.4455	-0.2455
Leg length					0.7668	-0.4916	-0.3082
Total lamellae						-0.4865	-0.3222
Vertebral scale rows							-0.7292

	Axilla–Groin
SVL	0.9352
Head length	0.8983
Head width	0.9048
Arm length	0.8821
Leg length	0.8843
Total lamellae	0.7067
Vertebral scale rows	-0.4831
Ventral scale rows	-0.2248

Appendix 2 Primer information for genes used in study. Unless otherwise specified, primers were used for both PCR and sequencing. If annealing temperature is specified, the basic PCR protocol found below was used. If not, a touchdown protocol was used, see below (Chapter 1).

ND2 (Annealing temperature = 56)
Met.f6: AAGCTTTCGGGCCCATACC (PCR & Sequencing)
Spheno.R: TAGGYGGCAGGTTGTAGCCC (PCR)
ND2.SphR: CTCTTDTTTGTRGCTTTGAAGGC (Sequencing)

ATPSB
ATPSB.F: TACCATGARATGATTGAATCTGGRGTCAT
ATPSB.R: CKAGCACGAGCACCTGGTGGGTCRTTCAT

SELT (Annealing temperature = 54)
SELT.F: GTTATYAGCCAGCGGTACCCAGACATCCG
SELT.R: GCCTATTAAYACTAGTTTGAAGACTGACAG

NAT15 (Annealing temperature =57)
NAT15.F: ATCAGAGGGGTTCTCAAAGATGG
NAT15.R: AGAGAAGGCTCTGGGCTTGTCGGTA

FOXP2
FOXP2.F: ACATTCMGACAAATACAACATTCCCATGTC
FOXP2.R: GCATTTTTATAAAATTCRTAGTTTGGGGC

LDHA
LDHA.F: GCAGATACACTBTGGGGAATCCAG
LDHA.R: TKGGCTGGTACTACAGYTRGACA

NOS1 (Annealing temperature = 58)
NOS1.F: GTGGGCAGGATYCAGTGGTCCAAGCT
NSO1.R: CTGAGATTCCCTTTGTTAGTGGC

Basic PCR Protocol:
95 for 1 min
(94 for 30 sec, 45 seconds the annealing temperature, 72 for 1 min) x38
72 for 10 min

Touchdown PCR protocol (for ATPSB & LDHA):
94 for 1 min
(94 for 30 sec, 61 for 30 sec, 68 for 1:30 min) x5
(94 for 30 sec, 59 for 30 sec, 68 for 1:30 min) x5
(94 for 30 sec, 57 for 30 sec, 68 for 1:30 min) x5
(94 for 30 sec, 50 for 30 sec, 68 for 1:30 min) x25

Touchdown PCR protocol (for FOXP2):
94 for 1 min
(94 for 30 sec, 57 for 30 sec, 72 for 1 min) x5
(94 for 30 sec, 55 for 30 sec, 72 for 1 min) x5
(94 for 30 sec, 53 for 30 sec, 72 for 1 min) x5
(94 for 30 sec, 50 for 30 sec, 72 for 1 min) x25

Appendix 3 List of genetic samples used in project and associated Genbank numbers for each gene. KU = University of Kansas, Biodiversity Institute; CAS = California Academy of Sciences; LSUHC = La Sierra University, Lee Grismer; FMNH = Field Museum of Natural History; TNHC = Texas Natural History Collection, University of Texas, Austin; USNM = Smithsonian Institution; TreeBASE = Several sequences were less than 200 bp in length, and are not accessioned in Genbank, see TreeBASE alignments. [N]No voucher specimen; [P] Specimen deposited at the Philippine National Museum

Species Taxon Name	Voucher #	ND2	ATPSB	SELT	NAT15	FOXP2	NOS1	LDAH
Eutropis bontocensis	KU 304878	KF235233	KF234787	KF235081	KF234935	KF234861	KF235010	KF235154
Eutropis bontocensis	KU 304881	KF235234	KF234788	KF235082	KF234936	KF234862	KF235011	KF235155
Eutropis bontocensis	KU 304882	KF235235	KF234789	KF235083	KF234937	KF234863	KF235012	KF235156
Eutropis bontocensis	KU 314026	KF235236	KF234790	KF235084	KF234938	KF234864	KF235013	KF235157
Eutropis bontocensis	KU 314032	KF235238	KF234791	KF235085	KF234939	KF234865	KF235014	KF235158
Eutropis bontocensis	KU 335111	KF235228	KF234786	KF235080	KF234934	KF234860	KF235009	KF235153
Eutropis bontocensis	KU 335112	KF235229	——	——	——	——	——	——
Eutropis bontocensis	KU 335113	KF235230	——	——	——	——	——	——
Eutropis bontocensis	KU 335122	KF235231	——	——	——	——	——	——
Eutropis bontocensis	KU 335123	KF235232	——	——	——	——	——	——
Eutropis bontocensis	KU 314025	KF235236	——	——	——	——	——	——
Eutropis cumingi	FMNH 259453	KF235239	KF234792	KF235086	KF234940	KF234866	KF235015	KF235159
Eutropis cumingi	FMNH 266254	KF235254	KF234797	KF235091	KF234945	KF234870	KF235020	KF235164
Eutropis cumingi	KU 320489	KF235257	KF234798	KF235092	KF234946	KF234871	KF235021	KF235165
Eutropis cumingi	KU 308933	KF235263	KF234802	KF235096	KF234950	KF234875	KF235025	KF235169
Eutropis cumingi	FMNH 258984	KF235264	KF234803	KF235097	KF234951	KF234876	KF235026	KF235170
Eutropis cumingi	RMB 9591[N]	KF235397	KF234852	KF235145	KF235001	KF234926	KF235073	KF235220
Eutropis cumingi	KU 306216	KF235401	KF234853	KF235146	KF235002	KF234927	KF235074	KF235221
Eutropis cumingi	KU 335134	KF235253	KF234796	KF235090	KF234944	TreeBASE	KF235019	KF235163
Eutropis cumingi	KU 327382	KF235245	——	——	——	——	——	——
Eutropis cumingi	KU 327383	KF235246	——	——	——	——	——	——
Eutropis cumingi	KU 327385	KF235247	——	——	——	——	——	——
Eutropis cumingi	KU 335135	KF235249	——	——	——	——	——	——
Eutropis cumingi	KU 335139	KF235250	——	——	——	——	——	——
Eutropis cumingi	KU 335132	KF235251	——	——	——	——	——	——
Eutropis cumingi	KU 335133	KF235252	——	——	——	——	——	——
Eutropis cumingi	KU 304009	KF235265	——	——	——	——	——	——
Eutropis cumingi	KU 304745	KF235266	——	——	——	——	——	——
Eutropis cumingi	KU 304746	KF235267	——	——	——	——	——	——
Eutropis cumingi	KU 314022	KF235297	——	——	——	——	——	——
Eutropis cumingi	KU 314023	KF235298	——	——	——	——	——	——
Eutropis cumingi	KU 330070	KF235365	——	——	——	——	——	——
Eutropis cumingi	KU 325106	KF235410	——	——	——	——	——	——
Eutropis indeprensa	LSUHC 6160	KF235403	KF234855	KF235148	KF235004	KF234929	KF235076	KF235223
Eutropis indeprensa	KU 302883	KF235275	KF234810	KF235104	KF234958	KF234883	KF235033	KF235177
Eutropis indeprensa	KU 304027	KF235280	KF234814	KF235107	KF234962	KF234887	KF235037	KF235181

Eutropis indeprensa	KU 304028	KF235281	KF234815	KF235108	KF234963	KF234888	KF235038	KF235182
Eutropis indeprensa	KU 306992	KF235282	KF234816	KF235109	KF234964	KF234889	KF235039	KF235183
Eutropis indeprensa	KU 306993	KF235283	KF234817	KF235110	KF234965	KF234890	KF235040	KF235184
Eurtopis macularia	KU 328458	KF235415	KF234824	KF235117	KF234972	KF234897	KF235046	KF235191
Eutropis m. multicarinata	KU 320025	KF235240	KF234793	KF235087	KF234941	KF234867	KF235016	KF235160
Eutropis m. multicarinata	KU 310149	KF235292	KF234821	KF235114	KF234969	KF234894	KF235043	KF235188
Eutropis m. multicarinata	KU 310155	KF235293	KF234822	KF235115	KF234970	KF234895	KF235044	KF235189
Eutropis m. multicarinata	KU 311246	KF235335	KF234831	KF235124	KF234979	KF234904	KF235053	KF235198
Eutropis m. multicarinata	EMD 257[P]	KF235342	KF234836	——	KF234984	KF234909	KF235058	KF235203
Eutropis m. multicarinata	KU 320026	KF235241	——	——	——	——	——	——
Eutropis m. multicarinata	ACD 7409[P]	KF235328	——	——	——	——	——	——
Eutropis m. multicarinata	ACD 7436[P]	KF235329	——	——	——	——	——	——
Eutropis m. multicarinata	EMD 232[P]	KF235341	——	——	——	——	——	——
Eutropis m. multicarinata	KU 310153	KF235392	——	——	——	——	——	——
Eutropis m. multicarinata	KU 310151	KF235390	——	——	——	——	——	——
Eutropis m. borealis	KU 327754	KF235375	KF234846	KF235139	KF234995	KF234920	KF235068	KF235214
Eutropis m. borealis	KU 323210	KF235357	KF234841	KF235134	KF234990	KF234915	KF235063	KF235209
Eutropis m. borealis	KU 325794	KF235361	KF234842	KF235135	KF234991	KF234916	KF235064	KF235210
Eutropis m. borealis	KU 331728	KF235366	KF234843	KF235136	KF234992	KF234917	KF235065	KF235211
Eutropis m. borealis	KU 331729	KF235367	KF234844	KF235137	KF234993	KF234918	KF235066	KF235212
Eutropis m. borealis	TNHC 62990	KF235373	KF234845	KF235138	KF234994	KF234919	KF235067	KF235213
Eutropis m. borealis	KU 306804	KF235389	KF234849	KF235142	KF234998	KF234923	——	KF235217
Eutropis m. borealis	KU 327369	KF235394	KF234850	KF235143	KF234999	KF234924	KF235071	KF235218
Eutropis m. borealis	FMNH 266253	KF235414	KF234859	KF235152	KF235008	KF234933	KF235079	KF235227
Eutropis m. borealis	KU 323210	KF235307	——	——	——	——	——	——
Eutropis m. borealis	TNHC 62997	KF235308	——	——	——	——	——	——
Eutropis m. borealis	KU 327366	KF235310	——	——	——	——	——	——
Eutropis m. borealis	KU 327549	KF235311	——	——	——	——	——	——
Eutropis m. borealis	KU 327387	KF235312	——	——	——	——	——	——
Eutropis m. borealis	KU 327557	KF235313	——	——	——	——	——	——
Eutropis m. borealis	KU 327560	KF235314	——	——	——	——	——	——
Eutropis m. borealis	KU 327562	KF235315	——	——	——	——	——	——
Eutropis m. borealis	KU 327567	KF235316	——	——	——	——	——	——
Eutropis m. borealis	KU 327568	KF235317	——	——	——	——	——	——
Eutropis m. borealis	ACD 3045[P]	KF235318	——	——	——	——	——	——
Eutropis m. borealis	ACD 3206[P]	KF235319	——	——	——	——	——	——
Eutropis m. borealis	KU 306196	KF235333	——	——	——	——	——	——
Eutropis m. borealis	KU 308125	KF235334	——	——	——	——	——	——
Eutropis m. borealis	KU 302877	KF235330	——	——	——	——	——	——
Eutropis m. borealis	KU 323204	KF235353	——	——	——	——	——	——
Eutropis m. borealis	KU 323222	KF235358	——	——	——	——	——	——
Eutropis m. borealis	KU 323223	KF235359	——	——	——	——	——	——
Eutropis m. borealis	KU 325793	KF235360	——	——	——	——	——	——
Eutropis m. borealis	TNHC 62992	KF235374	——	——	——	——	——	——
Eutropis m. borealis	TNHC 62993	KF235376	——	——	——	——	——	——
Eutropis m. borealis	KU 304837	KF235386	——	——	——	——	——	——
Eutropis m. borealis	KU 307536	KF235388	——	——	——	——	——	——
Eutropis m. borealis	KU 313911	KF235398	——	——	——	——	——	——
Eutropis m. borealis	ACD 2269[P]	KF235404	——	——	——	——	——	——
Eutropis m. borealis	KU 324812	KF235409	——	——	——	——	——	——
Eutropis m. borealis	KU 325050	KF235411	——	——	——	——	——	——
Eutropis m. borealis	KU 325051	KF235412	——	——	——	——	——	——
Eutropis m. borealis	RMB 3942[P]	KF235413	——	——	——	——	——	——
Eutropis m. borealis	KU 323202	KF235352	——	——	——	——	——	——

Eutropis m. borealis	KU 323199	KF235349	——	——	——	——	——	——
Eutropis m. borealis	KU 323200	KF235350	——	——	——	——	——	——
Eutropis m. borealis	KU 323206	KF235355	——	——	——	——	——	——
Eutropis m. borealis	KU 323205	KF235354	——	——	——	——	——	——
Eutropis m. borealis	KU 323201	KF235351	——	——	——	——	——	——
Eutropis m. borealis	KU 302905	KF235400	——	——	——	——	——	——
Eutropis sp. Palau	CAS 237940	KF235406	KF234857	KF235150	KF235006	KF234931	——	KF235225
Eutropis sp. Palau	CAS 238095	KF235407	KF234858	KF235151	KF235007	KF234932	KF235078	KF235226
Eutropis sp. Palau	CAS 238220	KF235272	KF234807	KF235101	KF234955	KF234880	KF235030	KF235174
Eutropis sp. Palau	CAS 248247	KF235273	KF234808	KF235102	KF234956	KF234881	KF235031	KF235175
Eutropis sp. Palau	CAS 248808	KF235274	KF234809	KF235103	KF234957	KF234882	KF235032	KF235176
Eutropis sp. Palau	USNM 577453	KF235300	——	——	——	——	——	——
Eutropis sp. Palau	USNM 577438	KF235299	——	——	——	——	——	——
Eutropis sp. Palau	USNM 577449	KF235301	——	——	——	——	——	——
Eutropis sp. Palau	USNM 577450	KF235302	——	——	——	——	——	——
Eutropis sp. Palau	USNM 577454	KF235303	——	——	——	——	——	——
Eutropis sp. Palau	USNM 577457	KF235304	——	——	——	——	——	——
Eutropis sp. Palau	USNM 577458	KF235305	——	——	——	——	——	——
Eutropis sp. Palau	USNM 577477	KF235306	——	——	——	——	——	——
Clade A	KU 327372	KF235248	KF234795	KF235089	KF234943	KF234869	KF235018	KF235162
Clade A	CDS 5300[P]	KF235339	KF234834	KF235127	KF234982	KF234907	KF235056	KF235201
Clade A	KU 327370	KF235405	KF234856	KF235149	KF235005	KF234930	KF235077	KF235224
Clade B	KU 306810	KF235289	KF234819	KF235112	KF234967	KF234892	TreeBASE	KF235186
Clade B	KU 306811	KF235290	KF234820	KF235113	KF234968	KF234893	KF235042	KF235187
Clade B	GVAG 280[P]	KF235343	KF234837	KF235129	KF234985	KF234910	KF235059	KF235204
Clade B	GVAG 281[P]	KF235344	KF234838	KF235130	KF234986	KF234911	TreeBASE	KF235205
Clade B	GVAG 294[P]	KF235345	——	KF235131	KF234987	KF234912	KF235060	KF235206
Clade C	KU 306203	KF235258	KF234799	KF235093	KF234947	KF234872	KF235022	KF235166
Clade C	KU 306194	KF235259	KF234800	KF235094	KF234948	KF234873	KF235023	KF235167
Clade C	KU 306199	KF235262	KF234801	KF235095	KF234949	KF234874	KF235024	KF235168
Clade C	KU 305176	KF235276	KF234811	KF235105	KF234959	KF234884	KF235034	KF235178
Clade C	KU 314104	KF235296	KF234823	KF235116	KF234971	KF234896	KF235045	KF235190
Clade C	KU 306200	KF235255	——	——	——	——	——	——
Clade C	KU 306197	KF235256	——	——	——	——	——	——
Clade C	KU 306195	KF235260	——	——	——	——	——	——
Clade C	KU 306198	KF235261	——	——	——	——	——	——
Clade C	KU 305177	KF235277	——	——	——	——	——	——
Clade C	KU 331836	KF235284	——	——	——	——	——	——
Clade C	KU 331838	KF235285	——	——	——	——	——	——
Clade C	KU 315006	KF235295	——	——	——	——	——	——
Clade C	KU 302874	KF235331	——	——	——	——	——	——
Clade C	KU 302876	KF235332	——	——	——	——	——	——
Clade C	KU 321832	KF235347	——	——	——	——	——	——
Clade C	KU 310871	KF235399	——	——	——	——	——	——
Clade D	KU 311449	KF235268	KF234804	KF235098	KF234952	KF234877	KF235027	KF235171
Clade D	KU 311406	KF235278	KF234812	——	KF234960	KF234885	KF235035	KF235179
Clade D	KU 311407	KF235279	KF234813	KF235106	KF234961	KF234886	KF235036	KF235180
Clade E	KU 314098	KF235269	KF234805	KF235099	KF234953	KF234878	KF235028	KF235172
Clade E	KU 315012	KF235271	KF234806	KF235100	KF234954	KF234879	KF235029	KF235173
Clade E	KU 320030	KF235243	KF234794	KF235088	KF234942	KF234868	KF235017	KF235161
Clade E	KU 327373	KF235321	KF234826	KF235119	KF234974	KF234899	KF235048	KF235193
Clade E	KU 335269	KF235322	KF234827	KF235120	KF234975	KF234900	KF235049	KF235194
Clade E	KU 335270	KF235323	KF234828	KF235121	KF234976	KF234901	KF235050	KF235195
Clade E	KU 335271	KF235324	KF234829	KF235122	KF234977	KF234902	KF235051	KF235196

Clade E	KU 335272	KF235325	KF234830	KF235123	KF234978	KF234903	KF235052	KF235197
Clade E	KU 314106	KF235396	KF234851	KF235144	KF235000	KF234925	KF235072	KF235219
Clade E	KU 320028	KF235242	——	——	——	——	——	——
Clade E	KU 335273	KF235244	——	——	——	——	——	——
Clade E	KU 315011	KF235270	——	——	——	——	——	——
Clade E	KU 310156	KF235294	——	——	——	——	——	——
Clade E	ACD 6484[P]	KF235326	——	——	——	——	——	——
Clade E	ACD 6485[P]	KF235327	——	——	——	——	——	——
Clade E	KU 315009	KF235346	——	——	——	——	——	——
Clade E	KU 332773	KF235368	——	——	——	——	——	——
Clade E	KU 334226	KF235369	——	——	——	——	——	——
Clade E	KU 334227	KF235370	——	——	——	——	——	——
Clade E	KU 334228	KF235371	——	——	——	——	——	——
Clade E	KU 334229	KF235372	——	——	——	——	——	——
Clade E	KU 314105	KF235395	——	——	——	——	——	——
Clade E	KU 310152	KF235391	——	——	——	——	——	——
Clade E	KU 310154	KF235393	——	——	——	——	——	——
Clade F	KU 304872	KF235287	KF234818	KF235111	KF234966	KF234891	KF235041	KF235185
Clade F	KU 323198	KF235348	KF234839	KF235132	KF234988	KF234913	KF235061	KF235207
Clade F	KU 323207	KF235356	KF234840	KF235133	KF234989	KF234914	KF235062	KF235208
Clade F	KU 304727	KF235384	KF234848	KF235141	KF234997	KF234922	KF235070	KF235216
Clade F	RMB 944[P]	KF235309	KF234825	KF235118	KF234973	KF234898	KF235047	KF235192
Clade F	KU 304767	KF235286	——	——	——	——	——	——
Clade F	KU 304940	KF235288	——	——	——	——	——	——
Clade F	KU 308074	KF235291	——	——	——	——	——	——
Clade F	KU 323224	KF235320	——	——	——	——	——	——
Clade F	KU 329522	KF235363	——	——	——	——	——	——
Clade F	KU 329523	KF235364	——	——	——	——	——	——
Clade F	KU 304618	KF235378	——	——	——	——	——	——
Clade F	KU 304871	KF235387	——	——	——	——	——	——
Clade F	MVD 059[P]	KF235408	——	——	——	——	——	——
Clade F	KU 329521	KF235362	——	——	——	——	——	——
Clade F	KU 304688	KF235382	——	——	——	——	——	——
Clade F	KU 304689	KF235383	——	——	——	——	——	——
Clade F	KU 304750	KF235385	——	——	——	——	——	——
Clade F	KU 304620	KF235379	——	——	——	——	——	——
Clade F	KU 304641	KF235380	——	——	——	——	——	——
Clade F	KU 304642	KF235381	——	——	——	——	——	——
Clade G	KU 304013	KF235377	KF234847	KF235140	KF234996	KF234921	KF235069	KF235215
Clade G	KU 320491	KF235337	KF234832	KF235125	KF234980	KF234905	KF235054	KF235199
Clade G	KU 320492	KF235338	KF234833	KF235126	KF234981	KF234906	KF235055	KF235200
Clade G	KU 302873	KF235340	KF234835	KF235128	KF234983	KF234908	KF235057	KF235202
Clade G	LSUHC 6178	KF235402	KF234854	KF235147	KF235003	KF234928	KF235075	KF235222
Clade G	KU 320490	KF235336	——	——	——	——	——	——

Appendix 4 Locality information for all individuals include in study. KU = University of Kansas Biodiversity Institute; CAS = California Academy of Sciences; LSUHC = La Sierra University (Lee Grismer); FMNH = Field Museum of Natural History; TNHC = Texas Natural History Collection, University of Texas, Austin; USNM = Smithsonian Institution; [N]No voucher specimen; [P]Specimen deposited at the Philippine National Museum; [M]Specimen examined for morphological analysis.

Catalog #	Species Taxon Name	Country	Landmass	Province	Municipality
KU 327370	Clade A	Philippines	Mindanao	South Cotobato	Tampakan
KU 327372[M]	Clade A	Philippines	Mindanao	South Cotobato	Tampakan
CDS 5300[P]	Clade A	Philippines	Mindanao	South Cotabato	Tampakan
KU 306810[M]	Clade B	Philippines	Panay	Antique	San Remigio
KU 306811[M]	Clade B	Philippines	Panay	Antique	San Remigio
GVAG 280[P]	Clade B	Philippines	Panay	Antique	Sibalom
GVAG 281[P]	Clade B	Philippines	Panay	Antique	Sibalom
GVAG 294[P]	Clade B	Philippines	Panay	Antique	Sibalom
KU 302874[M]	Clade C	Philippines	Panay	Antique	Pandan
KU 302876[M]	Clade C	Philippines	Panay	Antique	Pandan
KU 305176[M]	Clade C	Philippines	Panay	Antique	Pandan
KU 305177[M]	Clade C	Philippines	Panay	Antique	Pandan
KU 306194[M]	Clade C	Philippines	Dinagat	Dinagat	Loreto
KU 306195[M]	Clade C	Philippines	Dinagat	Dinagat	Loreto
KU 306197	Clade C	Philippines	Luzon	Camarines del Sur	Presentacion
KU 306198	Clade C	Philippines	Luzon	Camarines del Sur	Baao
KU 306199[M]	Clade C	Philippines	Luzon	Camarines del Sur	Presentacion
KU 306200[M]	Clade C	Philippines	Samar	Eastern Samar	Taft
KU 306202[M]	Clade C	Philippines	Samar	Eastern Samar	Taft
KU 310783[M]	Clade C	Philippines	Samar	Eastern Samar	Taft
KU 302875[M]	Clade C	Philippines	Panay	Antique	Pandan
KU 306203	Clade C	Philippines	Samar	Eastern Samar	Taft
KU 305174[M]	Clade C	Philippines	Panay	Antique	Pandan
KU 306205[M]	Clade C	Philippines	Samar	Eastern Samar	Taft
KU 306204[M]	Clade C	Philippines	Samar	Eastern Samar	Taft
KU 310781[M]	Clade C	Philippines	Samar	Eastern Samar	Taft
KU 314104[M]	Clade C	Philippines	Mindanao	Agusan del Sur	San Francisco
KU 315006[M]	Clade C	Philippines	Mindanao	Zamboanga City	Pasonanca
KU 321832	Clade C	Philippines	Mindanao	Zamboanga City	Pasonanca
KU 331836[M]	Clade C	Philippines	Cebu	Cebu	Argao
KU 331837[M]	Clade C	Philippines	Cebu	Cebu	Argao
KU 331838	Clade C	Philippines	Cebu	Cebu	Argao
KU 310340[M]	Clade C	Philippines	Samar	Eastern Samar	Taft
KU 311406	Clade D	Philippines	Palawan	Palawan	Rizal
KU 311407[M]	Clade D	Philippines	Palawan	Palawan	Rizal
KU 311449[M]	Clade D	Philippines	Palawan	Palawan	Brooke's Point
KU 310152[M]	Clade E	Philippines	Dinagat	Dinagat	Loreto
KU 310154[M]	Clade E	Philippines	Dinagat	Dinagat	Loreto

KU 310156[M]	Clade E	Philippines	Dinagat	Dinagat	Loreto
KU 314098[M]	Clade E	Philippines	Mindanao	Agusan del Sur	Bunawan
KU 314105[M]	Clade E	Philippines	Mindanao	Agusan del Sur	Bunawan
KU 314106[M]	Clade E	Philippines	Mindanao	Agusan del Sur	Bunawan
KU 315009[M]	Clade E	Philippines	Mindanao	Zamboanga City	Pasonanca
KU 315011	Clade E	Philippines	Mindanao	Zamboanga City	Pasonanca
KU 315012	Clade E	Philippines	Mindanao	Zamboanga City	Pasonanca
KU 320028[M]	Clade E	Philippines	Mindanao	Agusan del Sur	San Francisco
KU 320030[M]	Clade E	Philippines	Mindanao	Misamis Oriental	Gingoog City
KU 327373	Clade E	Philippines	Mindanao	Davao del Sur	Kiblawan
KU 332773[M]	Clade E	Philippines	Bohol	Bohol	Valencia
KU 334226[M]	Clade E	Philippines	Mindanao	Misamis Oriental	Gingoog City
KU 334227	Clade E	Philippines	Mindanao	Misamis Oriental	Gingoog City
KU 334228[M]	Clade E	Philippines	Mindanao	Misamis Oriental	Gingoog City
KU 334229[M]	Clade E	Philippines	Mindanao	Misamis Oriental	Gingoog City
KU 335269[M]	Clade E	Philippines	Siargao	Siargao del Norte	Dapa
KU 335270[M]	Clade E	Philippines	Siargao	Siargao del Norte	Dapa
KU 335271	Clade E	Philippines	Siargao	Siargao del Norte	Del Carmen
KU 335272	Clade E	Philippines	Siargao	Siargao del Norte	Dapa
KU 335273[M]	Clade E	Philippines	Siargao	Siargao del Norte	Pilar
KU 335274[M]	Clade E	Philippines	Siargao	Siargao del Norte	Pilar
KU 335275[M]	Clade E	Philippines	Siargao	Siargao del Norte	Pilar
ACD 6484[P]	Clade E	Philippines	Siargao	Siargao del Norte	Pilar
ACD 6485[P]	Clade E	Philippines	Siargao	Siargao del Norte	Pilar
KU 304618[M]	Clade F	Philippines	Camiguin	Cagayan	Calayan
KU 304620[M]	Clade F	Philippines	Camiguin	Cagayan	Calayan
KU 304641	Clade F	Philippines	Camiguin	Cagayan	Calayan
KU 304642	Clade F	Philippines	Camiguin	Cagayan	Calayan
KU 304688[M]	Clade F	Philippines	Camiguin	Cagayan	Calayan
KU 304689[M]	Clade F	Philippines	Camiguin	Cagayan	Calayan
KU 304727[M]	Clade F	Philippines	Camiguin	Cagayan	Calayan
KU 304750	Clade F	Philippines	Camiguin	Cagayan	Calayan
KU 304767[M]	Clade F	Philippines	Camiguin	Cagayan	Calayan
KU 304871[M]	Clade F	Philippines	Calayan	Cagayan	Calayan
KU 304872[M]	Clade F	Philippines	Calayan	Cagayan	Calayan
KU 304940	Clade F	Philippines	Calayan	Cagayan	Calayan
KU 308074	Clade F	Philippines	Camiguin	Cagayan	Calayan
KU 323198[M]	Clade F	Philippines	Luzon	Aurora	Maria Aurora
KU 323207	Clade F	Philippines	Luzon	Aurora	Maria Aurora
KU 323224[M]	Clade F	Philippines	Luzon	Aurora	Maria Aurora
KU 329521[M]	Clade F	Philippines	Luzon	Ilocos Norte	Adams
KU 329522[M]	Clade F	Philippines	Luzon	Ilocos Norte	Adams
KU 329523[M]	Clade F	Philippines	Luzon	Ilocos Norte	Adams
RMB 944[P]	Clade F	Philippines	Luzon	Aurora	Maria Aurora
MVD 059[P]	Clade F	Philippines	Luzon	Cagayan	Penablanca
KU 302873[M]	Clade G	Philippines	Semirara	Antique	Caluya
KU 304013[M]	Clade G	Philippines	Lubang	Occidental Mindoro	Lubang
KU 320490	Clade G	Philippines	Lubang	Occidental Mindoro	Lubang
KU 320491[M]	Clade G	Philippines	Lubang	Occidental Mindoro	Lubang
KU 320492[M]	Clade G	Philippines	Lubang	Occidental Mindoro	Lubang
LSUHC 6178[M]	Clade G	Malaysia	Turtle	Sabah	
KU 328458	*Eutropis macularia*	Thailand		Nakhon Si Thammarat	
KU 304878[M]	*Eutropis bontocensis*	Philippines	Calayan	Cagayan	Calayan
KU 304873[M]	*Eutropis bontocensis*	Philippines	Calayan	Cagayan	Calayan

KU 304874[M]	*Eutropis bontocensis*	Philippines	Calayan	Cagayan	Calayan
KU 304886[M]	*Eutropis bontocensis*	Philippines	Calayan	Cagayan	Calayan
KU 304883[M]	*Eutropis bontocensis*	Philippines	Calayan	Cagayan	Calayan
KU 304888[M]	*Eutropis bontocensis*	Philippines	Calayan	Cagayan	Calayan
KU 304887[M]	*Eutropis bontocensis*	Philippines	Calayan	Cagayan	Calayan
KU 304881[M]	*Eutropis bontocensis*	Philippines	Calayan	Cagayan	Calayan
KU 304882[M]	*Eutropis bontocensis*	Philippines	Calayan	Cagayan	Calayan
KU 304889[M]	*Eutropis bontocensis*	Philippines	Calayan	Cagayan	Calayan
KU 304890[M]	*Eutropis bontocensis*	Philippines	Calayan	Cagayan	Calayan
KU 304892[M]	*Eutropis bontocensis*	Philippines	Calayan	Cagayan	Calayan
KU 314025	*Eutropis bontocensis*	Philippines	Batan	Batanes	Basco
KU 314026[M]	*Eutropis bontocensis*	Philippines	Sabtang	Batanes	Sabtang
KU 314027[M]	*Eutropis bontocensis*	Philippines	Sabtang	Batanes	Sabtang
KU 314028[M]	*Eutropis bontocensis*	Philippines	Sabtang	Batanes	Sabtang
KU 314029[M]	*Eutropis bontocensis*	Philippines	Sabtang	Batanes	Sabtang
KU 314030[M]	*Eutropis bontocensis*	Philippines	Sabtang	Batanes	Sabtang
KU 314032[M]	*Eutropis bontocensis*	Philippines	Sabtang	Batanes	Sabtang
KU 335111	*Eutropis bontocensis*	Philippines	Luzon	Mountain	Bontoc
KU 335112[M]	*Eutropis bontocensis*	Philippines	Luzon	Mountain	Bontoc
KU 335113	*Eutropis bontocensis*	Philippines	Luzon	Mountain	Bontoc
KU 335122	*Eutropis bontocensis*	Philippines	Luzon	Mountain	Bontoc
KU 335123	*Eutropis bontocensis*	Philippines	Luzon	Mountain	Bontoc
CAS 61344	*Eutropis bontocensis*	Philippines	Luzon	Mountain	Bontoc
FMNH 258984	*Eutropis cumingi* (Cordlllera Mountains)	Philippines	Luzon	Kalinga	Balbalan
FMNH 259453	*Eutropis cumingi* (Cordlllera Mountains)	Philippines	Luzon	Kalinga	Balbalan
FMNH 266254	*Eutropis cumingi*	Philippines	Luzon	Zambales	
KU 304009[M]	*Eutropis cumingi*	Philippines	Lubang	Occidental Mindoro	Lubang
KU 304745[M]	*Eutropis cumingi*	Philippines	Camiguin Norte	Cagayan	Calayan
KU 304746[M]	*Eutropis cumingi*	Philippines	Camiguin Norte	Cagayan	Calayan
KU 306216	*Eutropis cumingi*	Philippines	Luzon	Cagayan	Pamplona
KU 308933[M]	*Eutropis cumingi*	Philippines	Luzon	Nueva Vizcaya	Quezon
KU 314022[M]	*Eutropis cumingi*	Philippines	Batan	Batanes	Ivana
KU 314023[M]	*Eutropis cumingi*	Philippines	Batan	Batanes	Ivana
KU 320489[M]	*Eutropis cumingi*	Philippines	Lubang	Occidental Mindoro	Lubang
KU 325106[M]	*Eutropis cumingi*	Philippines	Luzon	Aurora	Casiguran
KU 327378[M]	*Eutropis cumingi*	Philippines	Luzon	Isabela	San Mariano
KU 327382[M]	*Eutropis cumingi*	Philippines	Luzon	Isabela	San Mariano
KU 327383[M]	*Eutropis cumingi*	Philippines	Luzon	Isabela	San Mariano
KU 327385[M]	*Eutropis cumingi*	Philippines	Luzon	Isabela	San Mariano
KU 330070	*Eutropis cumingi*	Philippines	Luzon	Cagayan	Gonzaga
KU 335132	*Eutropis cumingi*	Philippines	Luzon	La Union	
KU 335133	*Eutropis cumingi*	Philippines	Luzon	La Union	
KU 335134	*Eutropis cumingi* (Cordlllera Mountains)	Philippines	Luzon	Mountain	Bontoc
KU 335135	*Eutropis cumingi*	Philippines	Luzon	Zambales	
KU 335139	*Eutropis cumingi*	Philippines	Luzon	Zambales	
RMB 9591[N]	*Eutropis cumingi*	Philippines	Batan	Batanes	Ivana
KU 302883[M]	*Eutropis indeprensa*	Philippines	Mindoro	Oriental Mindoro	Victoria
KU 304027[M]	*Eutropis indeprensa*	Philippines	Mindoro	Occidental Mindoro	Sablayan
KU 304028	*Eutropis indeprensa*	Philippines	Mindoro	Occidental Mindoro	Sablayan
KU 304032[M]	*Eutropis indeprensa*	Philippines	Mindoro	Occidental Mindoro	Sablayan
KU 304035[M]	*Eutropis indeprensa*	Philippines	Mindoro	Occidental Mindoro	Sablayan
KU 306992[M]	*Eutropis indeprensa*	Philippines	Mindoro	Occidental Mindoro	Calintaan
KU 306993	*Eutropis indeprensa*	Philippines	Mindoro	Occidental Mindoro	Calintaan
LSUHC 6160	*Eutropis indeprensa*	Malaysia	Borneo	Sabah	

FMNH 266253	*Eutropis m. borealis*	Philippines	Luzon	Zambales	Palauig
KU 302877	*Eutropis m. borealis*	Philippines	Polillo	Quezon	Polillo
KU 302905	*Eutropis m. borealis*	Philippines	Negros	Negros Oriental	Valencia
KU 304837[M]	*Eutropis m. borealis*	Philippines	Babuyan Claro	Cagayan	Calayan
KU 306196[M]	*Eutropis m. borealis*	Philippines	Luzon	Camarines del Sur	Baao
KU 306804[M]	*Eutropis m. borealis*	Philippines	Panay	Antique	San Remigio
KU 307536	*Eutropis m. borealis*	Philippines	Polillo	Quezon	Polillo
KU 308125[M]	*Eutropis m. borealis*	Philippines	Catanduanes	Catanduanes	Gigmoto
KU 313911[M]	*Eutropis m. borealis*	Philippines	Luzon	Camarines Norte	Labo
KU 323199[M]	*Eutropis m. borealis*	Philippines	Luzon	Aurora	Maria Aurora
KU 323200[M]	*Eutropis m. borealis*	Philippines	Luzon	Aurora	Maria Aurora
KU 323201[M]	*Eutropis m. borealis*	Philippines	Luzon	Aurora	Maria Aurora
KU 323202[M]	*Eutropis m. borealis*	Philippines	Luzon	Aurora	Maria Aurora
KU 323204[M]	*Eutropis m. borealis*	Philippines	Luzon	Aurora	Maria Aurora
KU 323205[M]	*Eutropis m. borealis*	Philippines	Luzon	Aurora	Maria Aurora
KU 323206[M]	*Eutropis m. borealis*	Philippines	Luzon	Aurora	Maria Aurora
KU 323210[M]	*Eutropis m. borealis*	Philippines	Luzon	Aurora	Baler
KU 323222	*Eutropis m. borealis*	Philippines	Luzon	Aurora	San Luis
KU 323223[M]	*Eutropis m. borealis*	Philippines	Luzon	Aurora	San Luis
KU 324812[M]	*Eutropis m. borealis*	Philippines	Luzon	Aurora	Casiguran
KU 325050[M]	*Eutropis m. borealis*	Philippines	Luzon	Aurora	San Luis
KU 325051[M]	*Eutropis m. borealis*	Philippines	Luzon	Aurora	San Luis
KU 325793	*Eutropis m. borealis*	Philippines	Luzon	Nueva Vizcaya	Quezon
KU 325794	*Eutropis m. borealis*	Philippines	Luzon	Nueva Vizcaya	Quezon
KU 327366[M]	*Eutropis m. borealis*	Philippines	Luzon	Isabela	San Mariano
KU 327369[M]	*Eutropis m. borealis*	Philippines	Polillo	Quezon	Burdeos
KU 327387	*Eutropis m. borealis*	Philippines	Luzon	Isabela	San Mariano
KU 327549[M]	*Eutropis m. borealis*	Philippines	Luzon	Isabela	San Mariano
KU 327557[M]	*Eutropis m. borealis*	Philippines	Luzon	Isabela	San Mariano
KU 327560	*Eutropis m. borealis*	Philippines	Luzon	Isabela	Cabagan
KU 327562[M]	*Eutropis m. borealis*	Philippines	Luzon	Isabela	San Mariano
KU 327567[M]	*Eutropis m. borealis*	Philippines	Luzon	Isabela	San Mariano
KU 327568	*Eutropis m. borealis*	Philippines	Luzon	Isabela	San Mariano
KU 327754	*Eutropis m. borealis*	Philippines	Luzon	Kalinga	Tabuk
KU 331728[M]	*Eutropis m. borealis*	Philippines	Siquijor	Siquijor	Siquijor
KU 331729[M]	*Eutropis m. borealis*	Philippines	Siquijor	Siquijor	Siquijor
ACD 3045[P]	*Eutropis m. borealis*	Philippines	Luzon	Isabela	San Mariano
ACD 3206[P]	*Eutropis m. borealis*	Philippines	Luzon	Cagayan	Gattaran
ACD 2269[P]	*Eutropis m. borealis*	Philippines	Luzon	Isabela	San Mariano
RMB 3942[P]	*Eutropis m. borealis*	Philippines	Luzon	Sorsogon	Irosin
TNHC 62990	*Eutropis m. borealis*	Philippines	Negros	Negros Oriental	Valencia
TNHC 62992	*Eutropis m. borealis*	Philippines	Luzon	Camarines Sur Prov.	Naga City
TNHC 62993	*Eutropis m. borealis*	Philippines	Luzon	Albay	Tiwi
TNHC 62997	*Eutropis m. borealis*	Philippines	Luzon	Zambales	Olongapo
KU 310149[M]	*Eutropis m. multicarinata*	Philippines	Dinagat	Dinagat	Loreto
KU 310151[M]	*Eutropis m. multicarinata*	Philippines	Dinagat	Dinagat	Loreto
KU 310153[M]	*Eutropis m. multicarinata*	Philippines	Dinagat	Dinagat	Loreto
KU 310155[M]	*Eutropis m. multicarinata*	Philippines	Dinagat	Dinagat	Loreto
KU 311246[M]	*Eutropis m. multicarinata*	Philippines	Leyte	Leyte	Baybay
KU 320025[M]	*Eutropis m. multicarinata*	Philippines	Mindanao	Agusan del Sur	San Francisco
KU 320026	*Eutropis m. multicarinata*	Philippines	Mindanao	Agusan del Sur	San Francisco
EMD 257[P]	*Eutropis m. multicarinata*	Philippines	Mindanao	Surigao del Sur	Cantilan
ACD 7409[P]	*Eutropis m. multicarinata*	Philippines	Leyte	Southern Leyte	Sogod
ACD 7436[P]	*Eutropis m. multicarinata*	Philippines	Leyte	Southern Leyte	Sogod

EMD 232[P]	*Eutropis m. multicarinata*	Philippines	Mindanao	Surigao del Sur	Calintaan
CAS 237940[M]	*Eutropis sp*. Palau	Palau	Carp	Ngercheu	
CAS 237940[M]	*Eutropis sp*. Palau	Palau	Carp	Ngercheu	
CAS 238095[M]	*Eutropis sp*. Palau	Palau	Carp	Ngercheu	
CAS 238097[M]	*Eutropis sp*. Palau	Palau	Carp	Ngercheu	
CAS 238098[M]	*Eutropis sp*. Palau	Palau	Carp	Ngercheu	
CAS 238099[M]	*Eutropis sp*. Palau	Palau	Carp	Ngercheu	
CAS 238100[M]	*Eutropis sp*. Palau	Palau	Carp	Ngercheu	
CAS 238101[M]	*Eutropis sp*. Palau	Palau	Carp	Ngercheu	
CAS 238220[M]	*Eutropis sp*. Palau	Palau	Ngerebelas	Ngcheangel	
CAS 248247	*Eutropis sp*. Palau	Palau	Ngerebelas	Ngcheangel	
CAS 248248[M]	*Eutropis sp*. Palau	Palau	Ngerebelas	Ngcheangel	
CAS 248248[M]	*Eutropis sp*. Palau	Palau	Ngerebelas	Ngcheangel	
CAS 248808[M]	*Eutropis sp*. Palau	Palau	Babeldaob	Ngaraard	
USNM 577438	*Eutropis sp*. Palau	Palau	Babeldaob		
USNM 577449	*Eutropis sp*. Palau	Palau	Oreor		
USNM 577450	*Eutropis sp*. Palau	Palau	Oreor		
USNM 577453	*Eutropis sp*. Palau	Palau	Carp	Ngercheu	
USNM 577454	*Eutropis sp*. Palau	Palau	Carp	Ngercheu	
USNM 577457	*Eutropis sp*. Palau	Palau	Beliliou		
USNM 577458	*Eutropis sp*. Palau	Palau	Beliliou		
USNM 577477	*Eutropis sp*. Palau	Palau	Pulo Anna		

Appendix 5 Maximum likelihood gene trees for nuclear loci.

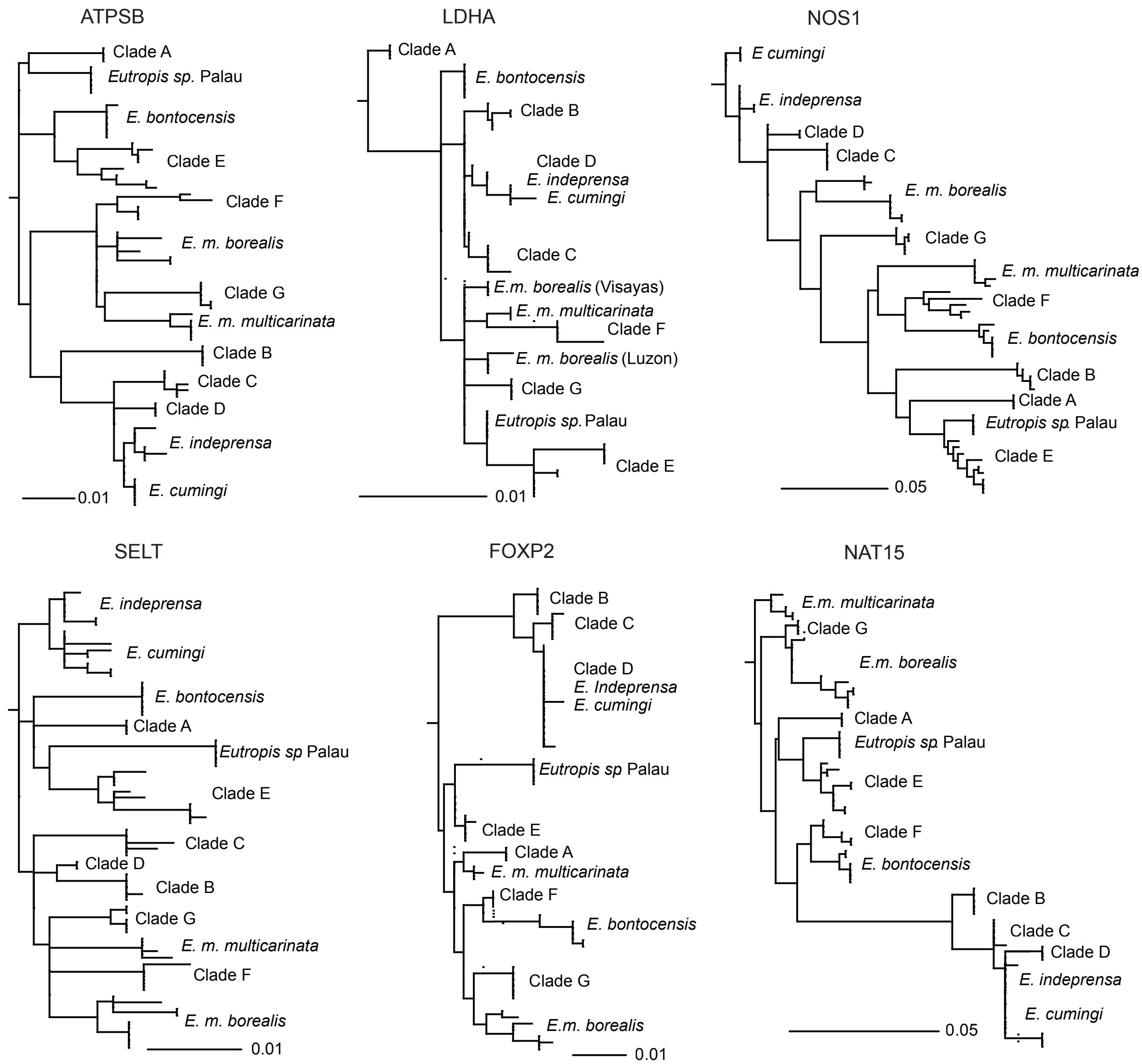

Appendix 6 Locality Information for specimens used in study. KU = Biodiversity Institute, University of Kansas; CES = Center for Ecological Sciences, Indian Institute of Science; LSUHC = La Sierra University, Lee Grismer; FMNH = Field Museum of Natural History, CAS = California Academy of Sciences; ZMFK = Zoologisches Forschungsmuseum Alexander Koenig; TNHC = University of Texas Natural History Collection; JAM = Jim McGuire, Museum of Vertebrate Zoology, University of California Berkeley; [P]Specimen deposited at Philippine National Museum; [N]No voucher specimen

Species Taxon Name	Catalog#	Country	Landmass	Province/State	District/Municipality
Dasia Grisea	KU 305574	Philippines	Luzon	Camarines del Sur	Ligao
Eutropis madaraszi	ZMFK 15976	Sri Lanka			
E.macropthalma	ZMFK 71716	Indonesia	Java		
Emoia atrococtata	KU 304896	Philippines	Calayan	Cagayan	Calayan
Eutropis allapallensis	CES 09/902	India		Tamil Nadu	
Eutropis allapallensis	CES 09/844	India		Karnataka	
Eutropis beddomii	CES 10/804	India		Orissa	
Eutropis beddomii	CES 09/1012	India		Andhra Pradesh	
Eutropis bibronii	CES 10/809	India		Orissa	
Eutropis bontocensis	KU 304878	Philippines	Calayan	Cagayan	Calayan
Eutropis bontocensis	KU 314026	Philippines	Sabtang	Batanes	Sabtang
Eutropis bontocensis	KU 335111	Philippines	Luzon	Mountain	Bontoc
Eutropis carinata	CES 11/810	India		Andhra Pradesh	
Eutropis carinata	CES 09/945	India		Orissa	
Eutropis Clade A	KU 327372	Philippines	Mindanao	South Cotobato	Tampakan
Eutropis Clade A	CDS 5300[P]	Philippines	Mindanao	South Cotabato	Tampakan
Eutropis Clade A	KU 327370	Philippines	Mindanao	South Cotobato	Tampakan
Eutropis Clade B	KU 306810	Philippines	Panay	Antique	San Remigio
Eutropis Clade B	KU 306811	Philippines	Panay	Antique	San Remigio
Eutropis Clade B	GVAG 280[P]	Philippines	Panay	Antique	Sibalom
Eutropis Clade C	KU 306194	Philippines	Dinagat	Dinagat Islands	Loreto
Eutropis Clade C	KU 314104	Philippines	Mindanao	Agusan del Sur	San Francisco
Eutropis Clade C	KU 306199	Philippines	Luzon	Camarines del Sur	Presentacion
Eutropis Clade D	KU 311406	Philippines	Palawan	Palawan	Rizal
Eutropis Clade D	KU 311407	Philippines	Palawan	Palawan	Rizal
Eutropis Clade D	KU 311449	Philippines	Palawan	Palawan	Brooke's Point
Eutropis Clade E	KU 335270	Philippines	Siargao	Siargap del Norte	Dapa
Eutropis Clade E	KU 335271	Philippines	Siargao	Siargap del Norte	Del Carmon
Eutropis Clade E	KU 320030	Philippines	Mindanao	Misamis Oriental	Gingoog City

Eutropis Clade E	KU 314106	Philippines	Mindano	Agusan del Sur	Bunawan
Eutropis Clade F	KU 304872	Philippines	Calayan	Cagayan	Calayan
Eutropis Clade F	KU 323207	Philippines	Luzon	Aurora	Maria Aurora
Eutropis Clade F	KU 323198	Philippines	Luzon	Aurora	Maria Aurora
Eutropis Clade G	KU 304013	Philippines	Lubang	Occidental Mindoro	Lubang
Eutropis Clade G	LSUHC 6178	Malaysia		Sabah	
Eutropis Clade G	KU 302873	Philippines	Semirara	Antique	Caluya
Eutropis clivicola	CES 10/801	India		Kerala	
Eutropis clivicola	CES 09/1026	India		Kerala	
Eutropis cumingi	KU 335134	Philippines	Luzon	Mountain	Bontoc
Eutropis cumingi	FMNH 258984	Philippines	Luzon	Kalinga	Balbalan
Eutropis cumingi	RMB 9591[N]	Philippines	Batan	Batanes	Ivana
Eutropis cumingi	KU 308933	Philippines	Luzon	Nueva Vizcaya	Quezon
Eutropis grandis	JAM 11362	Indonesia	Sulawesi		
Eutropis grandis	JAM 11488	Indonesia	Sulawesi		
Eutropis grandis	RMB 1611[N]	Indonesia	Sulawesi		Siuna
Eutropis indeprensa	KU 304027	Philippines	Mindoro	Occidental Mindoro	Sablayan
Eutropis indeprensa	LSUHC 6160	Malaysia	Borneo	Sabah	
Eutropis indeprensa	KU 306992	Philippines	Mindoro	Occidental Mindoro	Calintaan
Eutropis longicaudata	LSUHC 9242	Vietnam		Ba Ria-Vung Tau	
Eutropis longicaudata	LSUHC 3787	Malaysia	Pulau Tioman	Pahang	
Eutropis longicaudata	CAS 216129	Myanmar		Mandalay	Pyin Oo Lwin
Eutropis longicaudata	FMNH 255518	Lao PDR		Champasak	Mounlapamok
Eutropis longicaudata	KU 328457	Thailand		Nakhon Ratchisma	
Eutropis longicaudata	CAS 230469	Myanmar		Shan	Taunggyi
Eutropis longicaudata	CAS 235354	Myanmar		Chin	Mintatt
Eutropis macularia	KU 328458	Thailand		Nakhon Si Thammarat	
Eutropis macularia	FMNH 255529	Lao PDR		Champasak	Mounlapamok
Eutropis macularia	LSUHC 7244	Malaysia		Perak	
Eutropis macularia	KU 328459	Thailand		Nakhon Ratchisma	
Eutropis macularia	FMNH 261841	Cambodia		Kampong Speu	
Eutropis macularia	CES 11/811	India		Andhra Pradesh	
Eutropis macularia	CES 09/964	India		Tripura	
Eutropis macularia	CAS 229618	Myanmar		Tanintharyi	Kawthoung
Eutropis macularia	CAS 230589	Myanmar		Shan	Ywa Ngan
Eutropis macularia	CAS 239728	Myanmar		Bago	Pyi
Eutropis macularia	KU 328462	Thailand		Nakhon Ratchisma	
Eutropis m. borealis	KU 331728	Philippines	Siquijor	Siquijor	Siquijor
Eutropis m. borealis	TNHC 62990	Philippines	Negros	Negros Oriental	Valencia
Eutropis m. borealis	KU 306804	Philippines	Panay	Antique	San Remigio
Eutropis m. borealis	FMNH 266253	Philippines	Luzon	Zambales	Palauig
Eutropis m. borealis	KU 323210	Philippines	Luzon	Aurora	Baler
Eutropis m. borealis	KU 325794	Philippines	Luzon	Nueva Vizcaya	Quezon

Eutropis m. multicarinata	KU 320025	Philippines	Mindanao	Agusan del Sur	San Francisco
Eutropis m. multicarinata	KU 310149	Philippines	Dinagat	Dinagat Islands	Loreto
Eutropis m. multicarinata	KU 310155	Philippines	Dinagat	Dinagat Islands	Loreto
Eutropis multifasciata	CAS 232271	Myanmar		Sagaing	Khandi
Eutropis multifasciata	KU 322323	Philippines	Luzon	Aurora	Baler
Eutropis multifasciata	TNHC 59044	Indonesia	Sulawesi	Propinsi Sulawesi Tengah	Kabupaten Poso
Eutropis multifasciata	CES 09/925	India		Assam	
Eutropis multifasciata	KU 320061	Philippines	Luzon	Laguna	Los Banos
Eutropis multifasciata	KU 306207	Philippines	Luzon	Camarines del Sur	Baao
Eutropis multifasciata	KU 306210	Philippines	Luzon	Cagayan	Pamplona
Eutropis multifasciata	KU 324211	Philippines	Bohol	Bohol	Bilar
Eutropis multifasciata	KU 321587	Philippines	Mindanao	Zamboanga City	Pasonanca
Eutropis multifasciata	KU 306777	Philippines	Panay	Antique	San Remigio
Eutropis multifasciata	KU 308984	Philippines	Palawan	Palawan	Puerto Princessa
Eutropis multifasciata	RMB 1424[N]	Indonesia	Sulawesi	Propinsi Sulawesi Tengah	Kabupaten Poso
Eutropis multifasciata	ACD 1380[P]	Philippines	Palawan		
Eutropis multifasciata	ACD 2541[P]	Philippines	Luzon	Isabela	
Eutropis multifasciata	KU 335213	Philippines	Luzon	Bulacan	Norzagaray
Eutropis multifasciata	DSM 1681[N]	Philippines	Luzon	Bulacan	Norzagaray
Eutropis multifasciata	PNMH/CMNH H 1419	Philippines	Mindanao	Davao City	Calinan
Eutropis multifasciata	KU 328986	Thailand		Nakhon Si Thammarat	
Eutropis multifasciata	RMB 1428[N]	Indonesia	Sulawesi	Propinsi Sulawesi Tengah	Kabupaten Poso
Eutropis multifasciata	TNHC 59035	Indonesia	Sulawesi	Propinsi Sulawesi Tengah	Kabupaten Poso
Eutropis multifasciata	TNHC 59043	Indonesia	Sulawesi	Propinsi Sulawesi Tengah	Kabupaten Poso
Eutropis multifasciata	TNHC 59044	Indonesia	Sulawesi	Propinsi Sulawesi Tengah	Kabupaten Poso
Eutropis multifasciata	TNHC 58928	Indonesia	Sulawesi	Propinsi Sulawesi Tengah	Kabupatan Banggai
Eutropis multifasciata	RMB 1657[N]	Indonesia	Sulawesi	Propinsi Sulawesi Tengah	Kabupatan Banggai
Eutropis nagarjuni	CES 10/839	India		Andhra Pradesh	
Eutropis novemcarinata	CAS 215714	Myanmar		Sagaing	Mon Ywa
Eutropis quadricarinata	CAS 232429	Myanmar		Kachin	Myitkyina
Eutropis quadricarinata	CAS 240682	Myanmar		Kachin	Myitkyina
Eutropis rudis	TNHC 59050	Indonesia	Sulawesi	Propinsi Sulawesi Tengah	Kabupatan Banggai
Eutropis rudis	JAM 7517	Indonesia	Sulawesi		
Eutropis rudis	FMNH 230155	Malaysia		Sabah	Lahad Datu
Eutropis rudis	FMNH 269117	Malaysia		Sarawak	Bintulu
Eutropis rudis	LSUHC 4078	Malaysia	Borneo	Sarawak	
Eutropis rudis	LSUHC 6177	Brunei	Borneo		
Eutropis rudis	TNHC 59045	Indonesia	Sulawesi	Propinsi Sulawesi Tengah	Kabupatan Banggai
Eutropis rudis	TNHC 59048	Indonesia	Sulawesi	Propinsi Sulawesi Tengah	Kabupatan Banggai

Eutropis rugifera	KU 315013	Philippines	Mindanao	Zamboanga City	Pasonanca
Eutropis rugifera	KU 321833	Philippines	Mindanao	Zamboanga City	Pasonanca
Eutropis rugifera	JAM 10392	Indonesia	Sulawesi		
Eutropis rugifera	LSUHC 4067	Malaysia	Borneo	Sarawak	
Eutropis rugifera	LSUHC 8929	Malaysia		Johor	
Eutropis rugifera	KU 321834	Philippines	Mindanao	Zamboanga City	Pasonanca
Eutropis rugifera	JAM 10262	Indonesia	Sulawesi		
Eutropis sp. Palau	CAS 238095	Palau	Carp Island	Ngercheu Islands	
Eutropis sp. Palau	CAS 238220	Palau	Ngerebelas	Ngcheangel Atoll	
Eutropis sp. Palau	CAS 248247	Palau	Ngerebelas	Ngcheangel Atoll	
Eutropis trivittata	CES 10/849	India		Andhra Pradesh	
Eutropis trivittata	CES 09/976	India		Maharashta	
Mabuya mabouya	KU 214970	Peru		Madre de Dios	
Trachylepis perrotetii	KU 290460	Ghana			

Appendix 7 Table of Genbank numbers for individuals used in study. KU = Biodiversity Institute, University of Kansas, CES = Center for Ecological Sciences, Indian Institute of Science, LSUHC = La Sierra University, Lee Grismer, FMNH = Field Museum of Natural History, CAS = California Academy of Sciences, ZMFK = Zoologisches Forschungmuseum Alexander Koenig, TNHC = University of Texas Natural History Collection, JAM = Jim McGuire, Museum of Vertebrate Zoology, University of California Berkeley; [P] Specimen deposited at Philippine National Museum; [N]No voucher specimen.

Species Taxon Name	**Catalog#**	**ND2**	**ATPSB**	**SELT**	**NAT15**	**FOXP2**	**NOS1**	**LDAH**
Dasia grisea	KU 305574	KJ574688	KJ574416	KJ574973	KJ574644	KJ574456	KJ574757	KJ574501
Emoia atrococtata	KU 304896	KJ574690	KJ574417	KJ574974	KJ574645	KJ574458	KJ574758	KJ574503
Eutropis allapallensis	CES 09/902	KJ574682	KJ574412	———	KJ574636	KJ574457	KJ574756	KJ574502
Eutropis allapallensis	CES 09/844	KJ574689	———	———	KJ574635	———	———	KJ574497
Eutropis beddomii	CES 10/804	KJ574684	———	———	KJ574638	KJ574452	———	KJ574504
Eutropis beddomii	CES 09/1012	KJ574683	———	———	KJ574637	KJ574451	———	KJ574498
Eutropis bibronii	CES 10/809	KJ574691	KJ574413	———	KJ574639	KJ574453	KJ574759	KJ574505
Eutropis carinata	CES 11/810	KJ574685	KJ574415	———	KJ574641	———	———	KJ574506
Eutropis carinata	CES 09/945	———	KJ574414	———	KJ574640	KJ574454	———	KJ574499
Eutropis clivicola	CES 10/801	KJ574687	———	———	KJ574643	KJ574460	———	KJ574508
Eutropis clivicola	CES 09/1026	KJ574686	———	———	KJ574642	KJ574455	———	KJ574500
Eutropis grandis	JAM 11362	KJ574693	KJ574419	KJ574693	KJ574647	KJ574461	KJ574761	KJ574509
Eutropis grandis	JAM 11488	KJ574694	KJ574420	KJ574977	KJ574648	KJ574462	KJ574762	KJ574510
Eutropis grandis	RMB 1611[N]	KJ574746	KJ574444	KJ574999	KJ574672	KJ574488	KJ574785	KJ574534
Eutropis longicaudata	LSUHC 9242	KJ574700	KJ574425	KJ574982	KJ574653	KJ574467	KJ574766	KJ574515
Eutropis longicaudata	LSUHC 3787	KJ574699	KJ574424	KJ574981	KJ574652	KJ574466	KJ574765	KJ574514
Eutropis longicaudata	FMNH 255518	KJ574698	KJ574423	KJ574980	KJ574651	KJ574465	KJ574764	KJ574513
Eutropis longicaudata	KU 328457	KJ574697	KJ574422	KJ574979	KJ574650	KJ574464	KJ574763	KJ574512
Eutropis longicaudata	CAS 216129	KJ574695	KJ574421	KJ574978	KJ574649	KJ574463	———	KJ574511
Eutropis longicaudata	CAS 230469	KJ574696	———	———	———	———	———	———
Eutropis macropthalma	ZMFK 71716	———	KJ574450	———	———	KJ574496	KJ574791	KJ574545
Eutropis macularia	CAS 235354	KJ574703	KJ574426	KJ574983	KJ574654	KJ574469	KJ574767	KJ574517
Eutropis macularia	FMNH 255529	KJ574706	KJ574428	KJ574985	KJ574656	KJ574471	KJ574769	KJ574519
Eutropis macularia	LSUHC 7244	KJ574708	KJ574430	KJ574987	KJ574658	KJ574473	KJ574771	KJ574521
Eutropis macularia	KU 328459	KJ574704	KJ574427	KJ574984	KJ574655	KJ574470	KJ574768	KJ574518
Eutropis macularia	FMNH 261841	KJ574707	KJ574429	KJ574986	KJ574657	KJ574472	KJ574770	KJ574520
Eutropis macularia	CES 11/811	KJ574752	———	———	KJ574675	KJ574468	KJ574787	KJ574516
Eutropis macularia	CES 09/964	———	KJ574446	———	KJ574674	KJ574490	———	KJ574537
Eutropis macularia	CAS 229618	KJ574701	———	———	———	———	———	———
Eutropis macularia	CAS 230589	KJ574702	———	———	———	———	———	———
Eutropis macularia	CAS 239728	KJ574736	———	———	———	———	———	———

Eutropis macularia	KU 328462	KJ574705	———	———	———	———	———	———
Eutropis madaraszi	ZMFK 15976	———	KJ574449	KJ575003	KJ574681	KJ574495	KJ574790	KJ574544
Eutropis multifasciata	CAS 232271	KJ574713	KJ574432	KJ574989	KJ574660	KJ574475	KJ574773	KJ574523
Eutropis multifasciata	KU 322323	KJ574718	KJ574433	KJ574990	KJ574661	KJ574476	KJ574774	KJ574524
Eutropis multifasciata	TNHC 59044	KJ574745	KJ574443	KJ574991	KJ574662	KJ574477	KJ574775	KJ574525
Eutropis multifasciata	CES 09/925	KJ574712	———	———	KJ574677	KJ574492	———	KJ574539
Eutropis multifasciata	KU 320061	KJ574710	———	———	———	———	———	———
Eutropis multifasciata	KU 306207	KJ574714	———	———	———	———	———	———
Eutropis multifasciata	KU 306210	KJ574715	———	———	———	———	———	———
Eutropis multifasciata	KU 324211	KJ574716	———	———	———	———	———	———
Eutropis multifasciata	KU 321587	KJ574717	———	———	———	———	———	———
Eutropis multifasciata	KU 306777	KJ574719	———	———	———	———	———	———
Eutropis multifasciata	KU 308984	KJ574720	———	———	———	———	———	———
Eutropis multifasciata	RMB 1424[N]	KJ574733	———	———	———	———	———	———
Eutropis multifasciata	ACD 1380[P]	KJ574734	———	———	———	———	———	———
Eutropis multifasciata	ACD 2541[P]	KJ574735	———	———	———	———	———	———
Eutropis multifasciata	KU 335213	KJ574738	———	———	———	———	———	———
Eutropis multifasciata	DSM 1681[N]	KJ574739	———	———	———	———	———	———
Eutropis multifasciata	KU 328986	KJ574740	———	———	———	———	———	———
Eutropis multifasciata	PNM 1419	KJ574741	———	———	———	———	———	———
Eutropis multifasciata	RMB 1428[N]	KJ574742	———	———	———	———	———	———
Eutropis multifasciata	TNHC 59035	KJ574743	———	———	———	———	———	———
Eutropis multifasciata	TNHC 59043	KJ574744	———	———	———	———	———	———
Eutropis multifasciata	TNHC 58928	KJ574748	———	———	———	———	———	———
Eutropis multifasciata	RMB 1657[N]	KJ574749	———	———	———	———	———	———
Eutropis nagarjuni	CES 10/839	KJ574754	———	———	KJ574678	KJ574493	———	KJ574540
Eutropis novemcarinata	CAS 215714	KJ574721	KJ574434	KJ574992	KJ574663	KJ574478	KJ574776	KJ574526
Eutropis quadricarinata	CAS 232429	KJ574722	KJ574435	———	KJ574664	KJ574479	KJ574777	KJ574536
Eutropis quadricarinata	CAS 240682	KJ574737	KJ574442	———	KJ574671	KJ574487	KJ574784	KJ574533
Eutropis rudis	TNHC 59050	KJ574751	KJ574445	KJ575000	KJ574673	KJ574489	KJ574786	KJ574535
Eutropis rudis	JAM 7517	KJ574726	KJ574439	KJ574996	KJ574668	KJ574483	KJ574781	KJ574530
Eutropis rudis	FMNH 230155	KJ574723	KJ574436	KJ574993	KJ574665	KJ574480	KJ574778	KJ574527
Eutropis rudis	FMNH 269117	KJ574724	KJ574437	KJ574994	KJ574666	KJ574481	KJ574779	KJ574528
Eutropis rudis	LSUHC 4078	KJ574728	———	———	———	———	———	———
Eutropis rudis	LSUHC 6177	KJ574729	———	———	———	———	———	———
Eutropis rudis	TNHC 59045	KJ574747	———	———	———	———	———	———
Eutropis rudis	TNHC 59048	KJ574750	———	———	———	———	———	———
Eutropis rugifera	KU 315013	KJ574692	KJ574418	KJ574975	KJ574646	KJ574459	KJ574760	KJ574507
Eutropis rugifera	KU 321833	KJ574709	KJ574431	KJ574988	KJ574659	KJ574474	KJ574772	KJ574522
Eutropis rugifera	JAM 10392	KJ574725	KJ574438	KJ574995	KJ574667	KJ574482	KJ574780	KJ574529
Eutropis rugifera	LSUHC 4067	KJ574727	KJ574440	KJ574997	KJ574669	KJ574484	KJ574782	KJ574531
Eutropis rugifera	LSUHC 8929	KJ574731	KJ574441	KJ574998	KJ574670	KJ574485	KJ574783	KJ574532
Eutropis rugifera	KU 321834	KJ574711	———	———	———	———	———	———
Eutropis rugifera	JAM 10262	KJ574730	———	———	———	———	———	———
Eutropis trivittata	CES 10/849	———	———	———	———	KJ574486	———	KJ574543
Eutropis trivittata	CES 09/976	KJ574732	———	———	KJ574680	———	———	KJ574542
Mabuya mabouya	KU 214970	KJ574753	KJ574447	KJ575001	KJ574676	KJ574491	KJ574788	KJ574538
Trachylepis perrotetii	KU 290460	KJ574755	KJ574448	KJ575002	KJ574679	KJ574494	KJ574789	KJ574541

Species Taxon Name	Catalog#	MC1R	RP40	R35
Dasia grisea	KU 305574	KJ574546	KJ574883	KJ574792
Emoia atrococtata	KU 304896	———	———	KJ574795
Eutropis allapallensis	CES 09/902	KJ574548	KJ574885	KJ574794
Eutropis allapallensis	CES 09/844	KJ574547	KJ574884	KJ574793
Eutropis beddomii	CES 10/804	KJ574550	KJ574887	KJ574797
Eutropis beddomii	CES 09/1012	KJ574549	KJ574886	KJ574796
Eutropis bibronii	CES 10/809	———	KJ574888	KJ574798
Eutropis bontocensis	KU 304878	KJ574552	KJ574890	KJ574800
Eutropis bontocensis	KU 314026	KJ574553	KJ574891	KJ574801
Eutropis bontocensis	KU 335111	KJ574551	KJ574889	KJ574799
Eutropis carinata	CES 11/810	KJ574555	KJ574893	KJ574803
Eutropis carinata	CES 09/945	KJ574554	KJ574892	KJ574802
Eutropis Clade A	KU 327372	KJ574561	KJ574899	KJ574809
Eutropis Clade A	CDS 5300[P]	KJ574597	KJ574935	KJ574845
Eutropis Clade A	KU 327370	KJ574625	KJ574963	KJ574873
Eutropis Clade B	KU 306810	KJ574577	KJ574915	KJ574825
Eutropis Clade B	KU 306811	KJ574578	KJ574916	KJ574826
Eutropis Clade B	GVAG 280[P]	KJ574599	KJ574937	KJ574847
Eutropis Clade C	KU 306194	KJ574563	KJ574901	KJ574811
Eutropis Clade C	KU 314104	KJ574581	KJ574919	KJ574829
Eutropis Clade C	KU 306199	KJ574564	KJ574902	KJ574812
Eutropis Clade D	KU 311406	KJ574572	KJ574910	KJ574820
Eutropis Clade D	KU 311407	KJ574573	KJ574911	KJ574821
Eutropis Clade D	KU 311449	KJ574567	KJ574905	KJ574815
Eutropis Clade E	KU 335270	KJ574595	KJ574933	KJ574843
Eutropis Clade E	KU 335271	KJ574596	KJ574934	KJ574844
Eutropis Clade E	KU 320030	KJ574557	KJ574895	KJ574805
Eutropis Clade E	KU 314106	KJ574608	KJ574946	KJ574856
Eutropis Clade F	KU 304872	KJ574576	KJ574914	KJ574824
Eutropis Clade F	KU 323207	KJ574601	KJ574939	KJ574849
Eutropis Clade F	KU 323198	KJ574600	KJ574938	KJ574848
Eutropis Clade G	KU 304013	KJ574606	KJ574944	KJ574854
Eutropis Clade G	LSUHC 6178	KJ574621	KJ574959	KJ574869
Eutropis Clade G	KU 302873	KJ574598	KJ574936	KJ574846
Eutropis clivicola	CES 10/801	KJ574560	KJ574898	KJ574808
Eutropis clivicola	CES 09/1026	KJ574559	KJ574897	KJ574807
Eutropis cumingi	KU 335134	KJ574562	KJ574900	KJ574810
Eutropis cumingi	FMNH 258984	KJ574566	KJ574904	KJ574814
Eutropis cumingi	RMB 9591[N]	KJ574609	KJ574947	KJ574857
Eutropis cumingi	KU 308933	KJ574565	KJ574903	KJ574813
Eutropis grandis	JAM 11362	KJ574568	KJ574906	KJ574816
Eutropis grandis	JAM 11488	KJ574569	KJ574907	KJ574817
Eutropis grandis	RMB 1611[N]	KJ574629	KJ574967	KJ574877
Eutropis indeprensa	KU 304027	KJ574574	KJ574912	KJ574822

Eutropis indeprensa	LSUHC 6160	KJ574622	KJ574960	KJ574870
Eutropis indeprensa	KU 306992	KJ574575	KJ574913	KJ574823
Eutropis longicaudata	LSUHC 9242	KJ574586	KJ574924	KJ574834
Eutropis longicaudata	LSUHC 3787	KJ574585	KJ574923	KJ574833
Eutropis longicaudata	FMNH 255518	KJ574584	KJ574922	KJ574832
Eutropis longicaudata	KU 328457	KJ574583	KJ574921	KJ574831
Eutropis longicaudata	CAS 216129	KJ574582	KJ574920	KJ574830
Eutropis macropthalma	ZMFK 71716	KJ574634	KJ574972	———
Eutropis macularia	CAS 235354	KJ574589	KJ574927	KJ574837
Eutropis macularia	FMNH 255529	KJ574591	KJ574929	KJ574839
Eutropis macularia	LSUHC 7244	KJ574593	KJ574931	KJ574841
Eutropis macularia	KU 328459	KJ574590	KJ574928	KJ574838
Eutropis macularia	FMNH 261841	KJ574592	KJ574930	KJ574840
Eutropis macularia	CES 11/811	KJ574587	KJ574925	KJ574835
Eutropis macularia	CES 09/964	KJ574588	KJ574926	KJ574836
Eutropis madaraszi	ZMFK 15976	KJ574633	KJ574971	KJ574882
Eutropis m. borealis	KU 331728	KJ574604	KJ574942	KJ574852
Eutropis m. borealis	TNHC 62990	KJ574605	KJ574943	KJ574853
Eutropis m. borealis	KU 306804	KJ574607	KJ574945	KJ574855
Eutropis m. borealis	FMNH 266253	KJ574631	KJ574969	KJ574879
Eutropis m. borealis	KU 323210	KJ574602	KJ574940	KJ574850
Eutropis m. borealis	KU 325794	KJ574603	KJ574941	KJ574851
Eutropis m. multicarinata	KU 320025	KJ574556	KJ574894	KJ574804
Eutropis m. multicarinata	KU 310149	KJ574579	KJ574917	KJ574827
Eutropis m. multicarinata	KU 310155	KJ574580	KJ574918	KJ574828
Eutropis multifasciata	CAS 232271	KJ574611	KJ574949	KJ574859
Eutropis multifasciata	KU 322323	KJ574612	KJ574950	KJ574860
Eutropis multifasciata	TNHC 59044	KJ574628	KJ574966	KJ574876
Eutropis multifasciata	CES 09/925	KJ574610	KJ574948	KJ574858
Eutropis nagarjuni	CES 10/839	KJ574613	KJ574951	KJ574861
Eutropis novemcarinata	CAS 215714	KJ574614	KJ574952	KJ574862
Eutropis quadricarinata	CAS 232429	KJ574615	KJ574953	KJ574863
Eutropis quadricarinata	CAS 240682	KJ574627	KJ574965	KJ574875
Eutropis rudis	TNHC 59050	KJ574630	KJ574968	KJ574878
Eutropis rudis	JAM 7517	KJ574619	KJ574957	KJ574867
Eutropis rudis	FMNH 230155	KJ574616	KJ574954	KJ574864
Eutropis rudis	FMNH 269117	KJ574617	KJ574955	KJ574865
Eutropis rugifera	KU 315013	KJ574558	KJ574896	KJ574806
Eutropis rugifera	KU 321833	KJ574594	KJ574932	KJ574842
Eutropis rugifera	JAM 10392	KJ574618	KJ574956	KJ574866
Eutropis rugifera	LSUHC 4067	KJ574620	KJ574958	KJ574868
Eutropis rugifera	LSUHC 8929	KJ574623	KJ574961	KJ574871
Eutropis sp. Palau	CAS 238095	KJ574626	KJ574964	KJ574874
Eutropis sp. Palau	CAS 238220	KJ574570	KJ574908	KJ574818
Eutropis sp. Palau	CAS 248247	KJ574571	KJ574909	KJ574819
Eutropis trivittata	CES 10/849	KJ574624	———	KJ574872

Eutropis trivittata	CES 09/976	———	KJ574962	———
Mabuya mabouya	KU 214970	———	———	KJ574880
Trachylepis perrotetii	KU 290460	KJ574632	KJ574970	KJ574881

Appendix 8 Individual Maximum Likelihood gene trees for each locus.

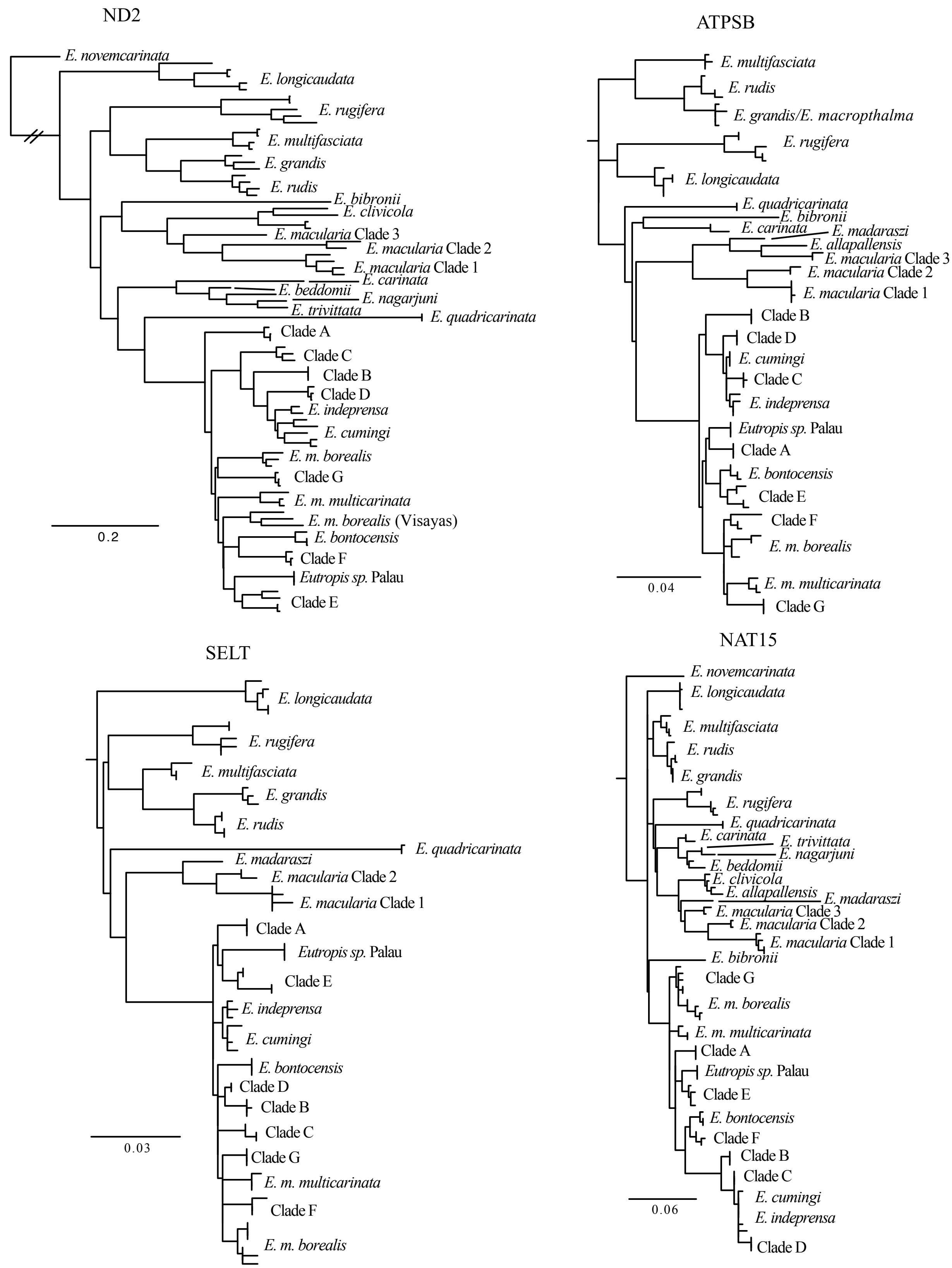

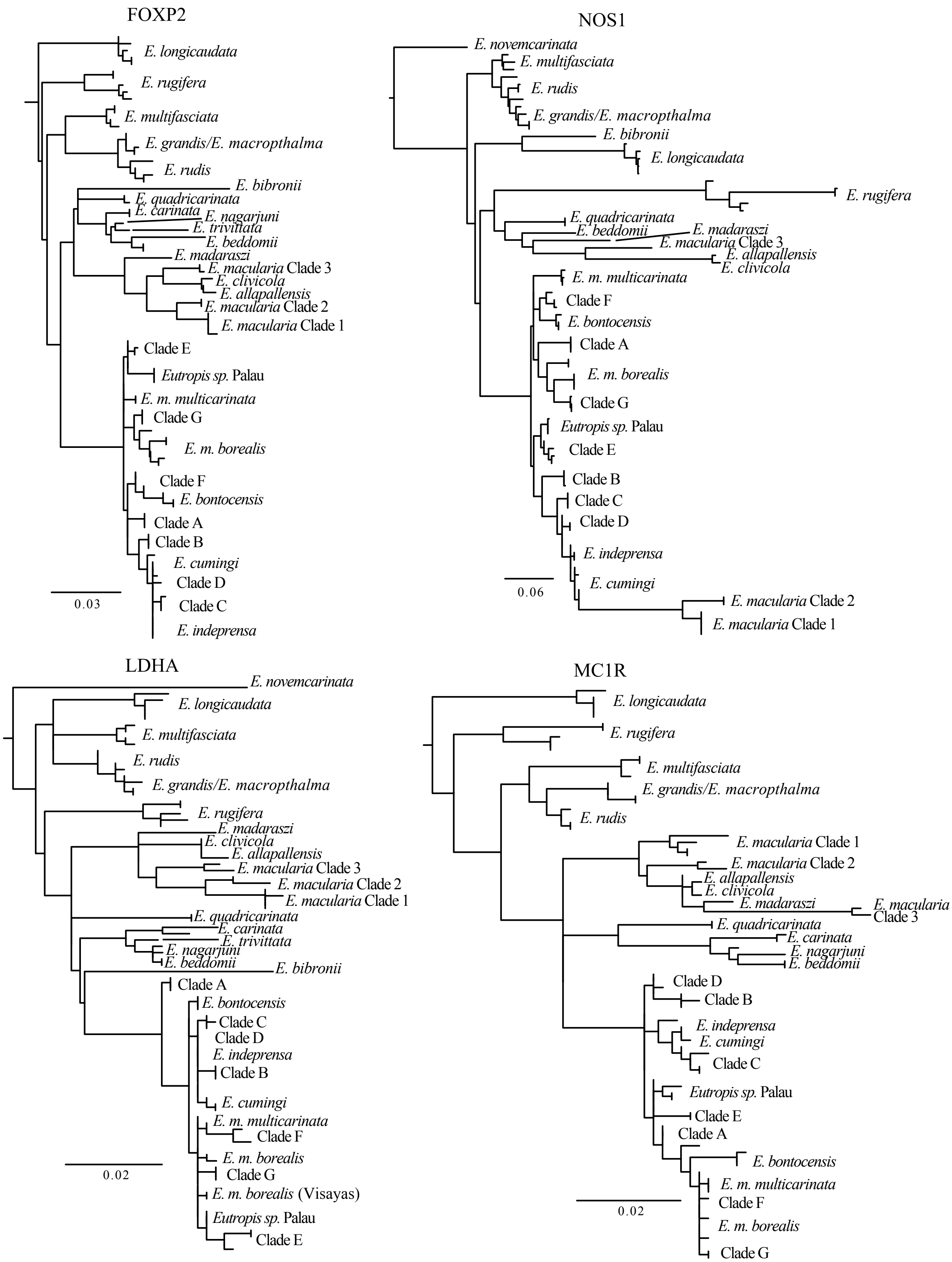

FOXP2
E. longicaudata
E. rugifera
E. multifasciata
E. grandis/E. macropthalma
E. rudis
E. bibronii
E. quadricarinata
E. carinata
E. nagarjuni
E. trivittata
E. beddomii
E. madaraszi
E. macularia Clade 3
E. clivicola
E. allapallensis
E. macularia Clade 2
E. macularia Clade 1
Clade E
Eutropis sp. Palau
E. m. multicarinata
Clade G
E. m. borealis
Clade F
E. bontocensis
Clade A
Clade B
E. cumingi
Clade D
Clade C
E. indeprensa
0.03
NOS1
E. novemcarinata
E. multifasciata
E. rudis
E. grandis/E. macropthalma
E. bibronii
E. longicaudata
E. rugifera
E. quadricarinata
E. beddomii
E. madaraszi
E. macularia Clade 3
E. allapallensis
E. clivicola
E. m. multicarinata
Clade F
E. bontocensis
Clade A
E. m. borealis
Clade G
Eutropis sp. Palau
Clade E
Clade B
Clade C
Clade D
E. indeprensa
E. cumingi
E. macularia Clade 2
E. macularia Clade 1
0.06
LDHA
E. novemcarinata
E. longicaudata
E. multifasciata
E. rudis
E. grandis/E. macropthalma
E. rugifera
E. madaraszi
E. clivicola
E. allapallensis
E. macularia Clade 3
E. macularia Clade 2
E. macularia Clade 1
E. quadricarinata
E. carinata
E. trivittata
E. nagarjuni
E. beddomii
E. bibronii
Clade A
E. bontocensis
Clade C
Clade D
E. indeprensa
Clade B
E. cumingi
E. m. multicarinata
Clade F
E. m. borealis
Clade G
E. m. borealis (Visayas)
Eutropis sp. Palau
Clade E
0.02
MC1R
E. longicaudata
E. rugifera
E. multifasciata
E. grandis/E. macropthalma
E. rudis
E. macularia Clade 1
E. macularia Clade 2
E. allapallensis
E. clivicola
E. madaraszi
E. macularia
Clade 3
E. quadricarinata
E. carinata
E. nagarjuni
E. beddomii
Clade D
Clade B
E. indeprensa
E. cumingi
Clade C
Eutropis sp. Palau
Clade E
Clade A
E. bontocensis
E. m. multicarinata
Clade F
E. m. borealis
Clade G
0.02

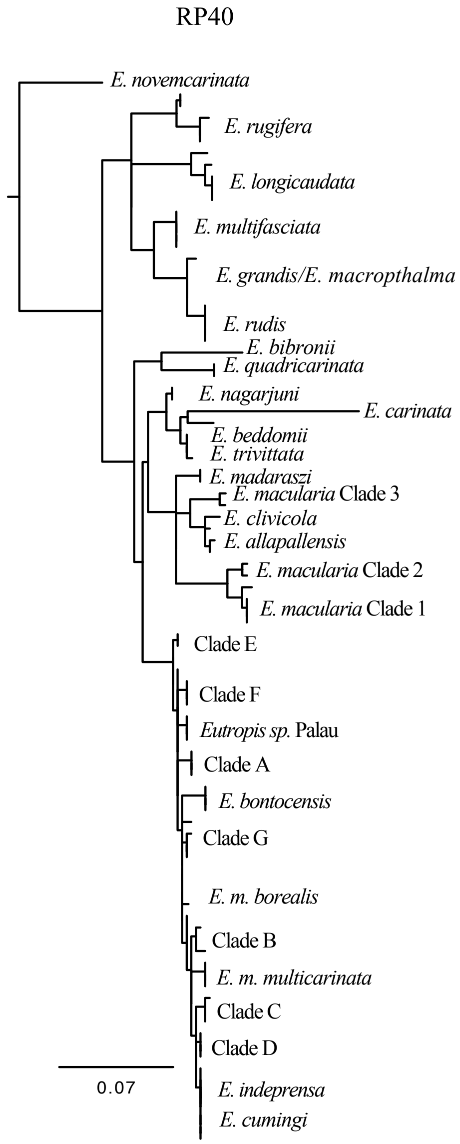
RP40
E. novemcarinata
E. rugifera
E. longicaudata
E. multifasciata
E. grandis/E. macropthalma
E. rudis
E. bibronii
E. quadricarinata
E. nagarjuni
E. carinata
E. beddomii
E. trivittata
E. madaraszi
E. macularia Clade 3
E. clivicola
E. allapallensis
E. macularia Clade 2
E. macularia Clade 1
Clade E
Clade F
Eutropis sp. Palau
Clade A
E. bontocensis
Clade G
E. m. borealis
Clade B
E. m. multicarinata
Clade C
Clade D
E. indeprensa
E. cumingi
0.07

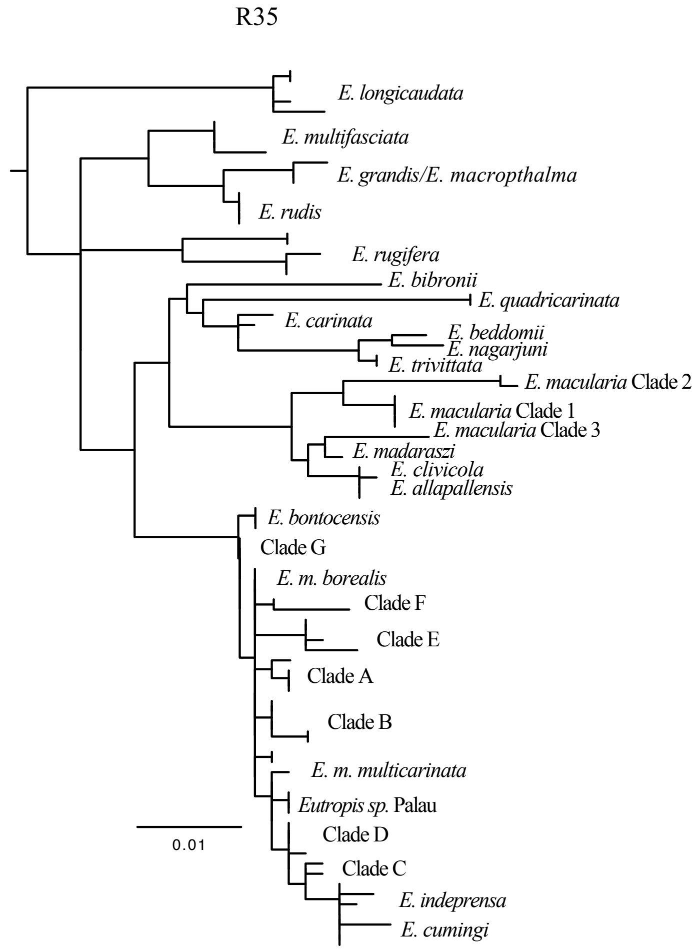
R35
E. longicaudata
E. multifasciata
E. grandis/E. macropthalma
E. rudis
E. rugifera
E. bibronii
E. quadricarinata
E. carinata
E. beddomii
E. nagarjuni
E. trivittata
E. macularia Clade 2
E. macularia Clade 1
E. macularia Clade 3
E. madaraszi
E. clivicola
E. allapallensis
E. bontocensis
Clade G
E. m. borealis
Clade F
Clade E
Clade A
Clade B
E. m. multicarinata
Eutropis sp. Palau
Clade D
Clade C
E. indeprensa
E. cumingi
0.01

Appendix 9 Results from BayesTraits biogeographic character-state reconstructions. Pie graphs represent relative probabilities of each state at each node. Red = India/Sri Lanka, Yellow = Sundaland, Purple = Mainland Asia, Black = Philippines. Green = Luzon PAIC + Mindoro , Blue = Mindanao PAIC, Brown = Visayan PAIC, Orange = Palawan + Borneo.

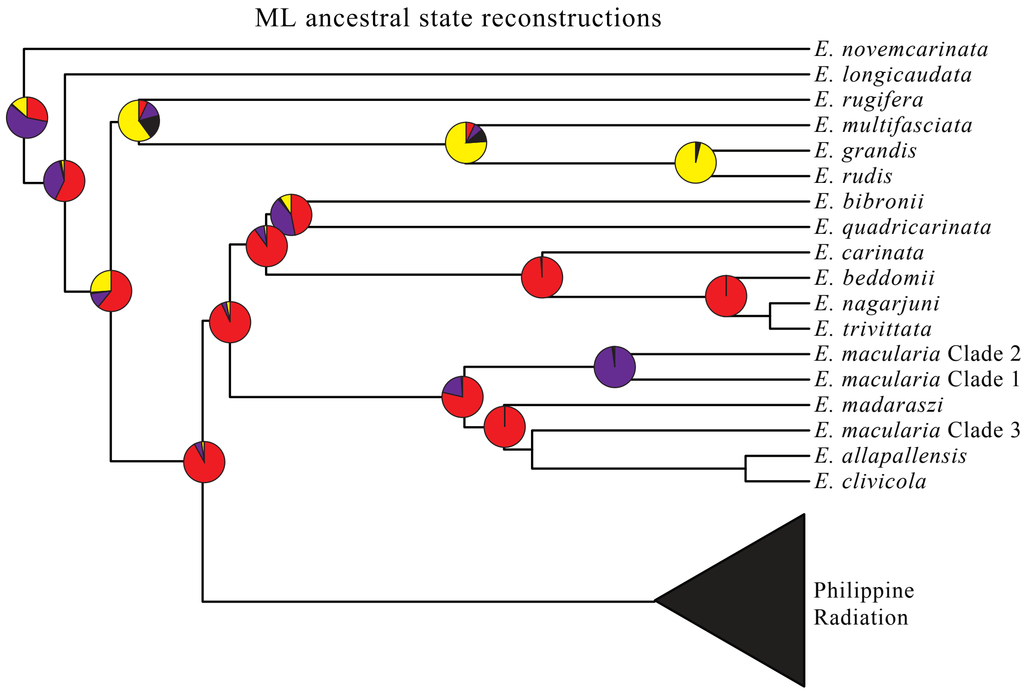

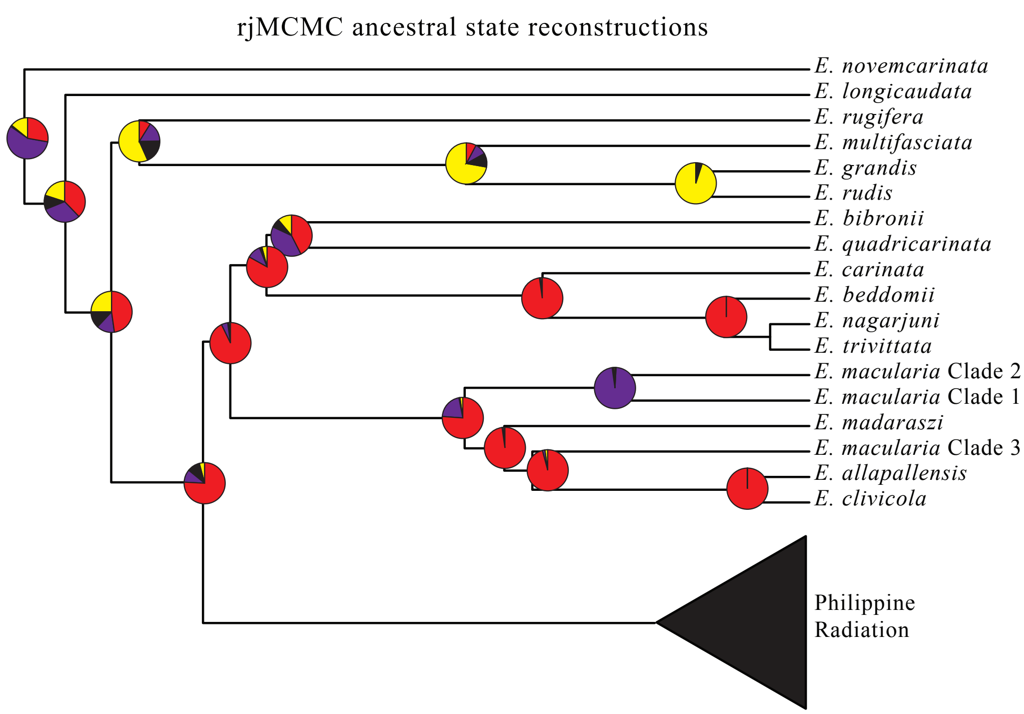

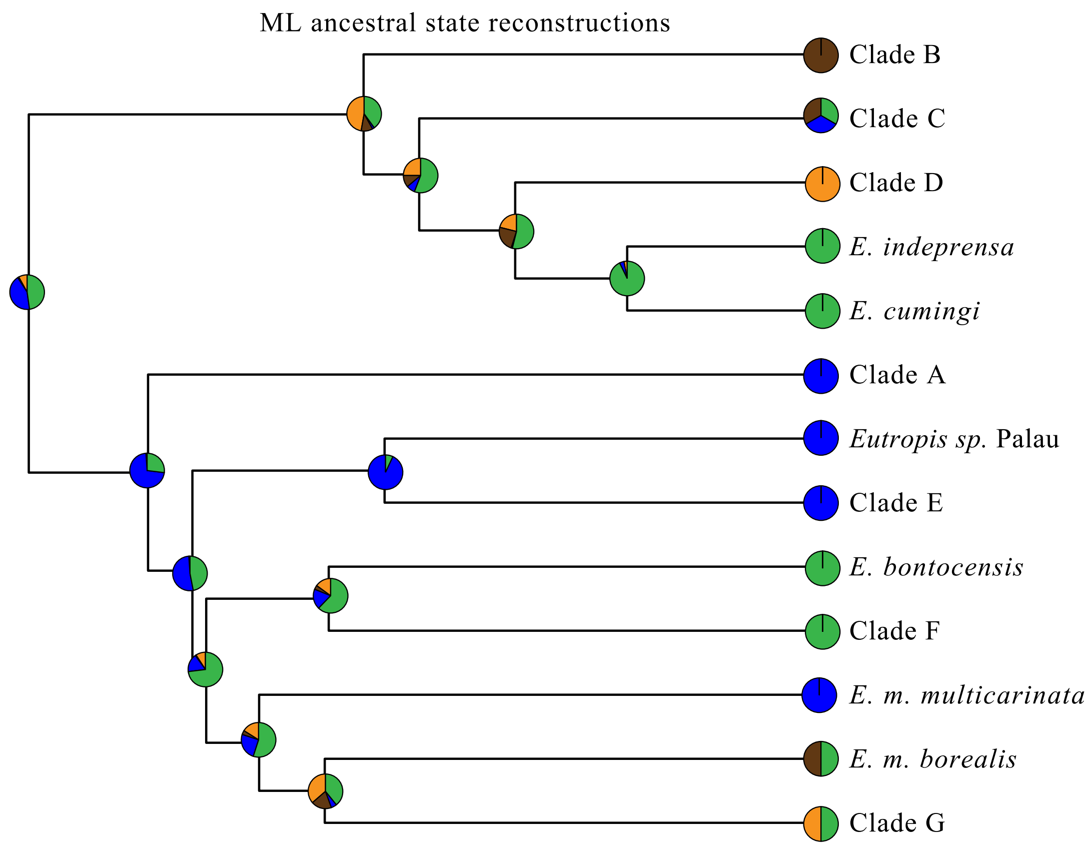
ML ancestral state reconstructions
Clade B
Clade C
Clade D
E. indeprensa
E. cumingi
Clade A
Eutropis sp. Palau
Clade E
E. bontocensis
Clade F
E. m. multicarinata
E. m. borealis
Clade G

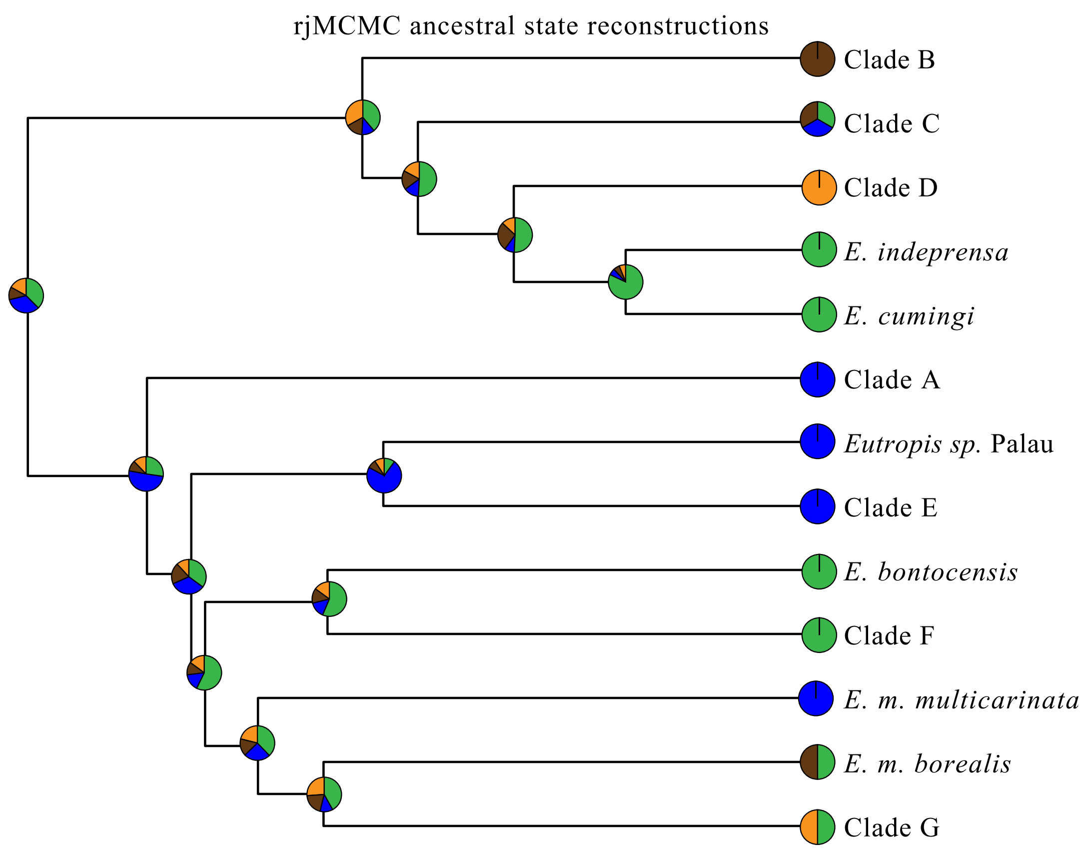
rjMCMC ancestral state reconstructions
Clade B
Clade C
Clade D
E. indeprensa
E. cumingi
Clade A
Eutropis sp. Palau
Clade E
E. bontocensis
Clade F
E. m. multicarinata
E. m. borealis
Clade G

Appendix 10 Locality information for *E. multifasciata* individuals sampled in study. KU = Biodiversity Institute, University of Kansas, LSUHC = La Sierra University, Lee Grismer, FMNH = Field Museum of Natural History, CAS = California Academy of Sciences, TNHC = University of Texas Natural History Collection, [P]Specimen deposited at Philippine National Museum; [N]No voucher specimen

Catalog #	Country	Landmass	Province/State	Genetic Data	Morphological Data
KU 322325	Philippines	Luzon	Aurora	x	x
KU 322324	Philippines	Luzon	Aurora	x	
KU 322323	Philippines	Luzon	Aurora	x	x
KU 322322	Philippines	Luzon	Aurora	x	x
KU 322326	Philippines	Luzon	Aurora	x	x
KU 322321	Philippines	Luzon	Aurora	x	x
KU 322327	Philippines	Luzon	Aurora	x	x
CAS 205004	Myanmar		Ayeyarwady	x	x
CAS 212916	Myanmar		Ayeyarwady	x	x
CAS 205006	Myanmar		Ayeyarwady	x	
CAS 212917	Myanmar		Ayeyarwady	x	x
CAS 212913	Myanmar		Ayeyarwady	x	x
CAS 222707	Myanmar		Ayeyarwady	x	x
CAS 222688	Myanmar		Ayeyarwady	x	x
CAS 204995	Myanmar		Rakhine	x	
CAS 221128	Myanmar		Rakhine	x	
CAS 223201	Myanmar		Rakhine	x	x
CAS 239758	Myanmar		Rakhine	x	x
CAS 239805	Myanmar		Rakhine	x	x
CAS 240068	Myanmar		Rakhine	x	x
CAS 239993	Myanmar		Rakhine	x	x
KU 304747	Philippines	Camiguin Norte	Cagayan	x	
KU 304654	Philippines	Camiguin Norte	Cagayan	x	
KU 304748	Philippines	Camiguin Norte	Cagayan	x	
KU 304557	Philippines	Camiguin Norte	Cagayan	x	
KU 328797	Philippines	Luzon	Albay	x	x
KU 328796	Philippines	Luzon	Albay	x	x
TNHC 62906	Philippines	Luzon	Camarines Sur	x	x
TNHC 62908	Philippines	Luzon	Camarines Sur	x	x
KU 306207	Philippines	Luzon	Camarines Sur	x	x
KU 313836	Philippines	Luzon	Camarines Norte	x	
KU 306208	Philippines	Luzon	Sorsogon	x	
KU 332777	Philippines	Bohol	Bohol	x	x
KU 324211	Philippines	Bohol	Bohol	x	x
KU 332778	Philippines	Bohol	Bohol	x	x
KU 332776	Philippines	Bohol	Bohol	x	x
KU 332775	Philippines	Bohol	Bohol	x	x
KU 332774	Philippines	Bohol	Bohol	x	x
KU 335110	Philippines	Luzon	Cagayan	x	
KU 335124	Philippines	Luzon	Cagayan	x	
KU 335125	Philippines	Luzon	Cagayan	x	

KU 307538	Philippines	Luzon	Cagayan	x	
KU 307539	Philippines	Luzon	Cagayan	x	
ACD 3209[P]	Philippines	Luzon	Cagayan	x	
ACD 3328[P]	Philippines	Luzon	Cagayan	x	
ACD 3330[P]	Philippines	Luzon	Cagayan	x	
KU 329377	Philippines	Luzon	Bulacan	x	x
KU 329379	Philippines	Luzon	Bulacan	x	
KU 329376	Philippines	Luzon	Bulacan	x	
KU 328942	Philippines	Luzon	Bulacan	x	x
KU 328943	Philippines	Luzon	Bulacan	x	x
KU 328940	Philippines	Luzon	Bulacan	x	
KU 328941	Philippines	Luzon	Bulacan	x	x
KU 320061	Philippines	Luzon	Laguna	x	
TNHC 62909	Philippines	Luzon	Zambales	x	
TNHC 62910	Philippines	Luzon	Zambales	x	
TNHC 62911	Philippines	Luzon	Zambales	x	
LSUHC 7113	Malaysia	Pulau Langkawi	Kedah	x	
LSUHC 7119	Malaysia	Pulau Langkawi	Kedah	x	
LSUHC 7121	Malaysia	Pulau Langkawi	Kedah	x	
LSUHC 7114	Malaysia	Pulau Langkawi	Kedah	x	
LSUHC 7526	Malaysia	Pulau Langkawi	Kedah	x	
LSUHC 7810	Cambodia			x	
FMNH 263340	Cambodia		Koh Kong	x	
FMNH 263341	Cambodia		Koh Kong	x	
LSUHC 7747	Cambodia			x	
FMNH 257250	Cambodia		Siem Reap	x	
FMNH 261830	Cambodia		Koh Kong	x	
FMNH 261835	Cambodia		Mondolkiri	x	
FMNH 262952	Cambodia		Ratanakiri	x	
FMNH 262953	Cambodia		Stung Treng	x	
FMNH 255516	Lao PDR		Bolikhamxay	x	
FMNH 255530	Lao PDR		Champasak	x	
FMNH 258731	Lao PDR		Vientiane	x	
KU 328465	Thailand		Nakhon Ratchisma	x	
KU 328466	Thailand		Nakhon Ratchisma	x	
KU 328467	Thailand		Nakhon Ratchisma	x	
FMNH 255596	Vietnam		Nghe An	x	
FMNH 255597	Vietnam		Nghe An	x	
KU 304017	Philippines	Mindoro	Occidental Mindoro	x	
KU 308402	Philippines	Mindoro	Occidental Mindoro	x	
KU 305434	Philippines	Mindoro	Occidental Mindoro	x	x
KU 305435	Philippines	Mindoro	Occidental Mindoro	x	x
KU 305436	Philippines	Mindoro	Occidental Mindoro	x	
KU 305433	Philippines	Mindoro	Occidental Mindoro	x	
KU 305437	Philippines	Mindoro	Occidental Mindoro	x	x
KU 304023	Philippines	Mindoro	Occidental Mindoro	x	
KU 305438	Philippines	Mindoro	Occidental Mindoro	x	x
KU 304026	Philippines	Mindoro	Occidental Mindoro	x	
KU 304024	Philippines	Mindoro	Occidental Mindoro	x	x
KU 302886	Philippines	Negros	Negros Occidental	x	
CDS GS 46[P]	Philippines	Negros	Negros Occidental	x	
KU 320486	Philippines	Negros	Negros Oriental	x	
KU 302910	Philippines	Negros	Negros Oriental	x	
KU 314100	Philippines	Mindanao	Agusan del Sur	x	x

KU 314101	Philippines	Mindanao	Agusan del Sur	x	x
KU 314102	Philippines	Mindanao	Agusan del Sur	x	x
KU 314103	Philippines	Mindanao	Agusan del Sur	x	x
KU 314099	Philippines	Mindanao	Agusan del Sur	x	x
PNMH 1419[P]	Philippines	Mindanao	Davao City	x	
KU 331496	Vietnam		Dien Bien	x	
KU 331497	Vietnam		Dien Bien	x	
KU 331498	Vietnam		Dien Bien	x	
LSUHC 7060	Malaysia		Pahang	x	
LSUHC 7058	Malaysia		Pahang	x	
LSUHC 6482	Malaysia		Pahang	x	
LSUHC 7059	Malaysia		Pahang	x	
LSUHC 8053	Malaysia		Pahang	x	
LSUHC 6470	Malaysia		Pahang	x	
ACD 1380[P]	Philippines	Palawan	Palawan	x	
KU 309488	Philippines	Palawan	Palawan	x	
KU 309487	Philippines	Palawan	Palawan	x	
KU 309489	Philippines	Palawan	Palawan	x	x
KU 309490	Philippines	Palawan	Palawan	x	
KU 327362	Philippines	Palawan	Palawan	x	
KU 327361	Philippines	Palawan	Palawan	x	x
KU 327363	Philippines	Palawan	Palawan	x	
KU 308984	Philippines	Palawan	Palawan	x	
KU 309167	Philippines	Palawan	Palawan	x	x
KU 309000	Philippines	Palawan	Palawan	x	
KU 309168	Philippines	Palawan	Palawan	x	x
KU 309169	Philippines	Palawan	Palawan	x	x
KU 306220	Philippines	Luzon	Cagayan	x	x
KU 306222	Philippines	Luzon	Cagayan	x	x
KU 306221	Philippines	Luzon	Cagayan	x	x
KU 306214	Philippines	Luzon	Cagayan	x	x
KU 306215	Philippines	Luzon	Cagayan	x	x
KU 306213	Philippines	Luzon	Cagayan	x	x
KU 306219	Philippines	Luzon	Cagayan	x	x
KU 306211	Philippines	Luzon	Cagayan	x	
KU 306212	Philippines	Luzon	Cagayan	x	x
KU 302894	Philippines	Panay	Antique	x	
KU 302893	Philippines	Panay	Antique	x	
KU 302895	Philippines	Panay	Antique	x	x
KU 302891	Philippines	Panay	Antique	x	x
KU 302890	Philippines	Panay	Antique	x	x
KU 302892	Philippines	Panay	Antique	x	x
CAS 229541	Myanmar		Tanintharyi	x	
CAS 229563	Myanmar		Tanintharyi	x	
KU 328986	Thailand		Nakhon Si Thammarat	x	
KU 328464	Thailand		Nakhon Si Thammarat	x	
KU 302900	Philippines	Polillo	Quezon	x	x
KU 302902	Philippines	Polillo	Quezon	x	x
KU 302901	Philippines	Polillo	Quezon	x	x
KU 302896	Philippines	Polillo	Quezon	x	
KU 302897	Philippines	Polillo	Quezon	x	x
KU 302898	Philippines	Polillo	Quezon	x	x
KU 302903	Philippines	Polillo	Quezon	x	x
KU 302887	Philippines	Sibuyan	Romblon	x	

KU 302888	Philippines	Sibuyan	Romblon	x	
KU 315362	Philippines	Tablas	Romblon	x	
KU 315363	Philippines	Tablas	Romblon	x	
KU 302904	Philippines	Tablas	Romblon	x	
KU 310784	Philippines	Samar	Eastern Samar	x	
KU 310785	Philippines	Samar	Eastern Samar	x	
KU 307537	Philippines	Luzon	Isabela	x	
ACD 2279[P]	Philippines	Luzon	Isabela	x	
ACD 3038[P]	Philippines	Luzon	Isabela	x	
ACD 3165[P]	Philippines	Luzon	Isabela	x	
ACD 3166[P]	Philippines	Luzon	Isabela	x	
KU 309886	Philippines	Camiguin Sur	Camiguin	x	
KU 302885	Philippines	Guimaras	Guimaras	x	
KU 308653	Philippines	Luzon	Nueva Vizcaya	x	
KU 324212	Philippines	Masbate	Masbate	x	
KU 324210	Philippines	Negros	Negros Occidental	x	
RMB 1428[N]	Indonesia	Sulawesi	Propinsi Sulawesi Tengah	x	
TNHC 59035	Indonesia	Sulawesi	Propinsi Sulawesi Tengah	x	
TNHC 59044	Indonesia	Sulawesi	Propinsi Sulawesi Tengah	x	
RMB 1424[N]	Indonesia	Sulawesi	Propinsi Sulawesi Tengah	x	
TNHC 59043	Indonesia	Sulawesi	Propinsi Sulawesi Tengah	x	
RMB 1657[N]	Indonesia	Sulawesi	Propinsi Sulawesi Tengah	x	
TNHC 58928	Indonesia	Sulawesi	Propinsi Sulawesi Tengah	x	
KU 306777	Philippines	Panay	Antique	x	x
KU 306778	Philippines	Panay	Antique	x	x
CAS 229736	Myanmar		Tanintharyi	x	x
CAS 229739	Myanmar		Tanintharyi	x	
CAS 229760	Myanmar		Tanintharyi	x	
CAS 243809	Myanmar		Tanintharyi	x	x
CAS 243735	Myanmar		Tanintharyi	x	x
CAS 243698	Myanmar		Tanintharyi	x	x
CAS 229788	Myanmar		Tanintharyi	x	x
LSUHC 4402	Malaysia	Pulau Tioman	Pahang	x	
LSUHC 4403	Malaysia	Pulau Tioman	Pahang	x	
LSUHC 3785	Malaysia	Pulau Tioman	Pahang	x	
KU 315008	Philippines	Mindanao	Zamboanga City	x	
KU 321590	Philippines	Mindanao	Zamboanga City	x	x
KU 321587	Philippines	Mindanao	Zamboanga City	x	x
KU 321588	Philippines	Mindanao	Zamboanga City	x	x
KU 321589	Philippines	Mindanao	Zamboanga City	x	x
KU 315007	Philippines	Mindanao	Zamboanga City	x	x
CAS 205005	Myanmar		Ayeyarwady		x
CAS 222687	Myanmar		Ayeyarwady		x
CAS 239812	Myanmar		Rakhine		x
CAS 239814	Myanmar		Rakhine		x
KU 324209	Philippines	Luzon	Albay		x
KU 306217	Philippines	Luzon	Camarines Sur		x
KU 306209	Philippines	Luzon	Camarines Sur		x
KU 329378	Philippines	Luzon	Bulacan		x
KU 328939	Philippines	Luzon	Cagayan		x
KU 304019	Philippines	Mindoro	Occidental Mindoro		x
KU 304025	Philippines	Mindoro	Occidental Mindoro		x

KU 304018	Philippines	Mindoro	Occidental Mindoro	x
KU 309091	Philippines	Palawan	Palawan	x
KU 309490	Philippines	Palawan	Palawan	x
KU 302899	Philippines	Polillo	Quezon	x
CAS 243828	Myanmar		Tanintharyi	x

Appendix 11 Multiplexed Shotgun Genotyping—Illumina Deep Sequencing Mapping Protocol

Isolate genomic DNA

DNA Quantification – Qubit or Picogreen

Dilute DNA to a standard concentration

- Dilute each sample to a DNA concentration of 5–10 ng/µL (this is flexible, you need to deposit 50 ng of DNA per sample for the digestion, so calculate a workable concentration).
- Protocol is for 10 µL of template at 5 ng/µL concentration.

DAY 1

Digest the genomic DNA samples with restriction enzyme.

1. Prepare a digestion master mix. For each 10 µL (50 ng DNA) sample we need:

2 µL	NEB buffer 4
0.2 µL	BSA (100X) (only if using MseI, not needed for NdeI)
X µL	Restriction enzyme (3 U): 0.3 µL for MseI, 0.15 µL for NdeI
10 – X – vol BSA µL	water (7.5 µL for MseI; 7.85 µL for NdeI)
10 µL	total

Example: master mix for NdeI digestion (make 105x per plate).

210 µL	NEBbuffer 4 (2 × 105)
No BSA needed	(For MseI this is 21 µL.)
16 µL	NDE1 enzyme (0.15 × 105). For MseI this is 31.5 µL.
824 µL	water (7.85 × 105). For MseI this is 787.5 µL
1050 µL	total

2. Add 10 µL of master mix to each 10 µL sample (50 ng DNA). Use strip tubes, multi-channel pipette to distribute to plate.
3. Spin samples down on centrifuge.
4. Incubate at 37°C for 3h in a thermocycler. Inactivate at 65°C for 20 minutes in a thermocycler.

Ligate bar-coded adapters and pool samples.

5. For each sample of digested genomic DNA we need:

5 µL	ligase buffer.
0.2 µL	T4 ligase , high concentration (400U)
0.5 µL	adapter oligos (10 µM stock solutions)- Add to each well first
24.3 µL	water
30 µL	total

Prepare a master mix of ligase buffer, ligase and water (105x per plate) in a 15 mL falcon tube. Do NOT include adapter oligos:

525 µL	ligase buffer.
21 µL	T4 ligase , high concentration (400U)
2552 µL	water
3098 µL	total

6. Pipet 0.5 µL of unique adapter oligos to each sample using a multichannel pipette. *BE VERY CAREFUL NOT TO CROSS-CONTAMINATE THE ADAPTOR OLIGOS!!!!! Do not thaw adapter oligos more than 3 times.*
7. Pour ligase mastermix onto a clean trough. Using a multichannel pipette add 29.5 µL of mastermix to each sample. Gently mix by tapping plate.
8. Ligate in a thermocycler at 16°C for 3 hours, followed by 10 minutes at 65°C for heat inactivation.

Ethanol (or isopropanol) precipitate.

9. Pipet 100 µL of 3M sodium acetate pH 5.2 in a clean trough. Add 1/10th volume (5 µL) of sodium acetate to each sample using a multichannel pipette.
    - *Be careful not to contaminate samples between plates if you don't change tips!*
10. Pour 5 mL of isopropanol into a clean trough. Add 1 volume (50 µL) of isopropanol to each sampl using a multichannel pipette.
    - *Be careful not to contaminate samples between plates.*
11. Pool ligation reactions into a 15mL falcon polypropylene tube.
    - Use a 200 µL pipette to get most of liquid.
    - VERY briefly spin down plates, then use a 20 µL pipette to get out rest of liquid.
12. Add 1 µL glycogen to each set of pooled samples and mix gently by inversion. You should see DNA precipitate in your solution.
13. Chill overnight at 4°C.

DAY 2 (long day)

Ethanol (or isopropanol) precipitation

1. Pellet the precipitate by centrifuging at 4000 RCF for 30 minutes at 4°C.
2. Carefully pour off the supernatant.
3. Wash the sides of the tube with cold 70% ethanol (Use at least 1ml).
4. Centrifuge at 4000 RCF for another 5 minutes and pour off the supernatant. It is important to get as much liquid out as possible, use kimwipe to soak up.
5. Let air dry in hood for ~30 minutes or until the ethanol is gone.
6. Resuspend the pellet in 100 µL (more if needed, by 100 µL increments, but remember to adjust subsequent bead volume) TE pH 8. Pipet solution in and out for faster resuspension. Incubate at RT for 30 minutes, and then at 37C for 15 minutes to ensure that is fully resuspended.
    - *Pour gel and take AMPure beads out of fridge during waiting time.*
7. Transfer each set of pooled samples to separate 1.5ml MC tubes.

Bead purification using the Agencourt AMPure PCR purification kit.

8. Allow beads to come to room temperature prior to use. Swirl bottle to resuspend beads. (Illumina protocol recommends vortexing vigorously. Just make sure that there are no clumps of beads still stuck to the sides of the bottle, then vortex again, just to be sure the solution is homogenized!)
9. Add 150 µL (1.5 volume, more if you added more TE in resuspension step) of beads, mix by pipetting up and down 10 times, making sure that the beads are resuspended homogeneously.
10. Incubate at room temperature for 15 min.

11. **PLACE on MAGNET.**
    - *Make sure that the bottom of the tube is not below the bottom level of the magnet. Use taped labels to prop tube up.*
12. Incubate for 10 min (or until solution becomes clear).
13. Remove and discard supernatant, take care not to disturb the beads!
    - *Hold tube steady while pipetting out supernatant. The beads may drop, but should still stay on the side of the tube. Just be sure not to pipet them up. Pipet out about 100 μL at a time.*
14. Add 200 μL of 70% ETOH (Agencourt recommends freshly made). Pipet it over the beads.
15. Incubate at room temperature for 1 min.
16. Remove and discard supernatant, again being careful not to disturb the beads
17. Repeat ETOH wash.
18. Air dry for 20 min or until dry.
19. **REMOVE FROM MAGNET**
20. Resuspend in 40 μL of TE – after you have gotten the beads resuspended, pipet up and down 10 times to mix thoroughouly
21. Incubate at room temperature for 2 min.
22. **Place back on magnet** for 5 min (or until solution becomes clear).
23. **(Keep on magnet!)** Transfer supernatant to a new tube.

SIZE SELECTION (GEL ELECTROPHORESIS & EXTRACTION)

MAKE GEL

24. Use 100mL gel in large gel casting tray and 12 well thick comb. Do not put the comb in the gel until after it is poured.
25. Add 100 mL 1x TAE to flask.
26. Add GTG very slowly, in increments letting it soak in and disperse across the surface of the liquid. Add agarose and then swirl to mix.
    - 1 g agarose
    - 1 g NuSieve GTG agarose
27. Weigh beaker + solution together, record weight
28. Microwave for 1 min 15 sec or until bubbles appear, then remove and swirl until you get the chunks to disappear (GTG agarose is more difficult than regular agarose to get into solution)
29. Microwave at boiling for 45–60 sec.
30. Re-weigh beaker + solution. Add distilled water to reach original weight, swirl solution to homogenize.
31. Cool to ~65°C by running flask under cool water in sink. Add 4.5 μL EtBr.
32. Pour into casting tray, place comb in gel and let sit until set, probably at least 30 minutes. Put in fridge if you aren't ready.

RUN GEL

33. Combine 40 μL sample with 8 μL special dye (6x orange dye) in tube. Run ladder and sample in separate lanes, separate samples with ladder. Ladder: Fermentas Generuler 50 bp. Use 1 X TAE for running buffer. Special dye: 80% glycerol, 0.05% BPB and 0.05% XC in water
34. Pour TAE into the gel chamber, but do not submerge the gel. Stop pouring when the TAE is just above the bottom of the gel.

35. Load the samples into the dry wells. Skip a lane between each sample. Into the skipped lanes, load ladder (Fermentas GeneRuler 50bp ladder).
36. Using a pipette top off each well with running buffer, but do not exceed the capacity of the well, i.e., do not let the buffer spill out of the well.
37. Run the gel at 70V for 10-15 minutes or longer as needed to allow the DNA to enter the gel.
38. Pour enough TAE to fully submerge the gel.
39. Continue to run the gel at 70V for a total of two hours. This is flexible. Run the gel for long enough to get good separation of the ladder bands.

GEL EXTRACTION

40. Label a new 1.5 mL tube(s) and record its weight.
41. Using a new disposable scalpel for each sample cut band between 250–300 bp ladder bands on the transilluminator (keep 200–250bp or 300–400bp as a back up). With the gel on UV light box, and the UV light on, quickly make vertical incisions in the gel for each of your samples. Turn off the UV light, and remove the pieces from the gel and place into pre-weighed MC tubes. It is very important that you minimize the amount of UV exposure that the DNA receives! The cut gel pieces can be saved until the next day, if you are pressed for time.
42. Re-weigh the tube with the gel and record its weight. Calculate the weight of the gel slice.

<u>Qiagen gel extraction</u>

43. Add 3 volumes **Buffer QG** to 1 volume gel (100mg ~ 100 μL). For > 2% agarose gels, add 6 volumes Buffer QG.
44. Incubate at 37°C or room temperature (original protocol calls for 50°C) for 30–45 minutes or until gel has completely dissolved. Vortex the tube every 5 minutes to help dissolve gel.
45. After the gel slice has dissolved completely, check that the color of the mixture is yellow (similar to Buffer QG without dissolved agarose). If the color of the mixture is orange or violet, add 10 μL 3 M sodium acetate, pH 5.0, and mix. The color of the mixture will turn yellow.
46. Add 1 gel volume of isopropanol to the sample and mix. Incubate for 1 minute.
47. Place a QIAquick spin column in a provided 2mL collection tube.
48. To bind DNA, apply the sample to the QIAquick column and centrifuge for 1 min at 17,900 x g (13,000 rpm). Discard flow-through and place the QIAquick column back into the same tube. For sample volumes of >800 μL, load and spin again.
49. If the DNA will subsequently be used for sequencing, in vitro transcription or microinjection, add 500 μL **Buffer QG** to the QIAquick column and centrifuge for 1 min at 17,900 x g (13,000 rpm). Discard flow-through and place the QIAquick column back into the same tube.
50. To wash, add 750 μL **Buffer PE** to QIAquick column and centrifuge for 1 min at 17,900 x g (13,000 rpm). Pipet onto the walls to wash them. Discard flow-through and place the QIAquick column back into the same tube. Let the column stand 2–5 min after addition of Buffer PE.
51. Centrifuge the QIAquick column once more in the provided 2 mL collection tube for 1 min at 17,900 x g (13,000 rpm) to remove residual wash buffer.
52. Place QIAquick column into a clean 1.5mL microcentrifuge tube.

53. To elute DNA, add 22 μL (Modified for increased DNA concentration. Original protocol asks for 50 or 30 μL) **Buffer EB** (10 mM Tris-Cl, pH 8.5) to the center of the QIA quick membrane, let the column stand for 1 min, and then centrifuge the column for 1 min.

DNA Quantification—Qubit

54. Qubit 2 μL of sample using Quantit HS assay. If using BR assay, you will probably need to Qubit 10 μL of sample.

DAY 3

1. You will need 2ng of template DNA for the PCR step. Calculate the volume of template DNA you will use for PCR:
   - If Qubit concentration < 2 ng/μL, you will need 2/Qubit concentration μL of template. Example: If Qubit reading is 1.5 ng/μL, use (2/1.5) = 1.33 μL template for PCR.
   - If Qubit concentration > 2 ng/μL, it is advisable to dilute your template. Take (2 ng/Qubit concentration) × 20 = Y (in μL) of template and add 20 – Y μL of water. Use 1 μL of this diluted template for PCR. Example: If Qubit reading is 13.9 ng/μL, take (2/13.9) × 20 = 2.88 μL template and add 17.12 μL water. Use 1 μL of this mixture for PCR.

Amplify bar-coded fragments using the Phusion PCR kit and FC1 and FC2 primers.
For a single library, we will perform 4 reactions each at 14 cycles. These reactions will be pooled together in a single tube after PCR for cleaning. In a 50 μL reaction you will need:

25 μL	2x Phusion Buffer Master Mix
2.5 μL	FC1 (10 μM) primer
2.5 μL	FC2 (10 μM) primer
X μL	(2 ng template DNA)-Need to calculate volume
20 – X μL	water

2. Pipet the required volume of water into each of the 4 PCR tubes.
3. Pipet the required volume of template DNA into each of the 4 PCR tubes.
4. Pipet 2.5 μL of each primer onto the inside wall of each PCR tube. Take care not to let the primers come into contact with each other to avoid primer dimer creation.
5. Wash down the primers into solution by pipetting in 25 μL of master mix into each tube.
6. Run the FC_PCR program in Tomoko's folder on the Dyad thermocycler. Run the minimum number of PCR cycles required to generate sufficient DNA for the flow cell. See "Quantify the libraries by qPCR" and "Determine Cluster Numbers for Control Library." The number of cycles may need to be increased to 18 if you have <2 ng DNA. The program should be:

Step 1	98°C	30 sec	
Step 2	98°C	10 sec	
Step 3	64°C	20 sec	14 cycles
Step 4	72°C	20 sec	
Step 5	72°C	7 min	
Step 6	4°C	hold	

7. Pool all four PCR products into a single tube for cleaning.

Bead purify using the Agencourt AMPure PCR purification kit

*Allow beads to warm to room temperature first

FIRST WASH

8. Swirl bottle to resuspend beads.
9. Add 160 μL (0.8 volume) of beads, mix.
10. Incubate at room temperature for 5 min.
11. Place on magnet for 10 min or until solution is clear.
12. Aspirate and discard supernatant (Make sure not to aspirate any beads).
13. Add 200 μL of ETOH 70%, wash by inverting.
14. Mix/wash by inverting tubes while on magnet.
15. Incubate at room temperature for 1 min.
16. Aspirate and discard supernatant.
    Take out any supernatant stuck in the cap.
17. Repeat ETOH wash.
18. Air dry for 20 min or until beads are dry.

Always on magnet

19. Remove the tube from the magnet and resuspend beads in 100 μL of **<u>TE</u>** (or half volume of pooled reactions**.**
20. Incubate at room temperature for 1 min.
21. Place back on magnet for 5 min.
22. Transfer supernatant to a new tube.

SECOND WASH

23. Perform a second bead purification the same as the first, but use 80 μL of beads and resuspend with 20 μL of **<u>Qiagen EB buffer</u>**.
24. Not a bad idea to run a gel and look for a band of correct size and check that there is no primer dimer.

Appendix 12 Additional specimens examined, all specimens are from the Philippines.

Eutropis bontocensis CALAYAN ISLAND: Cagayan Province: Municipality of Calayan: Barangay Magsidel: KU 304873, 304874, 304878, 304881–304883, 304886–304890, 304892; SABTANG ISLAND: Batanes Province: Municipality of Sabtang: Barangay Chavayan: KU 314026–314030, 314032; Luzon Island: Cordillera Mountain Range: Mountain Province: Municipality of Bontoc: KU 335121; Municipality of Sabangan: CAS 61344 (paratype); Benguet Province: Municipality of Baguio CAS 61327 (paratype).

Eutropis borealis See type description.

Eutropis caraga See type description.

Eutropis cumingi LUBANG ISLAND: Occidental Mindoro Province: Municipality of Lubang: Barangay Vigo: KU 304009, 320489; CAMIGUIN NORTE ISLAND: Cagayan Province: Municipality of Calayan: Barangay Balatubat: KU 304745, 304746; BATAN ISLAND: Batanes Province: Municipality of Ivana: Barangay Salagao, Sitio Imnadyed: KU 314022, 314023; SABTANG ISLAND: Batanes Province: Municipality of Sabtang: Barangay Chavayan: KU 314025; LUZON ISLAND: Nueva Vizcaya Province: Municipality of Quezon: Barangay Maddiangat, Sitio Dayog 308933; Zambales Province: Municipality of Botolan: Barangay Porac, Ramon Magsaysay Technological University Campus: KU 335139; Municipality of San Felipe CAS 15473 (holotype); Sierra Madre Mountain Range: Aurora Province: Municipality of Casiguran: Barangay Casapsipan, IDC forestry land 325106; Isabela Province: Municipality of San Mariano: Barangay Dibuluan, Sitio Apaya, Apaya Creek area: KU 327378, 327382; Barangay Dibuluan, Sitio Dunoy, Dunoy Lake area: KU 327383; Barangay Dibuluan, Dibnatis Ridge, Dibanti River area: KU 327385.

Eutropis englei MINDANAO ISLAND: Cotabato Province: Cotabato Coast, Tatayan to Saub: MCZ 26289 (holotype), MCZ 26290 (paratype).

Eutropis gubataas See type description.

Eutropis indeprensa MINDORO ISLAND: Occidental Mindoro Province: Municipality of Victoria: Barangay Loyal: KU 302883; Municipality of Sablayan: Barangay Batong Buhay, Butalai, Mount Siburan: KU 304027, 304032, 304035; Municipality of Calintaan: Barangay Malpalon: KU 306992; Municipality of San Jose: 500 yards south of Bugsanga River: CAS 86663 (paratype)

Eutropis islamaliit See type description.

Eutropis lapulapu See type description.

Eutropis multicarinata DINAGAT ISLAND: Dinagat Islands Province: Municipality of Loreto: Barangay Santiago, Sitio Cambinlia, Mount Camblinia: KU 310149, 310151, 310153, 310155; MINDANAO ISLAND: Agusan del Sur Province: Municipality of San Francisco: Barangay Bagusan, Mount Magdiwata: KU 320025; LEYTE ISLAND: Leyte Province:

Municipality of Baybay: Pilim, San Vicente: KU 311246; Municipality of Burauen: CAS-SU 24657